PROCESS ENGINEERING STUDIES FOR BIODEGRADATION OF REACTIVE RED 120 DYE BY *Pseudomonas aeruginosa* JU_CHE_01

Thesis submitted by

DEEPA GOSWAMI

DOCTOR OF PHILOSOPHY (ENGINEERING)

DEPARTMENT OF CHEMICAL ENGINEERING

FACULTY COUNCIL OF ENGINEERING & TECHNOLOGY

JADAVPUR UNIVERSITY

KOLKATA, INDIA

2026

JADAVPUR UNIVERSITY
KOLKATA-700032, INDIA

INDEX NO.188/19/E of 2019, dated 27/06/2019

1. Title of the thesis: **Process Engineering Studies for Biodegradation of Reactive Red 120 Dye by *Pseudomonas aeruginosa* JU_CHE_01**

2. Name, Designation & Institution of the Supervisors:

- Dr. Chanchal Mondal
  Associate Professor
  Department of Chemical Engineering
  Jadavpur University, Kolkata, West Bengal

- Dr. Biswanath Bhunia
  Assistant Professor
  Department of Bio Engineering
  National Institute of Technology, Agartala, Tripura

3. List of Publications:
   List of Journal Paper:

- **Deepa Goswami**, Jayanti Mukherjee, Chanchal Mondal, Biswanath Bhunia, **"Bioremediation of azo dye: A review on strategies, toxicity assessment, mechanisms, bottlenecks and prospects"**. Science of the Total Environment. **2024**. 954:176426
- **Deepa Goswami**, Priyanka Sarkar, Jayanti Mukherjee, Chanchal Mondal, Biswanath Bhunia, **"Improved biodegradation of Reactive Red 120 by *Pseudomonas aeruginosa* JU_CHE_01: Isolation, characterization, and statistical optimization".** Clean-Soil, Air, Water. **2025**. 53(7): 1-12
- **Deepa Goswami**, Chanchal Mondal, Biswanath Bhunia,"**Kinetic modelling of high concentration Reactive Red 120 biodegradation by *Pseudomonas aeruginosa* JU_CHE_01 and post-treatment phytotoxicity analysis**". Environmental Technology. 2025 (Under review)

4. List of Patents: Nil

5. List of Presentations in National/International Conference:

- **Deepa Goswami,** Chanchal Mondal, Biswanath Bhunia, **"Biodegradation of Reactive Red 120 by *Pseudomonas aeruginosa* JU_CHE_01: Optimization of Process Parameters"** presented in the 1st International Conference on "Enhancing health through

Environment, Biotechnology and Entrepreneuship (Green Bio-merge,2024)" organized by Department of Biotechnology, Brainware University, Kolkata from 22nd February to 24th February, 2024.

- **Deepa Goswami,** Chanchal Mondal, Biswanath Bhunia, **"Isolation, Screening and Morphological Identification of Reactive Red 120 Dye Decolorizing Bacteria from Textile Dye Effluent"** presented in the International Conference on "Climate change, Ecosystems and Natural Resource Management for Sustainable Livelihood" organized by Sripat Singh College, Rani DhanyaKumari College, Murshidabad, West Bengal, India and Universal Wiser Publisher-Singapore from 10th October to 11th October, 2023.

Statement of Originality

I, Deepa Goswami, registered on 27th June 2019 do hereby declare that this thesis entitled "**Process Engineering Studies for Biodegradation of Reactive Red 120 Dye by *Pseudomonas aeruginosa* JU_CHE_01**" contains literature survey and original research work done by the undersigned candidate as part of Doctoral studies.

All information in this thesis have been obtained and presented in accordance with existing academic rules and ethical conduct. I declare that, as required by these rules and conduct, I have fully cited and referred all materials and results that are not original to this work.

I also declare that I have checked this thesis as per the "Policy on Anti Plagiarism, Jadavpur University, 2019", and the level of similarity as checked by iThenticate software is 1 %.

Deepa Goswami

Signature of the candidate

Date: 13.02.26

Certified by the Supervisor(s): (Signature with date, seal)

1. 13/02/26

Associate Professor
CHEMICAL ENGINEERING DEPARTMENT
JADAVPUR UNIVERSITY
Kolkata-700 032

2. 13.2.26

Dr. Biswanath Bhunia
Assistant Professor
BIO ENGINEERING DEPARTMENT
NATIONAL INSTITUTE OF TECHNOLOGY, AGARTALA
Agartala, Tripura
Pin-799046

CERTIFICATE FROM THE SUPERVISORS

This is to certify that the thesis entitled **"Process Engineering Studies for Biodegradation of Reactive Red 120 Dye by *Pseudomonas aeruginosa* JU_CHE_01"** submitted by **Ms. Deepa Goswami**, who got her name registered on **27th June 2019** [Registration No. 1021902006 (Ref. No. D-7/E/365/19)] for the award of Ph.D. (Engineering) degree of Jadavpur University is absolutely based upon her own work under the supervision of **Dr. Chanchal Mondal** (Supervisor), Associate Professor, Department of Chemical Engineering, Jadavpur University, Kolkata, West Bengal and **Dr. Biswanath Bhunia** (Co-supervisor), Assistant Professor, Department of Bio Engineering, National Institute of Technology, Agartala, Tripura, and that neither her thesis and nor any part of the thesis has been submitted for any degree or any other academic award anywhere before.

1. _____ 12/2/19

Signature of the supervisor

and Date with Office Seal

Dr. Chanchal Mondal
Associate Professor
Department of Chemical Engineering
Jadavpur University, Kolkata, West Bengal

Associate Professor
CHEMICAL ENGINEERING DEPARTMENT
JADAVPUR UNIVERSITY
Kolkata-700 032

2. _____ 12/2/19

Signature of the supervisor

and Date with Office Seal

Dr. Biswanath Bhunia
Assistant Professor
Department of Bio Engineering
National Institute of Technology
Agartala, Tripura

Dr. Biswanath Bhunia
Assistant Professor
BIO ENGINEERING DEPARTMENT
NATIONAL INSTITUTE OF TECHNOLOGY, AGARTALA
Agartala, Tripura
Pin-799046

ACKNOWLEDGEMENTS

First of all, I would like to express my gratitude and sincere thanks to **Dr. Chanchal Mondal**, Associate Professor, Department of Chemical Engineering, Jadavpur University, Kolkata and **Dr. Biswanath Bhunia**, Assistant Professor, Department of Bio Engineering, National Institute of Technology, Agartala, Tripura, for constant encouragement and valuable guidance during execution of the research work. I am deeply grateful to them for their unwavering support during a challenging period and for their steadfast belief in my ability to complete this work. Their guidance, enthusiasm, and expertise have been a constant source of motivation throughout my Ph.D. journey. Their thoughtful suggestions have strengthened my resolve and provided the mental strength needed to pursue this research. Without their invaluable assistance, encouragement, and insightful recommendations, the successful completion of this work would not have been possible.

My further gratitude goes to my mother, Mrs. Swapna Goswami; my father, Mr. Kashinath Goswami; and my brother, Mr. Rajib Goswami, for their unwavering love, support, and encouragement throughout this journey. Their constant belief in me has been my greatest source of strength and motivation.

I would also like to thank all the professors, staffs and research scholars of Department of Chemical Engineering, Jadavpur University and Department of Bio Engineering, National Institute of Technology, Agartala, for extending generous help whenever needed.

Deepa Goswami 12.02.26

DEEPA GOSWAMI
CHEMICAL ENGINEERING DEPARTMENT
JADAVPUR UNIVERSITY
KOLKATA- 700032

PREFACE

The primary goal of this research is to investigate the ability of isolated potent bacteria to decolorize high concentrations of the di-azo dye Reactive Red 120 in the presence of minimal amount of carbon and nitrogen source. The thesis is structured into five principal chapters, succeeded by the references section. Chapter 1 is the introduction; this chapter provides an overview of the use of synthetic colorants in the textile industry. Chapter 2 is review of literature; this chapter includes the literature available to support the current research. Chapter 3 is materials and methods; this chapter included several materials and methods utilized in the present study. Chapter 4 is findings and analysis; this chapter is predicated on the conducted tests. Chapter 5 is conclusion and future recommendations; this chapter delineates the significant conclusion derived from the results and discussions presented in the preceding sections.

ABSTRACT

The increasing usage of dyes across multiple industries, including textiles, tannery, plastics, paper, and paints, has contributed to an alarming increase in both human and environmental exposure to these chemicals. It is well-known that the textile sector in India is a major source of harmful pollutants. The effluent produced by textile factories contains substantial amounts of unfixed dyes, commonly found in wastewater, posing a potential environmental risk. The physicochemical effluent treatment methods are incapable of achieving complete degradation of resistant synthetic dyes in effluents, owing to their lightfastness, stability, colorfastness and decomposition resistance. Biological treatment approaches for dye decolorization have lately gained popularity due to their cost-effectiveness and environmental sustainability, making them applicable to a diverse range of colors. The isolation of microorganisms from contaminated sites is thought to become more successful in treating both refractory and xenobiotic pollutants because they have been acclimatized to the harmful effect of the contaminants. Therefore, it is vitally necessary to have a full knowledge of the biological treatment procedures and many components required to attain the target performance.

In the initial phase of the study, six morphologically distinct bacterial strains were derived from a textile effluent sample obtained from the outlets of textile industrial units and industrial dye-contaminated soil, which exhibited a significant likelihood of contamination by di-azo Reactive Red 120 dyes. A significant number of viable isolates were chosen for further investigation due to their impressive tolerance and optimal decolorization efficiency. The powerful strain was determined to be *Pseudomonas aeruginosa* JU_CHE_01 determined through morphological and biochemical profiling along with 16S rRNA gene analysis. Next, the NCBI Gene Bank database was updated with the 16S rRNA gene sequence. The unadulterated bacterial strain was assessed for the removal of six model azo dyes: Reactive

Red 13, Acid Black 194, Methyl Orange, Reactive Yellow 135, Congo Red, and Direct Violet 1. This strain demonstrated tolerance to elevated dye concentrations, achieving maximal decolorization for all six model colors. Consequently, microorganisms capable of digesting Reactive Red 120 (RR120) dye shown remarkable efficacy and metabolic adaptability.

Five process variables were assessed for optimal conditions utilizing the Taguchi methodology. Two media components (glucose and yeast extract) and three physicochemical parameters (pH, temperature, and inoculum dose) were improved due to their substantial effects on RR120 biodegradation. The L-18 Orthogonal Arrays (OA) framework was employed in the design of many experimental researches. The L-18 Orthogonal Arrays (OA) framework was employed in the design of many experimental researches. To determine the crucial elements and ideal circumstances for increasing RR120 dye breakdown, the obtained experimental findings was examined employing the Signal-to-noise (S/N) ratio and a "bigger is better" methodology. The validation of the expected data by confirmatory investigations demonstrated that under optimal conditions of yeast extract and glucose, each at 1 g/L concentration, 8 pH, 37°C temperature, and 10% (v/v) inoculum dose, a 97.63% degradation of the RR120 dye could be attained within 48 hours, resulting in a 66.75% improvement in RR120 degradation. ANOVA revealed that the carbon (glucose) and nitrogen (yeast extract) sources significantly affected RR120 biodegradation, contributing 27.933% and 19.526%, respectively, followed by pH at 4.664%, temperature at 13.476%, and inoculum dose at 28.951%.

This work clarifies the kinetics of facultative anaerobic biological growth and the degradation of RR120 using the isolated bacterium *Pseudomonas aeruginosa* JU_CHE_01, which can decolorize 600 mg L^{-1} of RR120, marking the highest concentration recorded for biodegradation to date. The results from the batch degradation experiments revealed that

Pseudomonas aeruginosa JU_CHE_01 demonstrated substrate inhibition kinetics, with the Haldane model accurately representing this research outcome. The biokinetic parameters employed for the growth of biomass estimation included a maximum specific growth rate of μ_{max}= 0.18 h^{-1}, a half-saturation coefficient of K_s = 345 mg L^{-1}, and an inhibition coefficient of K_i = 83.34. A post-treatment research was conducted to assess the phytotoxicity of the biodegraded products by germination of seed and root elongation assays on *Cicer arietinum*, *Vigna mungo,* and *Vigna radiata*. The results indicated a significant reduction in phytotoxicity during biodegradation, along with improved germination rates and assessment of root growth in treated specimens against control groups. The findings demonstrate that the bacterial strain effectively eliminates RR120 and mitigates its harmful environmental impacts. This work demonstrates the effectiveness of bacterial biodegradation in addressing high-concentration textile dyes like RR120, with kinetic modeling providing valuable insights for process enhancement. The decrease in phytotoxicity confirms the environmental safety of the biodegraded products, promoting the advancement of sustainable wastewater treatment techniques.

Keywords: Azo dye, Reactive Red 120 dye, Biodecolorization, Optimization, Kinetics

CONTENTS

Page No.

LIST OF TABLES

LISTS OF FIGURES

ABBREVIATIONS

BOD: Biochemical oxygen demand
COD: Chemical oxygen demand
TOC: Total organic carbon
TDS: Total dissolved solids
TSS: Total suspended solids
DNA: Deoxyribonucleic acid
RNA: Ribonucleic acid
MBM: Mineral base medium
BLAST: Basic local alignment search tool
DOE: Design of experiments
ANOVA: Analysis of variance
SEM: Scanning electron microscope
UV-vis: Ultraviolet visible
IUPAC: International Union for Pure and Applied Chemistry
MEGA 11: Molecular Evolutionary Genetics Analysis version 11
NaOH: Sodium hydroxide
NCBI: National Center for Biotechnology Information
RPM: Revolutions per minute
S: Substrate
K_m: Michaelis-Menten constant
V: Velocity
V_{max}: Maximum substrate consumption rate

SYMBOLS

%: Percentage
˚C: Degree Celsius
×g: Centrifugal force
g: Gram
h: Hour
L: Liter
s: Second
t: Time
v/v: Volume/Volume
w/v: Weight/Volume
µM: Micromolar
cm: Centimeter
mg: Milligram
min: Minute
mL: Milliliter
mM: Millimolar
mm: Millimeter
mol: Mole

CHAPTER 1

INTRODUCTION

1.1. Introduction

Accelerated urban growth raises the need for rapid industrial development, which damages the environment. Massive wastewater releases from the industrial sector reduce freshwater availability, which, if left untreated, can cause pollution issues worldwide (D. Dutta, Arya, & Kumar, 2021; B. J. Singh, Chakraborty, & Sehgal, 2023). Artificial colorants are widely employed across industries including-printing, textile, tannery, paint, plastic, and cosmetics because of their vibrant and rich colors. Typically, the dyeing industries use 100,000 synthetic dyes and dye-stuffs; of these, a portion (around ten to fifteen percent) of the unfixed dyes are introduced into water bodies untreated (Goswami, Mukherjee, Mondal, & Bhunia, 2024). Dye residues present at 1.0 mg L^{-1} were sufficient to cause color change in water. The presence of colors in wastewater is a definite indication that untreated wastewater has been released into aquatic environments (Azanaw, Birlie, Teshome, & Jemberie, 2022). Hazardous substances like dyes and other chemicals are released into the wastewater from these dyeing companies, posing a risk affecting human health and depleting the biota in water bodies (Sohini Dutta et al., 2024). Untreated wastewater enters water bodies, changing their pH, BOD, and COD levels as well as decreasing their ability to absorb sunlight, which disrupts the system's biodiversity. Due to their elevated levels of total organic carbon (TOC) and chemical oxygen demand (COD), color sewage processing is difficult and can harm the environment by changing pH and increasing COD, which may color water systems where the effluents are deposited (A. Saxena & Gupta, 2020). In addition to being hazardous, the dye's complex structure and its breakdown products are mutagenic and may harm living organisms. Thus, before being released into any ecosystem, such industrial effluents must have their amount of unfixed dyes reduced (Panwar, Mahajan, & Kaushal, 2023). Chromophore groups have a role in the molecular structure of dyes that are classified according to their applications. These chromophores are made up of several functional groups that are widely utilized in the dyeing process, including azo, anthraquinone, triphenylmethane, nitro, carbonyl, and various additional groups (Bhatia, Sharma, Singh, & Kanwar, 2017). The type of dye determines how much is emitted into the aquatic environment; basic dyes release 2% of the dye, while reactive dyes release 50%. Azo colors, the greatest prevalent category of artifical colors, are typically synthesized by combining electron-rich nucleophilic groups, including hydroxy acids and amino acids, with aromatic primary amines that have undergone diazotization. Conventional techniques face greater difficulty in removing these colors due to their high water solubility (Benkhaya, M'rabet, & El Harfi, 2020a; Hassan &

Carr, 2018). Reusing and treating industrial effluents has become a more appealing option for these industries due to the rising cost of water for industry. Discharges from dye manufacturing processes and textile sectors is challenging to handle because of the dyes' intricate aromatic compounds and synthetic history, making them more persistent and harder to biodegrade (Al-Tohamy et al., 2022). Textile sectors are working to create effluent remediation technology in order to abide by environmental legislation that limits the discharge of wastewater. Dye removal presents unique challenges because of its great resistance to traditional treatment procedures (Periyasamy, 2024).

Physico-chemical techniques, including adsorption, coagulation-flocculation, chemical oxidation, and membrane filtering, are extensively utilized for the treatment of textile wastewater owing to their swift color elimination and operational ease. Nonetheless, these techniques predominantly accomplish color transfer or phase separation instead of actual destruction of dye molecules. Adsorption and coagulation transfer contaminants from the liquid phase to a solid phase, producing substantial quantities of dye-laden sludge that necessitate further handling, treatment, and disposal, thereby elevating operational costs and environmental impact (Ahmed et al., 2022).

Chemical treatments frequently require elevated dosages, strict pH regulation, and energy-consuming processes. Moreover, inadequate oxidation or coagulation may lead to the generation of secondary harmful by-products, which might provide additional environmental hazards. Advanced oxidation techniques, while effective, are economically unfeasible for large-scale applications due to substantial reagent and energy demands. Membrane-based systems encounter issues pertaining to membrane fouling, elevated maintenance expenses, and restricted longevity (Donkadokula, Kola, Naz, & Saroj, 2020).

Conversely, biological degradation is a more environmentally sustainable and economically viable option, as it facilitates the decomposition of dye molecules into simpler, less harmful metabolites under mild working conditions. Biological processes produce negligible secondary waste, utilize reduced energy, and can be modified to accommodate diverse effluent compositions. Biological systems possess constraints, such as susceptibility to shock loads, inhibitory dye concentrations, and the necessity for optimum working conditions.

Although physico-chemical approaches efficiently facilitate quick color removal, their drawbacks concerning cost, sludge production, and sustainability render biological degradation a more favorable and complementary strategy, especially for long-term and large-scale textile wastewater treatment (Kapoor, Danish, Singh, Rafatullah, & HPS, 2021).

The dye is rendered fully inert and converted into a non-toxic chemical state through this biodegradation process, making it a viable technique. A greater degree of dye breakdown and decolorization can be attained by utilizing microorganisms under optimized aerobic or anaerobic environments (Zafar, Bukhari, & Rehman, 2022).
Three main categories can be used to divide bioremediation strategies:

- Utilizing the target molecule as a carbon source.
- Co-metabolism refers to the process by which an enzyme attacks a target chemical without using it as a source of carbon.
- The target molecule enters an organism and becomes concentrated there instead of being digested at all (bioaccumulation) (Kapoor et al., 2021).

The fabric industries in India are considered earliest components of the nation's economic framework, with a history spanning several centuries. Even today, India's textile sector division remains a major contributor to its exports and overall foreign trade. Approximately 11% of total exports are made up of textiles from India (Gokilavani). To expand manufacturing capacity and raise the industry's cost competitiveness, fifty textile parks are being built. In Madhya Pradesh (M.P.), there are more than 55 textile mills are established. Madhya Pradesh exports $325 million worth of textiles annually. In addition, the sources claimed that the state government is under pressure to decrease regulations, including as anti-pollution standards, even as it hopes to draw in investments totalling 10,500 crore in the textile industry to expand its installed spindle capacity. The textile industry has informed the state government that certain other states have also given the industry similar relaxations. According to Gargava (2021), the state pollution control board is determined about its "zero discharge" policy for industrial waste (Gargava, 2021). On December 18, 2012, the state cabinet made a significant decision by approving subsidies for textile mills in an effort to increase investment in that industry (Gupte, 2012). A comprehensive examination of microbial systems' roles in the biological remediation of toxicants and environmental contaminants is recommended given the present state of environmental contamination. Therefore, an effort is made to investigate and comprehend the function of microbial systems for dye bioremediation and industrial wastewater in the current research project.

1.2. Motivation and Hypothesis

Dyeing refers to the application of an organic substance to a material for the purpose of altering its color. Most colors are found in nature, however due to their photo-stability, artificial synthetic dyes generated from petroleum-based chemicals are increasingly utilized. One of the major categories of contaminants that conventional technologies find difficult to eliminate is dyes produced from different industrial wastewater (Lellis, Fávaro-Polonio, Pamphile, & Polonio, 2019). Any pollutants in the ecosystem can be eliminated by biological methods called biodegradation, which uses microorganisms to break down different types of organic substances. Treating dye wastewaters using bacteria to biodegrade synthetic colors is an efficient and alternative approach that has several benefits. Biological treatment is an economical process that generates non-toxic by-products upon mineralization and needs minimal operating costs. Lower pollutant concentrations that would be impossible to achieve through chemical and physical methods can also be used with this technology. A broad spectrum of microbiological organisms, including fungi, bacteria, yeast, and algae can degrade various dye pollutants in a variety of anaerobic and aerobic environments when taking into account the primary and secondary metabolic processes. Among all industrial wastewaters, textile wastewaters are thought to be the most harmful. According to reports, effluent from textile industries is an excellent source to isolate bacteria that decolorize dyes. The fundamental strategy of bioremediation is to increase the native microorganisms' efficiency to facilitate better degradation. Research suggests that bacteria decolorize textile effluents far more effectively and quickly, resulting in full decolorization. Since azo dyes lack electrons due to the existence of their azo linkage, these dyes generally do not function as carbon sources. Carbon sources serve a crucial function to donate electrons during the azo dye reduction, significantly contributing to the microbial processes involved in their decolorization and degradation (Chakraborty, Basak, Dutta, Bhunia, & Dey, 2013). A multitude of research has been conducted using diverse medium consisting of mixtures of yeast extract and glucose, and other carbon sources. Observations revealed that medium composed of glucose and yeast extract have better azo dye decolorization ability in comparison to any other media (Anwar et al., 2014; Radhika Birmole & Aruna, 2019). The inclusion of nitrogen and carbon sources increases the overall cost of the decolorization process, making it more expensive. Therefore, a novel approach to treating textile effluents is necessary to effectively remove harmful contaminants from the environment. With the evidence presented above, it would be more economical to isolate and enhance bacteria from

textile wastewaters to expedite in order to improve degradation and removal of dye color. The biodegradation process is influenced by several environmental conditions, including temperature, pH, inoculum volume, oxygen availability, and nutrients. Increased dye breakdown and decolorization can be attained by employing microorganisms in aerobic or anaerobic conditions that are optimized. It has been found that a number of process parameters, in addition to nutrient medium, significantly affect bacterial metabolism, which reduces the efficacy of degradation. To attain optimal decolorization in industrial settings, it is crucial to refine several factors of the method by assessing their combined impact on the biodegradation process (Ajaz, Rehman, Khan, Nisar, & Hussain, 2019). An additional key element affecting the effectiveness of degradation is the rate of degradation or decolorization. It is an essential aspect that needs to be examined since the rate at which the pollutant degrades indicates how effective the decolorization procedure is. There is no such studies have been performed on the facultative anaerobic decolorization of widely used high concentrations of Reactive Red 120 (RR120), a di-azo dye under the presence of minimal nitrogen and carbon sources. Moreover, no investigations have been performed on the degradation kinetics of RR120 dye at high concentrations.

1.3. Objectives

The objective of this study is to decolorize toxic di-azo dye RR120 with high concentration using a pure bacterial strain. The objectives of the proposed research work might be summed up as follows:

- Isolation and characterization of RR120 dye degrading isolated strain.
- Optimization of the operational parameters for enhanced RR120 dye degradation using isolated strain.
- Investigation of batch kinetics for the RR120 dye biodegradation using isolated strain and phytotoxicity analysis.

1.4. Novelty and Innovativeness of the Present Work

Azo dyes represent a significant category of synthetic colorants extensively utilized in the textile sector, characterized by their structural complexity, persistence, and possible environmental toxicity. Multiple researches have documented physicochemical and biological methods for the remediation of azo dye-contaminated effluents. Nonetheless, despite comprehensive research, the practical application of biological dye degradation

processes is constrained by factors such as low dye tolerance, excessive food requirements, and insufficient process-level optimization. This investigation provides various novel contributions.

This study's primary innovation is the effective biodegradation of a high concentration (600 ppm) of RR120, a structurally intricate and sulfonated azo dye, in nutrient-limited environments. Most previously described investigations attain dye decomposition at relatively low concentrations and depend on substantial external carbon and nitrogen replenishment. In contrast, the bacterial strain utilized in this work employs merely 1 g/L of glucose as the carbon source and 1 g/L of yeast extract as the nitrogen source, indicating a significantly enhanced substrate utilization efficiency. This method accurately represents the properties of actual textile wastewater and improves the economic viability of the treatment process.

A further significant original feature is the utilization of a recently isolated bacterial strain, *Pseudomonas aeruginosa* JU_CHE_01 (*P. aeruginosa* JU_CHE_01), which demonstrates considerable tolerance and degrading efficacy towards RR120. While representatives of the genus *Pseudomonas* have been shown for dye degradation, the efficacy of biodegradation is markedly strain-specific. Strain *P. aeruginosa* JU_CHE_01's exceptional degrading ability at high dye concentrations sets it apart from previously documented strains and underscores its potential use in industrial wastewater treatment.

This study enhances current understanding by employing a process engineering-focused methodology instead of restricting the research to microbe screening or flask-scale decolorization. A systematic assessment of operational parameters, nutritional needs, and degrading efficacy yields engineering insights crucial for scaling and reactor design. This comprehensive method connects laboratory-scale biodegradation research with practical wastewater treatment implementations.

Furthermore, reducing nutrient supplementation enhances environmental sustainability by mitigating secondary contamination, excessive biomass accumulation, and total treatment expenses. This integrates the research with contemporary trends in sustainable and eco-friendly wastewater treatment technology.

In conclusion, although previous research has focused on azo dye biodegradation, the uniqueness of our study lies in its integration of high dye load treatment, reduced nutritional necessity, strain-specific efficacy, and process engineering evaluation. These factors combined augment the practical significance and industrial usability of the biodegradation procedure for RR120 contaminated textile effluents.

1.5. Layout of the thesis

The entire thesis is arranged into five major chapters, followed by the reference section.

Chapter I: Introduction

This chapter offers a summary of synthetic colorant utilization in the textile sector. It contains the motivation and working hypothesis of the research project. The importance of the research work, gaps, and specific objectives are discussed.

Chapter II: Literature review

The literature that is accessible to support the present research work is included in this chapter. This chapter primarily focuses on present issues, research conclusions, and potential future research directions that could be included in this investigation.

Chapter III: Materials and methods

This chapter encompassed several materials and methodologies employed in the current investigation. It offers an in-depth description of the techniques employed in the current study for the bacterial strain that decolorize dyes, including enrichment, isolation, screening, and identification. Additionally, pure strain phytotoxicity investigations, degradation kinetics, decolorization experiments, and process parameter optimization of RR120 dye is illustrated in this chapter.

Chapter IV: Results and discussion

This chapter is based on the experiments being done. Information regarding the isolation, morphological, molecular, biochemical and physiological characterization of potent dye-decolorizing bacterial strains from textile effluent is presented in the first section. It also describes the decolorization investigations and the influence of varied operational parameters on the efficiency of color removal of dyes. To achieve the highest possible biodecolorization, the Taguchi method is employed in order to improve five operational conditions: carbon source, nitrogen source, pH, temperature, and inoculum volume. Haldane model is used to investigate the kinetics of decolorization. Analytical techniques used for the analysis of dye degraded products for RR120 dye by isolated bacterial strain are explained. This section illustrates the plant toxicity investigations of the crude dye and its degradation metabolites.

Chapter V: Conclusion and future recommendations

The important conclusion reached in consideration of the results and discussions in the previous parts is outlined in this chapter. It also offers recommendations for further studies in this pertinent area.

CHAPTER 2

LITERATURE REVIEW

2.1. Dyes

Dye is an organic compound that is colored and can be used to change or add color to other substances. Since the beginning of time, people have painted and dyed various materials using colors. Most dyes are found in nature, but because of their photo-stability, man-made synthetic colors created from petrochemicals are now employed. Colors are utilized extensively in the paper, plastics, textiles, tanning, cosmetics and food sectors (F. D. Chequer et al., 2013).

2.2. History of Dyes

All colors originated from natural elements until the mid-19th century. The earliest accounts of coloring date back to 2600 BC in ancient China (Ingamells, 1993). Prior to the development of artificial colorants, natural dyes made from plant, vegetable, or mineral sources were utilized for coloring. The disadvantages of employing natural colors have included the necessity for numerous steps during the dyeing process, a slow shift in developments, along with the requirement for color fastness properties on an alternative substrate, all of which require in-depth information-based study to identify potential applications (Merdan, Eyupoglu, & Duman, 2017).

Early in the 20th century, W.H. Perkin was the first to discover a synthetic dye, mouve (Aniline purple, Tyran purple), which had superior dyeing properties and he replaced natural dyes with synthetic dyes. The synthetic dyes have been designed to possess chemical and physical features that fulfill the requirements of advanced, high-quality, and reliably reproducible operating systems (Welham, Willis, & Kerr, 2000). The utilization of synthetic dyes as coloring substances has markedly increased across several sectors. The global textile industries consume around 30 million tons of dyes annually, and this amount is growing at a rate of 3%. Approximately 700,000 tons of artificial dyes are manufactured annually, with around 10,000 functionally distinct dyes utilized across various industrial sectors (Zollinger, 2003).

2.3. Physical and Chemical Basis of Dye

A dye's color in solution is caused by the dye molecule's selective absorption of specific visible light wavelengths. The remaining light wavelengths are transferred, arrive at the retina, and produce the color that is seen. The dye molecule's ability to absorb visible light energy allows its electrons to be excited from a lower energy state (the ground state) to a greater amount of energy (the excited state). The energy difference, ΔE that exists from the excited state to the ground state is determined by the Planck's relationship stated in Eq. 2.1.

$$\Delta E = hv \text{ or } \Delta E = \frac{hc}{\lambda} \quad (2.1)$$

where h denotes Planck's constant, v represents the absorbed light frequency, λ signifies the absorbed light wavelength, and c indicates the constant speed of light. The energy involved in the dye's transition from a stable to an excited electronic state is therefore inversely related to the wavelength of light that the dye absorbs. Therefore, less excitation energy is required for a red-colored dye that absorbs bluish-green light with longer wavelengths than for a yellow dye that captures a short wavelength (blue) light (Christie, 2014).

According to the O. Witt, a dye contains two basic structural elements, chromophores and auxochromes. Chromophores (from Greek, Kuroma = color + Phors = carrier) possess a decentralized electron system characterized by conjugated double bonds, resulting in color; molecules possessing such a group are classified as chromogens. Certain groups can enhance color when they are present in a molecule with chromophores, even though they cannot produce color on their own. These are referred to as auxochromes (Greek, auxanein = to increase). The auxochromes -NH_3, -COOH, -OH, -NH (basic), -SOH (acidic), -NR and -NHR represent the most efficacious examples (Agrawal, Tipre, Patel, & Dave, 2017).

2.4. Nomenclature of Dyes

Color Index (C.I.) designations or commercial trade names are used to identify dyes. Most dyes have three parts to their commercial names. First, there is the color; second, there is the manufacturer's trademark that identifies the dye and the class it belongs to; and third, there is a code that specifies the dye and other important attributes. The application class, color, and sequential number combine to create the C.I. Generic Name, e.g., C.I. Acid Yellow 36, C.I. Reactive Black 5. Upon the disclosure of a dye's chemical structure by its producer, the dye receives a specific five-digit number under the C.I. (Constitution) system (Hunger, 2007a).

2.5. Dye Classification

Based on the characteristics, structure, and affinity for the substrate molecules, dyes can be categorized into different classes. Dye molecules have a physical adsorption and covalent bonding affinity with cellulose fiber. Although they vary in their characteristics and modes of application, all dyes and pigments give the appearance of being colored because they absorb particular light wavelengths (Gregory, 1990). The chromophore, which consists of elements like carbon, nitrogen, oxygen, and sulfur, is the area of the dye molecule that imparts color. It captures light between the visible spectrum range (400 to 800 nm) by altering the double and single bonds in the dye molecule (Gomes, 2001). Dyes are categorized into nitro and nitroso, azo (monoazo, disazo, triazo, polyazo), triarylmethane, anthraquinone, indigo, etc. based on the kind of chromophores found in the structures. It is possible to alter a chromophore's ability to absorb light by attaching a functional group called an auxochrome to it. Auxochromic groups that are most widely recognized include -OH, $-NH_2$, $-SO_3H$, -COOH, -NHR, and $-NR_2$, etc (F. D. Chequer et al., 2013).

Dyes were categorized in a number of ways, with the primary classifications based on the kind of material, the presence of the respective chromophores, and the methods of application.

2.5.1. Classification depending on the material type:

Dyestuffs are typically classified according to their production origin, which are outlined as follows:

- **Natural Dyes:**

Natural colors sourced from plant, mineral and invertebrate origins. The predominant types are plant-based vegetable dyes derived from bark, roots, berries, wood and leaves. Many natural sources, include small-scale lac insects, sea snails, cochineal, shellfish, sawfly larvae, snout caterpillars, Kermes, etc., or plants like beetroot red, sappan wood, weld, dyer's broom, cornflower, Deptford pink, Indian pokeweed, madder, turmeric, indigo, Jack fruits, Onion, tea waste, Henna, safflower, rose, marigold flowers, saffron, logwood, Cutch, Fustic, Weld, Woad, pomegranate rind, etc. (AlAshkar & Hassabo, 2021; Balfour-Paul, 2012; Cannon & Cannon, 1994; Cardon, Prunac, & Andary, 1996; Kant, 2011; Mcyotto et al., 2021; Weigle, 1974).

- **Synthetic Dyes:**

Petrochemicals are utilised as the principal raw components for dye production, which are utilized in daily life because they are more affordable to produce, have brighter colors, and have better colorfastness on a wider range of substrates. Some examples of synthetic dyes include azo, anthraquinone, mordant, acid, basic etc.

2.5.2. Classification based on the types of chromophores found in their structures

Azo dyes: A notable group of synthetic organic coloring agents known as azo dyes use azo groups, or -N=N, as their primary chromophore (Goswami et al., 2024). An aromatic amine is attached to aromatic molecules and diazotized to create these azo dyes, which results in an intense color. This supplies between 60 and 70 percent of the colors employed in the food and textile sectors. The examples of azo dyes are represented in **Figure 2.1**.

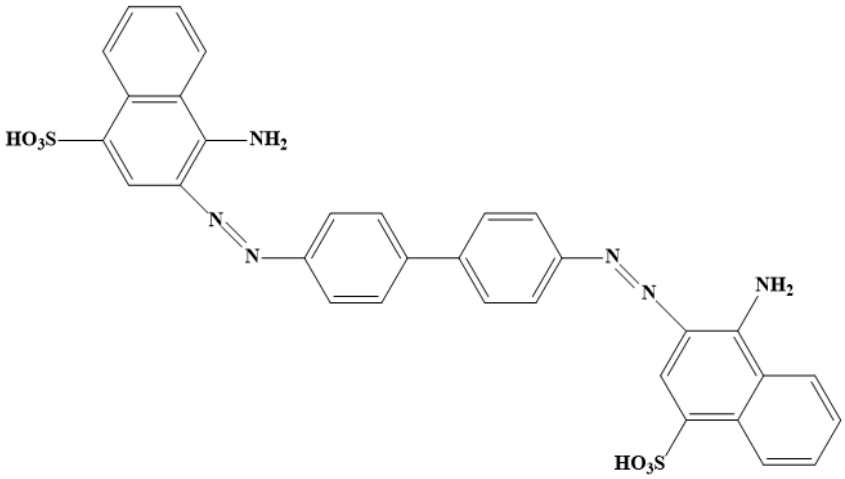

Congo Red

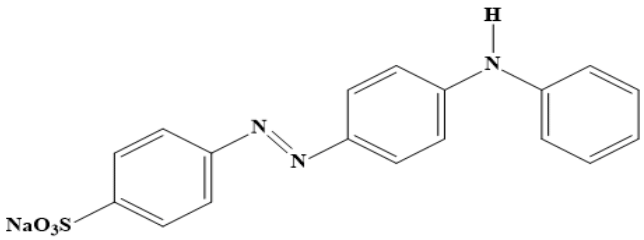

Acid Orange 5

Figure 2.1: Examples of azo dyes

Nitro and nitroso dyes: Dyes that employ -OH groups as an auxochrome and nitro (-NO_2) or nitroso (-N=O) groups as a chromophore (Benkhaya, M'rabet, & El Harfi, 2020b). Nitro and nitroso dye samples are shown in **Figure 2.2**.

Fast Green O **Martius Yellow**

Figure 2.2: Examples of nitro and nitroso dyes

Anthraquinone dyes: These organic dyes have molecular structures that are derived from anthraquinone. Anthraquinone is colorless by itself; however, by including groups that donate electrons, like hydroxyl or amino groups at the 1, 4, 5, and 8 locations, it can be colored red to blue (Hunger, 2007b). Their exceptional light fastness puts them in a category. In 1901, Rene Bohn discovered Indanthrone, also known as C.I. Vat Blue 4, which was the first synthetic vat dye based on anthraquinone. Anthraquinone dye examples are shown in **Figure 2.3**.

Purpurin **Alizarin**

Figure 2.3: Examples of anthraquinone dye

Triarylmethane dyes: These are the organic substances that make up the structure of triphenylmethane. These chemicals are produced industrially and come in bright colors (Wu, Doan, & Upreti, 2008). This consists of a quinoid as one of three aromatic rings bonded to a central carbon. There are four auxochromes in it: -NH_2, -NR_2, and -OH. **Figure 2.4** provides examples of triarylmethane.

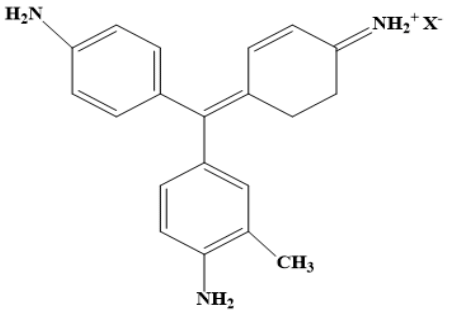

Basic Violet 14

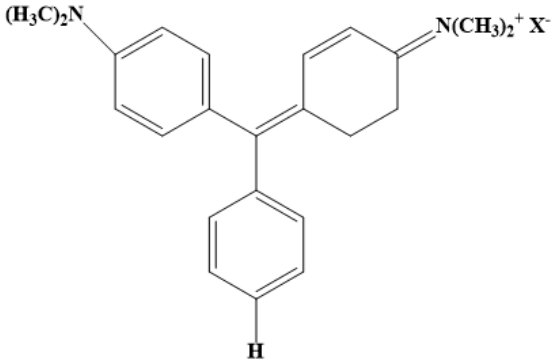

Malachite Green

Figure 2.4: Examples of triarylmethane dyes

Indigo dyes: The organic dye indigo has a blue color. Historically, indigo was produced organically from certain plant leaves, and this technique was economically crucial because blue dye was scarce. Synthetic indigo dye, one of the primary colors used in cotton dyeing and printing, is produced in thousands of tons per year. In 1865, German chemist Adolf von Baeyer started working on the indigo synthesis. He first illustrated the production of indigo from isatin in 1878, and then from 2-nitrobenzaldehyde in 1880. He eventually articulated the fundamental structure of indigo in 1883 (Baeyer, 1883). Indigo and its derivatives are poorly soluble in organic solvents because of intra- and intermolecular hydrogen bonding. **Figure 2.5** illustrates the basic structure of the indigo dye.

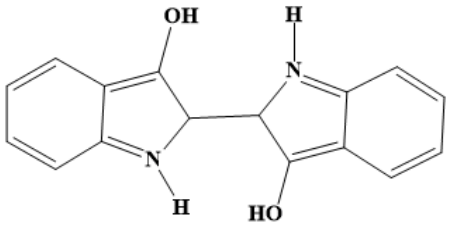

Indigo

Figure 2.5: Examples of indigo dyes

2.5.3. Categorization according to methods of application

The quality of the fabrics and the dye both influence the application techniques. They are classified in accordance with the implementation approach. These are as follows:

Acid dyes: Applied to the material at low pH because of carboxylic groups or sulphonic acid, it is highly water soluble. These dyes establish ionic connections between the anionic dyes and the cationic groups of the fibers ($-NH_3^+$), for instance nylon, acrylic, wool, and silk. The molecular weights of such colors vary between two hundred and one thousand; greater molecular weights correspond to diminished leveling characteristics (Waring & Hallas, 2013). The most prevalent chemical structures of acid dyes include azo, triarylmethane and anthraquinone. **Figure 2.6** shows various types of acid dyes.

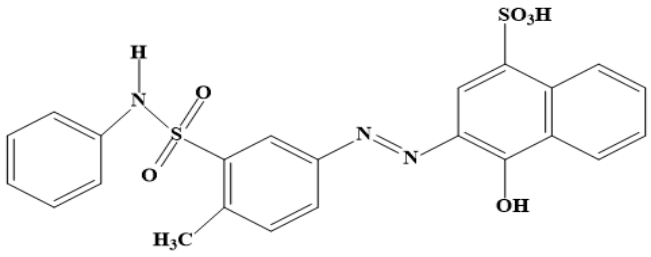

Acid Orange 19

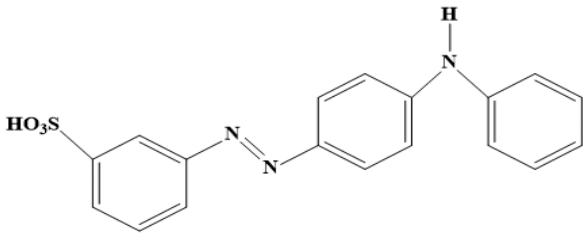

Acid Yellow 36

Figure 2.6: Examples of acid dyes

Basic dyes: Basic dyes dissolve readily in water and offer bright colors with poor light-fastness. They possess a noticeable liking for wool, acrylic, and silk fibers (Tang & Kan, 2020). The reason it works so well on acrylic fiber is that the negatively charged copolymer and dye functional groups like $-NR_3^+$ or $=NR_2^+$ have a strong ionic contact. The most common compounds of basic dyes include azo, triarylmethane, diarylmethane and anthraquinone. **Figure 2.7** illustrates instances of basic dyes.

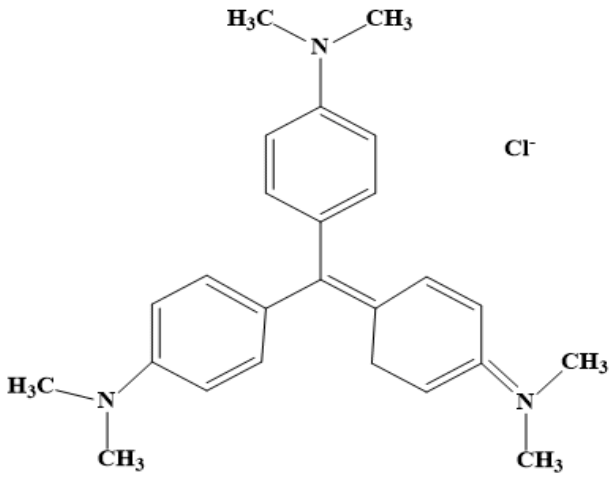

Crystal Violet

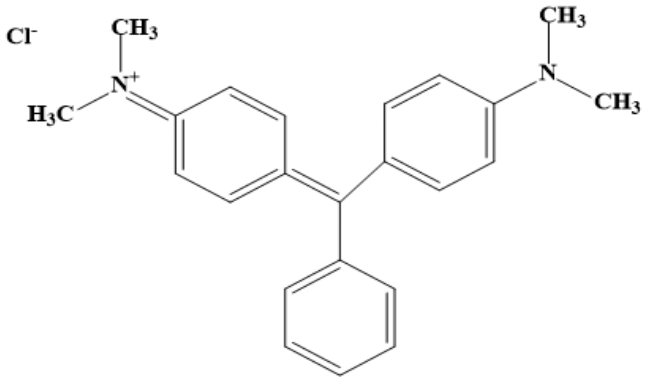

Malachite Green

Figure 2.7: Examples of basic dyes

Disperse dyes: They exhibit water-insolubility, are non-ionic, and possess colloidal characteristics, having polar groups ($-NO_2$ and -CN) that enhance Vander-Walls, dipole interactions and solubility. They are mainly used in the high-temperature dyeing of polyester

materials. Such colors are used in dispersed solutions to materials for colloidal absorption. Depending on the fabric's homogeneity and the dyes' absorption into the fibers, the pH and temperature of the dye bath can change (Rippon & Evans, 2020). Disperse dyes are categorized as mono-azo, di-azo, nitro, anthraquinonoid, or aminoketone dyes classified by their chemical composition. In **Figure 2.8**, the examples of dispersed dyes are provided.

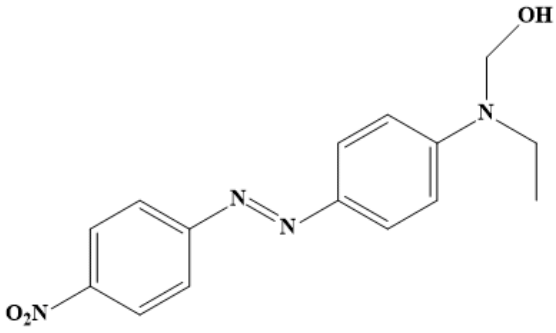

Disperse Red 1

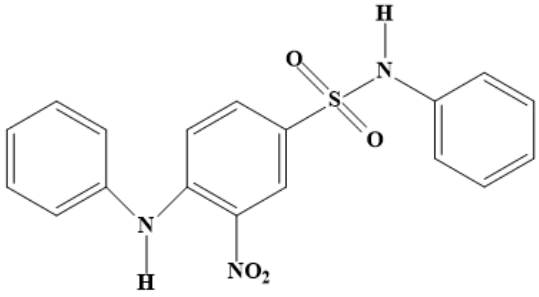

Disperse Yellow 42

Figure 2.8: Examples of disperse dyes

Direct dyes: They can be either anionic or cationic and are soluble in water. Through hydrogen bonding or Van der Waals interaction, they have an affinity for the fabric (cotton, silk, jute, and linen). These colors, which are mostly made up of amines and phenols with basic or acidic auxochromes, have also been employed as biological stains and pH indicators. The dyeing effluent exhibits considerable color loss due to the weak interactions between the fiber and direct dyes, resulting in poor wash fastness (Allen, 2013). In order to fix the dye on fibers, cationic bulking agents are used in a specific way. In **Figure 2.9**, direct dye examples are shown.

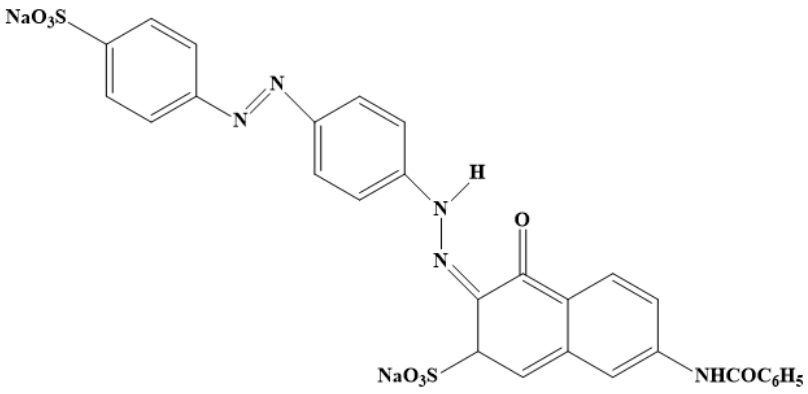

Direct Red 81

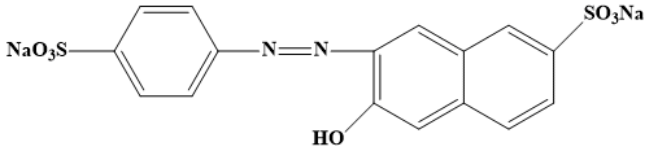

Direct Yellow 11

Figure 2.9: Examples of direct dyes

Reactive dyes: These dyes were initially discovered in 1956, and thereafter, particularly in industrialized nations, their use has increased. It was anticipated that 3,50,000 tons of reactive colors were produced annually in 2011 (DeLuca, 2017). It consists of chromophore (-OH,-NH, or-SH), which binds to the fibers (cotton, silk, wool, and nylon) by means of covalent bonds. The chemical breakdown of reactive groups occurring throughout the dyeing process increases the probability of vibrant effluents when utilizing these dyes. Reactive colors are more expensive than direct colors, but their light fastness and color fastness are excellent (Shu et al., 2019). Reactive dyes' strong chemical connection with the fabric gives them the most desirable characteristics, including permanence and washing resistance. The main structural components of reactive dyes are azo, phthalocyanine, anthraquinone, and metal-complex azo. Reactive dye examples are displayed in **Figure 2.10**.

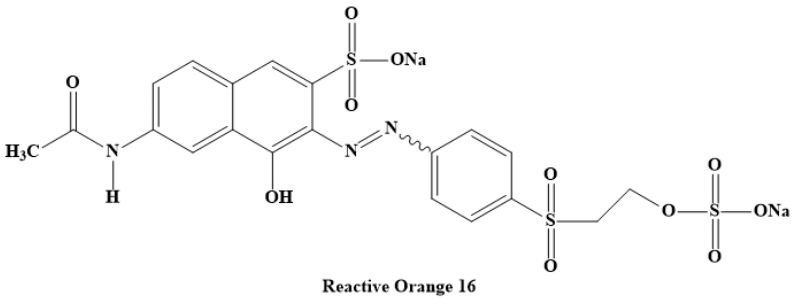

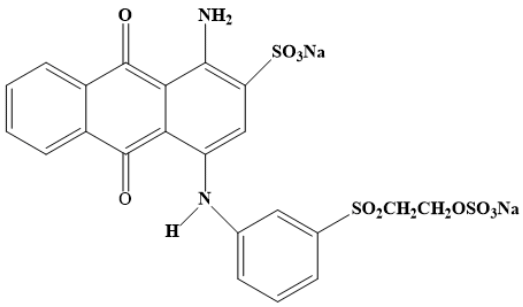

Figure 2.10: Examples of reactive dyes

Vat dyes: About 15% of all dyes used as textile dyes are vat dyes, which have anthraquinones or indigoids as their basic components. These dyes are water-insoluble. A reducing compound (sodium dithionite/hydrosulfite: $Na_2 S_2 O_4$) and an alkali (sodium hydroxide: NaOH) must be present to convert the dyes into their hydrophilic leuco form before dyeing. This creates a soluble substance termed the leuco dye, which has a definite predilection for cellulosic fibers. Therefore, in order to retain the color in the fiber, they are initially provided in a diminished soluble state and then oxidized to an unable to dissolve state (Benkhaya, M'rabet, Lgaz, El Bachiri, & El Harfi, 2022). A well-known vat dye is indigo. **Figure 2.11** illustrates some vat dye examples.

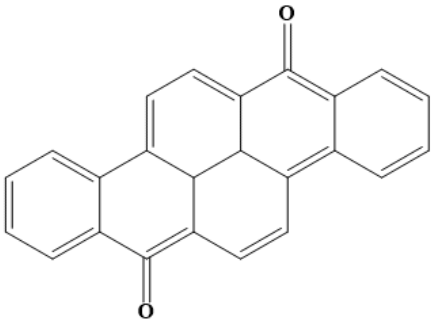

Vat Yellow 4

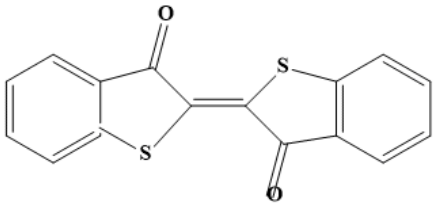

Vat Red 41

Figure 2.11: Examples of vat dyes

Sulfur dyes: Similar to vat dyes, sulfur dyes do not dissolve in water and involve oxidation and reduction processes. Sulfur dyes make up around 15% of all dyes produced and they are complex polymeric aromatics made of heterocyclic sulfur rings (El Harfi & El Harfi, 2017). It is frequently employed in two types of processes: batch and continuous, for the dyeing of cotton and linen. It is possible to increase the effectiveness of the sulfur dyeing process by using electrochemical reduction techniques. Although the color fastness and light fastness of these dyes are excellent, too much chlorine will eliminate the color (Shekhawat, Patra, Patra, & Bag, 2024). **Figure 2.12** depicts some examples of sulfur dye.

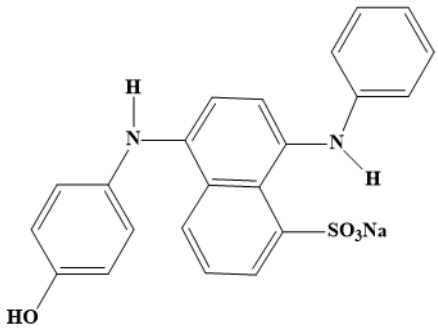

Sulfur Green 3

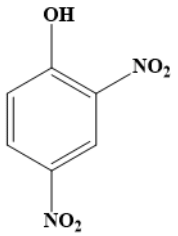

Sulfur Black 1

Figure 2.12: Examples of sulfur dyes

Mordant dyes: The chemical mordant is used in mordant dyes to improve the dye molecule's ability to hold color in fibers. Usually, they are metal salts (potassium or sodium dichromate), bark extracts, tannic acid, sumac, oleic acids, stearic acids, which bind well to both the fibers and the dye. They are utilized as "fixing agents" to enhance color stability in silk, leather, wool, and modified cellulose-based fibers. The predominant structures include oxazine, azo, and triarylmethane (Kamal El-Dean, Ahmed, Mohamed, Hussain, & Hashem, 2019). Mordant dye examples are shown in **Figure 2.13.**

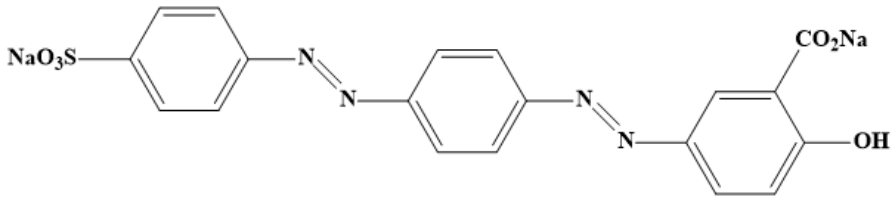

Mordant Orange 6

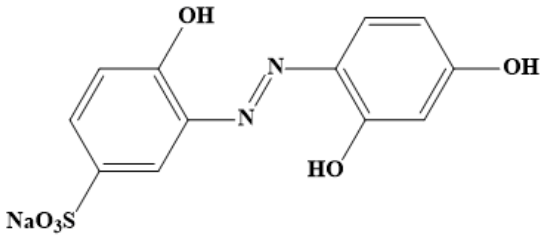

Mordant Red 5

Figure 2.13: Examples of mordant dyes

Pigment dyes: These dyes are not ionized, non-dissolvable chemicals that retain their particle structure during processing. In a water-based solution, dispersing agents are employed to distribute them. They are combined with thickeners to print on a variety of fabrics. The most widely used pigment colorants are either metal complex phthalocyanines, which include green and blue, or azo compounds, which include yellow, orange, and red. Quinacridone and anthraquinone are two other pigment dyes that have been added to the fabric (Marzec, 2014). **Figure 2.14** shows the structures of organic pigments.

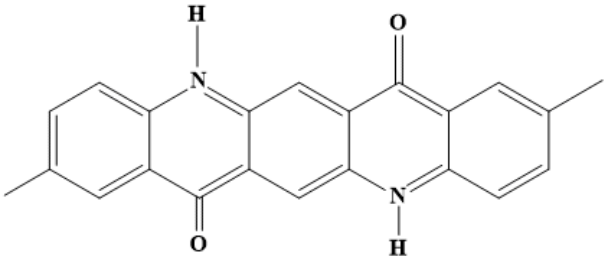

Pigment Red 122

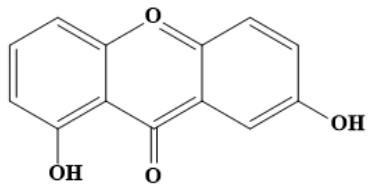

Xanthone

Figure 2.14: Examples of pigment dyes

Solvent dyes: Non-ionic colors known as solvent dyes are used to color non-polar materials like waxes, polymers, varnish, and ink. The production of textiles has recently made greater use of them. These diazo compounds experienced certain chemical changes that resulted in their loss of ionization ability (Sahu & Poler, 2024). The most prevalent structures include phthalocyanine, triarylmethane, anthraquinone, and diazo compounds. The examples of solvent dye are presented in **Figure 2.15**.

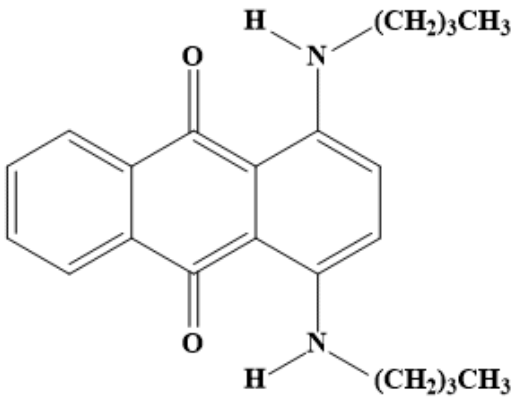

Solvent Blue 35

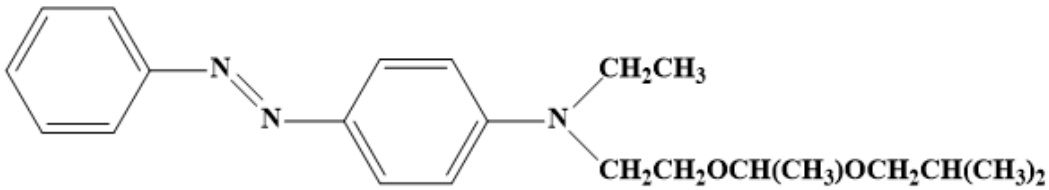

Solvent Yellow 124

Figure 2.15: Examples of solvent dyes

2.6. Azo Dyes

The primary group of artificial colors is the azo dye class, which are usually prepared by coupling nucleophilic groups with a high electron density, such as hydroxy acids and amino acids, with aromatic primary amines that have been diazotized. It presents greater challenges to eliminate these colors using conventional methods because of their significant water solubility (Benkhaya et al., 2020a; Hassan & Carr, 2018). The common structural characteristic of azo colorants is an azo (-N=N-) bond, which is joined to two sp^2 carbon atoms on either side. Typically, diazotization of the azo group results in a pair of aromatic ring structures. The term "monoazo dyes" or "pigments" refers to the predominant commercially relevant azo dyes, which have one azo functional group; however, many also comprise diazo, triazo, or higher-order azo groups (Christie, 2014). An example of an azo dye structure is depicted in **Figure 2.16**.

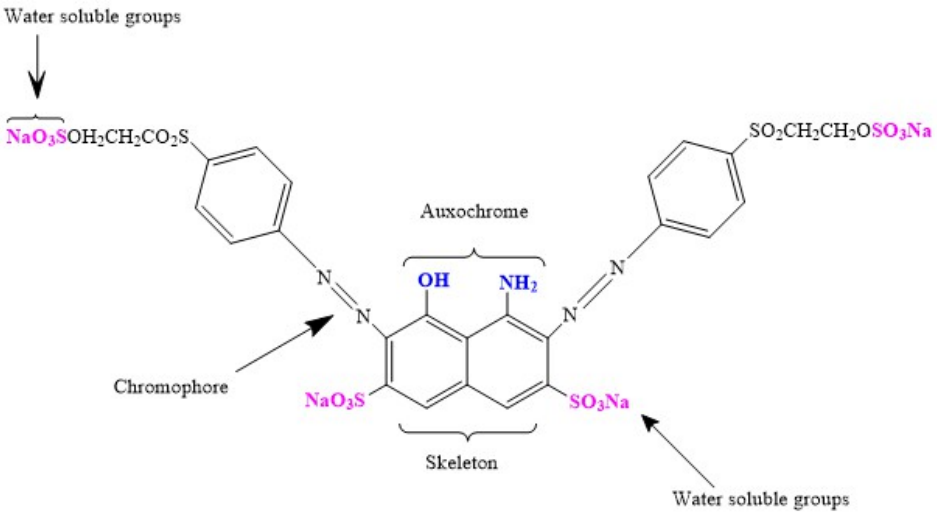

Figure 2.16: Azo dye composition (Benkhaya et al., 2020a)

A two-step reaction process is used to create azo dyes for industrial use:

Stage I (Diazotisation)

In order to create a diazonium salt, sodium nitrite is used to treat a main aromatic amine, also known as the diazo component, in an acidic environment at low temperatures (**Figure 2.17**).

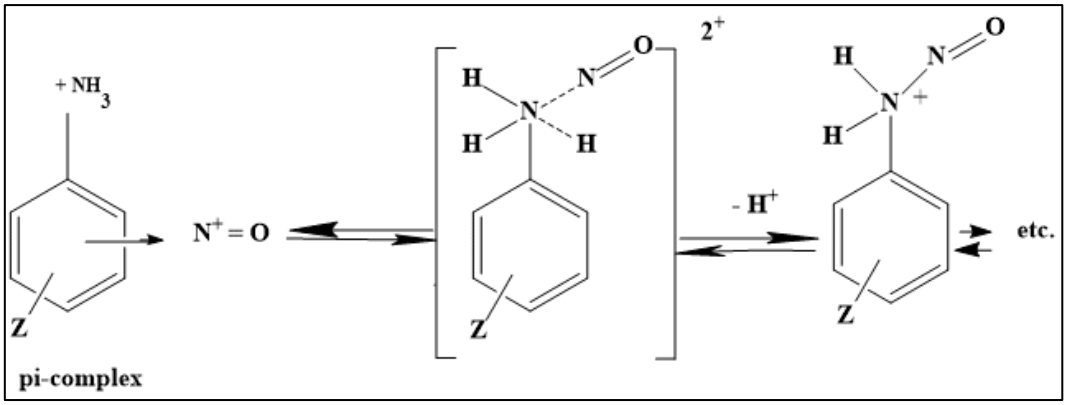

Figure 2.17: The diazotization mechanism (Christie, 2014)

Stage II (Azo coupling)

This rather unstable diazonium salt is then generated and reacts with amine containing an aromatic ring, phenol, or derivative of an α-keto acid to synthesize the azo color (**Figure 2.18**).

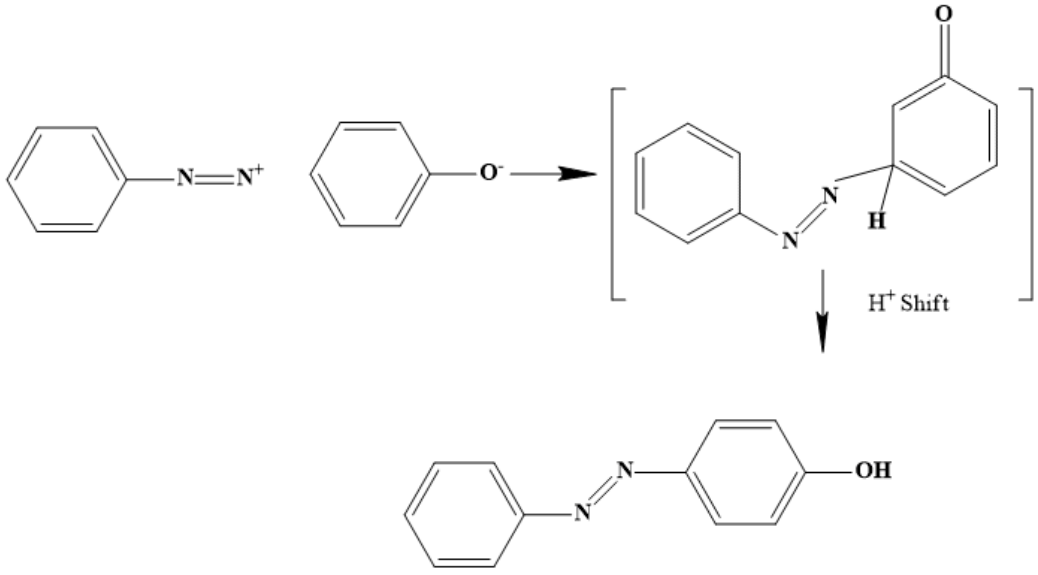

Figure 2.18: Azo coupling reaction between phenol and benzoenediazonium chloride (Christie, 2014)

Azo dyes constitute a major class of commonly used colorants due to their manufactured in enormous numbers (around 80% globally) and have the greatest color variety (Cheng et al., 2021). Worldwide, more than 3000 distinct azo dye combinations are created for commercial

use (V. Selvaraj, Karthika, Mansiya, & Alagar, 2021) and it is illustrated in the classification in **Figure 2.19** (Ajmal et al., 2016). **Figure 2.20** shows different categories of azo dye.

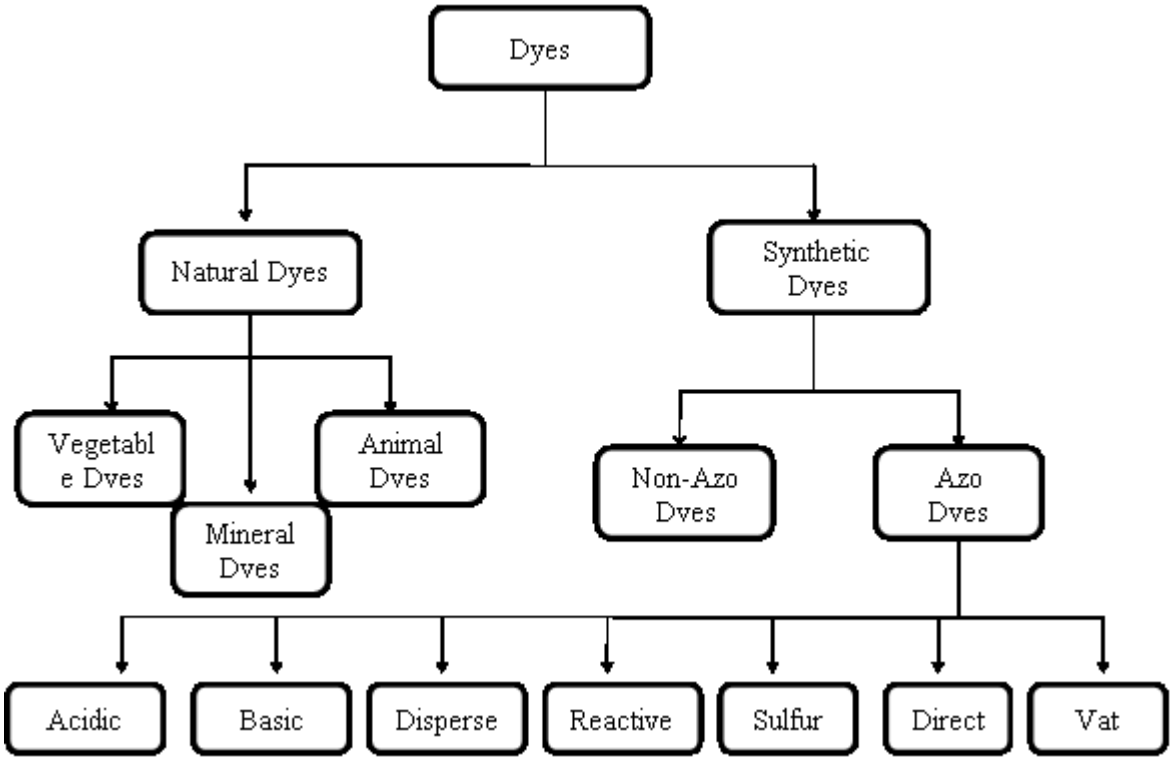

Figure 2.19: Dye products utilized in the textile sector (Ajmal et al., 2016)

Dye molecules with light-absorbing properties contain azo groups, which can be substituted with carboxyl, nitro, amino, hydroxyl, and chloro groups (J.-S. Chang, Kuo, Chao, Ho, & Lin, 2000). Azo dyes are frequently used because they are easier and less expensive to make than natural dyes, and they are available in a wider range of colors. They are also known for their intense coloration, stability, structural plasticity, extended shelf life, and resistance to light and moisture (Bera & Tank, 2021; Brüschweiler & Merlot, 2017; Chung, 2016). Examples of azo colors include Basic Yellow 40, Methyl Orange, Disperse Red 1, and Congo Red.

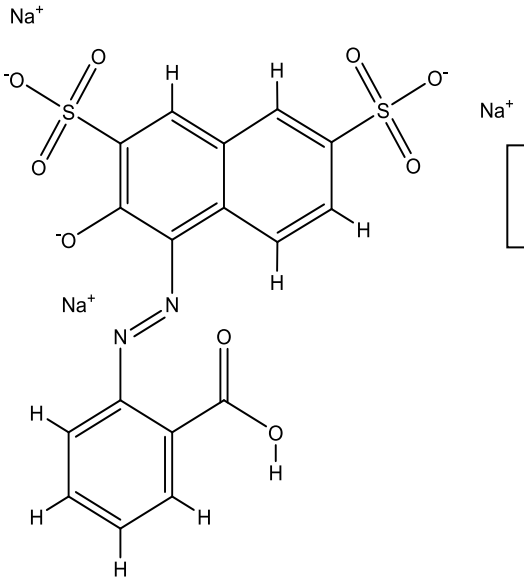

Mono-azo
(Acid Red B)

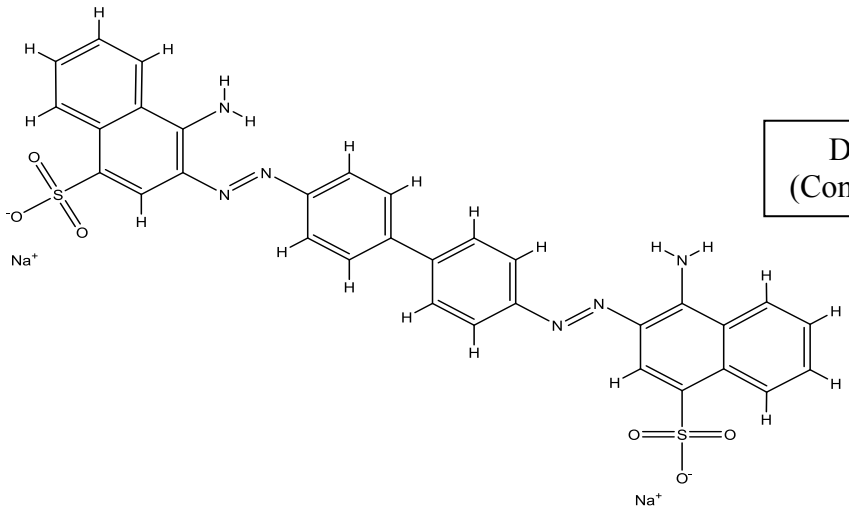

Di-azo
(Congo Red)

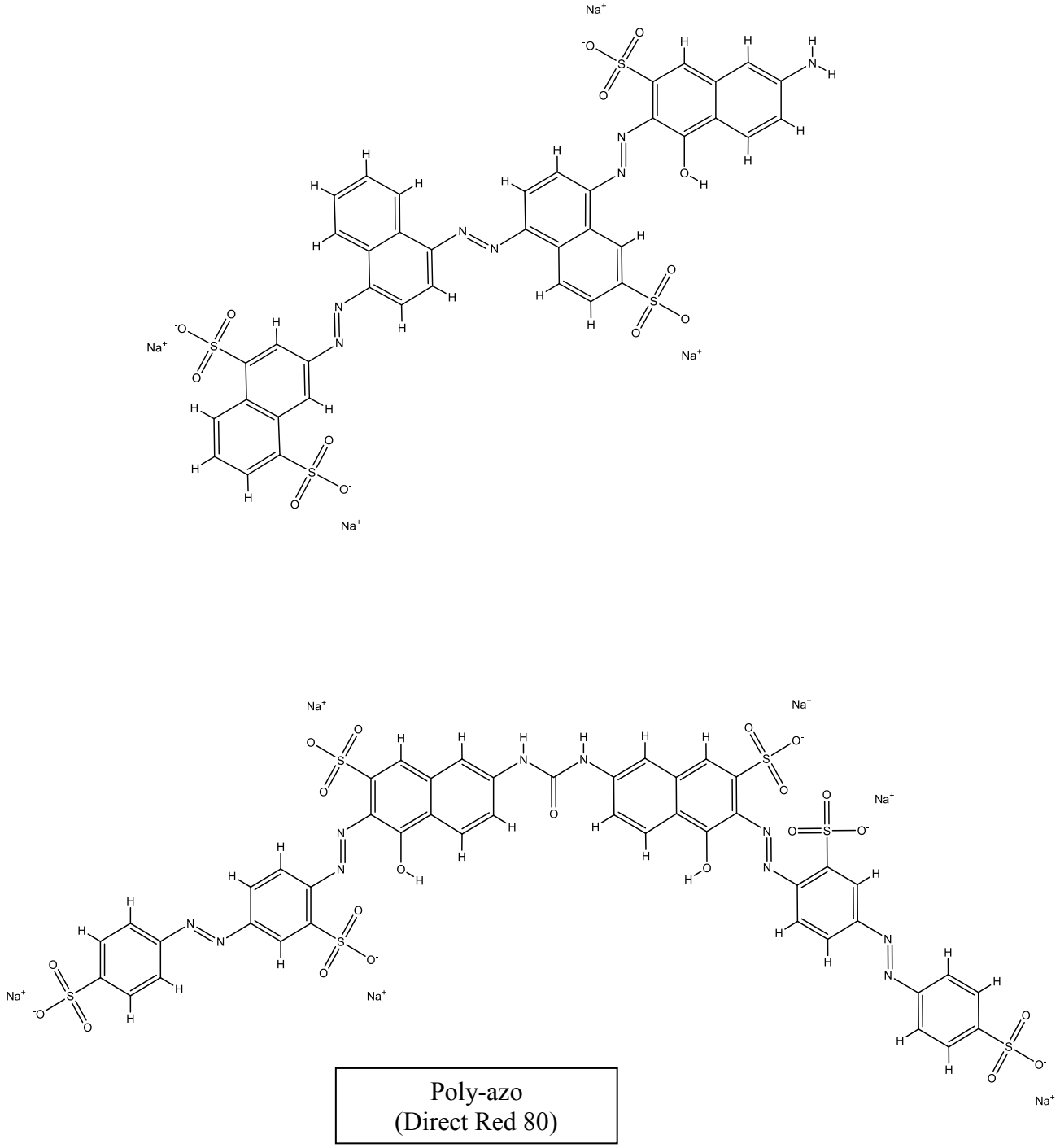

Figure 2.20: Categorization of azo dyes in accordance with different azo group numbers (N. Ali et al., 2020; Feng, Yan, & Zhang, 2009; SILVA, SILVA, & Takashima, 2015; Zarei et al., 2017)

RR120 is a synthetic diazo dye widely employed in the textile sector for dyeing cotton and cellulosic fibers. RR120 is characterized by two azo (–N=N–) linkages, many sulfonate ($–SO_3^-$) groups, and a high molecular weight aromatic structure, all of which enhance its water solubility and fiber affinity. The existence of many aromatic rings augments molecular stability, whereas sulfonate groups confer a negative charge, hence enhancing resistance to microbial absorption and enzymatic degradation. Moreover, the azo linkages function as electron-deficient sites necessitating reductive cleavage, usually facilitated by azoreductase enzymes in low-oxygen environments. Owing to its intricate structure, RR120 is deemed highly refractory and persistent in aquatic ecosystems, and its partial degradation may produce aromatic amines with potential toxicity. The structural attributes of RR120 render it a formidable target for wastewater treatment, hence validating its selection as a model dye for assessing resilient biodegradation and process engineering methodologies (Anastopoulos et al., 2024). **Figure 2.21** shows a structure of RR120 dye.

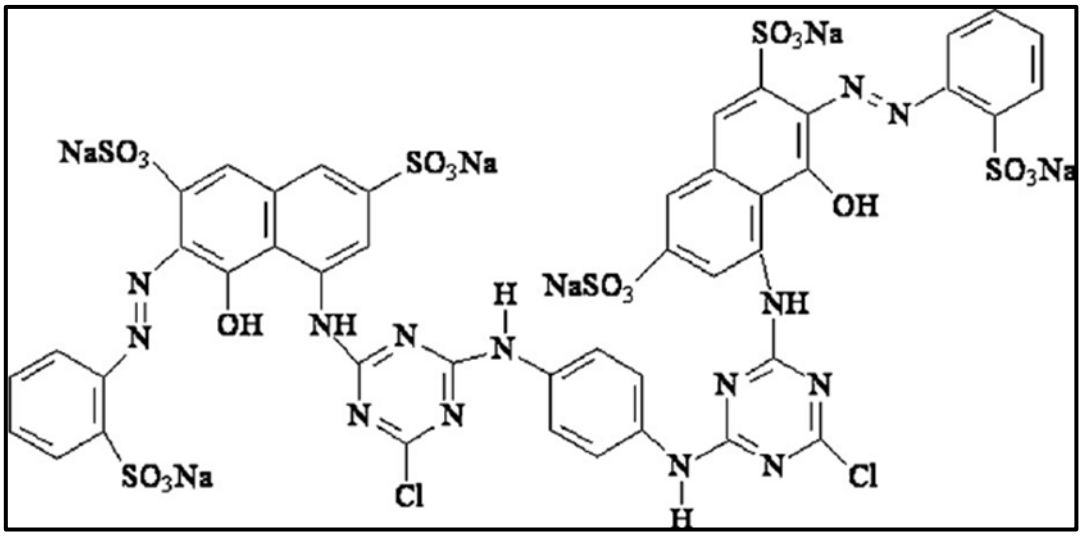

Figure 2.21: Structure of RR120 dye

2.7. Ecotoxicity of Azo Dyes

The textile sector significantly contributes to environmental contamination by releasing large volumes of colored wastewater into nearby lakes and rivers without sufficient treatment for effluent. Since such azo dyes are xenobiotic and have a wayward nature, their high pH and abundance of hazardous metals and chemicals have a prolonged influence on life (V. Selvaraj et al., 2021). According to their molecular configuration, the detrimental effects of the aromatic amines generated during reduction are visible in relation to the original substance.

Recent studies have investigated the genetic toxicity of various azo dyes (Hassan & Carr, 2018; Shindhal et al., 2021). Many investigations on the synthesis and breakdown of metabolites have been conducted in an effort to identify the most effective strategies for reducing these substances' harmful effects on living things. Despite the possibility that they all share a chemical structure and belong to related groups, each color has quite different biological and toxicological properties (A. Chen, Yang, Zhou, Sun, & Ding, 2018). Paper, ink, and textiles are made with Basic Red 9 dye, which poses environmental hazards and has the capacity to induce cancer in humans (Foguel et al., 2015). Disperse Red 1, a widely used dye with carcinogenic qualities, is used in dyeing (F. M. D. Chequer et al., 2009). Nucleic acids (RNA and DNA) are easily embedded by the Azure-B dye. In humans, crystal violet dye causes skin irritation, affects the digestive tract, and leads to chemical cystitis, along with renal and respiratory malfunctions (S. Mani & Bharagava, 2016). **Table 2.1** offers important details about the hazardous consequences of using azo dyes.

Table 2.1: Impact of azo dyes on nature and mankind

Sr. No.	Azo dyes	Hazardous Effects	Reference
1	Tartrazine	Mitochondrial dysfunction, developmental neurotoxicity, renal failure, hepatotoxicity, and altered exploratory behavior in zebrafish embryos/larvae	(Haridevamuthu et al., 2024)
2	Cationic blue SD-GSL	Inhibits superoxide dismutase activity, cell division, and Chlorophyll-a (Chl-a) synthesis in Chlorella vulgaris algae	(Jie Liang, Zhang, & Zhu, 2024)
3	Trypan blue	Hepatotoxicity and nephrotoxicity in freshwater fish Cirrhinus mrigala	(Hussain et al., 2022)
4	Disperse Red 1	Cause damage to DNA	(Lellis *et al*., 2019)
5	Sunset yellow	Lead to behavioral impairment by oxidative stress, chromosomal abnormality, and prefrontal cortex injury.	(Kamali et al., 2023)
6	Congo red	Carcinogenic, mutagenic, Cytotoxic (genotoxic, hemotoxic, and neurotoxic) effects on human	(Siddiqui et al., 2023)

7	Acid blue 113	Neurobehavioral alterations and developmental toxicity in zebrafish larvae and embryos	(Tippabathani, Nellore, Kathirkannan, & Nachiyar, 2022)
8	Direct Blue 297	Influence the proliferation of mouse blood cells	(T. Islam, Repon, Islam, Sarwar, & Rahman, 2023)
9	Sudan IV	Genotoxicity, cytotoxicity effects in mice	(Eteng et al., 2022)
10	Basic red 51	Genotoxicity, cell cycle arrest and carcinogenicity in zebrafish embryos	(Abe, Soares, de Oliveira, & Gravato, 2018)
11	Methyl red	Highly toxic and mutagenic by nature	(Kataria, Rawat, Tomar, Gaurav, & Kumar, 2022)
14	Reactive Black 5	Lowers the rate of the ammonification process and urease activity in the atmosphere of Earth	(Wielewski, Zuccolotto, Soares, Prola, & Liz, 2020)
15	Reactive Orange 16	Mutagenic consequences	(T. Islam et al., 2023)

2.7.1. Impacts of azo dyes on aquatic environments

The need for drinkable water is significantly increasing (G. Chen et al., 2021; Y.-G. Chen et al., 2021; V. Gupta, Garg, Capalash, Gupta, & Sharma, 2015). Toxin deposition in terrestrial and aquatic ecosystems has severely damaged environments due to damage caused by humans, and it will permanently contaminate nature and significantly lower water quality (Soni, Keswani, Bhatt, Kumar, & Singh, 2021). Large amounts of organic pollutant-containing effluents such as azo dyes are disposed of by the textile sector. In comparison to untreated wastewater, the breakdown of azo dyes, whether before to or subsequent to disposal, results in treated waste water containing amino acid derivatives potentially exhibiting greater toxicity than their precursors (Khalaj, Kamali, Khodaparast, & Jahanshahi, 2018; Mudhoo, Ramasamy, Bhatnagar, Usman, & Sillanpää, 2020). Textile dye effluent discharge into water bodies adversely affects aquatic vegetation. More clearly, the inherent issue with dye is the way sunlight is reflected and absorbed by water. It obstructs the entry of

light inside the euphotic region of lakes and oceans (Jieying Liang et al., 2017). Significant ecological consequences arise, leading to disruptions in aquatic biodiversity and suppression of photosynthesis in aquatic plants (M. D. Khan, Abdulateif, Ismail, Sabir, & Khan, 2015). In addition, human dermatitis, allergies, mutations, and skin irritations may result from exposure to these toxic effluents. These conditions can produce an array of significant issues, such as declining the quality of water (color and odor) and making the water dangerous (Sarvajith, Reddy, & Nancharaiah, 2018). A greater quantity of textile colorants in water reduces oxygen supply, obstructs sunlight, harms aquatic vegetation, and disrupts animal biological processes (Ghaedi et al., 2015). Wastewater with elevated levels of textile pigments and dyes exhibits significant concentrations of suspended solids, chemical oxygen demand (COD), total organic carbon (TOC), biological oxygen demand (BOD), and a fluctuating pH. These suspended particles hinder the exchange of gases by impeding water circulation across the fish's gills, perhaps resulting in mortality or stunted growth (Berradi et al., 2019). Reactive dyes, while enhancing the synthesis of erythrocytic small nuclei in juvenile fish as time progresses and dose-dependent manner, subsequently expedite the formation of gill micronuclei; they remain genotoxic to mature fish (K. Sharma, Sharma, Dhiman, Chadha, & Saini, 2022; Zheng et al., 2021). Hypoxia adversely affects their immunity and physiological reactions, rendering them more susceptible to many illnesses. Consequently, eating contaminated fish harms human health (Zheng et al., 2021). The cytotoxic effect on red blood cells was demonstrated to be greatly reduced by treatment, evidenced by a reduction in the frequency and intensity of poikilocytosis, a disorder marked by irregularly shaped red blood cells. Further investigating the toxicity and histology of industrial textile dye wastewater on *Poecilia reticulata*, Selvaraj et al. took up this investigation (D. Selvaraj, Leena, & Kamal, 2015). The investigation revealed several histological changes, including significant haemocyte infiltration within the inner lumen, displacement of the auxiliary branchial bar, injury to the intestinal villi, and proliferation of the main gill bar. Microalgae are vital to aquatic habitats because they are primary producers that are advantageous to the economy and the ecology. On the other hand, dye contamination in aquatic environments disrupts nutrient and energy transfer within food webs as well as microalgae development. The substantial amount of textile dye released into seas, lakes, rivers, and other aquatic habitats influence numerous parameters related to algal proliferation, including proteins, pigments, and additional nutrients. In toxicological investigations, algae are an excellent indicator of pollutants due to their greater susceptibility to contaminants than other species of aquatic life (J. Sharma, Sharma, & Soni, 2021). Cyanobacteria are especially prone to pollutants. Their

growth as well as the quantity of protein, minerals, pigments, and other nutrients they contain, are all significantly influenced by azo dyes (S. K. Ali & Saleh, 2012). The phytotoxicity of textile dyes is assessed using aquatic macrophytes as a natural ecological marker. Strong growth in a plant is determined by several measures, including number of fronds, dry weight, chlorophyll content and total frond area (Colin et al., 2016; H. Singh et al., 2021). Textile dye contamination is causing a complete transformation of the macrophyte's characteristics. Dye has been shown to significantly alter growth rate and impede the expansion of aquatic plants in multiple studies (Adomas, Sikorski, Bęś, & Warmiński, 2020; Hocini, Benabbas, Khellaf, Djelal, & Amrane, 2019; Lobiuc et al., 2018; Rápó et al., 2020; H. Singh et al., 2021). Lemna minor serves as a key food source within aquatic food webs. In order to determine how the colors Gentian Violet and Congo Red affected the quantity of naturally occurring amines that *L. minor* produced, a study was conducted. It is clear that these dyes hindered the development of *L. Minor*, chlorophyll biosynthesis and biomass production. Moreover, Gentian Violet exhibited greater lethality than Congo Red due to its interference with the biosynthetic pathway of biogenic amines. The findings demonstrate the extreme sensitivity of decarboxylase activity and biological amine concentrations (Adomas et al., 2020). The reactivity, toxicity, and functional moiety of azo dyes determine how they affect cyanobacteria, which can vary greatly. To evaluate the impacts of phytoplankton exposed to synthetic azo dye discharge from textiles, De Sousa et al. 2012 used columns of Winogradsky containing a microecosystem composed of water, soil (collected from the riverbed), and necessary nutrients (de Sousa et al., 2012). Moreover, research findings demonstrate that the Remazol Red Brilliant dye interferes with photosynthesis and causes ecological imbalances within the food chain. High amounts of azo dyes released by industrial effluents consequently have a detrimental effect on phytoplankton and various microorganisms in aquatic ecosystems (Alzain, Kalimugogo, Hussein, & Karkadan, 2023).

2.7.2. Environmental influence of released textile azo dyes on terrestrial ecosystems

Textile azo dyes or their effluents disturb the microbial flora in the soil and change its chemistry. These organic contaminants negatively impact plant germination and flowering processes. The development and health of a plant are primarily determined by the proportion of seeds that grow upon contact with textile dyes, as well as by growth performance and survival rate of seedlings (Arshad, Imran, & Ashraf, 2020). Moreover, the generation of dry matter is demonstrated by the sturdy, green stems of sprouting vegetation, which show a high

amount of chlorophyll and an intense process of photosynthesis. The coloration of industrial wastewater adversely impacts plant growth (Zou, Ning, Wang, & Zhou, 2019). Higher amount of color in polluted water also alters the seed's osmotic potential and decreases the quantity of aqueous oxygen present in saplings, or more accurately, seedlings, require (Hassan & Carr, 2018). Consequently, lower levels of chlorophyll impact photosynthetic activity, hinder plant development, and minimize the buildup of dry vegetation (A. Sharma et al., 2020). Research indicates that elevated abscisic acid levels lead to the degradation of chlorophyll and inhibit plants from growing by preventing the production of fresh chlorophyll (X. Zhu, Chen, Qiu, & Kuai, 2017). Furthermore, exposure to textile dye effluents may cause plants to collect more proline, a sign that the dyes are stressing them out (Ebency, Rajan, Murugesan, Rajesh, & Elayarajah, 2013). The deleterious genetic impacts on *Allium cepa* seedlings in presence of industrial discharge loaded with azo dyes are responsible for micronucleus and chromosome abnormalities. *A. cepa* meristematic cells demonstrate chromosomal abnormalities, micronuclei formation, and cell mortality when subjected to minimal dosages of the commercial black dye (Ventura-Camargo, Maltempi, & Marin-Morales, 2011). Wang and Keturi assert that the detrimental effects of toxic substances and azo dyes on polluted water storage reservoirs may be assessed rapidly, easily, consistently, and reliably through root-to-shoot ratios and seed germination percentage (L. Chang, Meier, & Smith, 1997; W. Wang & Keturi, 1990). Toxicity of plants bioassays can assess the synthetic azo dye toxicity and monitor environmental contamination (A. K. Gupta & Sinha, 2006). Textile wastewater contaminated with colors can enhance the synthesis of ethylene in plants. A toxicological study using Reactive Red HE3B (RR120) revealed oxidative stress and an elevated─frequency of chromosomal abnormalities containing micronuclei within root cells of certain plants. The dye itself initiated a considerably greater rate of damage to DNA, rather than the damage being mediated by its metabolites (X.-R. Xu & Li, 2010). The mechanisms of color and mineral absorption and deposition through crops and various other plants are influenced by a number of elements such as metallic constituents of the soil, and the dye's concentration in water (A. K. Gupta & Sinha, 2006). At different doses of azo dye, Oguntade and his colleagues examined the dry biomass, absorption of heavy metals and percentage growth of a potted plant called *Amaranthus cruentus L.* (Oguntade, Adetunji, Salako, Arowolo, & Azeez, 2018). The development and yield rates of Amaranthus were inhibited by an overabundance of azo dye solution; however, at lower azo-dye concentrations, the nutritional components had a favorable influence affecting plant development and yield. Additionally, Savin et al. 2008 discovered the hazardous properties of

these dyes have the ability to eradicate soil microbes, which would have a detrimental effect on agricultural productivity (Savin & Butnaru, 2008). Therefore, pretreatment and detoxification are consequently required when using wastewater, or industrial effluent, as the source of water for crop and vegetable cultivation.

2.7.3. Influence of textile azo dye exposure on humans and other organisms

Textile azo dyes exhibit significant toxicity and have been associated to numerous diseases including cancer in humans as well as animals (Jin et al., 2021; Tounsadi, Metarfi, Taleb, El Rhazi, & Rais, 2020). These dyes for textiles are linked to several diseases, such as central nervous system disorders and dermatitis. Specifically when exposed to dust, textile colors can irritate the dermis and ocular region upon ingestion or inhalation (Clark, 2011). Azo dyes possess capability to contaminate water bodies and infect fish and other aquatic organisms. Human consumption of these can result in long-term side effects such hypertension, random problems, and cramps. Furthermore, it was asserted that azo dyes derived from benzidine are linked to cancer formation in both human bladders and experimental animals (Sen, Raut, Bandyopadhyay, & Raut, 2016). Azo dyes are potentially carcinogenic, mutagenesis, and genotoxicity in both humans as well as other animals (Chung & Cerniglia, 1992). Liver azoreductase, intestine microbiota, and human skin microbiota can all decrease an azo dye. The carcinogenic characteristics of fragmented aromatic amines, such as benzidine, have been linked to a number of human malignancies. In regions characterized by advanced industrialization, a notable correlation exists between the widespread application of azo dyes as well as the elevated incidence of intestinal cancer. Many other human diseases have also been reported in addition to this (Chung, 2016). The textile dyes Disperse Red 1, Reactive Green 19 and Reactive Blue 2 pose a potential risk of prolonged genotoxic consequences for human well-being. Reactive Green 19 demonstrated genotoxicity in a dosage-dependent way, on the contrary, Reactive Blue 2 and Disperse Red 1 did not exhibit such effects (Leme et al., 2015). Research has shown intestinal microbes can enzymatically convert Sudan I, a lipid-soluble azo dye utilized in the textile and food sectors, into particular aromatic amines linked to cancer. The dye has the capacity to cause cancer, as do its metabolic by-products (Piątkowska, Jedziniak, Olejnik, Żmudzki, & Posyniak, 2018). Additionally, studies revealed cellular (HepG2) contamination caused by Disperse Red 1 dye may induce hepatoma and mutagenesis in human lymphocytes (Will, McDuffie, Olaharski, & Jeffy, 2016). Other ways that this harms DNA include frameshift mutations and base-pair replacement (F. M. D. Chequer et al., 2009). Disperse Orange 1 color shows cell-toxic properties that cause HepG2

cells to undergo apoptosis when it comes into contact with them (Ferraz, Grando, & Oliveira, 2011). A carcinogenic aromatic amine is formed as a result of Direct Blue 14 degradation when it comes into contact with bacterial species that are common on human epidermis; however, additional dyes, including Disperse Yellow 7, have been shown to break down in natural rivers and release carcinogenic amines (Balakrishnan et al., 2016). The spiral formations of double-stranded RNA and DNA are intercalated by the cationic dye Azure B (Haq & Raj, 2018). Additionally, the investigation assessed whether Azure B could block enzymes like glutathione reductase, essential for preserving the cell's redox homeostasis (Couto, Wood, & Barber, 2016). Animal studies have also documented the toxicological impacts of azo dyes. In rat bone marrow cells and spermatozoid cells, for example, the mitotic index and chromosome abnormalities show the cell-toxic and DNA-damaging effects of para dimethyl amino benzene (p-DAB). When rats are administered with p-DAB, their germ cells exhibit numerous chromosomal errors and nuclear abnormalities. Researchers have shown that the textile dyes induce clastogenicity, which is a process that causes human cells to produce micronuclei. Additionally, it has been discovered that the Disperse Blue 291 causes micronuclei to form, DNA fragmentation, and a rise in the rate of mammalian HepG2 cell apoptosis. Sudan azo dye has been demonstrated to have mutagenic and genotoxic effects on human bladders and those of other mammals. The specimen organisms also exhibit noted clastogenic and aneugenic properties of the azo dye (J. Han et al., 2020). Research has demonstrated that azo colors produce dysfunctional reproductive organs and teratogenic and cancerous consequences in rodents (Parrott, Bartlett, & Balakrishnan, 2016). These hydrophobic substances exert deadly impacts on the growth and survival of benthic species, including fish and mammals (Milani et al., 2018). **Figure 2.22** illustrates the influence of dye contamination on environmental conditions.

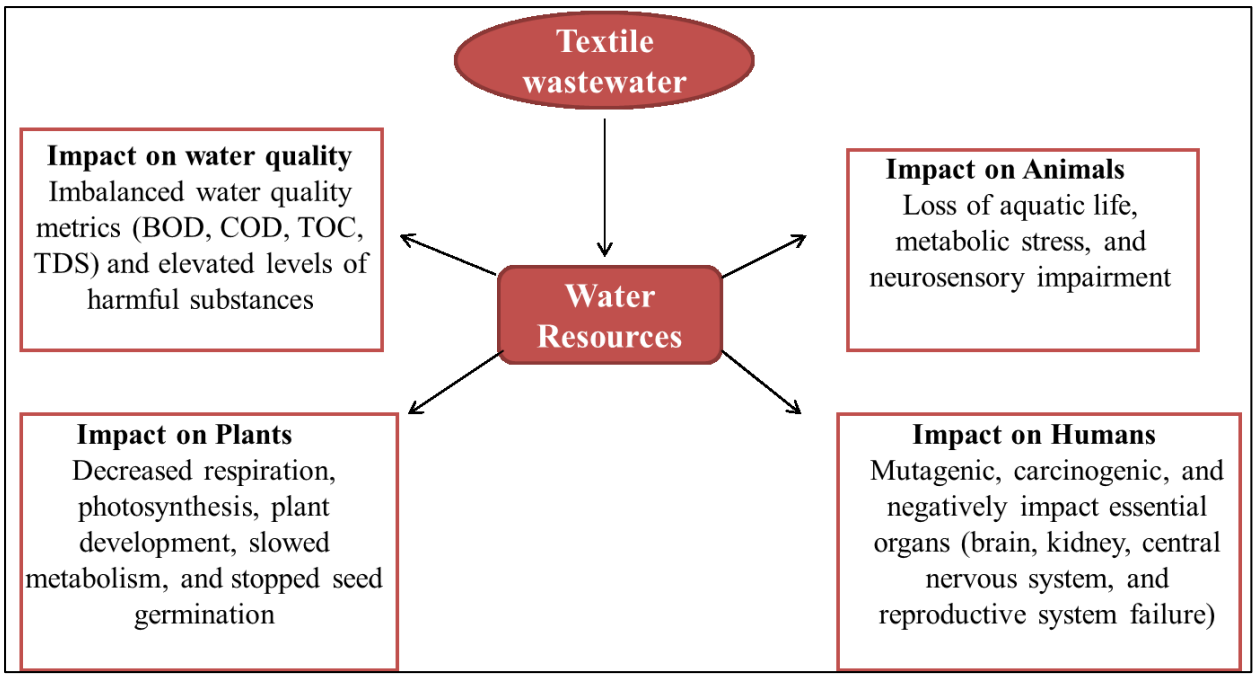

Figure 2.22: Impact of dye on the environmental conditions

2.8. Various approaches to treat wastewater including textile azo dyes

Currently, obtaining safe drinking water stands as one of the most significant worldwide issues because of restricted accessibility and human interference. Around 47% of the global population will lack access to drinkable water by the year 2030 (A. Islam et al., 2021). However, most moderate and less affluent nations lack the financial support to procure the expensive minerals required for water purification. The top exporters of all textile varieties are Europe, USA, China, India, and China, and these countries promote global economic expansion (Atkar, Pabba, Sekhar, & Sridhar, 2021; Darwesh, Ali, Matter, & Elsamahy, 2021). At present, there is no global legislative agreement regarding the handling of effluent notably those incorporating azo dyes. Wastewater management can employ an amalgam of physical, biological, and chemical approaches, contingent upon its characteristics. These are a few of the more widely used techniques.

Remediation method of Dyes

The usual amount of dye in effluent generated from textile sector varies between 0.6 to 0.8 gm L^{-1}; nevertheless, its strong durability in nature makes this compound difficult to degrade naturally and causes of environmental contamination (J. Jadhav, Parshetti, Kalme, & Govindwar, 2007). Consequently, it is essential to identify and design an efficient dye elimination methodology for treating such pollutant-laden waters. Textile waste water can be

addressed using several remediation methods. Various chemical and physical approaches have been applied for decolorizing textile–wastewater. Physico-chemical techniques have a lot of disadvantages. These procedures are labor-intensive, incapable of totally eliminating the dyes from their organic metabolites, and, last but not least, generate a significant volume of sludge, which may act as an auxiliary pollutant. Furthermore, because these procedures demand more energy and chemicals, they are not commercially feasible. In contrast to physicochemical methods, biological color removal and deterioration represents the most economical and ecologically sustainable method for mitigating water pollution (A. Singh et al., 2022).

2.8.1. Physical based treatment process

The physico-chemical techniques are widely used and well-established for eliminating dye from wastewater. This section will examine methods that are based on physicochemical process. Various physical techniques are employed to completely eliminate colored substances from effluent. The processes encompass membrane separation, coagulation-flocculation, adsorption, ion exchange, oxidation , and photo-degradation (Moghaddam, Moghaddam, & Arami, 2010; B. Shi, Li, Wang, Feng, & Tang, 2007). The adsorptive strategy is a commonly employed technique for eliminating various colors and pollutants. Since it is highly efficient, inexpensive, and simple to use, it is widely used (Al-Khaldi et al., 2015; Asmaly et al., 2016; Asmaly, Saleh, Laoui, Gupta, & Atieh, 2015). To eliminate dyes from wastewater, a broad spectrum of adsorbents is utilized, like activated carbon, bentonite clay, carbon tube nanostructures, wood, fly ash, ion exchangers, resin-based polymers, zeolites, metallicoxides, MXenes, metal-organic lattice structures, and various bio-based materials such as corn cobs, rice husks, wheat straw (Ihsanullah Ihsanullah, 2020; Arsalan Khalid, Zubair, & Ihsanullah, 2018; Vikrant et al., 2018). For the treatment of effluent, cost-effective nature, excellent restorative capability, and strong interaction of an adsorbent with the target molecules are desirable (A. J. Jadhav & Srivastava, 2013). One limitation of the adsorption process is that color molecules cannot be broken down by it. For the elimination of dyes from effluent containing dye, the coagulation method uses ferric chloride and ferrous sulphate (Huang et al., 2014). Furthermore, other research have shown the utilization of additional coagulants, including chitosan, magnesium chloride, poly-aluminum chloride, and aluminum chloride, in the treatment of textile effluent (Szyguła, Guibal, Ruiz, & Sastre, 2008). However, this technique is limited in its ability to apply dye decolorization due to its high cost, significant sludge output, and low dye removal effectiveness (Vikrant et al., 2018;

Yeap, Teng, Poh, Morad, & Lee, 2014). Furthermore, the efficacy of this physical methodology for eliminating dyes from wastewater contaminated with dyes varies according to the chemical nature of the dyes (Vandevivere, Bianchi, & Verstraete, 1998). Membrane filtration techniques employ membranes to eliminate dissolved dyes and decrease the color, BOD and COD values in effluent. The filter's type and porosity have been selected according to the chemical makeup of the effluent and a specific operating temperature (Dos Santos, Cervantes, & Van Lier, 2004). Membrane-based dye removal from wastewater offers some advantages, including minimal maintenance, a small environmental imprint, and simple operation and installation (Robinson, McMullan, Marchant, & Nigam, 2001; Rondon et al., 2015). However, it presents several limitations to employing this method for treating wastewater, including the formation of concentrated residue, high expense, difficulties treating huge volumes of dyes, and membrane clogging (Dos Santos et al., 2004). Resins used for ion exchange efficiently remove colors from wastewater and reduce its COD (Karcher, Kornmüller, & Jekel, 2002). This approach is ineffective for removing a broad spectrum of dyes. The benefits of this approach include fast solvent recovery, active elimination of soluble dye, and no loss of adsorbent during redevelopment. However, there are specific drawbacks, including elevated operational costs, the necessity for expensive chemical solvents, as well as limited color dispersion (G. Mishra & Tripathy, 1993).

2.8.2. Chemical based treatment process

Oxidation processes such as advanced oxidation processes (AOP), chemical treatment, ultraviolet irradiation, and photochemical methods are commonly employed chemical approaches to achieve complete color elimination from textile effluents (Kalyani, Telke, Dhanve, & Jadhav, 2009). Because it is easy and simple to apply, oxidation serves as a popular method to eliminate color from wastewater generated by various textile industries. Degradation of double-bonded dyes can be accomplished by oxidation techniques that involve chemical treatment. AOP methods, on the other hand, produce more hydroxyl radicals than typical chemical processes, making them superior. In case of AOP, iron salts (Fenton reagents) are used to remove complex organic contaminants, and UV-Vis radiation is used for semiconductor catalyst (photocatalysis degradation) (Mukherjee et al., 2023). These techniques are not appropriate for dispersing colors and have a number of disadvantages, such as producing a lot of sludge and emitting aromatic amines (Slokar & Le Marechal, 1998). Ozone finds extensive use as an oxidizer in order to purify drinkable water, eliminate many pollutants from wastewater, and quickly break down a variety of organic wastes (J.

Wang & Chen, 2020). Ozonation offers multiple significant advantages, such as diminished sludge generation, minimal rise in wastewater amount, and the creation of colorless, non-toxic waste water with low COD values post-treatment (Miralles-Cuevas et al., 2017). Conversely, the main drawbacks of the ozonation process include the harmful by-products generation and high operating costs. As the temperature rises, ozone becomes less soluble, pH, temperature, and salt concentration play critical roles in determining stability (Shabir et al., 2022). Photocatalytic treatment is currently the most extensively used and effective method in the area of environmental remediation. For instance, biochar-TiO_2 was employed by Fazal et al. (2020) to effectively degrade wastewater, with a photodegradation efficiency of almost 99.20% (Fazal et al., 2020). Different contaminants can be removed from wastewater using a straightforward process called sonocatalysis. Many contaminants, including dyes, can be broken down sonocatalytically by a combination of high pressure, high temperature, and radicals (Solayman et al., 2023). The merits and demerits of chemical and physical methods for eliminating dye from effluent from the **Table 2.2** presents data related to the textile sector.

Table 2.2: Benefits and drawbacks of chemicals and physical dye elimination techniques

(Al-Tohamy et al., 2022; Behera, Nayak, Banerjee, Chakrabortty, & Tripathy, 2021; Collivignarelli, Abbà, Miino, & Damiani, 2019; Soumi Dutta, Gupta, Srivastava, & Gupta, 2021; A. C. Jadhav & Jadhav, 2021; Mcyotto et al., 2021; Titchou et al., 2021; Yaseen & Scholz, 2019)

Different Approaches	Methods	Advantages	Disadvantages
Physical	Adsorption	• Low initial investment • Regenerative adsorbent • Flexible and easy to use • Used to eliminate many kinds of organic compounds • Exhibits a high flow rate effectively • Eliminates an extensive range of dyes	• The process is not self-monitored • The adsorbents are costly • This method only moves the removed contaminants from one phase to another • Long contact times are needed to achieve acceptable removal rates • The adsorbents quickly exhaust; and the method is non-destructive.
	Coagulation and flocculation	• Convenient to manage Rapid and effective for dye elimination • Large scale • Cost-effective • Completely eliminated upon removal of dye	• Uses hazardous substances • Creates concentrated sludge • pH-dependent

	Membrane filtration	• Greater permeability • Employed to get rid of all organic substances • Reasonable temperature resilience • Excellent resistance to adverse chemical conditions • No change in phase	• Expensive management • Regular replacement is necessary • Membrane fouling • High energy consumption • Decreases water penetration • Transfers pollutants from one phase to the next • Costly disposal
	Ion-exchange	• Minimal expense • Exceptional efficiency • No adsorbent loss	• Not appropriate for all dye types • pH-dependent
Chemical	Chemical oxidation	• Common chemical color removal method • Simple to use • Quick reaction time • Increases azo-bond cleavage • Completely removes dyes • No sludge generation	• High cost • Dependent on pH • Activation of hydrogen peroxide is arduous • Necessitates a catalyst for effective dye elimination
	Photolysis	• Not requiring extra catalysts or oxidizing agents • Economically feasible	• The medium may become more turbid due to photosensitizer action, which will prevent UV light from entering.
	Electro-chemical destruction	• Does not require additional chemicals • Does not generate sludge • Remove both soluble and insoluble dyes with efficiency.	• High power costs • Ineffective when compared to alternative techniques

Chemical (Advanced oxidation process)	Ozonation	• Application in gaseous state • Double-bonded conjugated chemicals without volume change • Rapid color removal • Extremely unstable atomic structure • No volume iteration	• High energy expenses • 20-minute ozone half-life • Sensitivity to pH • By products produced • Need for costly equipment • Short response time • proficient maintenance required • Issues related to sludge discharge, on-site generation
	Fenton reagents	• More advanced, efficient, and useful • Ability to break down and change the color of certain pollutants	• Low catalytic influence • Unsuitable and ineffectual in alkaline conditions (wastewaters are normally alkaline) • Less effective for copper phthalocyanine dye • High operating costs • Needs special disposal and additional investment • Challenging handle and transport • Functions in a limited pH range • Challenging in catalyst regeneration increased production of iron sludge
	Sono-catalytic process	• Potent with non-biodegradable materials • Successful with harmful or toxic chemical particles • Take less time • Do not produce chemicals to get rid of hazardous materials.	• Costly process • Requires a substantial quantity of dissolved oxygen (DO) • Ineffective at eliminating color • Hazardous to the environment.

	Photocatalytic treatment	• Ideal for long-lasting parts • Time-efficient • Uses minimal chemicals • Durable and efficacious in lowering COD levels.	• Secondary product generation • Poor performance in the presence of light • Catalyst misuse • High cost • Challenging in catalyst separation • Inadequate ability to transport the electrons and holes created by photocatalysis

2.8.3. Bio-mediated environmental restoration process

Bioremediation is a superior substitute to chemical and physical cleanup methods. Toxic organic wastes are transformed biologically into safe, non-toxic substances when using a biological treatment approach (LYNCH & MOFFAT, 2005). The biological agents with the highest possibility of cleansing dye wastewater are bacteria, yeast, algae, and fungi. These bacteria can improve decolorization, removal, and mineralization efficacy while reducing BOD, COD, TSS, turbidity, and TDS levels in wastewater contaminants (Kapoor et al., 2021). Microorganisms possess the capacity for adaptation to harmful substances, resulting in the rise of resistant strains that inhabit the environment and decompose pollutants through enzymes, or biocatalysts, which primarily facilitate metabolic processes (R. G. Saratale, Saratale, Chang, & Govindwar, 2011). The foremost advantage of biological treatment for dye-laden wastewater is the utilization of microorganisms with significant biodegradation capabilities, whether individually or in consortium (W. Liu et al., 2018). Degradation and adsorption constitute the two primary methods to treat textile wastewater with the aim of eliminating dyes (Popli & Patel, 2015). Both aerobic and anaerobic conditions may be utilized for these procedures. A varied assortment of charged compounds found in microbial cell walls, comprising amino, hydroxyl, carboxyl, phosphate, and various other ionic groups, is accountable for producing attraction forces in the treatment of effluent (Jafari, Soudi, & Kasra-Kermanshahi, 2014). Many enzymes derived from microorganisms demonstrated strong ability to degrade dyes effectively (AR Khataee, Dehghan, Ebadi, Zarei, & Pourhassan, 2010). According to literatures, ligninolytic peroxidase (Duran & Esposito, 2000), laccase (Hatvani & Mécs, 2001), tyrosinase (X. ZHANG & FLURKEY, 1997),

hexane-degrading oxidase (G. Saratale, Humnabadkar, & Govindwar, 2007), NADH-DCIP reductase (Bhosale, Saratale, & Govindwar, 2006), as well as aminopyrine-metabolizing demethylase enzyme (Salokhe & Govindwar, 1999) are the microbial enzymes that break down dyes. It has been documented that in the presence of the enzyme azoreductase, *Streptomyces* S27 and *E. gallinarum* are crucial to promote the breakdown of azo dyes (Dong et al., 2019). Laccase, an oxidative enzyme breaks down a lot of aromatic molecules (Bhatia et al., 2017). It has been investigated that *Brassica rapa* peroxidase's catalytic activity can degrade crystal ponceau 6R (Almaguer, Carpio, Alves, & Bassin, 2018). Since microbial proliferation is dependent on environmental conditions, it is essential to the biological remediation approach. The environment may be altered to promote microbial proliferation and optimize the efficacy of microorganisms in degrading contaminants, hence improving the bioremediation process (Shabir et al., 2022). Compared to physico-chemical methods, bioremediation offers multiple benefits for azo dye removal, including enhanced environmental sustainability, cost-effective, producing less sludge after treatment, fully mineralizing or producing non-toxic end products, having the ability to save energy, requiring fewer chemical reagents, being easier to implement, and requiring less water (Banat, Nigam, Singh, & Marchant, 1996; H. S. Rai et al., 2005). An essential part of the dye removal process is the functionality and resilience of specific microorganisms.

2.8.3.1. Azo dye contaminated wastewater treatment by Bacteria

Bacteria are extensively utilized in industrial effluent treatment because of their capacity to adapt in many environmental conditions, such as temperature, pH, and oxygen levels. Bacteria have been reported to decolorize faster in comparison to other microorganisms (Kalyani et al., 2009). Bacterial biodegradation or adsorption could trigger discoloration of the dye. Bacterial cells that absorb new colors experience deep coloring after adsorption, whereas those that shed their initial color experience biological degradation. In the instance of dye adsorption, colors may attach to bacterial surfaces through electrostatic, covalent interaction. Prior to further breakdown, it is usual for the dye to be attached to the bacterial surface during dye breakdown. Therefore, one of the most essential stages is adsorption. Peptidoglycan has reportedly been shown to be essential for the bacterial adsorption of colors. Moreover, surface functional groups participate significantly in bacterial-mediated adsorption process, with minimal dependence on chemical processes (H.-h. Li et al., 2019).

Under both monoculture and consortium conditions, bacteria have shown a strong capacity for mineralizing dyes (Jamee & Siddique, 2019; Karim, Dhar, & Hossain, 2018). Recent years have seen a substantial quantity of investigations regarding dye elimination from pure bacterial cultures utilizing *Pseudomonas* sp., *Bacillus* sp., *Sphingomonas* sp., *Rhodococcus*, *Proteus* and *Escherichia* (Elfarash, Mawad, Yousef, & Shoreit, 2017; N. Garg, Garg, & Mukherji, 2020) (Barathi, Karthik, Nadanasabapathi, & Padikasan, 2020; Wanyonyi, Onyari, Shiundu, & Mulaa, 2019) (L. Ali, Alhassani, Karuvantevida, Rauf, & Ashraf, 2014) (K.-Z. Xu et al., 2020) (Qi, Anke, Szymańska, & Tischler, 2017) (Mohanty & Kumar, 2020). In this area, mixed cultures are especially useful since certain microbial consortia can cooperate to carry out biodegradation operations (Jamee & Siddique, 2019; Mohanty & Kumar, 2020). A greater level of biodegradation and inorganic end-product formation is achieved in processing units that contain microbial mixtures owing to the synergistic metabolic functions within the microbial population. Regarding dye degradation, these systems demonstrate significant advantages compared to pure cultures. A single strain in a mixed microbial culture can either exploit the metabolites produced by coexisting microorganisms to further break down the dye molecule into aromatic amines or cause the dye molecule to break down at specified places. When microbial consortia are present and complementing biological agents facilitate the decomposition of aromatic amines, the process's efficiency and efficacy are improved (Sghaier et al., 2019). Microbes residing in unsafe conditions exhibit increased adaptability, transforming more hazardous chemicals into less harmful substances (Rathod & Archana, 2013). Various bacterial species can remove dyes in anaerobic, aerobic, and integrated anaerobic-aerobic systems (Guo et al., 2019a; Y. Zhu, Wang, Ni, & Hu, 2020).

2.8.3.1.1. Anaerobic Biodegradation

Under anaerobic circumstances, a number of microorganisms break down the dye molecule's highly electrophilic azo link by a non-specific enzymatic action. The anaerobic bacteria's nonspecific enzymatic activity allows facilitating the breakdown of azo dyes in textile wastewater, rendering this procedure better aligned for industrial applications. This approach offers the following advantages: (1) In the existence of small redox-active molecules, reactions take place at a pH of neutral and exhibit a high degree of nonspecificity. (2) Anaerobic bacteria, essential and optional, can be used to reduce azo dye and readily achieve oxygen depletion in static culture. (3) Improvement of azo dye reduction rates by extra carbon sources that wastewater systems often provide (Shah, 2019). Azo reductase enzymes utilize the redox mediator facilitating electron transport and adhere to the cell membrane in

an anaerobic environment. In contrast to cytoplasmic azoreductase, membrane azoreductase mediators have a different binding mechanism. Due to the oxygen sensitivity of azoreductase, the disintegration of azo dye compounds is best accomplished in oxygen-free conditions. The different dye forms and carbon source used have an impact on the rate of decolorization. The dye may become a terminal electron recipient in the electron transport chain as a result of anaerobic decolorization (P. Mani et al., 2019; Srivatsav, Devi, Reddy, & Venkant, 2019; Zahran, Ali-Tammam, Hashem, Aziz, & Ali, 2019).

2.8.3.1.2. Aerobic Biodegradation

In oxidative reactions, azo molecules are more sensitive due to the electron-withdrawing property of azo interactions. It has been demonstrated that colorant amounts can be lowered in aerobic treatment plants through non-enzymatic adsorption onto the sludge biomass. It is therefore impossible to discolor liquid azo dyes or other comparable colorants substances with conventional aerobic systems for wastewater treatment. It has been shown that the peroxidase produced by the Streptomyces genus *Sphingomonas* decolorizes azo dyes. Further research revealed several limitations regarding the disintegration of azo dye by aerobic bacteria, such as the requirement for extra energy and carbon sources to exist at the site of azo dye application for these microbes to make the azo dye disappear. Since azo dyes are not suitable as a substrate, it is necessary to generate energy from an organic carbon supplier. The elevated expense of the carbon substrate makes this economically unfeasible (Chittal, Gracias, Anu, Saha, & Rao, 2019; Shah, 2019).

2.8.3.1.3. Integrated anaerobic-aerobic systems

The integration of aerobic treatment with the hypoxic breakdown of azo dyes is anticipated to result in the complete mineralization of aromatic amines generated during the anaerobic process. This is a result of sulfonated amino aromatics and aromatic amines undergo total mineralization due to aerobic microorganisms. It can be done both concurrently and in a step-by-step manner. Aerobic and anaerobic phases can be integrated into a continuous system utilizing distinct vessels, or they can be mixed alternating in the same vessel as in previous operations. Anaerobic bacteria use azo dye reductive cleavage as the initial step in their biological breakdown of azo dyes. Few studies, therefore, recommend the efficient elimination of colors from effluent by combining consortium-enriched sludge utilized in sequential anaerobic and aerobic digestion. Due to their lack of electrons, azo dyes decolorize

in reducing environments, producing aromatic compounds that, in oxidative environments, change into harmless final products. **Figure 2.23** illustrates models that are capable of clarifying the anaerobic degradation of azo pigments. Reductive splitting of azo linkages forms the initial phase of hypoxic bacterial azo dye metabolism. This procedure is facilitated by a category of low-substrate-selective soluble cytosolic enzymes referred to as "azoreductases". Under anoxic circumstances, such enzymes mediate electron transfer from azo dyes to soluble flavins, therefore reducing the dye. For these enzymes, there are unknown in vivo cytoplasmic activities. A cell wall-bound azoreductase enzyme was discovered in *Sphingomonas* sp. by Guivarch and co-workers. This strain exhibits azoreductase activity in both membrane-bound and cytoplasmic forms. Research on *Sphingomonas xenophaga* proposed an alternate hypothesis about the wide-ranging degradation of azo colorants by bacteria. The extent of reduction was shown to increase upon the introduction of quinones, such as 2-hydroxy-1,4-naphthoquinone or anthraquinone-2-sulphonate, into the growth media. The produced hydroquinones undergo reduction to form the azo dye by a completely chemical redox reaction. Reduced inorganic molecules (such as Fe2Í and H_2S), which are results of certain purely anaerobic bacterial metabolic activities, can also reduce azo compounds in anaerobic environments (Shah, 2019).

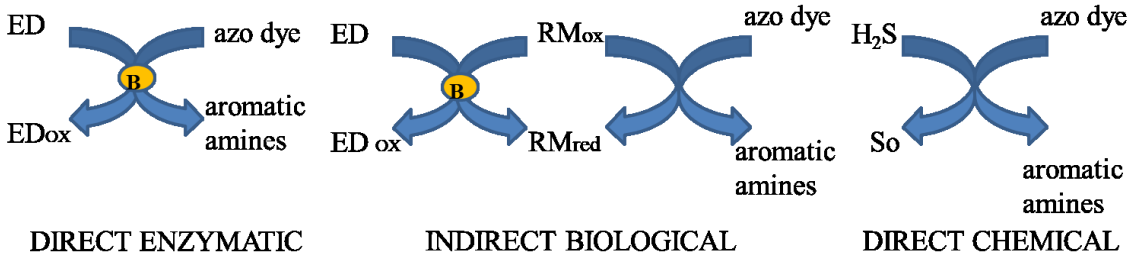

Figure 2.23: The processes by which bacteria reduce azo dyes anaerobically (ED=Electron Donor; EDox= Oxidized Electron Donor; B= Bacteria (enzyme system); RMred= Reduced Redox Mediator; RMox=Oxidized Redox Mediator)

Table 2.3 presents the findings from several investigations on biodegradation of azo dye-laden wastewater using bacteria.

Table 2.3: A summary of multiple investigations utilizing bacteria to facilitate azo dye degradation

Bacterial strain	Dye	Conditions (time (h), dye concentration (mg L^{-1}), T(^{o}C), pH)	Decolonization (%)	Reference
Bacillus cereus	Reactive Black 5	120, 99.1, 25, 9.0	97	(Wanyonyi et al., 2019)
Stenotrophomonas sp.	Acid Blue 29	125, 100, 30, 7.2	94	(M. D. Khan et al., 2021)
Shewanella haliotis RDB_1	Reactive Red 120	2.25, 50, 35, 7.4	100	(Radhika Birmole & Aruna, 2019)
Pseudomonas aeruginosa	Reactive Yellow 145	96, 50, 37, 7.0	100	(N. Garg et al., 2020)
Pseudomonas stutzeri AK6	Acid Blue 113	96, 300, 37, 7.4	86.2	(Joshi et al., 2020)
Klebsiella pneumoniae GM-04	Disperse Blue-284	24, 200, 37, 7.0	95	(Mustafa, Zahid, Ali, Abbas, & Rafatullah, 2021)
Lactobacillus acidophilus	Brillant Orange 3R	12, 750, 24, 11.5	99.3	(Ayed et al., 2019)
Thiosphaera pantotropha	Reactive Yellow 145	72, 50, 37, 7.5–8.0	100	(N. Garg et al., 2020)
Bacillus subtilis HAU-KK01	Congo Red	10, 40, 30, NA	92.8	(Sarim, Kukreja, Shah, & Choudhary, 2019)
Citrobacter sp.	Congo Red	120, 200, 35, 7.5	93	(Schmidt, Berghahn, Ilha, & Granada, 2019)
Oerskovia paurometabola	Acid Red 14	48, 20, 30, NA	96	(Franca et al., 2020)
Acinetobacter baumannii JC359	Reactive Black 5 (B-GDN), Reactive Red	72, 500, 37, 7.0	98.8% for B-GDN, 96% for RP and 96.2%	(Ameenude en, Unnikrishna

	120 (RP), Reactive Blue 19 (RNB)		for RNB	n, & Ramalinga m, 2021)
Ochrobactrum anthropi	Reactive Black 5	72, 400, 30, 7.0	100	(Cheng et al., 2021)
Pseudomonas aeruginosa MZ520730	Methyl Orange	12, 100, 30, 7	>99%	(Kishor et al., 2021)
Bacillus subtilis, Brevibacillus borstelensis, Bacillus firmus	Reactive Red 170	48, 40, 35, 7.0	>80	(Barathi, Aruljothi, Karthik, Padikasan, & Ashokkuma r, 2022)
Pseudomonas aeruginosa, Thiosphaera pantotropha ATCC 35512	Reactive Yellow 145	96, 100, 37, 7.0	100	(N. Garg et al., 2020)

NA- Not available

2.8.3.2. Azo dye bioremediation by genetically modified microorganisms:

When desired or alien genes-which are typically not a part of the host system-are added to an organism for any particular reason, the result is a genetically modified organism, or GMO. Studies have shown that, given the right circumstances, nature is capable of self-cleaning, however this process is insufficient and slow to get rid of contaminants (B. Mishra et al., 2019). Since synthetic azo dyes do not deteriorate naturally, it is difficult and time-consuming to break them down using conventional methods. Numerous microorganisms are available with regard to biological treatment of textile effluent, not all of them are capable of successfully decomposing the dye molecules due to varied wastewater conditions (G. Saxena, Kishor, Saratale, & Bharagava, 2020). Hence, to enhance the durability and rate of disintegration of the treatment, active bacteria must be genetically modified. Through the use of genetic engineering techniques, bacteria that have undergone genetic modification can enhance dye degradation (B. Mishra et al., 2021). Genetically modified microorganisms (GEM) are created in bioremediation applications using four main techniques: (i) changes to

the specificities and affinities of enzymes; (ii) bioprocess monitoring, growth, and control; (iii) pathway creation and control; (iv) bio-affinity methods for reducing toxicity and conducting endpoint analysis, chemical sensing, and bio-reporters (Srivastava, Rani, Patle, & Kumar, 2022). Genetically modified organisms, or GMOs, are produced through gene alteration or gene exchange between different species (V. Kumar, Chandra, Thakur, Saxena, & Shah, 2020). The recombinant *E. coli* BL21 degraded Methyl Orange dye after the isolation of azo reductase gene, azo K, from *Klebsiella pneumoniae* and its introduction into *E. coli* DH5α (Dixit & Garg, 2019). Azoreductase, derived from *Enterococcus faecalis*, is produced in *Escherichia coli*. The Lac gene construct was derived from fungi *Ganoderma lucidum* and translated into *P. pastoris*, resulting in a significant reduction of Methyl Orange levels. The lac21 gene, resembling the Lac gene was produced by *E. coli*, demonstrating its ability to degrade dye across a pH spectrum from 5 to 9 (Kapoor et al., 2021). **Table 2.4** delineates various outcomes from research on the remediation of azo dyes utilizing genetically engineered microorganisms.

Table 2.4: An overview of several investigations into the azo dyes breakdown using genetically engineered bacteria

Genetically modified microorganism	**Dye**	**Vector**	**Extracted Gene**	**Gene Extracted from**	**Gene Expressed in**	**Conditions (dye concentration (mg L^{-1}),time (h), pH, T(^{o}C))**	**Removal/Decolonization (%)**	**References**
Escherichia coli JM109 pGEX-AZR	Acid red GR	vector pGEX 4T-1	Azoreductase gene	*Rhodobacter sphaeroides* AS1.1737	*E. coli* JM109	150,12,9.0,30	90%	(A. Kumar et al., 2020)
Escherichia coli JM109 pGEX-AZR	Direct Blue 71	Vector pGEX 4T-1	Azoreductase gene	*Rhodobacter sphaeroides* AS1.1737	*E. coli* JM109	150,12,9.0,30	82%	(A. Kumar et al., 2020)
E. coli BL21 DE3	Azo dye	pET30a (+)	AzoG gene	*Halomonas sp.*	*E. coli* DH5α	100,NA, 7.5,30	NA	(Tian et al., 2019)

	wastewater			*strain* GT				
Escherichia coli BL21	Methyl Orange	Vector pGEM-T	AzoK gene	*K. pneumoniae* MGH 78,578	*E. coli* DH5α	100, 96, NA, 37	90%	(Dixit & Garg, 2019)

NA- Not available

2.9. Microbial strategies for the elimination of azo dyes

2.9.1. Biosorption

Microorganisms that may remove colors through adsorption has been previously documented in scientific literature, and biosorption involves both absorption and adsorption mechanisms. Since biosorption is strongly associated with the lipid and heteropolysaccharide constituents of cell walls, both dead and alive cells can engage in biosorption or bioaccumulation within the subsequent stage. Pretreatment can alter the capacity of the cell for absorption which improves the procedure and more effectively meets a particular demand. These modifications can be carried out by a range of compounds, including formaldehyde, bases and acids (Solís, Solís, Pérez, Manjarrez, & Flores, 2012). When dealing with large quantities of polluted material, biosorption is not the best option because it produces a lot of biomasses, some of which contain dyes and others which may contain other dangerous substances, which must be properly disposed of. Alternatively, since biosorption usually retains the dye intact and merely destroys the biomass, it only partially solves the problem (R. Khan, Bhawana, & Fulekar, 2013). **Table 2.5** delineates various findings from research about the application of microorganisms in biosorption to eliminate azo dyes.

Table 2.5: Microorganisms employ biosorption to decolorize azo dyes

Microorganisms Type	Microorganisms name	Dye	Reference
Bacteria	*Ochrobactrum pseudintermedium* C1	Congo Red	(I. Saha, Datta, & Biswas, 2023)
Macroalgae	*Lychaete pellucida*	Reactive Red 120, Reactive Green12, Reactive Brilliant Yellow 3G	(Khalaf, El-Sheekh, & Makhlof, 2023)
Fungi	*Aspergillus arcoverdensis* SSSIHL-01	Congo Red	(Skanda, Bharadwaj, Kar, Sai Muthukumar, & Vijayakumar, 2023)
Fungi	*Aspergillus tamarii* MWWAS8	Reactive Black 5	(R. Rai & Vijayakumar, 2023)

2.9.2. Enzymatic Deterioration

The elimination of dyes from aquatic ecosystems has highlighted the significance of microbial enzymes. These enzymes are known to catalyze the redox processes that contribute to the generation of azo bonds. Numerous researches have examined the capacity of oxidoreductases to decolorize azo dyes. Oxidoreductase enzyme is capable of catalyzing both reduction and oxidation procedure (Paul, Sangeetha, & Deepika, 2019). The microbial dye decolorization technique has employed most oxidoreductase enzymes, such as azoreductase, laccase, lignin and manganese peroxidase. **Table 2.6** provides a crucial summary of microbe-produced enzymes employed to efficiently degrade azo dyes.

Table 2.6: Azo dye biodegradation using microbial enzymes

Enzymes	Dye	Microorganisms	Reference
Azoreductase	Methyl Red	*Streptomyces* sp.	(Dong et al., 2019)
Laccase	Acid Blue 113, Acid Blue 52	*Penicillium chrysogenum strain* TSV1	(Senthilvelan et al., 2023)
Manganese peroxidase	Methyl Orange	*Cerrena unicolor* BBP6	(H. Zhang, Zhang, Zhang, & Geng, 2018)
Azo reductase	Methyl Red	*Zhihengliuella sp.* ISTPL4	(Takkar et al., 2022)
Azoreductase, flavin reductase, oxidoreductases	Reactive Black 5	*Shewanella* sp. SR1	(J. Liu et al., 2023)
Azoreductase	Basic Orange 2	*Escherichia coli*	(Ikram et al., 2022)
Laccases	T-blue, Yellow GR and Orange 3R	*Bacillus cereus*, *Pseudomonas parafulva*	(Khaled et al., 2022)
Azoreductase	Reactive Red, Reactive Black, Reactive Brown	*Bacillus subtilis*	(Krithika, Gayathri, Kumar, & Doss, 2021)
Laccase, Tyrosinase, Azo reductase, Riboflavin reductase	Golden Yellow HER	*Galactomyces geotrichum, Brevibacillus laterosporus*	(Patel, Tipre, & Dave, 2019)
Azoreductase, Lignin peroxidase, NADH-DCI	Reactive Blue 160	*Bacillus subtilis*	(Barathi, Aruljothi, Karthik, & Padikasan, 2020)

2.9.2.1. Azo-reductases

Azo-reductases can be divided into two categories according to their mechanism of action: flavin-dependent and flavin-independent (Bharathi, Nandagopal, Ranjithkumar, Gupta, & Djearamane, 2022). This enzyme is assisted in breaking down dye through the action of cofactors and redox-active coenzymes. These intermediates facilitate the passage of electrons from the azo reductase enzyme to the azo color. Under aerobic conditions, the breakdown of aromatic amines yields small molecules including water, ammonia, and carbon dioxide (P. Mani et al., 2019). In summary, the predominant breakdown of azo colors occurs in hypoxic circumstances, where the reduction of double bond formation occurs, subsequently leading to the aerobic process of mineralization. As azo dyes degraded, several auto-oxidized metabolites of the hazardous and cancer-causing aromatic compounds also developed. Membrane and cytoplasmically-bound redox-active azo-reductase enzymes employ diverse methods to decrease azo dyes (Patel, Tipre, & Dave, 2017). The anaerobic degradation of azo dyes is more efficient owing to the oxygen sensitivity of the azo-reductase enzyme. The molecules of azo dyes received two electrons at each stage of the breakdown process. The oxidizing and electron-accepting properties of these molecules lead to the formation of a hazardous mixture of colorless aromatic amines (Nikam et al., 2017). Various bacterial strains have proven to have purifiable azo-reductase, including *Variovorax paradoxus*, *Thermobifida fusca*, *Staphylococcus* sp., *Chlorella* sp., and numerous others (Meinert et al., 2018; Suzuki, Abe, Doi, & Ohshima, 2018). **Table 2.7** illustrates the azoreductase enzymatic activity observed in different microorganisms. **Figure 2.24** illustrates the process by which an azo dye is transformed into fewer hazardous substances facilitated by the enzyme azoreductase.

Table 2.7: Azoreductase enzymatic activity in different microorganisms

Dyes	Microorganisms	Azoreductase Enzyme activity (nmol min^{-1} mg^{-1})	References
Reactive Red 120	*Bacillus lentus* BI377	0.090 ± 0.004	(Oturkar et al., 2011)
Reactive Blue 59	*Alishewanella sp.* KMK6	3.09 ± 0.07	(Kolekar et al., 2013)
Reactive Black 5	*Providencia rettgeri* strain HSL1 and *Pseudomonas sp.* SUK1	3.75 ± 0.04	(Lade, Kadam, Paul, & Govindwar, 2015)
Acid Red 1	*Stenotrophomonas* sp. BHUSSp X2	1.8 ± 0.002	(L. Kumari, Tiwary, & Mishra, 2016)
Reactive Yellow F3R	*L. sphaericus* MTCC 9523	3.95 ± 0.12	(S. Srinivasan, Bankole, & Sadasivam, 2022)

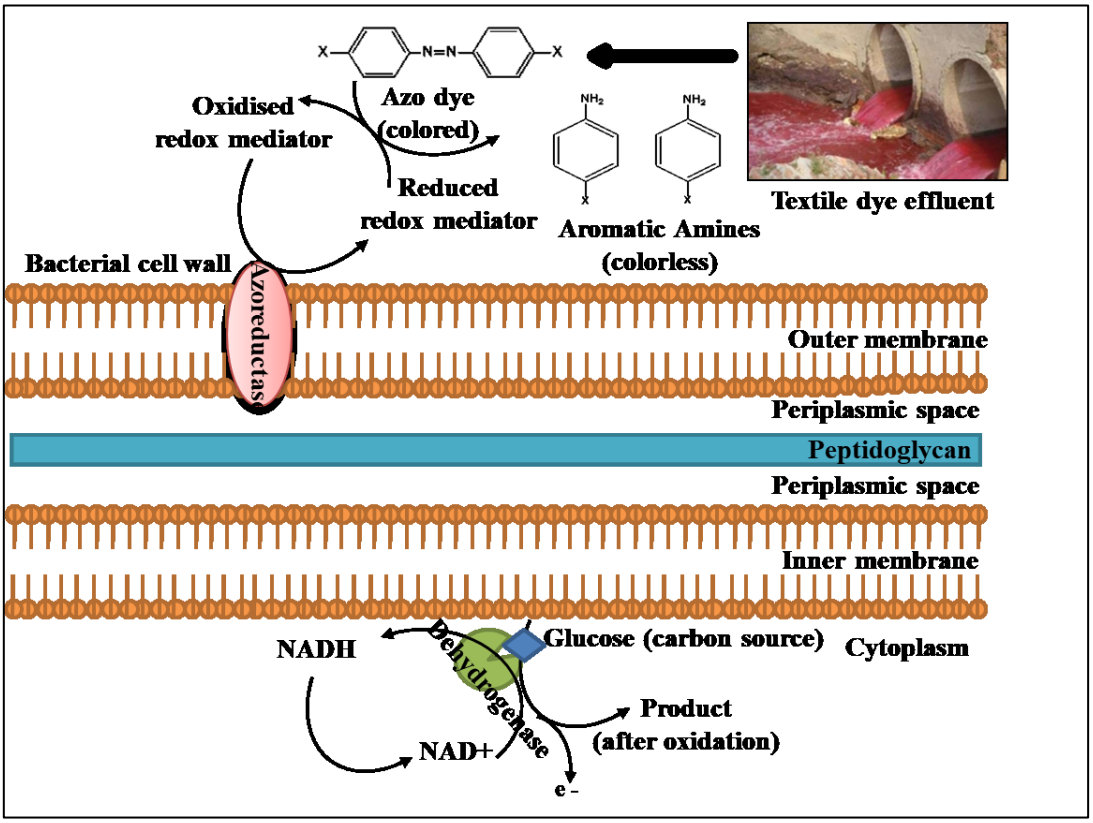

Figure 2.24: The bacterial enzyme azo reductase: a pathway involved in breakdown of azo dyes (Goud, Cha, Koyyada, & Kim, 2020)

2.9.2.2. Laccases

Laccase is a common type of oxidoreductase that is employed to act as biocatalyst for removing dyes from wastewater. An enzyme with several copper atoms is called laccase, or multi-copper oxidases. It has been demonstrated that laccase considerably decolorizes wastewater colors. Many microorganisms produce extracellular and intracellular laccases that can decolorize colors (Unuofin, Okoh, & Nwodo, 2019; K.-Z. Xu et al., 2020). Laccase-mediated activity towards a range of colors has been shown for fungal lipolytic enzymes. Laccases generally break down azo dyes without rupturing the azo bonds by using a broad free radical strategy (Kalme, Jadhav, Jadhav, & Govindwar, 2009). The laccase-catalyzed dye degradation mechanism follows a different route depending on the dye structure. Laccase enzyme functions as a small-molecule mediator of metabolites and effectively acts on a broad spectrum of non-aromatic and aromatic azo dyes (Galai, Korri- Youssoufi, & Marzouki, 2014). For degrading azo dyes, it employs a general free radical reaction to produce phenolic compounds rather than hazardous aromatic amines (Kapoor et al., 2021). **Figure 2.25** illustrates the degradation of Congo Red into lesser hazardous chemicals facilitated by the laccase enzyme.

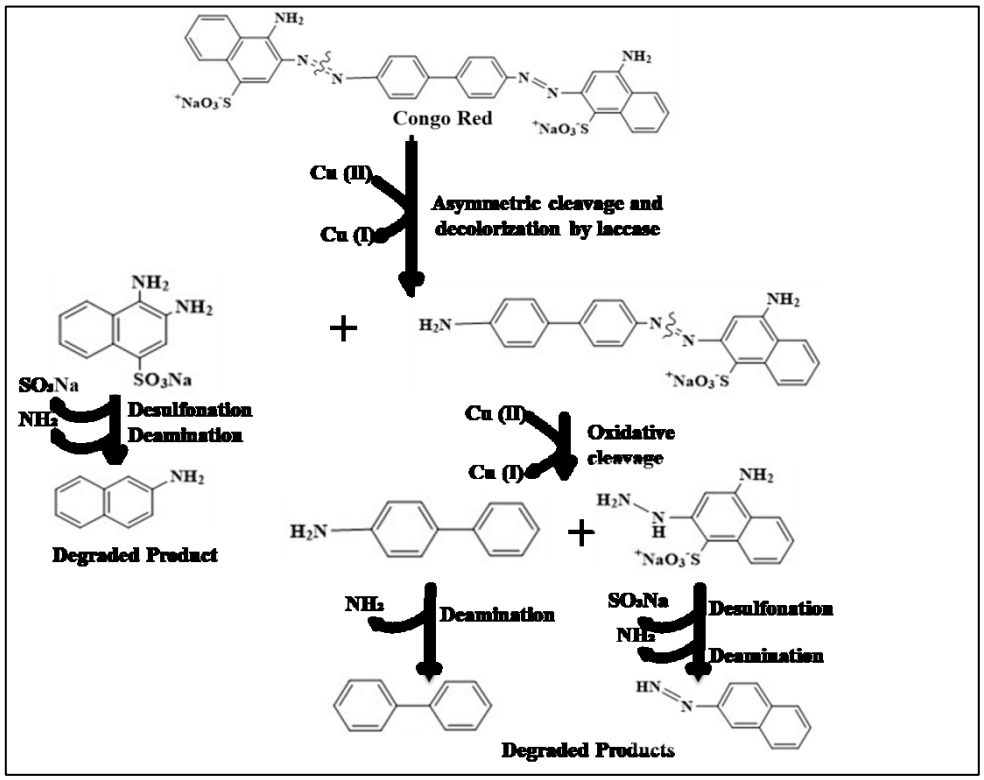

Figure 2.25: Congo Red Dye degradation mechanism of action of the fungus laccase enzyme (Goud et al., 2020)

2.9.2.3. Manganese peroxidase and lignin peroxidase

Manganese and lignin peroxidase belong to a class of peroxidase enzymes that are grouped based on the type of breakdown they cause (Falade et al., 2017). The majority of hemoproteins known as peroxidases are found in fungi, while some bacteria can also have them. In the presence of hydrogen peroxide, they speed up operations. Paszczynski and colleagues assert their capacity to breakdown a variety of colors. They explicitly stated that manganese and lignin peroxidase facilitate the breakdown of dyes and xenobiotic compounds (Pinheiro, Gradíssimo, Xavier, & Santos, 2022). Besides degrading lignin, manganese peroxidases are capable of decolorizing azo dyes. Furthermore, it was demonstrated to degrade Poly R-478, an extremely resilient high-molecular-weight dye. The source of manganese peroxidase was fungus *Phanaerochaete chrysosporium*. Nevertheless, it has been shown that azo dye Ranocid Fast Blue's color deterioration is caused by *Serratia marcescens* (M. Narayanan, Ali, & El-Sheekh, 2023). Moreover, *Pseudomonas desmolyticum* NCIM 2112 has been demonstrated to breakdown Direct Blue 6 utilizing tyrosinases, laccases, and lignin peroxidases (Ngo & Tischler, 2022). **Figure 2.26** illustrates the action mechanism of Methyl Orange in conjunction with the enzymes lignin peroxidase or manganese peroxidase.

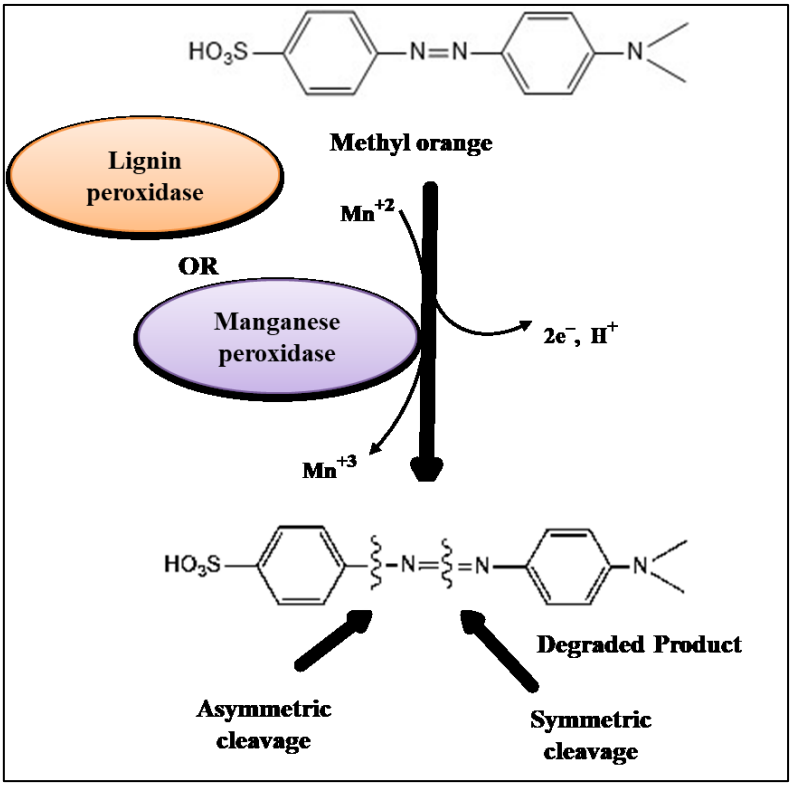

Figure 2.26: The function of Peroxidase enzyme in the Methyl Orange dye breakdown process (Goud et al., 2020)

2.9.2.4. NADH-DCIP reductase

Although they have limited uses in reducing azo dye, it has been reported that non-specific reductases, like NADH-DCIP reductase, play a role in azo dye decolorization. This enzyme is inefficient in vivo and has limited applications. NADH-DCIP reductase mediates the elimination of xenobiotic compounds that constitute the bacterial multi-enzyme complex. The enzyme NADH-DCIP reductase employs NADH as a source of electrons for conversion the blue DCIP compound into a colorless state (**Figure 2.27**) (Patel Jay, Vaishnav Darshit, Joshi Pavan, & Tipre Devayani, 2023).

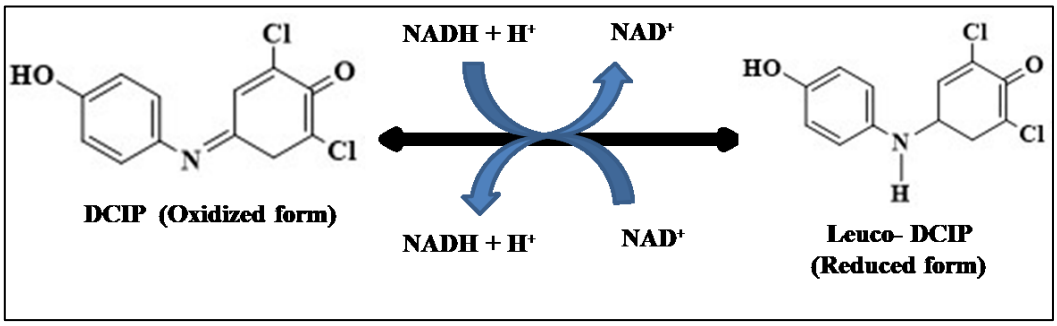

Figure 2.27: The function of NADH-DCIP reductase in dye breakdown (Patel Jay et al., 2023)

2.9.2.5. Veratrol alcohol oxidase (VAO)

VAO belongs to the group of enzymes called oxidoreductases. This enzyme generates aromatic aldehydes and H_2O_2 from two substrates: O_2 and a primary alcohol attached to an aromatic ring (Patel Jay et al., 2023).

Aromatic primary alcohol + O_2 → Aromatic aldehyde + H_2O_2

2.9.2.6. Polyphenol oxidase (Tyrosinase)

Polyphenol oxidases (PPOs) facilitate the hydroxylation of monophenols at the ortho position, resulting in the formation of O-diphenols, and subsequently catalyze the oxidative destruction of O-diphenols to generate O-quinones. O-quinone can be synthesized by polyphenol oxidases (PPOs) through the oxidation of tyrosine, a class of amino acids characterized by a singular phenolic ring. Tyrozinase is another name for PPOs. When molecular oxygen is present, PPO oxidizes certain phenolics to quinones. In industry, pure polyphenol oxidase was used to oxidize colored and phenolic compounds (Arti Mishra et al.,

2022). **Figure 2.28** depicts the function of polyphenol oxidase (tyrosinase) in catalyzing the transformation of L-tyrosine into O-quinone.

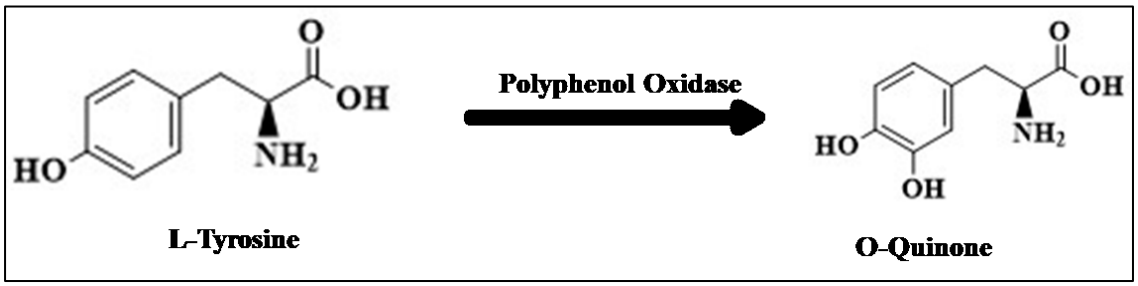

Figure 2.28: Polyphenol oxidase (Tyrosinase) facilitates the conversion of L-tyrosine into O-quinone (Patel Jay et al., 2023)

2.10. Enzymes Involved in RR120 Degradation

The degradation of azo dyes is a multi-step biochemical process that involves various enzymes; still, the earliest and most crucial stage is the breaking of the azo (–N=N–) link, which is chiefly responsible for dye decolorization. Among the enzymes documented in the literature, including laccases, lignin peroxidases, manganese peroxidases, monooxygenases, and dioxygenases, azoreductases are the enzymes most directly implicated in the breakdown of RR120 dye.

Azoreductase is the Principal Enzyme for RR120 Degradation. RR120 is a strongly sulfonated diazo dye, distinguished by:

- Two azo (–N=N–) bonds
- Greater molecular weight
- Numerous sulfonic acid groups that impede oxidative degradation

Due to these structural characteristics, oxidative enzymes alone (e.g., laccase, peroxidase) are typically ineffective in initiating the degradation of RR120. Instead, the reductive cleavage of azo bonds is crucial, primarily facilitated by NAD(P)H-dependent azoreductases. Azoreductases catalyze the reductive cleavage of azo bonds, transforming RR120 into colorless aromatic amines, which results in rapid decolorization. Numerous studies specifically document azoreductase-mediated degradation of reactive azo dyes, including RR120, under bacterial treatment, particularly by *Pseudomonas* species.

2.11. Factors influencing the breakdown of azo dyes

Design and operational factors influence microbial dye decolorization and degradation. Various factors, including pH level fluctuations, temperature variations, salinity conditions, dye concentrations, inoculum size, nutrient types, stirring velocity, and both under aerobic and anaerobic conditions, affect the microbial breakdown of dyes (Ayed, Mahdhi, Cheref, & Bakhrouf, 2011). A comprehensive examination of the impact of numerous elements on the microorganism-driven dye discoloration is vital to optimize appropriate treatment strategies. **Figure 2.29** illustrates the factors affecting the degradation process.

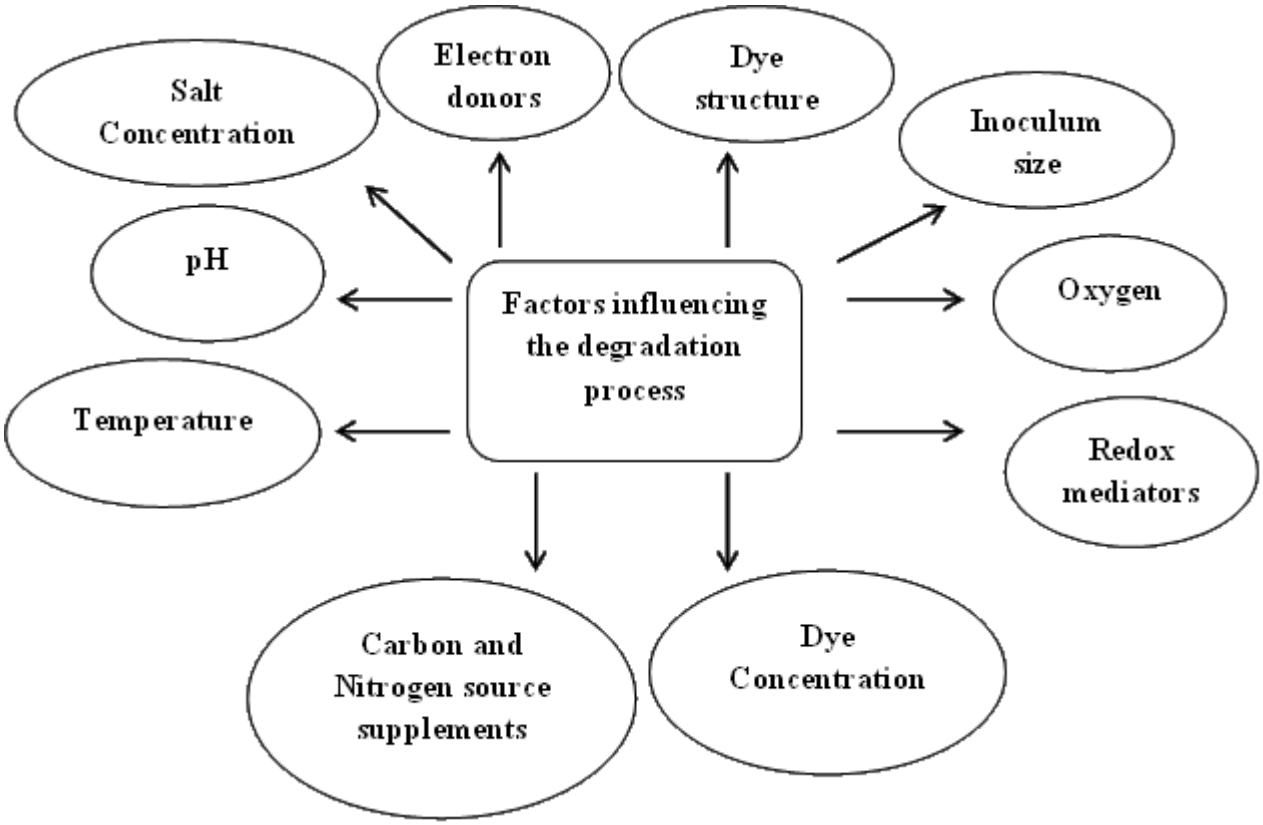

Figure 2.29: Parameters influencing the degradation process

2.11.1. Impact of pH

The pH indicates that dye decolorization is considerably affected by it, with optimal pH ranges differing according to the biological species. The environment may exhibit neutral, acidic, or basic pH levels, contingent upon the types of salts and dyes employed (Al-Amrani, Lim, Seng, & Ngah, 2014; Y. Shi et al., 2021). This stage determines the speed of the decolorization process. Bacteria exhibit optimal performance at pH values exceeding 7,

whereas fungus and yeast thrive at neutral or acidic pH levels in the context of color degradation. According to Tripathi and Srivastava, at pH 7*, Pseudomonas putida* decolored the Acid Orange 10 dye, whereas *P. aeruginosa* performed well in the pH range of 7 to 9 (A. Tripathi & Srivastava, 2011). When using *Lysinibacillus boronitolerans* CMGS-2, the pH range of 8-10 showed the most dye degradation (Basutkar & Shivannavar, 2019).

2.11.2. Impact of Temperature

The microbial dye degradation process is reliant upon temperature, which significantly affects microbial activity. Numerous metabolic processes, growth, enzyme synthesis, response mechanisms, biodegradation and biosorption are all impacted (R. Saratale, G. Saratale, J. Chang, & S. Govindwar, 2009b). As temperature rises, azo dye decolorization increases; but, at high temperatures, it decreases because of a reduction in cellular viability or denaturation of an azoreductase. The optimal temperature for bacterial cultivation is generally considered to range from 30°C to 40°C for the majority of bacteria. This will yield an accelerated rate of dye degradation. *Enterobacter* sp. EC3 exhibits enhanced decolorization of Reactive Black 5 at temperatures between 22°C and 37°C, while demonstrating reduced activity at temperatures of 42°C and above (H. Wang et al., 2009). According to Das and Mishra et al., a bacterial community consisting of *Bacillus pumilus* HKG212 and *Zobellella taiwanensis* AT 1-3 degrades Reactive Green 19 most effectively at 32.04°C (Das & Mishra, 2017). Since, temperature is the primary determinant of enzyme-based decolorization, as elevated temperatures cause the denaturation of enzymes. Nonetheless, scientists have employed some microorganisms and thermostable enzymes for discoloration of dyes at extremely elevated temperatures (Zhuang et al., 2020) showed evidence that the thermostable laccase enzyme is effective in decolorizing ten distinct dyes at 70°C (Y. Liu et al., 2017).

2.11.3. Effect of dye structure and concentration

The breakdown or discoloration of dye is influenced by both dye concentration and dye structure. It is possible that microorganisms that break down dyes release enzymes that do not detect low dye concentrations. Conversely, elevated dye concentrations can harm bacteria as well as prevents the enzyme from breaking down the dye by blocking its active sites (H.-h. Li et al., 2019). As the dye concentration rises, the degrading characteristics of microorganisms and their by-products diminish. According to a number of studies, the amount of dye gradually affects the decolorization effectiveness (Jamee & Siddique, 2019). Dye compounds

characterized by complex structures and elevated molecular weights demonstrate a reduced rate of decolorization, whereas dyes with small molecular weights and straightforward structures undergo rapid degradation by microbial organisms. The breakdown of dyes is substantially affected with the number of azo linkages and substituent groups. Azo bonds are susceptible to discoloration because of a substituent at the phenyl ring's para position (J. F. Li et al., 2019). Dye decolorization efficiency is affected by the dye's molecular complexity, which prevents the azo (-N=N-) link from cleaving. Nevertheless, it is possible for genetically modified bacteria to degrade highly concentrated colors (S. Varjani, Upasani, & Pandey, 2020). This suggests that dye and intermediate product concentrations have an effect on the process of deterioration and decolorization overall.

2.11.4. Impact of nutrients

For the decolorization process to continue, the substrate must include carbon and nitrogen (S. Varjani & Upasani, 2019). Azo dyes use redox mediators to absorb electrons that are produced when carbon is oxidized (Popli & Patel, 2015). For bacteria to decolorize azo dyes, various carbon sources, such as peptone, glucose, starch, and yeast extract, need to be available. Ammonium salts, peptone, beef extract, and some amino acids function as nitrogen sources that are vital for the production of cellular proteins (Bharathi & Rajalakshmi, 2019). These sources assist in breaking the azo bond by acting as electron donors. Coenzyme reducing equivalents are produced by oxidising organic substrates and act as an electron donor. Peptone, urea, beef, and yeast are combined to create NADH, which is needed to reduce azo dyes by one electron (Kapoor et al., 2021). Alalewi and Jiang observed that in the presence of starch, *Comamonas acidovorans* and *Burkholderia cepacia* decolorized the colors Direct Blue 75 and Acid Orange 7 (Aamr & Cuiling, 2012). Numerous investigators noted that supplementing with yeast extract removed a considerable amount of dye (Tian et al., 2021). Glucose is often believed the most accessible and optimal source of carbon due to the metabolic processes of colors or dye intermediates by microbes (Kishor et al., 2021). Reports state that phosphorus is a vital ingredient for microorganisms' development and proliferation (S. Varjani & Upasani, 2019). The impact of different nutrients on *Trichoderma asperellum*'s degradation of Crystal Violet, Cotton Blue, Methyl Violet and Malachite Green has been demonstrated by Marcharchand and Ting (Marcharchand & Ting, 2017).

2.11.5. Effect of inoculum

The process of the dye decolorization requires proper concentrations of microbial inoculum. Research has shown that a higher *B. cereus* inoculum level enhances Terasil Black decolorization. The ideal inoculum for decolorizing Acid Orange 7 was 4% *Pseudomonas putida* SKG-1 (Kapoor et al., 2021). Following a three-day exposure to an inoculum comprising 3% of the total volume of *Bacillus cereus* RMLAU1, Acid Orange 7 showed a 68% decolorization, according to Garg and Tripathi (S. K. Garg & Tripathi, 2013).

2.11.6. Effect of salts

A conductivity meter can be used to test the elevated electric conductivity of effluent from the dye in the dying process. Sodium nitrate ($NaNO_3$), Sodium sulfate (Na_2SO_4), and Sodium chloride (NaCl) are commonly used into the color bath to enhance ionic strength and facilitate dye fixing on textiles. Elevated concentrations of pollutants, such as acids, alkalis, and salts, are present in the effluents discharged by the dyeing sector. Dyes with higher salt concentrations can impede the pace of breakdown by limiting biological activity (Basutkar & Shivannavar, 2019). According to Anjaneya et al. most microbial activities are inhibited in saline environments; nevertheless, halotolerant bacteria can still decolorize azo dyes when salts are present (Anjaneya, Souche, Santoshkumar, & Karegoudar, 2011). Different azo dyes were decolored by *Serratia* sp. strain AXJ-M under the influence of high saline condition (greater than 6M NaCl) (Xuejiao et al., 2023). Khalid et al. showed that sodium chloride (NaCl, 40 g/L), Disperse Orange 3, Acid Red 88 and Reactive Black 5 completely decolorized within eight hours. However, *Shewanella putrefaciens* strain AS96 decolorized the dyes in 24 hours when the concentration of NaCl is 60 g/L (Azeem Khalid, Arshad, & Crowley, 2008).

2.11.7. Effect of oxygen

Literature shows that oxygen and agitation influence microbial metabolism (S. J. Varjani & Upasani, 2017). Anaerobic, semi-anaerobic, and aerobic environments are necessary for different microorganisms. Anaerobic decolorization treatments are more effective than aerobic ones when dyes contain electron-pulling groups. It is advised that for dyes to completely deteriorate, an aerobic treatment should come after the anaerobic treatment. *Galactomyces geotrichum* decolorized the dye mixture more quickly in aerobic medium than in anaerobic environments. *Bacillus lentus* decolorized RR120 by 98% in absence of oxygen

and 70% when oxygen is present (Oturkar et al., 2011). Although several studies have suggested that agitation may accelerate decolorization, the impact of agitation process on the degradation of microbes is controversial. Under quiescent conditions, decolorization increased, according to some researchers. The agitation facilitates better transportation of oxygen between the dye-containing solution and the microbial cells. Even though oxidative enzymes may require partial aeration to break down azo dye, reductive enzyme activities seem to favour static anaerobic circumstances. Amaranth dye was found to discolour by 91% in static conditions and to remove 68% of its colour when shaken over a 48-hour period. In contrast to 61% in static environments, 84% of Orange II decolorization was produced by *Aspergillus niger* when it was agitated. Fungi grow more quickly when agitation increases the oxygen and mass transfer to microorganisms in the culture media. Congo Red was more efficiently broken down by *A. niger* in aerobic than anaerobic circumstances due to improved oxygen transfer caused by shaking velocity (Kapoor et al., 2021). In contrast to stationary conditions, Kaushik and Malik reported color disappearance with agitation as a result of oxygen and nutrient distribution transfer (Kaushik & Malik, 2009). On the other hand, after 24 hours of contact, Kalyani et al. found that *Pseudomonas* species SUK1 had a low ability to degrade Reactive Red 2 dye while they were under agitation. At the same time, in static conditions, 96% decolorization was observed in 6 hours (Kalyani et al., 2009).

2.11.8. Effects of redox mediators and electron donors

The electron donating groups are responsible to remove the dye because they increase enzyme activity, which in turn triggers the dye reduction process. When different species compete for the same supply of electrons, the electron transport system becomes less efficient. Under the influence of electron-releasing groups, *Bacillus* species enhanced the removal of color of Reactive Orange 16 dye. An electron transport chain-connected multi-component system is used in bacterial anaerobic azo reduction processes to transmit electrons and oxidize electron donors. Van der Zee and Villaverde state that in oxygen-free bioreactors, the availability of electron donors is essential for the elimination of dye. Redox mediators transfer an electron donated by a primary electron donor source toward the final electron acceptor in order to function, which can speed up a reaction. Numerous substances, including riboflavin, cyanocobalamin, menadione, lawsone, anthraquinone-2-sulphonate (AQS) and flavin adenine dinucleotide (FAD) have all been identified as redox mediators. Under anaerobic conditions, decolorization is reduced by alternate ultimate electron acceptors including oxygen and nitrate, which should function in opposition to the azo dyes for electron

acceptance. Conversely, when oxygen is not present, the latter redox mediators might accelerate the processes of reductive decolorization. By promoting electron transport, quinone-based molecules function as mediators of redox reactions in both chemical and microbial contexts. When the redox potential of the system (or oxidizing or reducing capacity) was low, the rate of dye degradation was high, and as the redox potential increased, the rate of dye removal decreased (Kapoor et al., 2021).

2.12. Reusability and Recycling Potential of Azo Dye-Degrading Bacteria

Azo dyes, extensively utilized in textiles and several industries, present considerable environmental challenges owing to their persistence and toxicity. Microbial degradation presents a viable biological method for decomposing these substances; nonetheless, recyclability, which pertains to the reusability of the degrading organisms, treated water, or by-products in subsequent cycles, remains a crucial consideration for effective and scalable wastewater treatment. Research has investigated how bacteria, fungi, and consortia sustain degrading efficiency throughout numerous batches, frequently under optimum settings such as pH, salinity, and aeration, facilitating economical recycling without compromising viability (G. B. Singh, Vinayak, Mudgal, & Kesari, 2024).

2.12.1. Halophilic Bacteria in Elevated Salinity Environments

Halophilic and halotolerant bacteria from severe settings, such as the salt fields of Tibet, exhibit significant recyclability in the degradation of azo dyes like Direct Blue G (DBG). A 2022 study identified a microflora predominantly composed of Enterococcus species, which decolorized 600 mg L^{-1} DBG in high-salinity (up to 60 g/L NaCl) and low-oxygen wastewater, achieving nearly complete degradation and converting the toxic dye into low-toxicity metabolites, as verified by phytotoxicity tests and LC-MS analysis. Enzyme studies demonstrated enhanced activity of azo reductase, laccase, lignin peroxidase, NADH-DCIP reductase, and Mn-peroxidase, with intracellular levels increasing significantly after decolorization (e.g., NADH-DCIP from 5.77 to 40.99 U/min/mg protein at 60 g/L NaCl), indicating a synergistic degradation mechanism. The stability of microflora over salt gradients implied recyclability, indicating the potential for reusing industrial textile effluents without loss of viability.

This method emphasizes ecological significance, as the bacteria flourished in authentic saline environments, repurposing biomass for continual utilization while reducing secondary pollutants (Qiu et al., 2022).

2.12.2. Efficiency of Soil Bacteria and its Consortia

Bacillus species extracted from soil efficiently decompose methyl red and orange azo dyes, with recyclability assessed via multiple batch cycles. A study indicated a 78.57% breakdown of methyl red and 47.59% degradation of orange dye utilizing *Bacillus*, crediting the efficacy to azoreductase enzymes that sever the azo link (-N=N-), producing less toxic amines that can be reintroduced into the nitrogen cycle. The bacteria's capacity for spore formation improved recyclability, facilitating recovery through centrifugation and reuse in new dye-laden media with minimal activity reduction across multiple cycles.

Bacterial consortia enhance recyclability by dispersing metabolic burdens. A consortium of *Providencia rettgeri* and other strains effectively detoxified textile azo dyes, demonstrating continuous decolorization (up to 90-100%) across numerous batches via the processes of cell harvesting, washing, and reinoculation. Phytotoxicity assays verified the non-toxicity of the waste, facilitating the safe recycling of water for irrigation purposes (Gayathri, Kavi, Meena, Karthikeyan, & Ramesh, 2014).

2.12.3. Fungal and Mixed Microbial Systems

Fungi such as *Aspergillus* and *Phanerochaete* provide extracellular enzyme-mediated degradation, exhibiting significant recyclability in immobilized states. Research on white-rot fungi reveals the production of laccase and peroxidase, which mineralizes azo dyes into CO_2, water, and inorganic salts, enabling the trapping of fungal biomass in alginate beads for 5-10 reuse cycles with negligible efficiency loss (e.g., 85% decolorization maintained). An assessment highlighted fungal consortia that degrade Reactive Black 5, with recycled mycelia sustaining 70-90% activity due to immobilization safeguarding against hazardous intermediates.

Microbial fuel cells (MFCs) combine degradation with energy recovery, hence improving recyclability. A study on microbial fuel cells (MFCs) utilizing mixed bacterial populations demonstrated sustained degradation of azo dyes (e.g., 95% for Acid Orange 7) over several months, with anode biofilms autonomously regenerating by electron transfer, providing

power while treating wastewater for discharge. Biofilm stability guaranteed prolonged functioning without the need for reseeding (K. Li, 2003).

2.12.4. Optimization for Recurring Utilization

The recyclability depends on process parameters. A literature highlighted bacterial strains such as *Pseudomonas* and *Bacillus*, which can be reused through flocculation or membrane separation, attaining 80-95% degradation over 4-6 cycles by regulating pH (7-8) and utilizing glucose co-substrates that enhance azoreductase activity. Genetic engineering, namely the overexpression of laccase in *E. coli*, enhanced recyclability to over 10 cycles with 90% efficiency (Yang et al., 2024).

2.13. Analytical Techniques for Decolorization Studies

Several analytical approaches were employed to detect the metabolites that bacteria created as they mineralized reactive dyes. The most common technique to evaluate dye decolorization is UV–vis spectroscopy (Knapp & Newby, 1995). The dye's discoloration is shown by the primary peak disappearing at a maximum wavelength and additional peaks appearing within the ultraviolet range (R. Saratale, G. Saratale, J.-S. Chang, & S. Govindwar, 2009a). The optimum method for separating the dyes and their structurally identical intermediates has been shown to be thin-layer chromatography (TLC), which possesses the necessary separation power and spot ability. A distinct stationary phase can be used to compensate for infinite variations in the mobile phase mixtures. Another method used to validate the dye degradation investigation was high-performance thin-layer chromatography (HPTLC) (Mohana, Shrivastava, Divecha, & Madamwar, 2008). While the basic idea behind this technique is the same as that of TLC, there are certain benefits including automated utilization–techniques, greater responsiveness and thinner plates. High-performance liquid chromatography (HPLC) is the general term for liquid chromatography that requires relatively small packing materials at extremely high pressure. The formation of additional peaks with differing times of retention relative to the initial dye signifies dye breakdown, suggesting the formation of metabolites (G. D. Saratale, Chien, & Chang, 2010).

Fourier-transform infrared spectroscopy (FTIR) is among the most widely utilized techniques in infrared spectroscopy. The FTIR spectrum can elucidate the nature and intensity of interactions in dyes with diverse functional groups post-biodegradation, as well as provide insights into the dye breakdown mechanism. Gas chromatography mass spectrometry (GC–

MS) refers to the procedure where a liquid serves as the mobile phase, while liquid chromatography mass spectrometry (LC–MS) pertains to the scenario where the mobile phase is a liquid. Mass spectrometry utilizing both techniques is essential for identifying the metabolites produced following biodegradation. Furthermore, it determines the molecular masses and physical characteristics of the dye intermediates and can propose pathways for dye degradation (Telke, Kalyani, Dawkar, & Govindwar, 2009). Similar to this, nuclear magnetic resonance (NMR) is a common analytical approach that is applicable for quantitatively investigate substances in either a solid or liquid state and is helpful in acquiring information on the structures of molecules. According to some researches, the decolorization % before and after the treatment using the total organic carbon (TOC), biological oxygen demand (BOD), and chemical oxygen demand (COD) elimination rate can be employed to determine the biodecolorization efficiency (R. Saratale, Saratale, et al., 2009a; R. Saratale, Saratale, Kalyani, Chang, & Govindwar, 2009).

2.14. Evaluation of the toxicology of the Bio-Decolorization Products

The textile industry generates numerous synthetic dyes that pose significant environmental hazards. Before environmental discharge, it is crucial to assess the potential hazards and effects of the intermediates generated during biodegradation. Environmental exposure to textile wastewater can lead to artificial above-ground water sources discoloration and significant environmental problems, adversely affecting aquatic ecosystems and the quality of water. A multitude of studies regarding the role of microbial species in assessing wastewater toxicity has been recorded (Goswami et al., 2024; Pearce, Lloyd, & Guthrie, 2003). According to Jiang et al. (2020) the biodegradation of reactive dyes necessitates prolonged residence durations, which impact multiple aspects such as cellular transport and the dye's capacity to be stored or kept within the cells for disintegration (Jiang et al., 2020). Consequently, the dye-decolorization reaction in a comparatively short time eliminates dye bioaccumulation and long-term toxicity, both of which are essential for cell survival. When Rawat et al. (2016) reviewed the literature on detoxification from azo dyes, they found that few of the research were based on toxicity analyses, which suggested the dyes had little environmental significance (Rawat, Mishra, & Sharma, 2016).

2.15. Improvements in dye bioremediation bioreactors

Improving and developing efficient bioreactor technologies are important for the widespread implementation of the bioremediation approach (Vikrant et al., 2018). In order to convert substrates into products, entire cells or enzymes that are either free or immobilized can be found inside tanks or other vessels called bioreactors. Multiple closed-system bioreactors have previously been introduced in an effort to provide improved growth and controlled operating parameters. According to the needs of the applications, bioreactors can be broadly categorized as batch, semi-batch, or continuous operation (Agrawal, Tipre, & Dave, 2019). Various bioreactor types have been employed for dye biological remediation, contingent upon the design and intended anaerobic and aerobic applications. According to Narayanan & Narayan (2019), these types of bioreactors are stirred tanks, membranes, airlift, fluidized beds, semi-fluidized beds, moving beds, and packed beds (C. Narayanan & Narayan, 2019). Bioremediation is currently more successful since the bioreactor process is more carefully regulated (B. Wang, Wang, Chen, & Zhao, 2020). This is caused by advancements in machinery, sensors, and information technology as well as the creation of intelligent distributed sensors and actuators. Bioreactors have been thoroughly investigated for the effectiveness towards the bioremediation of several dyes.

2.15.1. Membrane bioreactors

Membrane bioreactors provide a variety of advantages, including minimum sludge generation, flexible design, small footprint, high effluent quality, and avoiding enzyme washout (Y. Li, Song, Yuan, Zhang, & Zhu, 2020). The filtration capability of the membrane increases treatment effectiveness by separating particles from fluids. The primary disadvantage of membrane bioreactors is membrane fouling, which shortens the reactor's lifespan (Berkessa, Yan, Li, Jegatheesan, & Zhang, 2020). About 99% of the dye may be degraded by the bacteria *Lactococcus lactis* in about 36 hours (You & Teng, 2009). According to Bai et al. (2020), a bioreactor membrane including methanomethylovorans and moranbacteria showed that the Methyl Orange removal can reach up to 883 mg per liter per day, with an almost complete degradation efficiency (Bai et al., 2020). Liu et al. utilized an anaerobic baffled membrane bioreactor to eliminate Methyl Orange by combining a membrane bioreactor and an anaerobic baffled reactor. The study showed complete decolorization of Methyl Orange after traversing four anaerobic process cells and entering the membrane bioreactor (J. Liu et al., 2018).

2.15.2. Stirred tank bioreactors

Stirred bioreactors are versatile and reproducible systems that are suitable for batch as well as continuous processes. Glass bioreactors are widely used in research because they are more robust, easier to clean, and don't create dead zones (Schirmer et al., 2018). Stirred tank bioreactors are the method of choice because of their excellent temperature and pH control, uniform mixing to reduce clogging, improved substrate contact, and homogeneous distribution. Stirred tank bioreactors are renowned for their low initial and ongoing expenses and their increased gas–liquid mass transport efficiency. The reactor achieved an 80% removal of COD and a 75% reduction in color after 96 hours of operation, using a wastewater feed rate between 0.92 and 3.7 g/Ld. Effective color removal from textile effluent is achievable using a continuous stirred tank bioreactor, concentrations as high as 200 mg L^{-1} were treated. Recent studies have proved the utilization of low-cost materials and novel methodologies in bioreactor design (Ihsanullah Ihsanullah et al., 2020).

2.15.3. Bioreactors with fixed or packed beds

The decolorization of textile wastewater has shown considerable promise for a number of fixed bed or packed bed bioreactors (Agrawal, Tipre, & Dave, 2023). A consortia of bacteria and yeast decolorized the actual textile effluent in a three-layer fixed bed reactor (Kurade, Waghmode, Patil, Jeon, & Govindwar, 2017). Over the course of seven days, the reactor showed ~78% COD reduction and >80% decolorization (at a flowrate of 100 mL/h). RR120 was completely degraded within four hours using an immobilized packed bed reactor (A. N. Kulkarni, Watharkar, Rane, Jeon, & Govindwar, 2018).

2.15.4. Airlift bioreactors

An intriguing alternative option for treating wastewater is the use of Airlift bioreactors. Airlift bioreactors are distinguished by their simple construction, affordable price, and minimal power usage. Mass transmission is however constrained by their lack of a mixing mechanism (Gholami, Zinatizadeh, Zinadini, McKay, & Sibali, 2020). Teerapatsakul et al. (2017) stated that an aromatic ring-structured dye was entirely eliminated using an airlift-type bioreactor with laccase enzyme and optimal operating conditions (Teerapatsakul, Parra, Keshavarz, & Chitradon, 2017). Within an air-lift reactor, *Bjerkandera adusta* OBR105 was employed to remove color from several dyes. According to Sodaneath et al. (2017), after

three days, the majority of the colors tested exhibited dye removal rates between 91 and 99% (Sodaneath et al., 2017).

2.15.5. Fluidized bed bioreactors

Due to their large reactor capacity, high power consumption, and erosion, these bioreactors have limited applications; nonetheless, they are advantageous because they can work continuously, mix evenly, and have better temperature control (Özkaya, Kaksonen, Sahinkaya, & Puhakka, 2019). The utilization of a fluidized bed bioreactor considerably enhanced the efficacy of dye removal (Nejatbakhsh et al., 2023). In a fluidized bed reactor operating at semi-pilot scale, Acid Yellow 36 dye shown good decolorization efficacy (92%) according to a study (A Khataee, Vahid, Aghdasinia, & Bagheri, 2018). *Bacillus subtilis* encapsulated in polyurethane foam (PUF) was employed in a multistage fluidized bed bioreactor to eradicate Congo Red. Following a 24-hour period at a dosage level of 100 mg L^{-1}, an optimal dye clearance rate of 92% was attained (Shalini & Setty, 2019).

2.15.6. Alternative bioreactors for dye bioremediation

Advancements in technology and the increasing utilization of bioreactors have led to the creation of more contemporary designs, such as hybrid and sequential bioreactors (Agrawal et al., 2019). A few additional bioreactor types, including bio-filters, rotating biological contactors and slurry phase bioreactors, have also been covered in the literature (Tekere, Jacob-Lopes, & Zepka, 2019).

CHAPTER 3

MATERIALS AND METHODS

3. Materials and Methods

3.1. Collection of sample

To isolate the decolorizing bacteria, a sample of textile dye-contaminated soil and wastewater was obtained from textile processing plants in West Bengal, India. The soil sample was stored in sterile plastic bags. Sterilized polypropylene bottles were used to collect water samples. During the sampling process, temperature, pH, color and odor were recorded at the location. Samples were kept for further analysis at 4°C.

3.2. Chemicals and reagents

A common di-azo dye called Reactive Red 120 (RR120) was used as the representative color for the present research. The dye, which was acquired from Sigma-Aldrich in India, was analytical grade (≥ 98% purity). Nutrient media, including nutrient agar and nutrient broth, procured from Hi-Media Laboratories (India). The following products were bought from Merck (India): Glucose (99% pure), Yeast Extract (99% pure), KH_2PO_4 (99% pure), K_2HPO_4 (99% pure), $MgSO_4.7H_2O$ (99% pure), NaCl (99% pure), $CaCl_2.2H_2O$ (99% pure), $FeSO_4.7H_2O$ (99% pure). Sterilized NaOH (1M) was employed to maintain the elevated pH of the media.

3.3. Isolation and characterization of RR120 dye degrading isolated strain

3.3.1. Culture medium for isolation and growth of RR120 dye degrading microorganism

An inorganic medium, augmented with a trace amount of yeast extract and glucose, was employed for isolation and biodegradation studies, comprising the following constituents (g L^{-1}) $MgSO_4.7H_2O$ 0.2, K_2HPO_4 1.5, KH_2PO_4 0.5, Yeast Extract 0.5, Glucose 0.5, NaCl 0.5, $CaCl_2.2H_2O$ 0.026 and $FeSO_4.7H_2O$ 0.0025. Agar was incorporated into the medium in an amount of 2.5% (w/v) to create the solid mineral base medium. Initially, the pH of the media was kept at 7. RR120 dye stock solutions were formulated at 10,000 mg L^{-1} concentration using double distilled water and Sodium hydroxide (NaOH). The effective solution was prepared by accurately diluting the stock sample. The calibration plot was created for RR120 dye and it was found that R2 ≈ 1.000 indicated linearity as illustrated in **Appendix I**. **Figure A1** shows the standard curve of RR120 dye. The ingredients of the liquid and solid mineral-based medium (MBM) is given in **Appendix II**. The bacterium was preserved through

routine biweekly transfers under aseptic conditions and subsequent to a 24-hour incubation period at 35°C, they were preserved at 4°C.

3.3.2. Isolation, screening, and selection of microbial strains capable of RR120 dye degradation

A soil sample contaminated by textile dyes was gathered from a local textile industry, West Bengal, India, known for its prolonged and intensive application of textile dyes. The acclimatization culture technique was used to isolate the potent dye-removing bacterial strain (Benali et al., 2020). The inoculum comprised 1 gram of soil contaminated with dye placed in 9 ml of a 0.85% saline solution was subjected to vortex for 5 minutes, and thereafter left to settle. Dye content was 50 mg L^{-1}, and a combination was created by blending 5 ml of soil solution with 45 ml of mineral base medium. The flasks were incubated at 35°C without agitation. Thereafter, the culture was moved to new medium that had been augmented with more RR120 until the distinctive red hue of the RR120 disappeared. A stepwise increase in concentration from 50 to 600 mg L^{-1} was performed, using 50 mg L^{-1} increments. For each RR120 concentration, the culture was subcultured three to four times in order to provide the microorganisms the optimal acclimatization. It was placed on top of a solid mineral base media that included 600 mg L^{-1} of RR120 dye. The potent bacteria's tolerance level was ascertained by progressively raising the dye concentration to 2000 mg L^{-1}. For 24 hours, the plates were maintained at 35℃. After displaying unique morphological traits on solid plates, the colonies were further refined by being re-streaked as isolated colonies on fresh MSM agar enriched with RR120 with a dye concentration of 600 mg L^{-1}. The identified isolate maintained separately in plates and stored at 4°C in glycerol stocks.

3.3.3. Characterization of the isolated strain

Using biochemical, optical microscopy, and molecular techniques, the potent selected bacterial strain was characterized.

3.3.3.1. Morphological Characterization

The Gram staining method was used to carry out the morphological investigations. Following the recommended procedure, isolated bacteria were gram-strained and studied using a phase-contrast light microscope (OPTIKA, Italy). Using a field emission scanning electron microscope (FESEM) (FEI INSPECT F50, USA), the bacterial cell's geometry was

examined. The images were taken at a 40000X magnification, using an accelerating voltage of 5 kV.

3.3.3.2. Molecular Characterization

As determined by 16S rRNA sequence homology with related species, a phylogenetic study of the isolated potent microbial strain was conducted. The DNA was examined and measured for quality after being removed from the pure cultures. Primers 8F and 1492R were employed to construct the 16S rRNA gene. The amplicons were sequenced utilizing the Sanger Big Dye Termination method (BDT v3.1 Cycle Sequencing kit) after capillary electrophoresis, yielding forward and reverse sequences on an ABI 3500 Genetic Analyzer. BLAST is then used to compare a representative sequence for the 16S rRNA gene to the NCBI GenBank unique database. The highest identity score is employed to choose the initial fifty sequences. The sequences are synchronized with Clustal W, a program for multiple alignments. A Kimura 2-parameter model (Kimura, 1980), was employed to evaluate the divergence in evolution of the sequences. MEGA 11 (S. Kumar, Stecher, & Tamura, 2016) was used for the evolutionary investigations, and the Neighbour Joining approach (Saitou & Nei, 1987) was used to reconstruct evolutionary history.

Using an online application tool, the thermodynamic parameters of the isolated strain were obtained, including its Gibb's free energy (ΔG), GC content, entropy (ΔS) and enthalpy (ΔH) (https://cail.cn/biotool/oligo/index) (Sandhibigraha, Chakraborty, Bandyopadhyay, & Bhunia, 2020).

3.3.3.3. Biochemical and physiological Characterization

The purified and effective bacterial isolate was characterized microbiologically and biochemically in accordance with Bergey's Manual of Systematic Bacteriology and Hicarbohydrate Kit (Himedia) (Brenner, Krieg, Staley, & Garrity, 2005).

3.3.3.4. Physiological Characterization

3.3.3.4.1. Impact of shaking and static conditions

Both static and agitated circumstances were used in the study on the discoloration of RR120 dye. A 10% (v/v) inoculum of the isolated bacterial strain was introduced to 100 mL flasks containing 20 mL of a liquid mineral-based medium with 200 mg L^{-1} of RR120 dye. The flasks underwent incubation for 48 hours maintained at 37°C while agitated at 150 RPM, both under shaking and static conditions.

3.3.3.4.2. The effect of the initial dye concentration on the efficiency of decolorization

The decolorization evaluation was conducted in 20 mL of mineral-based liquid media was dispensed into 100 mL flasks seeded with 10% (v/v) of isolated bacteria cultured for 48 hours. The initial doses of RR120 dye ranged from 100 to 1000 mg L^{-1}, were assessed to see how well the potent bacterial strain decolored. The flask was incubated in static condition for 48 hours at 37°C. All experiments were conducted in triplicate, and abiotic control (without bacterial culture) was also maintained.

3.3.3.4.3. Impact of incubation duration on decolorization efficiency

For the investigation, 20 milliliters of liquid mineral-based media included a dosage of 600 mg L^{-1} RR120 dye. Flasks were introduced with an overnight bacterial culture at 10% (v/v), and they then underwent incubation under static conditions. Additionally, abiotic control- that is, without bacterial culture was maintained and the experiments were conducted in triplicates.

3.3.3.4.4. Impact of pH on decolorization efficiency

The decolorization evaluation was conducted in 20 mL of mineral-based liquid media was dispensed into 100 mL flasks seeded with 10% (v/v) of isolated bacteria cultured for 48 hours. The pH of the media ranged from 5 to 12. The flask was incubated in static condition for 48 hours at 37°C. All experiments were conducted in triplicate, and abiotic control (without bacterial culture) was also maintained.

3.3.3.4.5. Impact of temperature on decolorization efficiency

The decolorization evaluation was conducted in 20 mL of mineral-based liquid media was dispensed into 100 mL flasks seeded with 10% (v/v) of isolated bacteria cultured for 48 hours. The temperature of the experiment ranged from 22 to 42℃. The pH of the media was 8. The flask was incubated in static condition for 48 hours. All experiments were conducted in triplicate, and abiotic control (without bacterial culture) was also maintained.

3.3.3.4.6. Impact of inoculum size on decolorization efficiency

The decolorization evaluation was conducted in 20 mL of mineral-based liquid media was dispensed into 100 mL flasks seeded with isolated bacteria cultured for 48 hours. The inoculum size ranged from 2 to 14% (v/v). The pH of the media was 8. The flask was incubated in static condition for 48 hours at 37°C. All experiments were conducted in triplicate, and abiotic control (without bacterial culture) was also maintained.

3.3.3.4.7. Impact of co-substrates on decolorization efficiency

The decolorization evaluation was conducted in 20 mL of mineral-based liquid media was dispensed into 100 mL flasks seeded with 10% (v/v) of isolated bacteria cultured for 48 hours. The pH of the media was 8. Different substrate (1% (w/v)) was utilized such as beef extract, peptone, NH_4Cl, $(NH_4)_2SO_4$, yeast extract, urea, starch, glucose, sucrose, lactose. The flask was incubated in static condition for 48 hours at 37°C. All experiments were conducted in triplicate, and abiotic control (without bacterial culture) was also maintained.

3.3.3.5. Characterization of Antibiotics susceptibility

In accordance with Benali et al., 2020, the disc diffusion assay was utilized to conduct antimicrobial susceptibility testing (AST) (Benali et al., 2020). Mueller-Hinton agar (MHA) and antibiotic discs (Hi-media, India) were utilized to evaluate the susceptibility of the identified bacterial strain to a panel of eight antimicrobial agents from eight different classes. A variety of antibiotics were used, including azithromycin (15 µg), cefradine (25 µg), ampicillin (10 µg), aztreonam (50 µg), ciprofloxacin (30 µg), doxycycline (30 µg), chloramphenicol (30 µg) and gentamicin (10 µg). The multiple antibiotic resistance (MAR) index was derived by dividing an isolate's antibiotic susceptibility by the whole amount of antibiotics tested against it (Taieb et al., 2021).

3.3.3.6. Evaluation of the isolated bacterial strain's metabolic diversity

The species' metabolic flexibility was assessed by introducing the robust bacteria into an inorganic medium enriched with 1% glucose and 1% yeast extract with the inclusion of diverse azo dye compounds such as Reactive Red 13 (RR13), Acid Black 194 (AB194), Methyl Orange (MO), Reactive Yellow 135 (RY135), Direct Violet 1 (DV1) and Congo Red (CR). A concentration of 200 mg L^{-1} of azo dye compounds was incorporated within the mineral nutrient solution. 2 milliliters of cells (OD600 = 1.0) added to each flask, the samples maintained at 37°C under static conditions for 48 hours. Post 48-hour incubation, the amounts of the residual dye components were quantified using a spectrophotometric method. Using a spectrophotometric method, the remaining dye component concentrations were determined at a wavelength of 532nm, 588nm, 464nm, 415nm, 499nm, 547nm respectively following the incubation period (Chakraborty et al., 2013; Kishor et al., 2021). The maximum wavelengths of the azo dyes were obtained by spectral scan using UV-VIS spectrophotometer (Perkin Elmer LAMBDA 365). The decolorization percentage was established as:

$$\%\ Decolorization = \frac{(Initial\ absorbance - Final\ absorbance)}{Initial\ absorbance} \text{ X } 100$$

3.4. Optimization of the operational parameters for enhanced RR120 dye degradation using isolated strain

3.4.1. Optimization with the Taguchi Design of Experiments orthogonal array methodology

Taguchi Design of tests (DOE) entails the creation of several experimental conditions via Orthogonal Arrays (OAs) to minimize empirical mistakes and improve the performance and repeatability of tests. This work incorporates robust design to mitigate the impact of noise components during optimization, resulting in a dynamic experimental design (Taguchi & Phadke, 1984). The planning, analyzing, validating, and conducting phases are the four independent steps.

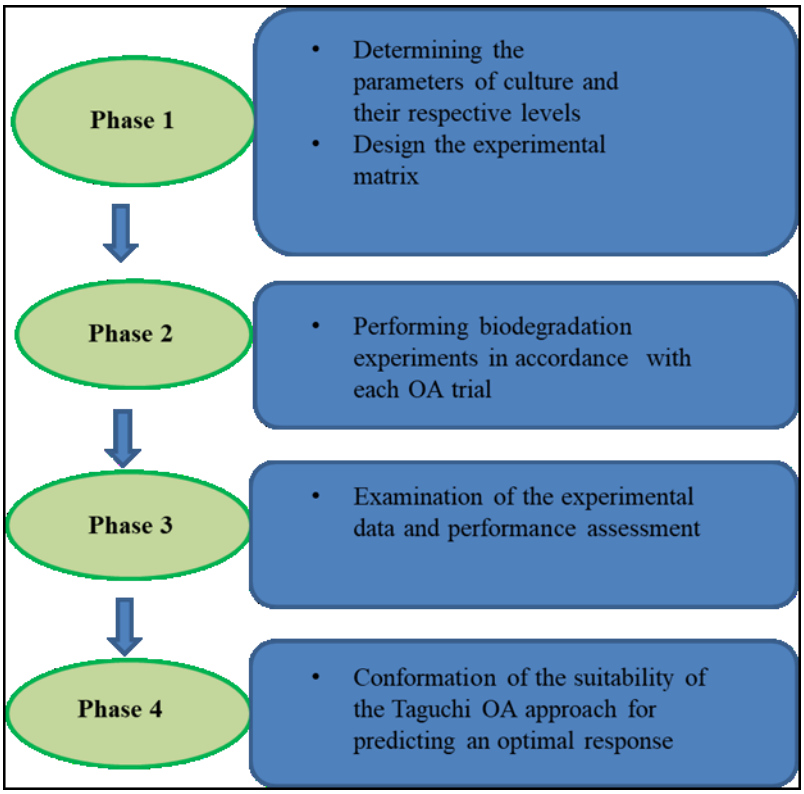

Figure 3.1: Flow diagram illustrating the stages in the Taguchi Methodology-based parameter optimization process

The Taguchi technique's process flow is shown in **Figure 3.1** Every stage is as important and is connected to its descendants in the flow chart, but it is also isolated from the others.

3.4.1.1. Design of experiments (phase 1)

A preliminary series of assessments, not detailed here, highlighted the many elements to be adjusted that significantly affect the biodegradation of RR120. Every variable was analyzed within the permissible range to make sure the effect of the factor was not obscured by the inherent process variation (K. K. Prasad, Mohan, Rao, Pati, & Sarma, 2005). Initially, the process variables that are most important regarding the degradation of RR120 dye were selected. To enrich the medium with carbon and nitrogen nutrients that were believed to be required for azo dye RR120 degradation experiments, yeast extract and glucose were employed in this study (Manogaran et al., 2021). Several physical conditions, including temperature, pH, and inoculum dosage, clearly affect the degradation of RR120 dye. Therefore, these process parameters are also included while evaluating biodegradation analysis. The Taguchi methodology used orthogonal arrays (OA) to build up numerous studies in order to optimize every process parameters. The preliminary investigation established the level of each element. Since the output variation of the process did not obscure the specific effects of the parameters, the range of feasibility was used to assess the extent of parameter analysis. The experimental data for designing the OAs was subjected to analysis via Qualitek-4 software (Nutek Inc., MI, USA), determine the best process conditions, assess process performance, and ascertain the relative importance of each component and the way they interact. A matrix was built for this inquiry by selecting the pertinent OAs using the software's automatic selection menu. The suitable OAs is determined by the quantity and magnitude of parameters, even if the Taguchi process employs a range of standardized OAs. Three levels of five components were used in this work to analyze the RR120 dye degradation **Table 3.1**, and an array of symbolic L-18 OAs was used to illustrate the experimental outcomes.

Table 3.1: Factors along with their respective levels

Serial no.	Factor code	Factor	Level-1	Level-2	Level-3
1	A	C-source (Glucose) (g/L)	0.5	1.0	1.5
2	B	N-source (Yeast extract) (g/L)	0.5	1.0	1.5
3	C	pH	6	8	10
4	D	Temperature(℃)	27	32	37
5	E	Inoculum dose % (v/v)	2	6	10

3.4.1.2. Biodegradation of RR120 by the isolate under specified conditions and parameters (phase 2)

Five milliliters of the culture were taken out after a specified period of time, and the remaining RR120 was measured by centrifuging it in a centrifuge machine (REMI) at 4000 rpm for 20 minutes at 4°C. The decolorization efficiency was determined using spectrophotometry (Perkin Elmer LAMBDA 365) by examining the supernatant from the culture at 535 nm (Rajendran, Kiruthika, Saranya, Mohan, & Vaishali, 2021). The decolorization percentage was defined as:

$$\%\ Decolorization = \frac{(Initial\ absorbance - Final\ absorbance)}{Initial\ absorbance}\ \text{X}\ 100$$

Experiments were performed three times, with the average results reported.

3.4.1.3. Evaluation of data and estimation of performance (phase 3)

The biodegradation experiments for each of the 18 trials (performed in triplicate) were carried out using a dye concentration of 600 mg L^{-1} (RR120). The process response (RR120 elimination) was analyzed under both ideal and current circumstances using the 'larger is better' feature of the Signal-to-Noise (S/N) ratio was employed to assess performance quality. It was represented using the signal-to-noise (S/N) ratio. In this instance, the signal represents the desired result, in which noise is defined as the standard deviation obtained from multiple attempts. The output quality attributes are computed using the signal-to-noise ratio and are presented as a deviation from the intended value. Equation (1) may be utilized to determine the S/N ratios of the experimental data.

$$\text{S/N} = -10\ \log_{10}\left(\frac{1}{n}\sum_{i=1}^{n}\frac{1}{y_i^2}\right) \qquad (1)$$

In this context, y represents the mean of the outcome (namely, biomass growth and RR120 degradation percentage), whereas n denotes the number of replications for each experiment.
Using the ideal process parameters from the Taguchi Methodology, confirmatory biodegradation tests were conducted to confirm the results.

3.4.1.4. Experimental model validation (phase 4)

To verify the optimal conditions established by the Taguchi experimental design, cultivation environments were assessed by a total of three sets of biodegradation tests.

3.5. Investigation of batch kinetics for the RR120 dye biodegradation using isolated strain and phytotoxicity analysis

3.5.1. Biodegradation kinetics study

In order to assess kinetic parameters, a batch shake flask experiment was conducted by introducing 2 mililiters of cells (OD600 ≈ 1.0) that had been previously acclimated at 600 mg L^{-1} of RR120 dye into 20 mililiters of an optimized inorganic medium, as well as 1 g L^{-1} yeast extract and 1 g L^{-1} glucose. Subsequently, the mixture was subjected to incubation for 48 hours at 37°C in a stationary environment. The media composition utilized for the breakdown investigation was described as (g L^{-1}): Glucose 1, Yeast Extract 1, KH_2PO_4 0.5, K_2HPO_4 1.5, NaCl 0.5, $MgSO_4.7H_2O$ 0.2, $CaCl_2.2H_2O$ 0.026, and $FeSO_4.7H_2O$ 0.0025. The medium contained RR120 dye at 600 mg L^{-1}, with carbon and nitrogen sources. Sampling was performed at 4-hour intervals to quantify residual RR120 dye and cell concentration.

3.5.2. The effect of temperature and pH on the specific growth rate and specific decay rate

This work investigated the impact of temperature on the kinetics by incubating the production media at several temperatures: 30, 35, 37, 40, 45^{o}C, while keeping the pH constant at 8. An investigation was conducted to evaluate the impact of pH on kinetic parameters by incubating production medium at different pH values, namely 6, 7, 8, 9, 10 while maintaining a constant temperature of 37^{o}C. Each batch process was conducted in the 100 ml conical flask with the medium composition kept constant. Each experiment was repeated three times to assure accuracy.

3.5.3. Phytotoxicity study

Plant model systems are often taken into consideration for toxicological study because of their complex eukaryotic structure. Common biotesting techniques to evaluate environmental contamination include the root-elongation bioassay and germination assessments. In this test, plant seeds are exposed to potentially harmful substances, and the index of seed germination and amount of growth of root are then evaluated. These bioassays offer a rather easy, dependable, a cost-effective and productive method for evaluating the potential phytotoxicity of this compound. Three distinct seed varieties were chosen for germination bio-testing in this study: *Cicer arietinum, Vigna radiate*, and *Vigna mungo*. The seeds that were chosen all had similar weights and sizes. A 0.1% $HgCl_2$ solution was used to surface sterilizes the seeds

after they had been cleansed using distilled water, and they underwent another thorough washing in distilled water. A thin layer of absorbent cotton topped with whatman filter paper (No. 1) was implanted on the exterior of the petri plates in order to conduct experiments for root growth and seed germination. The grains of *Vigna radiata*, *Cicer arietinum,* and *Vigna mungo* were immersed in distilled water prior to use for six hours, and then equal volume (5ml) of distilled water (Control), RR120 dye (600 mg L^{-1}) and biodegraded sample were added to the filter paper. The experiments were performed in duplicates. For five days, every petri dish was incubated at 37°C. Total quantity of germinated seeds and root (radicle) lengths of the seedlings treated within each test setup, it was recorded following the incubation phase. The formula shown below was employed to compute relative seed germination (RSG) (Enaime et al., 2020):

$$\text{RSG} = \frac{\text{Seed germination number in the sample}}{\text{Seed germination number in the control sample}} \text{ X } 100$$

In each experimental setup, the root lengths of the sample and the control were measured. The following equation was employed for determining the relative root growth (RRG) (Enaime et al., 2020):

$$\text{RRG} = \frac{\text{Root growth observed in the sample}}{\text{Root growth observed in the control}} \text{ X } 100$$

The following equation is employed to calculate the phytotoxicity index (PI), a crucial metric in phytotoxicity assessment (Rusan, Albalasmeh, Zuraiqi, & Bashabsheh, 2015):

$$\text{PI} = 1 - \frac{\text{Root length in the sample}}{\text{Root length in the control}}$$

PI value is ranging between 0 and 1, with a low PI value denotes a stimulatory effect and a high PI value implies higher toxicity (Rusan et al., 2015).

The subsequent formula is utilized to calculate the germination index (GI) (Enaime et al., 2020):

$$\text{GI (\%)} = \frac{\text{RSG X RRG}}{100}$$

As reported in the literature, the significance of GI values differs. For instance, a value below 40% signifies strong inhibition, while a range of 40–60% suggests significant inhibition. A range of 60–80% reflects minor inhibition, and values between 80–100% indicate no suppression of plant development (Trautmann & Krasny, 1998).

3.5.4. Statistical analysis

The statistical software package, Qualitek-4 software (Nutek Inc., MI, USA) is used to analyze the experimental design and carry out the regression analysis of the experimental data. For model parameter estimation, differential equation of the model was solved using Xpp out software using Runge-Kutta method. Graphpad Prism 5 software was used for nonlinear regression analysis.

CHAPTER 4

RESULTS AND DISCUSSION

4. Results and Discussion

The findings of this research are delineated into three objectives throughout three distinct sections, as mentioned below.

- Isolation and characterization of RR120 dye degrading isolated strain
- Optimization of the operational parameters for enhanced RR120 dye degradation using isolated strain.
- Investigation of batch kinetics for the RR120 dye biodegradation using isolated strain and phytotoxicity analysis

4.1. Isolation and characterization of RR120 dye degrading isolated strain

4.1.1. Dye decolorizing bacterial strain: Isolation and screening

Textile effluents have long been recognized as a valuable source for isolating of effective dye removal bacteria due to their toxic effect and capacity to adapt to high dye concentrations (Pokharia & Ahluwalia, 2013; A. A. Prasad & Rao, 2010). The acclimatization culture approach was employed to isolate a dye-decolorizing bacterial strain from textile wastewater obtained from the effluent of a textile production unit and from dye-contaminated soil. The amount of RR120 was elevated gradually, ranging from 50-600 mg L^{-1} with 50 mg L^{-1} increments. Additionally, the bacterial strain's tolerance threshold was ascertained. The chosen concentration was 600 mg L^{-1}, as it represented the highest degradation level reported to date. After demonstrating maximal decolorization efficacy of 600 mg L^{-1} of dyes by decolorizing >70% of 600 mg L^{-1}, six possible morphologically distinct isolates—JU_CHE_01, JU_CHE_02, JU_CHE_03, JU_CHE_04, JU_CHE_05 and JU_CHE_06 were chosen for further research (**Table 4.1**). Literature suggests that concentrations of reactive azo dye levels in textile effluents can fall within 10–50 mg L^{-1} (Laing, 1991) to 100–250 mg L^{-1} (Ghaly, Ananthashankar, Alhattab, & Ramakrishnan, 2014). In effluent, higher concentrations of dye have also been observed; Vandevivere et al. found reactive dye concentrations of 600–800 mg L^{-1}, while Koprivanac et al. recorded 7000 mg L^{-1} (Koprivanac, Bosanac, Grabaric, & Papic, 1993; Vandevivere et al., 1998). Consequently, a reliable approach for breaking down elevated levels of the textile azo dye RR120 is necessary.

However, changes in operating parameters may result in a higher amount of dye present in textile effluent. In light of the previously mentioned details, a dye level of 600 mg L^{-1} was

employed in this investigation to evaluate the decolorization effectiveness for RR120 dye. The JU_CHE_01 strain had the highest decolorization efficacy of RR120 dye at roughly 90% with 600 mg L^{-1} dye among other five isolates. The microbial strains found in the wastewater from textile industries demonstrate how microorganisms will adapt to harmful colors in order to survive. The decrease in the synergistic interaction that the bacteria can share in certain environmental conditions is responsible for the difference in their decolorization rate (Siemiatycki et al., 2004).

Table 4.1: Selecting the optimal strain of bacteria through screening

Microbial isolates	Size of colony	Form of colony	Pigmentation of colony	Elevation of colony	Maximum Decolorization (%) (600 mg L^{-1})
JU_CHE_01	Large	Circular	White	Raised	90
JU_CHE_02	Moderate	Irregular	Light pink	Flat	72
JU_CHE_03	Moderate	Irregular	Light pink	Raised	71
JU_CHE_04	Small	Circular	Red	Raised	89
JU_CHE_05	Large	Circular	Red	Flat	75
JU_CHE_06	Small	Irregular	White	Flat	70

4.1.2. Characterization of the isolated strain

4.1.2.1. Morphological Characterization

The bacterial isolate *P. aeruginosa* JU_CHE_01 displayed unique colony and cellular traits when cultured on nutrient agar plates. Colonies exhibited an uneven morphology, with an approximate diameter of 1 mm, characterized by a low convex elevation and borders that were whole to slightly undulate. The colonies exhibited a white hue and a smooth surface texture upon first isolation, subsequently appearing mucoid due to the formation of a slime layer. Colony opacity varied from translucent to opaque, indicating active metabolic response to diverse growth environments.

Microscopic analysis after Gram staining indicated that the isolate was Gram-negative, exhibiting rod-shaped morphology. The bacterial cells were primarily organized individually or sporadically in pairs. The average cell diameters were roughly 0.9-1.5 µm in length and about 0.5 µm in breadth, aligning with standard Pseudomonas morphology.

Figure 4.1, 4.2, and **4.3** shows images of colony morphology, cellular morphology obtained by gram staining method and the SEM analysis respectively.

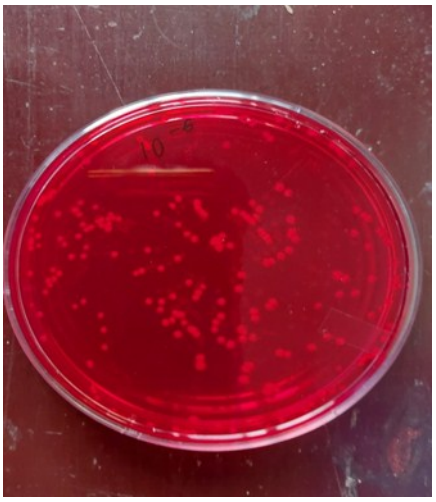

Figure 4.1: Image displaying the morphology of the isolate *P. aeruginosa* JU_CHE_01 colony on dye containing mineral agar plates

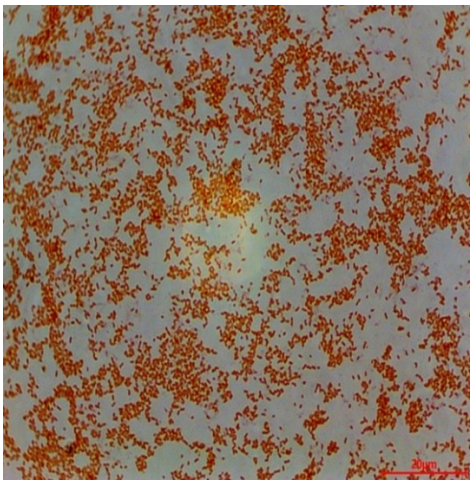

Figure 4.2: Cellular morphology of isolate *P. aeruginosa* JU_CHE_01 (gram staining image displayed in a light microscopy)

Figure 4.3: Scanning Electron Microscopy (SEM) picture of *P. aeruginosa* JU_CHE_01

4.1.2.2. Molecular Characterization

The identified potent microbial strain was subjected to phylogenetic analysis according to 16S rRNA sequence similarity with comparable species. After the strain's genomic DNA has been extracted, PCR was carried out using a particular designed primer for the 16S rRNA gene. **Figure 4.4** showed a single, clear 1,500 bps PCR amplicon band after resolution on a 1.2% agarose gel. 16S rRNA gene of this bacterial strain uploaded to the GenBank database of NCBI (www.ncbi.nlm.nih.gov) alongside the accession number OR388872. To conduct BLAST against the NCBI GenBank data, the 16S rDNA sequence served as the basis. The alignment table shown in **Table 4.2** contains information on additional adjacent homologs for microorganisms. It was determined that the isolated bacterial strain was *P. aeruginosa* (**Table A1**). **Figure 4.5** displays the phylogenetic tree with the greatest possibility, generated using the MEGA 11 program.

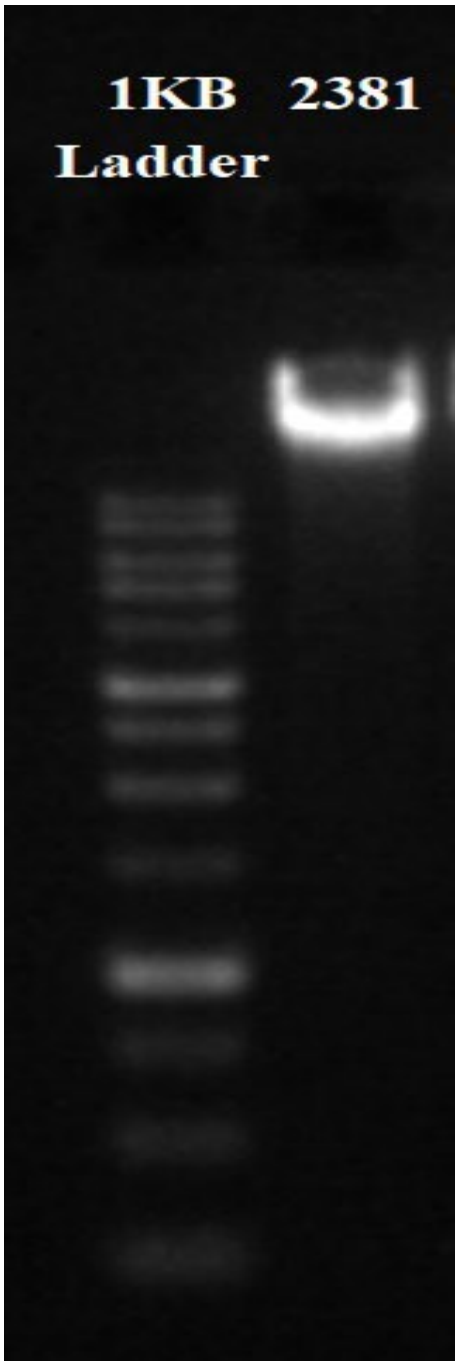

Figure 4.4: Agarose gel (1.2%) displaying a singular 1,500 bp fragment of 16S rDNA amplicon. Lane 1: 100 base pair DNA ladder; Lane 2: 16S rDNA amplification product

Table 4.2: Sequences that generate substantial alignments

Accession	Description	Max. Score	Total Score	Query coverage	E value	Maximum Identity
MW846270.1	*Pseudomonas aeruginosa* strain 25	1602	1602	83%	0.0	100.00%
MN647070.1	*Pseudomonas aeruginosa* strain CM3	1600	1600	83%	0.0	100.00%
MK503459.1	*Pseudomonas aeruginosa* strain E	1600	1600	83%	0.0	100.00%
KT232079.1	*Pseudomonas aeruginosa* strain AS36	1600	1600	83%	0.0	100.00%
KF929428.1	*Pseudomonas aeruginosa* strain AR01	1600	1600	83%	0.0	100.00%
MH084956.1	*Pseudomonas aeruginosa* strain Tn 6	1600	1600	83%	0.0	100.00%
EU194239.1	*Pseudomonas aeruginosa* strain CMG590	1600	1600	83%	0.0	100.00%
AY792969.1	*Pseudomonas aeruginosa*	1600	1600	83%	0.0	100.00%
MT353653.1	*Pseudomonas aeruginosa* strain OFAA14	1598	1598	83%	0.0	100.00%
MN611437.1	*Pseudomonas aeruginosa*	1598	1598	83%	0.0	100.00%
MN006645.1	*Pseudomonas aeruginosa* strain Pw3	1598	1598	83%	0.0	100.00%
KX214108.1	*Pseudomonas aeruginosa* strain 352CR	1598	1598	83%	0.0	100.00%
OR039660.1	*Pseudomonas aeruginosa* strain Y4	1598	1598	83%	0.0	100.00%
OR039115.1	*Pseudomonas aeruginosa* strain 2	1598	1598	83%	0.0	100.00%

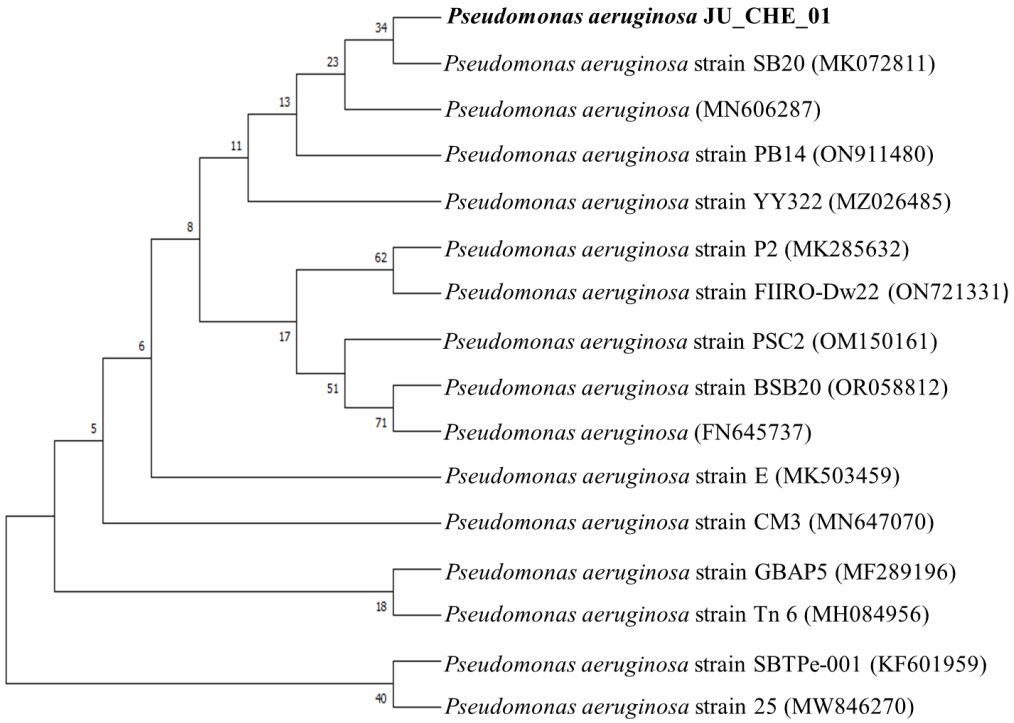

Figure 4.5: Phylogenetic tree illustrating the evolutionary relationships of *P. aeruginosa* JU_CHE_01 with fifteen taxa by the use of the Neighbor-Joining technique

4.1.2.3. Biochemical Characterization

The biochemical properties and physical features chosen isolate strain were conducted in accordance with the protocols outlined in Bergey's Manual of Systematic Bacteriology and Hicarbohydrate Kit (Himedia) (**Table 4.3**).

Table 4.3: Colony characterization and morphological, biochemical, physiological characteristics of the selected bacterial isolate

Shape	Irregular
Size	1 mm
Elevation	Low Convex
Color	White
Surface	Smooth-textured (fresh isolation); Mucoid-textured (in the presence of a slime layer)
Opacity	Translucent – Opaque
Gram staining	Negative
Cell shape	Rod-shaped
Cell arrangement	Single, pair (occasionally)
Cell size	Approximately length (0.9-1.5 μm) and width (0.5 μm)
Spore staining	Non spore former
Motility	Motile
Flagella	Uni-polar
Catalase	Positive
Oxidase	Positive
Urease	Positive
H_2S production	Positive
Nitrate reduction	Negative
Citrate utilization	Positive
Voges-Proskauer test	Negative
Methyl red test	Negative
Indole test	Negative
Starch hydrolysis	Negative
Gelatine hydrolysis	Positive
Lysine utilization	Negative
Ornithine utilization	Negative
Casein hydrolysis	Positive
Phenylalanine deamination	Negative
Carbohydrate Utilization	**Results**
Lactose	Negative
Xylose	Positive
Maltose	Negative
Fructose	Negative
Dextrose	Positive
Galactose	Positive
Raffinose	Negative
Trehalose	Negative

Melibiose	Positive
Sucrose	Negative
L-Arabinose	Positive
Mannose	Negative
Inulin	Negative
Sodium gluconate	Negative
Glycerol	Negative
Salicin	Negative
Dulcitol	Negative
Inositol	Negative
Sorbitol	Negative
Mannitol	Negative
Adonitol	Negative
Arabitol	Negative
Erythritol	Negative
α Methyl-D-glucoside	Negative
Rhamnose	Negative
Cellobiose	Negative
Melezitose	Negative
α Methyl-D-mannoside	Negative
Xylitol	Negative
ONPG	Negative
Esculin hydrolysis	Positive
D-Arabinose	Positive
Malonate utilization	Positive
Sorbose	Negative
Growth performance across a range of pH levels: 5.5 6.5 7.5 8.5 9.5 10.5 Growth performance across a range of NaCl conc. (%): 1 2 5 7 10 Growth performance across a range of	 + ++ +++ ++ ++ + +++ ++ - - -

temperature (°C): 4 25 30 37 45	 - + ++ +++ ++

Note: + = Scanty, ++ = Moderate, +++ = Heavy, – = No growth

4.1.2.4. Physiological Characterization

Degradation of RR120 dye influenced by diverse environmental parameters was tested using isolated potent bacterial strain in batch experiment.

4.1.2.4.1. Impact of dye decolorization at static and shaking environments

Physiological characteristics exhibited by the cells that impact the effectiveness of decolorization are greatly influenced by oxygen during the cell growth phase (Pearce et al., 2003). Microbial dye decolorization can be either stimulated or inhibited by oxygen availability. In a similar way, it has caused the aromatic chemicals to mineralize by hydroxylation into a non-toxic product (Aftab et al., 2011). **Figure 4.6** illustrates the effect of stationary and agitated conditions on dye degradation efficacy by *P. aeruginosa* JU_CHE_01 strains. The static condition showed maximum decolorization by isolated potent bacterial strain for RR120 dye, which is significantly higher than the shaking condition. The *P. aeruginosa* JU_CHE_01 strain achieved ≥ 90% decolorization of RR120 under static conditions, whereas ≤ 45% decolorization was recorded under shaking conditions. Consequently, it was shown that the azo dye decolorization is best achieved in an anaerobic, static environment. In aerobic conditions, lesser azoreductase activity is probably the cause of the reduced degree of decolorization. During this process it was observed that at oxygen rich environment as compared to static condition, decolorization was much less due to presence of oxygen. At the same time, static condition exhibited >90% decolorization since azoreductase enzymes become activated in less oxygenated environment. In a similar study, decolorization of Reactive Red 22 increased under static condition by *Pseudomonas luteola* species (B.-Y. Chen, 2002). The demand for oxygen is very low because *P. aeruginosa* JU_CHE_01 has

shown decolorization in a microaerophilic environment. This will conserve a substantial quantity of kinetic energy required for the aerobic system and reduce operational expenses.

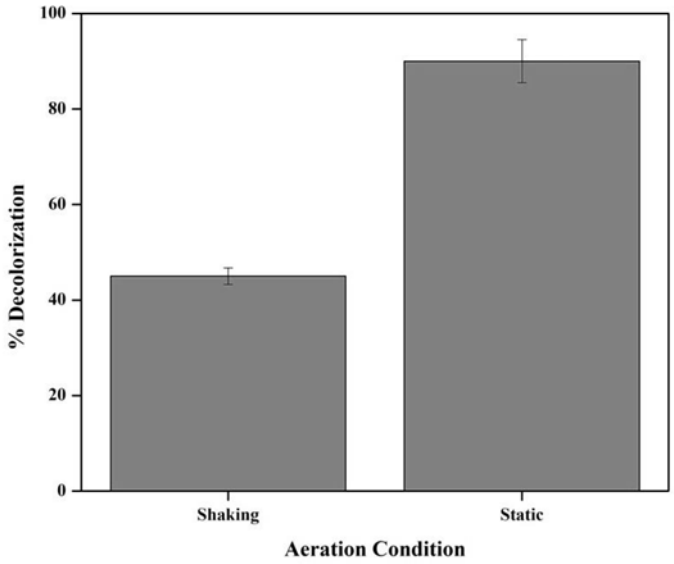

Figure 4.6: Impact of static and shaking circumstances on decolorization efficacy

4.1.2.4.2. Impact of incubation time on decolonization effectiveness

The incubation period affects dye bio-decolorization because the growth and metabolism of particular bacteria change with time. **Figure 4.7** showed the decolorization efficacy at a different time interval of RR120 dye by isolated strains. The findings indicate that isolated strain *P. aeruginosa* JU_CHE_01 achieved an increased decolorization efficacy of 90.02% and 50.24% respectively, following incubation periods of 48 and 24 hours. The interpretation of **Figure 4.7** suggested that a higher bacterial growth rate is associated with a higher decolorization efficacy. The data indicates a correlation between cell proliferation and the decolorization activity of the isolated strain (Ogugbue & Sawidis, 2011).

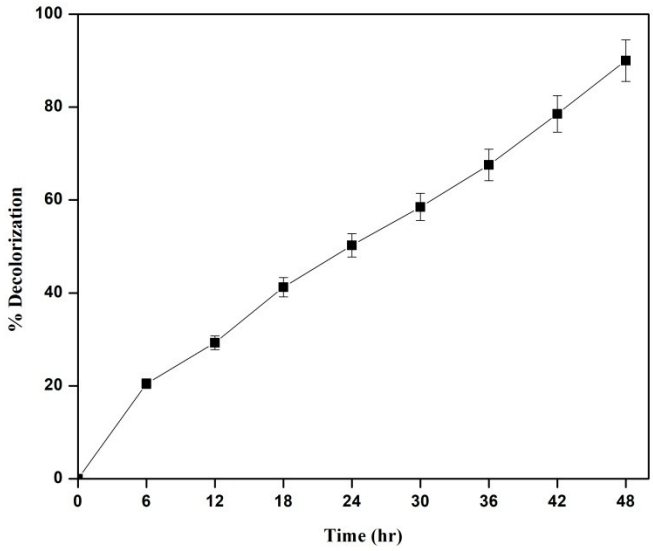

Figure 4.7: Impact of incubation duration on the decolorization efficacy of RR120 dye by *P. aeruginosa* JU_CHE_01

4.1.2.4.3. Impact of dye concentration on removal of color efficacy

The decolorization of dye is substantially affected by the dye concentration. The fact that the decolorization efficacy has decreased noticeably with rising dye levels might be a consequence of the dye's harmful impact on microorganisms or their ability to hinder the active site of enzymes. Consequently, it is crucial to investigate the capacity of the bacteria for tolerance as well as their ability to decolorize at increasing dye concentrations for industrial processes. The dye concentration observed in the dyeing workshop effluents is found ranging between 100 mg L^{-1} to 2000 mg L^{-1} (U. U. Jadhav, Dawkar, Ghodake, & Govindwar, 2008).

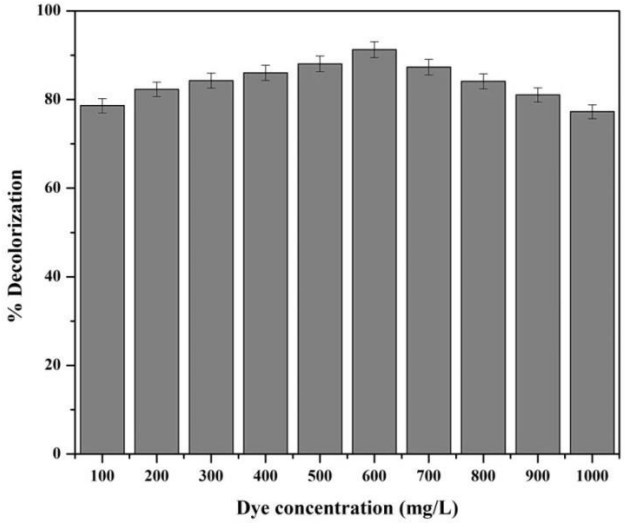

Figure 4.8: Effect of concentration of dye focusing on decolorization efficiency by *P. aeruginosa* JU_CHE_01

Figure 4.8 depicts the impact of initial dye concentration on the removal efficacy of color by *P. aeruginosa* JU_CHE_01. This isolated strain was used to investigate the decolorization capacity across a concentration range of 100 and 1000 mg L^{-1} and tolerance of RR120 dye upto 2000 mg L^{-1}. The decolorization efficiency of dye concentration of 100, 200, 300, 400, 500, 700, 800, 900, 1000 mg L^{-1} were observed 78%, 83%, 85%, 87%, 89%, 88%, 84%, 82%, 75% respectively. The isolate successfully achieved maximum decolorization efficacy while tolerating higher dye concentrations. The greatest amount of degradation was achieved at 600 mg L^{-1} of dye. For RR120, *P. aeruginosa* JU_CHE_01 strain showed >90% decolorization. The growth and efficacy of the microorganisms in decolorizing the dye are greatly impacted by further increases in dye concentration, which reduces the efficiency of decolorization. It was noted that elevating the initial concentration of RR120 led to diminished decolourisation kinetics, necessitating extended incubation periods to attain partial or equivalent colour removal at elevated dye concentrations. This is mostly attributable to the hazardous characteristics and degradation products of the dye (Ogugbue & Sawidis, 2011). The present research illustrates effective decolourisation of RR120 at elevated concentrations (600 mg/L) under regulated conditions; however, performance in real textile wastewater, which is characterized by greater dye concentrations and diverse contaminants, may differ and necessitates additional validation with real effluent samples.

4.1.2.4.4. Influence of Temperature, pH and Inoculum volume on decolorization effectiveness

Temperature, pH, and inoculum volume are critical variables that must be controlled to maximize the metabolic function of bacterial proliferation and dye decolorization. These variables affect multiple biochemical and enzyme-driven processes as well as cell growth. Because reactive dye procedures are frequently carried out in alkaline environments, pH is a crucial variable for industrial processes (Aksu & Tezer, 2000). The pH effect strongly influences bacterial metabolism and growth. Textile effluent is typically alkaline as a result of the high salt usage during dyeing; however its pH can vary. The pH is alkaline to create an affinity among the dye and cellulose-based fibers (Walters, Santillo, & Johnston, 2005). By analyzing the impact of pH in the range of 5 to 12, the decolorization effectiveness of the isolated strain of bacteria was evaluated (**Figure 4.9**). At slightly alkaline pH of 8, this bacterium showed the greatest decolorization efficiency. The decolorization efficiency was diminished at acidic pH as a result of suppressed bacterial growth and competition of H^+ ions with dye cations. The cell membrane becomes negatively charged at slightly alkaline pH, which maximizes the decolorization effectiveness by enhancing the interaction of cationic dye molecules via electrostatic interactions (Ayed, Chaieb, Cheref, & Bakhrouf, 2009). Due to the existence of a higher proportion of dye metabolites or a higher concentration of hydroxide ions, the decolorization efficiency declines at high pH levels (10 to 12) (Pearce et al., 2003).

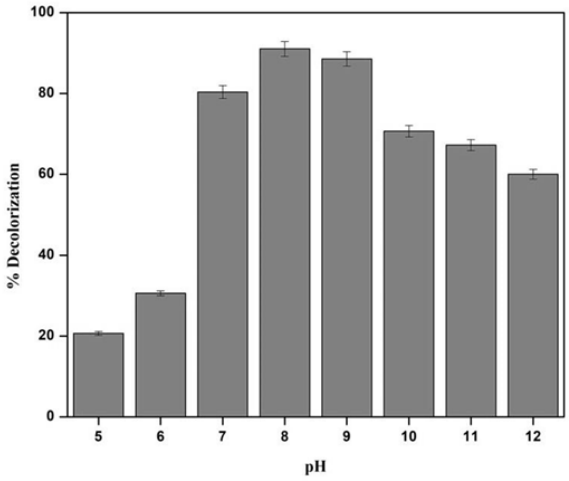

Figure 4.9: Influence of pH levels on RR120 decolorization performance

A crucial element influencing the metabolic activity of the bacteria is the incubation temperature, which should be taken into account while maximizing the biodegradation processes. To find the ideal decolorization effectiveness of the isolated strain, the investigations were conducted across a temperatures ranging from 22°C to 42°C (**Figure 4.10**).

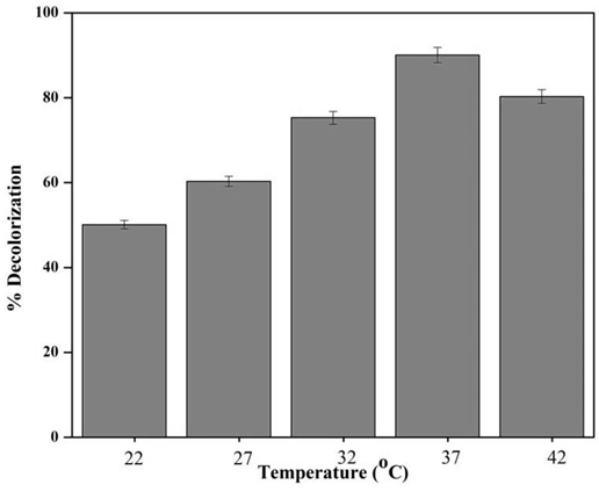

Figure 4.10: Impact of temperature on dye decolorization efficacy of RR120

Research indicates that elevating the temperature from 22°C to 37°C improves the color removal process. Strain *P. aeruginosa* JU_CHE_01 showed a maximum decolorization of 92.8% at 37°C. As the temperature rose above 40°C, the strain exhibited a significant decline in dye removal efficiency. At the optimal temperature, both decolorization efficacy and decolorization activity increased. At elevated temperatures, the enzyme activity is inhibited and cell viability is lost, which reduces the efficacy of decolorization (R. G. Saratale et al., 2011). Dye breakdown often takes place in the mesophilic temperature range. While psychophilic actions are slow, using thermophiles demands high temperatures and is not cost-effective (Beydilli, Pavlostathis, & Tincher, 2000).

In batch studies, microbes grow in a defined volume of nutrients, and the inoculum volume significantly impacts the efficacy of the procedure. An inoculum volume below the optimal range impairs biological activity, whereas a bigger amount has been linked to cell death and nutritional depletion, both of which have decreased the decolorization efficacy. The efficiency of decolorization of RR120 dye by *P. aeruginosa* JU_CHE_01 strain in response to different inoculum volumes is displayed in **Figure 4.11**. Observations revealed that with

an inoculum volume of 10% (v/v), the strain exhibited the highest decolourisation efficacy. Afterward, this strain showed that increasing the inoculum volume further reduced the decolorization efficiency. Ayed et al. (2009) found analogous findings indicating that as the volume of inoculum increased, the decolorization efficacy dramatically increased as well (Ayed et al., 2009). **Table 4.5** delineates research on the color removal of RR120 dye by diverse bacterial species.

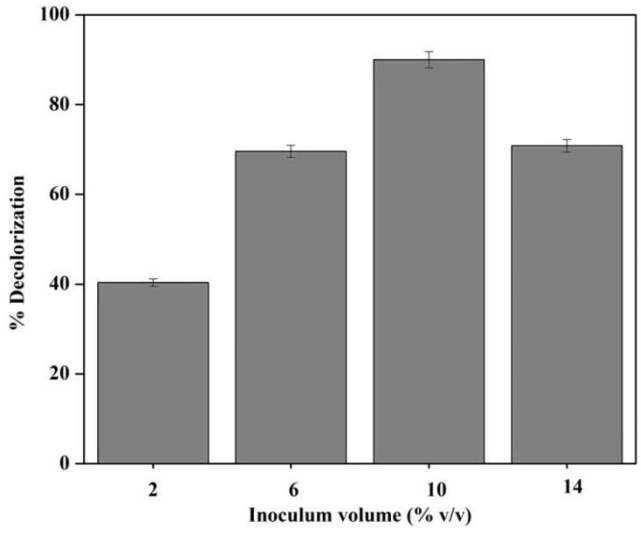

Figure 4.11: Impact of inoculum volume on decolorization efficacy of RR120 dye

4.1.2.4.5. The effect of co-substrate supplementation on decolorization performance

The supplementation with nitrogen and carbon sources to minimal salt medium can shorten the time required for isolated strain to decolorize specific dye. The decolorization process is significantly reliant on the incorporation of nitrogen and carbon sources, as dyes lack sufficient nitrogen and carbon (R. G. Saratale et al., 2011). The carbon-based sources are necessary for both the requirement for energy and the growth of microorganisms. Simultaneously, the organic nitrogen metabolism facilitates the regeneration of NADH, essential for the reductive breaking of bonds in dye molecules (Solis-Oba, Solís, Pérez, Manjarrez, & Flores, 2012).

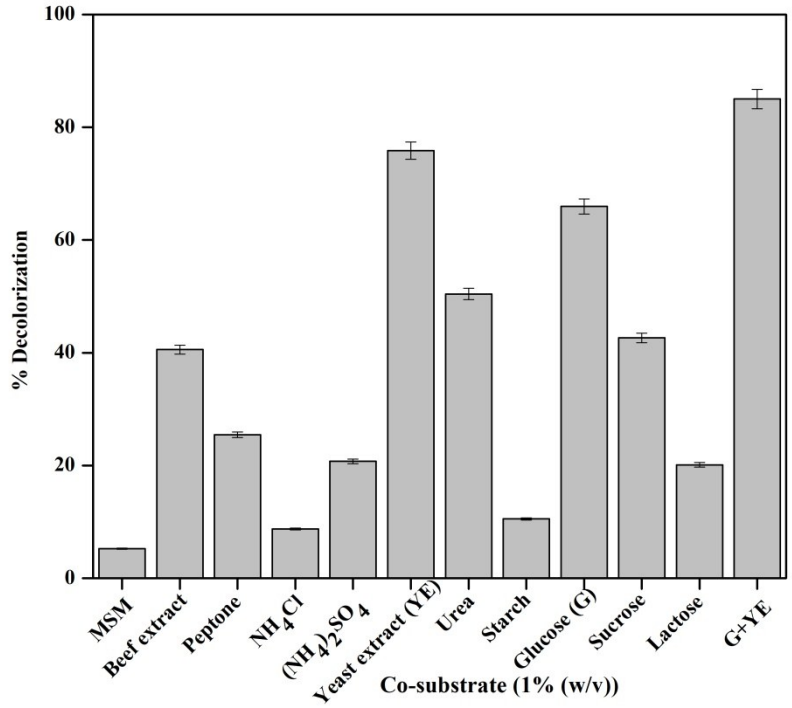

Figure 4.12: Influence of co-substrate supplementation on dye decolorization efficacy of RR120 by *P. aeruginosa* JU_CHE_01

For the model dye, only yeast extract showed the highest decolorization efficacy among the sources of nitrogen. It was found that yeast extract and glucose are the requirements necessary for the microbial strain to decolorize dye; the impact of several sources of carbon and nitrogen (1% (w/v)) were investigated. The results show that adding sources of nitrogen and carbon improved the effectiveness of decolorization.

The decolorization efficacy of RR120 by *P. aeruginosa* JU_CHE_01 varied considerably based on the type of co-substrate used. The observed decolorization percentages were as follows: MSM 5.26%, beef extract 40.56%, peptone 25.46%, NH_4Cl 8.75%, $(NH_4)_2SO_4$ 20.75%, yeast extract 75.86%, urea 50.42%, starch 10.53%, glucose 65.95%, sucrose 42.64%, lactose 20.12%, and glucose combined with yeast extract 85%. The combination of glucose (1 g/L) and yeast extract (1 g/L) yielded the highest decolorization effectiveness among the evaluated substrates. When provided separately, glucose or yeast extract facilitated only mild decolorization; however, their combined presence markedly improved bacterial metabolic activity, resulting in effective destruction of RR120 at a high concentration of 600 ppm. The synergistic effect arises from glucose acting

as a proficient carbon and electron donor, whereas yeast extract supplies vital nitrogen and growth elements necessary for enzymatic dye degradation.

The most effective carbon and nitrogen source was discovered to be yeast extract and glucose, which improved the effectiveness of decolorization (**Figure 4.12**). The decolorization effectiveness of yeast extract and glucose as co-substrates was evaluated in minimal salt media under ideal conditions, and **Figures 4.13** and **4.14** illustrate the results.

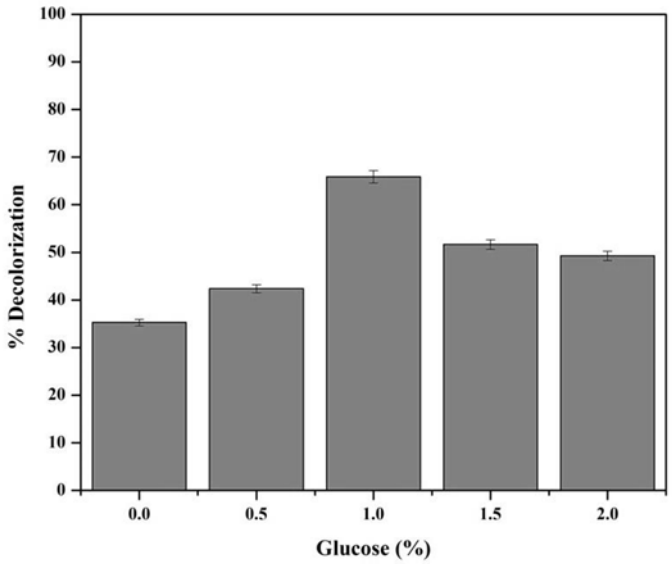

Figure 4.13: Impact of glucose content on the color removal efficacy of RR120 dye by *P. aeruginosa* JU_CHE_01

Figure 4.13 depicts the impact of glucose content on the color removal ability of isolated cultures for specific dyes. The glucose concentrations were varied throughout the trial, ranging from 0.0 to 2.0%. The highest decolorization efficiency was demonstrated by all strains at 1% glucose concentration. The decolorization efficiency was observed to decline with any additional carbon source increase above 1%. Metabolic regulation, including glucose/catabolic suppression, is the cause of the decrease in degradation efficiency at increasing glucose concentrations. During the repression, there is a good chance that cyclic AMP-dependent gene transcription will be inhibited; this may involve dye decolorization in some cases (J.-S. Chang et al., 2001). Consequently, during the experiment, the glucose concentration was kept at 1%.

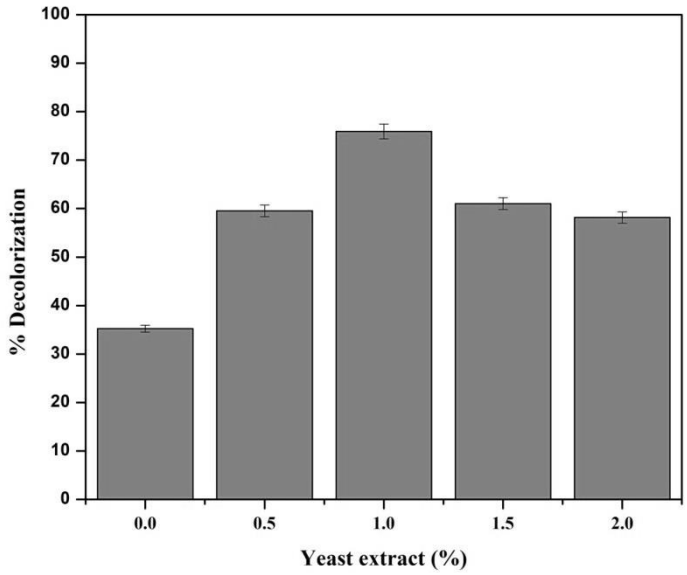

Figure 4.14: Influence of yeast extract content on the color removal efficiency of RR120 dye by *P. aeruginosa* JU_CHE_01

Minimal salt media was used to examine the decolorization effectiveness of isolated strains supplemented with various nitrogen sources under static conditions (**Figure 4.14**). An evaluation was made of the yeast extract content, which varied between 0.0 to 2.0%. The isolated strains exhibited highest decolorization efficacy when 1% of yeast extract was supplemented. The effectiveness of the decolorization process was not significantly affected by any additional increase in yeast extract concentration. Therefore, it was discovered that the best concentration of yeast extract for making the procedure affordable was 1%. Since NADH serves as an electron donor during bond reduction, the yeast extract was essential for this process (Jain, Shah, Chapla, & Madamwar, 2012). **Figure 4.17** illustrates the RR120 dye contaminated wastewater treatment using *P. aeruginosa* JU_CHE_01.

4.1.2.5. Characterization of Antibiotics susceptibility

The antimicrobial susceptibility or resistance of the isolated bacterial strain *P. aeruginosa* JU_CHE_01, which was tested against eight antibiotics, was listed in **Table 4.4**. Our research revealed that *P. aeruginosa* JU_CHE_01 was susceptible to Gentamicin, Doxycycline, Azithromycin, and Ciprofloxacin but resistant to Ampicillin and Cefradine. It was also intermediately sensitive to Chloramphenicol and Aztreonam. The MAR index is determined by the ratio of the total antibiotics administered and the number resisted by the isolate

(Ameenudeen et al., 2021). Consequently, resistance to two distinct antibiotics is indicated by a MAR index of 0.25. The antimicrobial susceptibility testing (AST) results using the disc diffusion technique is shown in **Figure 4.15**.

Table 4.4: Antimicrobial susceptibility test

Antimicrobial class	**Antimicrobial agent or Antibiotics**	**Dose (µg)**	**Diameter (mm)**	**Result**
Penicillin	Ampicillin	10	No clear zone	Resistant
Cephalosporin	Cefradine	25	No clear zone	Resistant
Phenicol	Chloramphenicol	30	13	Intermediate
Fluoroquinolones	Ciprofloxacin	30	42	Sensitive
Macrolide	Azithromycin	15	24	Sensitive
Monobactam	Aztreonam	50	25	Intermediate
Tetracycline	Doxycycline	30	19	Sensitive
Aminoglycoside	Gentamicin	10	24	Sensitive

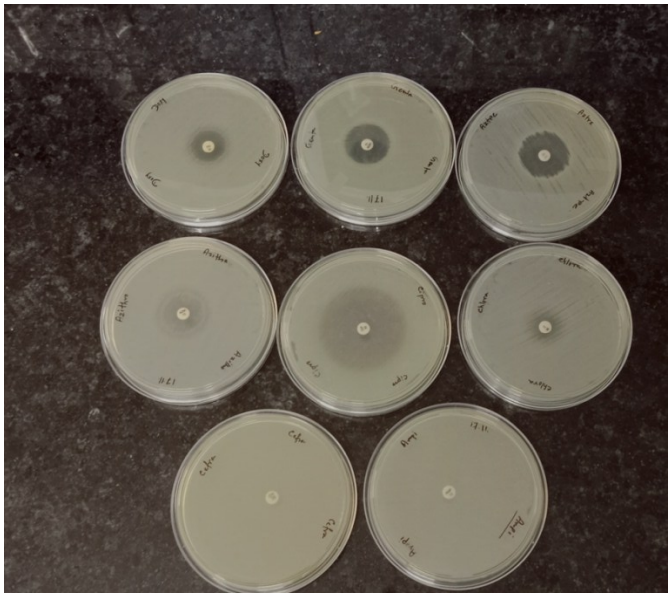

Figure 4.15: *P. aeruginosa* JU_CHE_01 antibiotic sensitivity analysis (AST) using the disk diffusion assay

4.1.2.6. Analysis of metabolic versatility of other azo dyes

The metabolic adaptability of *P. aeruginosa* JU_CHE_01 in presence of various azo dye compounds is presented in **Figure 4.16**. The outcomes indicated the ability of the isolated strain to deteriorate 92.20% Reactive Red 13 (RR13), 96.45% Acid Black 194 (AB194), 98.23% Methyl Orange (MO), 84.97% Reactive Yellow 145 (RY145), 90.04% Congo Red (CR), 89.72% Direct Violet 1 (DV1) after incubating for 48 hours at 37°C. Variations in degradation were seen after 48 hours of culture in inorganic media containing added yeast extract and glucose, as the capacity of various azo dye compounds to undergo decomposition and support growth is an inherent characteristic of the microorganism. According to literature, *Pseudomonas* species are well known for breaking down several hazardous compounds; however, this breakdown was often observed at lower concentrations (Wasi, Tabrez, & Ahmad, 2013). Furthermore, numerous different bacterial species, including *Pseudomonas* sp. (Kishor et al., 2021), *Alcaligenes* sp. (Ajaz et al., 2019), *Rhodococcus* sp. (S. Kumari, Debnath, Hari Sonawane, Teja Malkapuram, & Mohan Seepana, 2022) are capable of metabolizing a broad range of dye compounds, even though they are common, the degradation of various toxic azo dye compounds shows limited diversity. Consequently, scientists are searching for novel, potent microbial species possessing the ability to efficiently degrade diverse azo dyes at increased concentrations. As far as we know, *P. aeruginosa* JU_CHE_01 will represent the first bacterial species capable of metabolizing six distinct azo dye compounds at high concentrations after 48 hours of incubation. Due to its metabolic flexibility, *P. aeruginosa* JU_CHE_01 acts as an effective microorganism for bioremediation of effluents generated by textile processing that has been contaminated by various azo dye compounds.

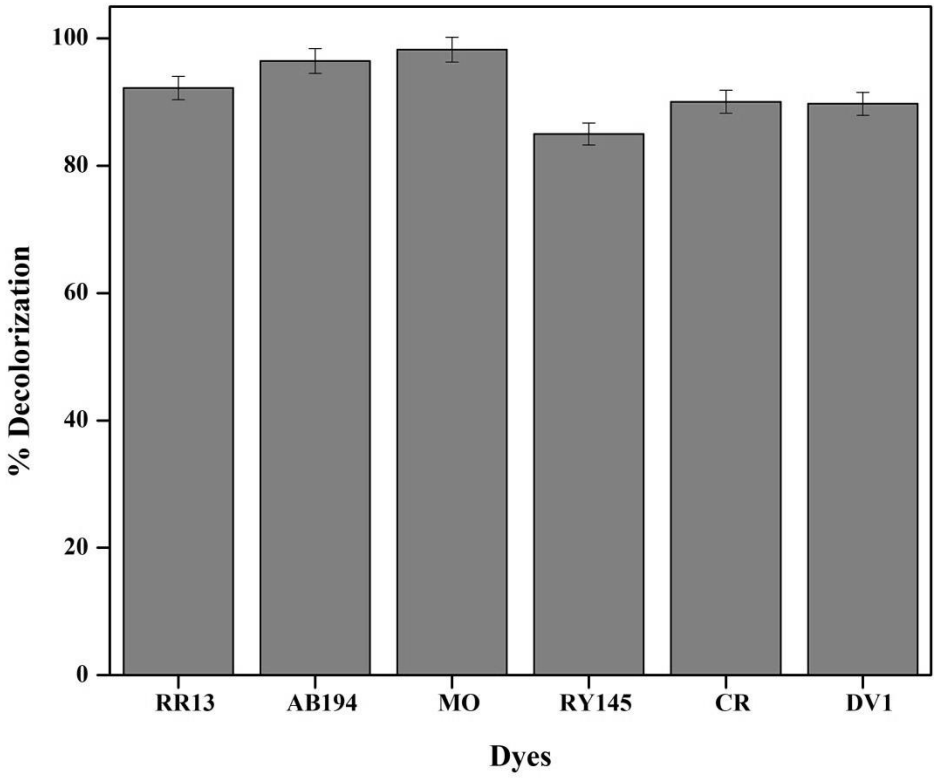

Figure 4.16: The metabolic versatility of *P. aeruginosa* JU_CHE_01 in presence various azo dye compounds

Table 4.5: Literature related to RR120 dye decolorization by bacterial species

Serial No.	Bacterial species	Experimental parameters (Dye concentration, pH, temperature)	Decolorization efficacy	References
1	*Bacillus lentus* BI377	500 mg L^{-1}, 8, 35℃	98% in 12hrs	(Oturkar et al., 2011)
2	*Acinetobacter junii* FA10.	200 mg L^{-1}, 7, 30℃	90% in 48hrs	(Anwar et al., 2014)
3	*Tistrella mobilis* JCM 21370	100µg L^{-1}, 7, 30℃	92.08% in 10 days	(K Lingappa, Sindhe Ananda, Sneha Horti, Begum Nabeela, & Ratkal Mahesh, 2023)
4	*Micrococcus* sp.	200 mg L^{-1}, 9, 35℃	82% in 24hrs	(Basutkar et al., 2019a)
5	*Pseudomonas* sp. strain DRY011	200 mg L^{-1}, 7.5, 30℃	90.9% in 24hrs	(Hafeez et al., 2018)
6	*Acinetobacter baumannii* JC359	500 mg L^{-1}, 7, 37℃	96% in 48hrs	(Ameenudeen et al., 2021)
7	*Shewanella putrefaciens* RDB_2	50 mg L^{-1}, 8, 35℃	100% in 3hrs	(D'souza, Birmole, & Aruna, 2020)
8	*Shewanella haliotis* RDB_1	50 mg L^{-1}, 8, 35℃	99% in 2.5hrs	(Radhika Birmole, 2021)

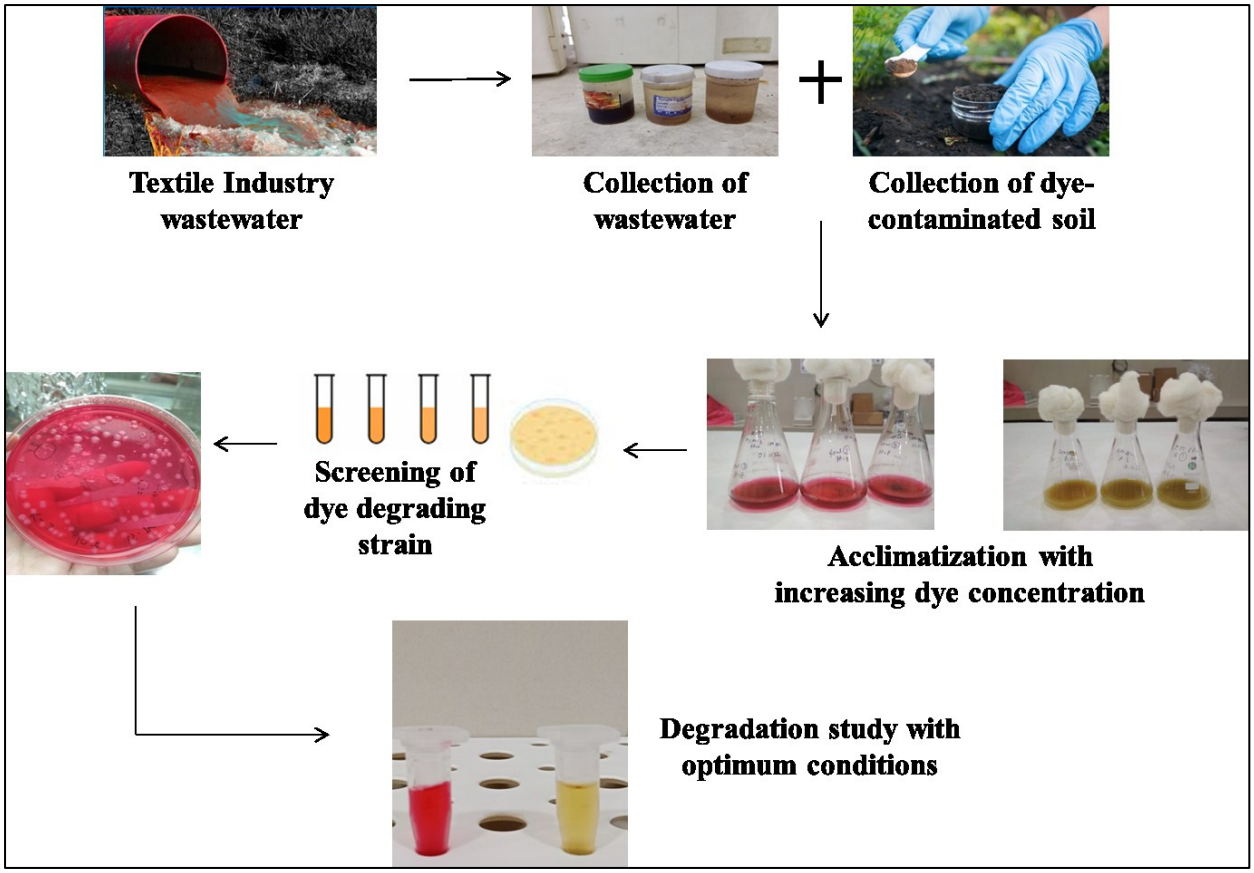

Figure 4.17: Treatment of RR120 dye contaminated wastewater by *P. aeruginosa* JU_CHE_01

4.2. Optimization of the operational parameters for enhanced RR 120 dye degradation using isolated strain

4.2.1. Evaluation of operational parameters on process output and Taguchi Optimisation Algorithm (OA)

Different microorganisms exhibit varying degrees of effectiveness in breaking down specific contaminants. Therefore, it is important to detect and isolate capable microorganisms, as well as determine and choose critical parameters and their appropriate range, prior to the development of bioremediation methods. Numerous physicochemical parameters, including nitrogen and carbon source, inoculum dosage, temperature, and pH, influence the microbial degradation of RR120. The optimization of process parameters ensures enhanced biodegradation with the maximization of resource utilization. Therefore, to enhance the breakdown of RR120 dye by the isolated highly active bacterial strain, a rigorous optimization procedure (Taguchi methodology) was utilized. **Table 4.6** displays the

experimental data acquired from the biodegradation investigations conducted under L-18 OA settings. Clearly, cultural elements influenced the efficiency of the biodegradation process. Individual factors are illustrated in **Table 4.7**. The variability in signal-to-noise ratio values at the L2-L1 level indicates the relative impact of each parameter on the specific outcome of the procedure (Taguchi & Phadke, 1984; Wahla, Iqbal, Anwar, Firdous, & Mueller, 2019). Greater differences are indicative of stronger consequences. An analysis of **Table 4.7** reveals that nitrogen source i.e. yeast extract had the greatest impact on the biodegradation of RR120 dye, followed by the carbon source (glucose), inoculum dosage, pH, and temperature. Elevating the levels of yeast extract and glucose above level 1 (0.5 g L^{-1}) to level 2 (1.0 g L^{-1}) significantly improved the biodegradation of RR120 dye. This behavior can be elucidated by the role of yeast extract and glucose serving as nitrogen and carbon sources, respectively, promote the production of cellular components and biomass growth (Abbasiliasi et al., 2017; N. Kulkarni, Shendye, & Rao, 1999). Upon cultivating the microbial culture in a medium enriched with higher concentrations of RR120 dye, the degradation rate of RR120 dye has been reported to rise with 1 g L^{-1} of substrate present. This phenomenon arises because of the heightened nutritional requirements of the microbial culture. Further augmentation of yeast extract and glucose concentration results in substrate inhibition, leading to reduced degradation of RR120 dye. RR120 dye is detrimental to microbial cells at high concentrations (Hanne, Kirk, Appel, Narayan, & Bains, 1993), and the tolerance threshold for RR120 dye toxicity varies among bacteria.

Most of the research on the breakdown of RR120 dye are centered within the range of 50 to 150 mg L^{-1} (Radhika Birmole & Aruna, 2019; D'souza et al., 2020). Earlier studies reported that *Micrococcus* sp. and *Bacillus* sp. are capable of metabolizing RR120 dye within a concentration levels between 200 to 500 mg L^{-1}. This occurs because the dye inhibits the growth of the majority of microorganisms (Basutkar et al., 2019a; Oturkar et al., 2011). Contrary to previous literature findings, the specific bacterial strain employed in this experiment demonstrated the capability to degrade RR120 at a dye level of 600 mg L^{-1} - when provided with 1 g L^{-1} yeast extract and 1 g L^{-1} of glucose serving as both a carbon and nitrogen source. Presently, this is the highly concentrated kind of RR120 dye that has demonstrated biodegradability. Because of the azo bond (-N=N-) found in RR120 dye, these are electron-deficient and cannot function as carbon sources. Carbon sources serve as electron donors in the reduction of azo dyes, facilitating microbial degradation and decolorization of these compounds. Incorporating glucose and yeast extract into the

breakdown of azo dyes improves the degradation of di-azo dye RR120 by supplying carbon and nitrogen that function as electron donors. A different set of researchers reported similar results, demonstrating that a newly discovered fungus *Galactomyces geotrichum* can break down the azo dye Acid Scarlet GR when provided with 0.1 g L^{-1} yeast extract and 2.0 g L^{-1} glucose as sources of nitrogen and carbon, respectively (Guo et al., 2019b). Research conducted by Kishor et al. (2021) found that *P. aeruginosa* MZ520730 can degrade Methyl Orange dye in under 24 hours when enhanced by the addition of 10 g L^{-1} of glucose and 5 g L^{-1} of peptone used as the carbon and nitrogen sources, respectively (Kishor et al., 2021). A crucial factor in RR120 dye degradation is inoculation dosage. The study found that at level 3, the process output exerted the most significant impact on the inoculum size. An increased inoculum volume optimizes the usage of dye molecules, thus improving the effectiveness of the decolorization process (Mohanty & Kumar, 2020). The biological activity is interrupted when the volume of the inoculum decreases below the optimal values. Therefore, augmenting the amount of inoculum will result in a reduction in substrate inhibition (Radhika Birmole & Aruna, 2019). Prior studies have reported similar results, showing a notable rise in decolorization effectiveness as the volume of inoculum increases (Ayed et al., 2009; Usha et al., 2012).

As shown in **Table 4.7**, pH ranked as the fourth most influential parameter for RR120 degradation at level 2, indicating that *P. aeruginosa* JU_CHE_01 is alkalophilic as a result of its high S/N value. RR120 demonstrates decreased toxicity, improved bioavailability, and optimal enzymatic activity within the alkaline pH range. The pH significantly affects dye decolorization performance, with optimal decolorization occurring in the 8.0–9.0 range. At acidic pH, restricted solubility may impede the utilization of bacterial cells, undermining enzymatic stability and diminishing decolorization efficacy. The translocation of color compounds through the cell membrane could represent a significant regulating element influencing the fading of the dye, thereby elucidating the influence of pH (Z. Wang, Liang, & Liang, 2013). Moreover, some investigations have demonstrated that the biodegradation of RR120 dye transpires at alkaline pH levels (Ameenudeen et al., 2021; Basutkar et al., 2019a; Manogaran et al., 2021).

Concerning RR120 dye degradation, it was shown that temperature exerted a significant influence. A temperature increase from 30°C to 37°C contributed to enhanced biodegradation of RR120 dye, presumably because to the elevated metabolic activity of *P. aeruginosa* JU_CHE_01. However, the degradation of RR120 dye was diminished by an increased

temperature from 37°C to 40°C. One hypothesis suggests that the procedure of decolorization and microbial proliferation are linked to the denaturation of protein and enzyme structures (R. G. Saratale et al., 2011). Moreover, this is widely recognized that a rise in temperature enhances the suppressive impact of the substrate and alters membrane fluidity (Cheng et al., 2021). In a distinct investigation, although bacteria could survive at 17°C, the decolorization rate was lesser to that observed at the optimal range of 27°C to 37°C. Conversely, temperatures of 47°C and 57°C impeded development, subsequently influencing the rate of decolorization (Ameenudeen et al., 2021). A bioprocess's constituent parts interact with one another to differing degrees and produce output with a range of values. To understand the functions of each parameter and their level, an examination of the interactions is necessary.

4.2.2. Influence of factor interaction on the RR120 degradation

Each biological event includes interactions among the elements of the process, leading to a multitude of interactions whose investigation may clarify the entire process. The severity index (SI) in **Table 4.8** quantifies the effects of a pair of factors interacting across varying degrees of interaction. Regarding biomass production (**Table 4.7**), nitrogen and carbon sources exhibited the most significant influence factors, succeeded by inoculum dose, temperature and pH. Yeast extract and temperature exhibited distinct high and low-impact factors; however, their combination resulted in the highest SI. Temperature (minimal effect factor) and pH (moderate impact factor) exhibited a significant SI value throughout their entire interaction. Furthermore, the smallest SI value was seen in the association–between yeast extract (high impact factor) and glucose (high effect factor). Consequently, the biodegradation of RR120 dye is determined by the interplay of multiple characteristics rather than the influence of a single one.

Table 4.6: L-18 OA (3^5) experimental design involving five factors and their respective levels, using RR120 dye biodegradation

Trial no.	A	B	C	E	F	RR120 biodegradation %		
1	1	1	1	1	1	32.19	42.73	38.29
2	1	2	2	2	2	61.53	59.92	65.09
3	1	3	3	3	3	62.7	66.22	67.12
4	2	1	1	2	2	54.77	49.87	54.49
5	2	2	2	3	3	99.66	98.71	98.32
6	2	3	3	1	1	57.76	55.93	54.37
7	3	1	2	1	3	60.29	57.1	62.12
8	3	2	3	2	1	57.49	52.02	56.71
9	3	3	1	3	2	61.16	63.36	64.27
10	1	1	3	3	2	55.16	57.95	50.17
11	1	2	1	1	3	59.6	63.23	60.21
12	1	3	2	2	1	53.5	46.06	53.94
13	2	1	2	3	1	60.64	56.3	59.14
14	2	2	3	1	2	71.56	71.15	78.91
15	2	3	1	2	3	67.71	64.63	72.59
16	3	1	3	2	3	61.12	58.91	61.24
17	3	2	1	3	1	62.57	63.16	65.7
18	3	3	2	1	2	59.42	54.2	53.93

Table 4.7: Main effects of factors

Factors	RR120 biodegradation (S/N Ratio)			
	Level 1	Level 2	Level 3	L2-L1
C-source (Glucose)	34.664	36.448	35.494	1.783
N-source (Yeast Extract)	34.499	36.623	35.484	2.123
pH	35.041	35.944	35.621	0.903
Temperature	34.965	35.26	36.381	0.294
Inoculum dose % (v/v)	34.453	35.537	36.616	1.083

Table 4.8: Severity Index determined for the first ten interaction points

Sl. No.	RR120 biodegradation				
	Pairs of interacting factors	Columns	SI (%)	Col	Opt
1	N-source x Temperature	3 x 5	30.41	6	[2,3]
2	pH x Temperature	4 x 5	27.67	1	[2,3]
3	C-source x Temperature	2 x 5	24.87	7	[2,3]
4	Temperature x Inoculum dose	5 x 6	23.12	3	[3,3]
5	C-source x Inoculum dose	2 x 6	16.08	4	[2,3]
6	pH x Inoculum dose	4 x 6	10.57	2	[2,3]

7	C-source x N-source	2 x 3	8.4	1	[2,2]
8	C-source x pH	2 x 4	7.45	6	[2,2]
9	N-source x pH	3 x 4	5.47	7	[2,2]
10	N-source x Inoculum dose	3 x 6	0.9	5	[2,3]

4.2.3. Analysis of Variance (ANOVA)

Analysis of Variance (ANOVA) served to interpret the experimental results, with the objective of determining the impact of every step variable and the statistically significant factors influencing the variation in the final outcome (Sarkar, Show, Tiwari, & Dey, 2024). An elevated F value indicates that the components in the experimental condition and their interaction are important. The F ratio and % contribution are deemed essential factors for determining the most important factor. The ANOVA and the percentage contribution of each component are shown in **Table 4.9**. When the error term's degrees of freedom dropped to approximately half of that of the experimental design, the components were aggregated, exceeding the 95% confidence level. According to ANOVA, the source of nitrogen (yeast extract) and source of carbon (glucose) exerted the most substantial influence on RR120 biodegradation, accounting for 27.933% and 19.526% respectively, followed by pH at 4.664%, temperature at 13.476%, and inoculum dose at 28.951%.

Table 4.9: ANOVA of process parameters for RR120 dye biodegradation

Factors	DOF (f)	Sum of squares (S)	Variance (V)	F-Ratio (F)	Pure Sum (S')	Percent P (%)
C-source	2	9.562	4.781	31.467	9.259	19.526
N-source	2	13.549	6.774	44.584	13.245	27.933
pH	2	2.515	1.257	8.277	2.211	4.664
Temperature	2	6.693	3.346	22.026	6.39	13.476
Inoculum dose	2	14.031	7.015	46.172	13.728	28.951
Other Error	7	1.063	0.151			5.45
Total	17	47.417				100.00%

4.2.4. Optimum circumstances for the biodegradation of RR120 dye

The Taguchi DOE technique indicates that the ideal parameters for the biodegradation of RR120 dye are: pH 8.0, temperature 37°C, yeast extract concentration 1.0 g L^{-1}, glucose concentration 1.0 g L^{-1} and inoculum dose of 10% (v/v) (**Table 4.10**). Employing equation 1 to calculate the anticipated S/N ratio in the ideal conditions for RR120 dye degradation, Taguchi projected the expected degradation percentage of RR120 dye to be 98.48%.

Table 4.10: Ideal circumstances and efficacy of RR120 dye biodegradation

Factors	Level Description	Level	Contribution (from S/N ratio)
C-source	2	2	0.912
N-source	2	2	1.087
pH	2	2	0.408
Temperature	3	3	0.845
Inoculum dose	3	3	1.08
Overall contribution of all factors			4.331
Current grand average of performance			35.535
Expected results at optimum condition			39.867

4.2.5. Experimental validation

The overall enhancement in process output is illustrated by the variance reduction plots comparing the existing and improved conditions for the biodegradation of RR120 dye. In the confirmatory biodegradation trials conducted under the ideal circumstances of Taguchi DOE, a biodegradation rate of 97.63% for RR120 was attained, hence validating the methodology (**Figure 4.18**).

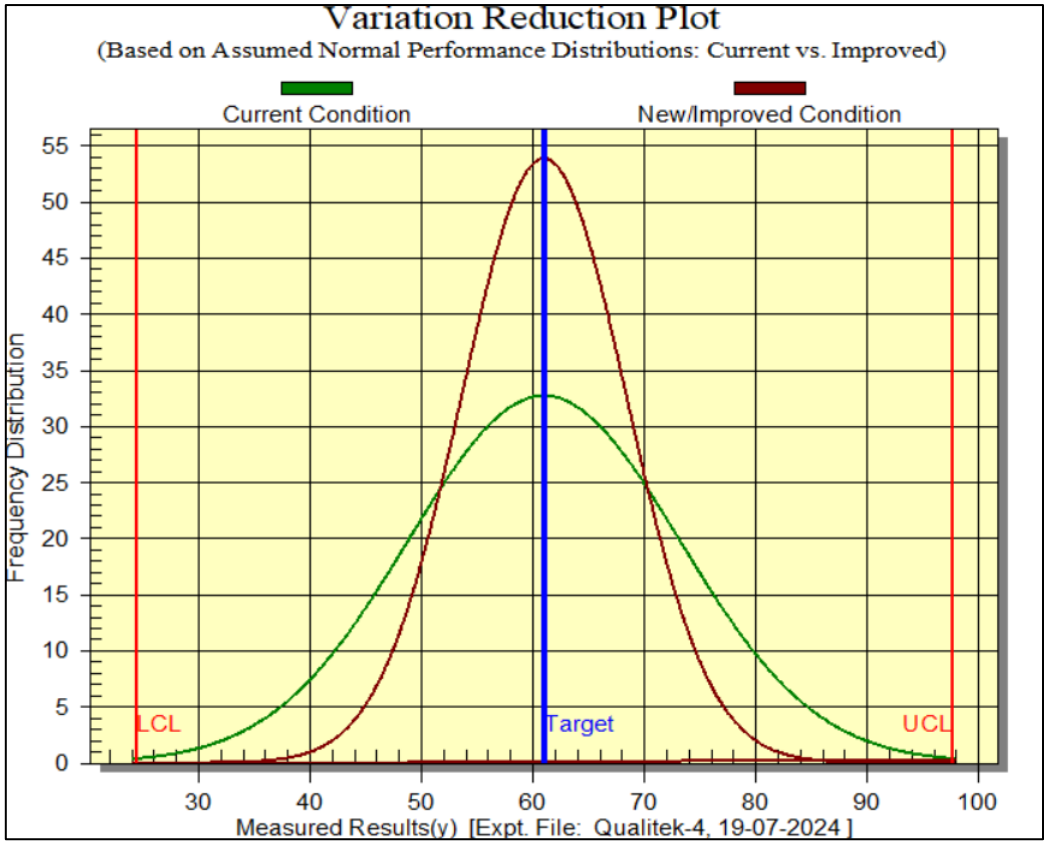

Figure 4.18: Plots showing variation reduction under current and optimized conditions for RR120 dye biodegradation

The 600 mg L^{-1} RR120 dye utilized in the decolorization and optimization study exceeds the dye concentration typically observed in textile effluent and prior research, as indicated by the available literature (**Table 4.11**).

Table 4.11: Efficiency of various microorganisms in degrading RR120 dye

Bacteria	Initial dye concentration	Tolerance	Media with Co-substrates	% decolorization	References
Tistrella mobilis JCM 21370	100µg L^{-1}	100 µg L^{-1}	Mineral based media containing 0.5 g/L yeast extract and 1 g/L glucose	92.08% in 10 days	(K Lingappa, Sindhe Ananda, Sneha Horti, Begum Nabeela, & Ratkal Mahesh, 2023)
Micrococcus sp.	200 mg L^{-1}	250 mg L^{-1}	Mineral based media with 1 g/L yeast extract and 1 g/L Maltose	82% in 24 hrs	(Basutkar et al., 2019b)
Pseudomonas sp.DRY011	200 mg L^{-1}	500 mg L^{-1}	Mineral based media with 1 g/L yeast extract	71.07% in 5 days	(Manogaran, Manogaran, Othman, Gunasekaran, & Abd Shukor, 2020)
Pseudomonas aeruginosa HF5	200 mg L^{-1}	200 mg L^{-1}	Mineral based media with 3 g/L yeast extract	> 90% in 24 hrs	(Hafeez et al., 2018)
Acinetobacter baumannii JC359	500 mg L^{-1}	1000 mg L^{-1}	Luria-Bertani	96% in 48 hrs	(Ameenudeen et al., 2021)
Pseudomonas aeruginosa JU_CHE_01	600 mg L^{-1}	2000 mg L^{-1}	Mineral based media containing 1 g/L yeast extract and 1 g/L glucose	97.63% in 48 hrs	**Present study**

4.3. Investigation of batch kinetics for the ReR120 dye biodegradation using isolated strain and phytotoxicity analysis

4.3.1. Cellular growth and RR120 dye biodegradation batch kinetics and biokinetic parameter evaluation

Analyzing the interactions and changes of chemical constituents bioconversion is crucial for forecasting environmental persistence and developing wastewater management strategies (Dang et al., 2022; Zambrano et al., 2023). Forecasting the fate and movement of carbon-based compounds necessitates an in-depth understanding of their biodegradation kinetics and an assessment regarding their biodegradation rates (Gul et al., 2023; Sonwani, Patel, Singh, Singh, & Rai, 2023). The inhibitory features of the target pollutants can affect the rate of biological degradation; mathematical modeling helps clarify the underlying mechanisms of the biochemical process.

The dynamics growth of cell in a batch reaction can be expressed as follows:

$$\frac{dX}{dt} = \mu X - k_d X \quad (1)$$

k_d can be considered negligible throughout the exponential period. Consequently, Equation (1) might be expressed as:

$$\frac{dX}{dt} = \mu X \quad (2)$$

$$\mu = \frac{1}{X}\frac{dX}{dt} \quad (3)$$

X denotes the cell concentration (g L^{-1}) at time t (h), whereas μ represents the specific growth rate (h^{-1}) (Bhunia, Basak, Bhattacharya, & Dey, 2012).

Furthermore, the specific degradation rate (q) is described as (Min, Xu, Fang, Chen, & Hu, 2020)

$$q = \frac{1}{X}\frac{dS}{dt} \quad (4)$$

The biomass yield coefficient $Y_{X/S}$, representing the proportion of production of biomass to concentration of substrate, can be shown as

$$Y_{X/S} = \frac{X-Xo}{So-S} \quad (5)$$

S_0 and S stand for initial substrate concentration (g L^{-1}) and substrate concentration (g L^{-1}), respectively, whereas X and X_0 represent cell concentration (g L^{-1}) and initial cell concentration (g L^{-1}), respectively (Basak, Bhunia, Dutta, Chakraborty, & Dey, 2014).

RR120 is a noted inhibitory substance that presents a threat to the majority of microorganisms. To simulate biomass development on hazardous substances and the ensuing substrate consumption, numerous models have been developed to describe substrate inhibition. The Haldane inhibition model's simple mathematical formulation and simplicity make it a popular kinetic model in biodegradation studies (Sonwani et al., 2023), and is represented as:

$$\mu = \frac{\mu_{max} S}{Ks + S + S^2/Ki} \quad (6)$$

Here, the maximal specific growth rate (h^{-1}) is denoted by μ_{max}, the saturation constant (g L^{-1}), the inhibitory constant by Ki, and the substrate concentration (g L^{-1}) by S.

To determine various kinetic parameters, multiple substrate inhibition models were applied, including the Edward model, Webb model, and Han and Levenspiel model. The following equations are used in these models:

Edward model: $\mu = \frac{\mu_{max} S}{(S+Ks+(S^2/Ki)(1+ S/Ks))}$ (7)

Webb model: $\mu = \frac{\mu_{max} S (1+m S/Ki)}{(S+Ks+S^2/Ki)}$ (8)

Han and Levenspiel model: $\mu = \frac{\mu_{max} S\left[1-\left(\frac{S}{S_i}\right)\right]^n}{S + Ks\left[1-\left(\frac{S}{S_i}\right)\right]^m}$ (9)

The precise maximum growth rate, $\mu *_{max}$, is frequently conflated with μ_{max}, a fitting parameter in substrate inhibition models that are mistakenly labeled as the ideal specific growth rate in the majority of published literature (Christen, Vega, Casalot, Simon, & Auria, 2012).

At $\frac{d\mu}{dS} = 0$, $S_m = \sqrt{KsKi}$ (10)

In the Haldane equation (6), the substitution of S_m yields the representation of $\mu *_{max}$ (Christen et al., 2012).

$$\mu *_{max} = \mu_{max} / (1+2\sqrt{Ks/Ki}) \quad (11)$$

Similarly, $q *_{max}$, the actual specific degradation rate, is determined by:

$$q^*_{max} = q_{max} / (1+2\sqrt{K's/K'i}) \quad (12)$$

Kinetic parameters, such as μ_{max}, K_i, K_s, and $Y_{X/S}$ were computed utilizing the aforementioned equations following the fitting of experimental results applied to substrate inhibition models through non-linear regression. All regression analyses were performed with GraphPad Prism 5 software, compatible with Windows 10. In a batch culture, *P. aeruginosa* JU_CHE_01 biodegraded RR120 dye. Glucose and yeast extract were included into an optimal inorganic medium at a dosage of 1 g L^{-1}. A 600 mg L^{-1} concentration of the RR120 dye was added to the culture. Azo dyes often are not used as carbon sources due to electron loss associated with the azo functional category (–N=N–). The kind and presence of sources of carbon, acting as electron donors in lowering the amount of azo dyes, influence the removal and deterioration of azo dyes (Chakraborty et al., 2013). Kinetics investigations are typically performed under the availability for carbon source. While azo dye is no longer considered a carbon source, glucose promotes bacterial proliferation and supplies electrons in order to decolorize azo dye. Consequently, the current study performed a kinetic analysis based on dye concentration. The residual substrate was illustrated using the identical graph employed to depict the experimental biomass data in relation to time (**Fig. 4.19**).

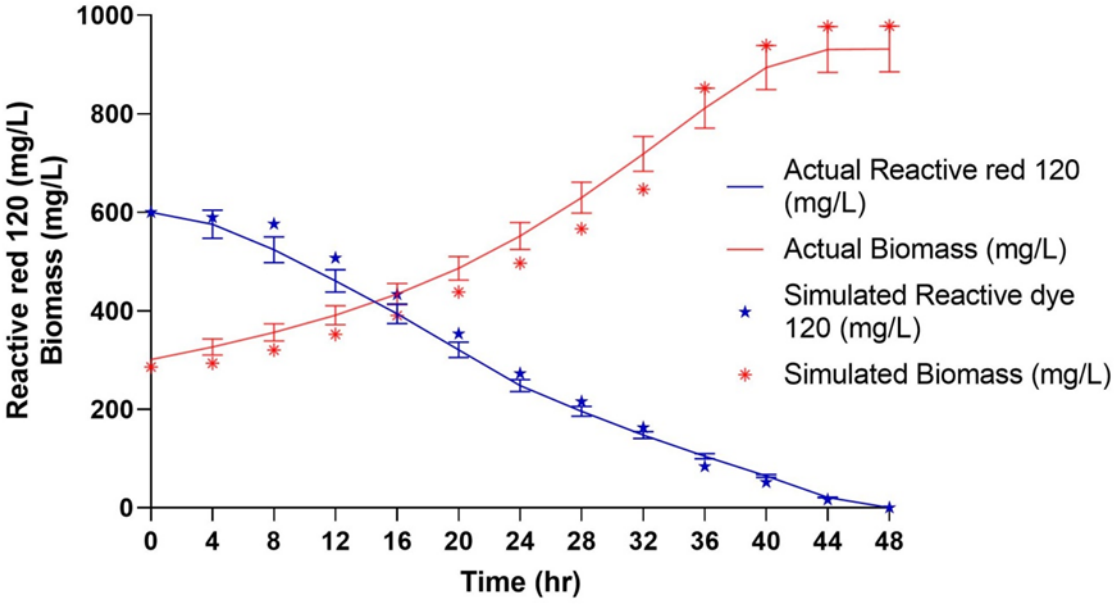

Figure 4.19: The residual substrate was illustrated using the identical graph employed to depict the experimental biomass data in relation to time

The present study utilized Graph-Pad Prism 5 to solve a nonlinear problem by nonlinear regression analysis. Kinetic parameters, such as μ, μ_{max}, K_i, and $K_s$were ascertained by correlating the experimental results. The bacterial strain's specific growth rate increased with substrate concentration to some extent, at which time it started to decrease. The concentration of RR120 dye determines the maximum specific growth rate, or μ_{max}, suggesting that RR120 dye is hazardous and suppresses biomass growth development at elevated concentrations. This confirms the reason for the observation. The decline in μ_{max} values with increased RR120 dye concentration may be ascribed to the isolated strain's stress response and the evident phytotoxic effects at elevated substrate levels. Substrate inhibition is characterized by a trend in substrate degradation rate that increases with concentration to some extent, subsequently diminishing, similar to the specific growth rate of biomass. The experimental data aligned effectively with the other models analyzed in this study; nevertheless, the Haldane model demonstrated the optimal match (**Table 4.12**). Substrate inhibition at high doses denotes a specific case of uncompetitive inhibition (Bailey & Ollis, 2018). It occurs when numerous substrate molecules bind to the enzyme's catalytic site, which is reserved for a single substrate molecule. This occurs because different components of the substrate molecules bind to certain sub-regions of the attachment site. At high substrate concentrations, this type of inhibition lowers the reaction rate if the ensuing molecular assembly is inactive

(Rajamohan & Rajasimman, 2013). The analysis and comparison of several substrate inhibition kinetic models were the key aims of this research (**Table 4.12**).

Table 4.12: Kinetic model parameters estimated for a batch investigation

Sr. No	Author	Equation	μ_{max} (hr^{-1})	K_s (mg L^{-1})	K_i	m	n	R^2	Ref.
1	Edward's Model	$\mu = \frac{\mu_{max} S}{(S + Ks + \left(\frac{S^2}{Ki}\right)\left(1+\frac{S}{Ks}\right))}$	0.07513	117.3	503.6			0.9782	(Edwards, 1970)
2	Haldane's Model	$\mu = \frac{\mu_{max} S}{Ks + S + \frac{S^2}{Ki}}$	0.18	345	83.34			0.999	(S.-J. Wang & Loh, 1999)
3	Han and Levenspiel 's model	$\mu = \frac{\mu_{max} S\left[1-\left(\frac{S}{S_i}\right)\right]^n}{S+K_i\left[1-\left(\frac{S}{S_i}\right)\right]^m}$	0.03687	87.92		11.27	0.2168	0.6455	(K. Han & Levenspiel, 1988)
4	Luong's Model	$\mu = \frac{\mu_{max} S\,(1-(\frac{S}{S_i})^n}{(S + Ks)}$	0.04660	48.98			0.2904	0.6063	(Luong, 1987)
5	Teisseir's Model	$\mu = \mu_{max}\left[exp\left(-\frac{S}{K_i}\right) - exp\left(-\frac{S}{K_i}\right)\right]$	0.1	127.5	358.8			0.9718	(Edwards, 1970)
6	Webb's Model	$\mu = \frac{\mu_{max} S(1 + m\frac{S}{Ki})}{(S + Ks + \frac{S^2}{Ki})}$	0.1	300	218.6	$9.7*10^{-8}$		0.7441	(Edwards, 1970)
7	Yona's Model	$\mu = \frac{\mu_{max} S}{(S + Ks + (\frac{S^2}{Ki})(1+\frac{S}{Ki}))}$	0.07513	117.3	503.6			0.9262	(Yano & Koga, 1969)
8	Aiba's Model	$\mu = \frac{\mu_{max} S}{Ks + S}\, e^{-\frac{S}{Ki}}$	0.1	200	421			0.8994	(Bhunia et al., 2012)

An estimated μ value was derived through simulation using Equation (6), and the anticipated value of q was obtained using Equation (12). **Figures 4.20 (a)** and **(b)** presented both the investigative and anticipated μ and q. A plot illustrating specific growth rate (μ) based on the concentration of substrate is demonstrated in **Figure 4.20**, which shows the extent of substrate inhibition that exists across the substrate range concentrations under analysis.

Consequently, an endeavor was undertaken to reconcile the investigation findings with the kinetic hypotheses of substrate inhibition. The trial and error approach demonstrated that the experimental results were in close accordance with Haldane's Model about cell growth and usage of RR120 dye. The model indicated that the degradation rate of RR120 dye exhibited

an inhibitory effect, characterized by an exponential pattern, corresponding with the substrate concentration that matched the growth discrepancy position (S.-J. Wang & Loh, 1999).

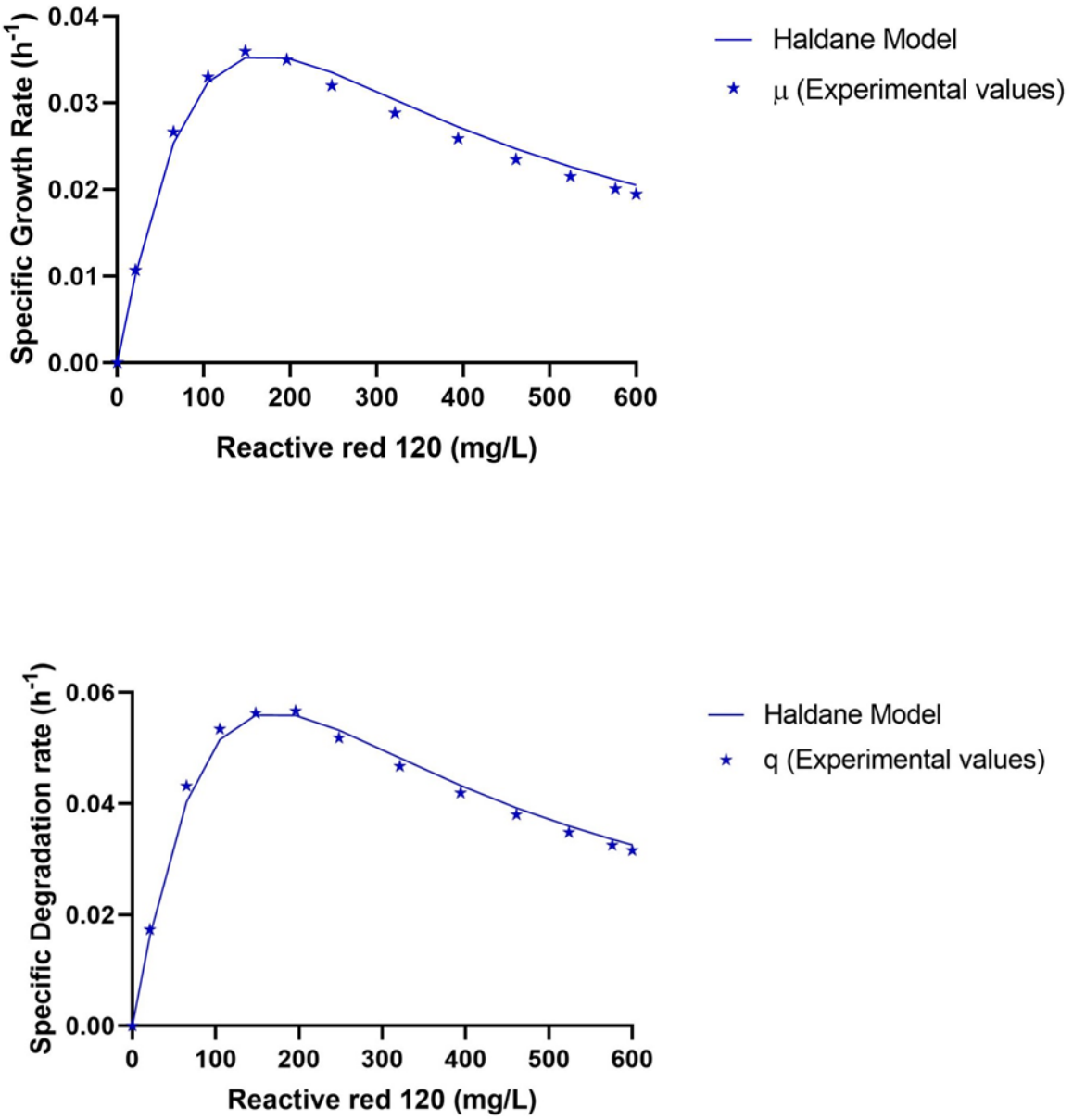

Figure 4.20: Evaluation of the relationship between (a) specific growth rates (μ) and initial substrate concentration, and (b) specific degradation rates (q) and initial substrate concentration

In the Haldane model, μ and μ_{max} represent the specific substrate degradation rate (h^{-1}) and the maximal substrate degradation rate (h^{-1}), respectively. The kinetic parameters μ_{max}, K_i, and K_s, were observed as around 0.18 h^{-1}, 345 mg L^{-1}, and 83.34, respectively. The critical

concentration of inhibitors for *P. aeruginosa* JU_CHE_01 was found to be 600 mg L^{-1}. The computed correlation coefficient (R^2) was 0.999. Haldane's model has a higher correlation coefficient than the other experimentally assessed substrate inhibition models in this investigation, suggesting that it is more applicable. By plotting the gradient of ΔX versus ΔS across a number of time periods, $Y_{x/s}$ is determinable. The inclination of the straight-line equation determines the numerical value of the function $Y_{x/s}$. The biomass value of 0.630 g per g of RR120 was acquired from the research evaluation of $Y_{x/s}$. The study's $Y_{x/s}$ value was noticeably low due to the environmental risks associated with RR120 dye. $Y_{x/s}$ levels in bacterial cultures typically range from 0.6 to 0.72 g/g. Biomass yield for *Pseudomonas putida* was 0.65 g g^{-1} when a hazardous chemical was utilized as the exclusive source of carbon (Livingston & Chase, 1989). Given that $Y_{x/s}$ reflects a fundamental trait of bacterial species, the outcomes may differ among diverse microorganisms. Furthermore, the yield is influenced by the specific types and concentrations of substrates, as well as the ambient conditions (Amin, Aboul-Enein, Abd-Elsalam, Wahba, & El-Refai, 2022). The breakdown of RR120 dye has been linked to an enzyme in the extracellular matrix that the bacterium releases. The diminishing efficacy of *P. aeruginosa* JU_CHE_01 was evaluated by collecting experimental data over a 48-hour period. For the mathematical computation of $Y_{x/s}$, exclusively the log phase data were used. RR120 dye is widely acknowledged as a growth-essential but limited substrate. Moreover, the computation of $Y_{x/s}$ omitted maintenance, as it is typically disregarded during the exponential growth phase (P. Saha, Madliya, Khare, Subudhi, & Bhaskara Rao, 2023).

As far as we know, there are currently no microorganisms that can break down RR120 dye with a concentration of 600 mg per liter. Based on the kinetic values obtained through the Haldane model, the present study showed that *P. aeruginosa* JU_CHE_01 exhibited notable growth and decolorization of 600 mg L^{-1} RR120 dye: K_s = 345 mg L^{-1}, K_i = 83.34, μ_{max}= 0.18 h^{-1}. The μ_{max} exhibited by *P. aeruginosa* JU_CHE_01 corresponds with prior results and exceeds many other bioremediation studies, indicating effective use of RR120 dye for metabolism and development. The maximal specific growth rate, $\mu *_{max}$, derived from Equation (11), is 0.035 h^{-1}. The K_s/K_i ratio has been utilized by several researches as an empirical metric for evaluating the magnitude of inhibition. An increased proportion indicates a greater degree of inhibition. Our analysis indicates a K_s/K_i ratio of 4.139. This observation illustrates the remarkable tolerance of *P. aeruginosa* JU_CHE_01 to inhibition. The values of

S_m, obtained from Equation (10), are calculated to be 169.56 mg L^{-1}. S_m represents the concentration of substrate associated with, $\mu *_{max}$, below which substrate availability restricts biomass growth and above which substrate presence inhibits growth. The discrepancies within the biokinetic values noted in the current investigation relative to other pertinent literature can be ascribed to differences with respect to biomass and environmental conditions, encompassing biomass type, adaptability, concentration, and the properties of the test substrate. Variations in biomass history and cultural settings lead to changes in metabolic phases and promote the dominance-of adaptive microbial species throughout the community (Rezouga, Hamdi, & Sperandio, 2009). **Table 4.13** presents an assessment of kinetic tests on several dye compounds conducted by different microorganisms.

However, directly comparing the biokinetic factors from this study with those in the existing literature is frequently impractical due to discrepancies in operational parameters, types of biodegrading organisms (both pure and consortium), substrate composition, and substrate inhibition models, which complicate reproduction efforts.

Table 4.13: Evaluation of kinetic properties for substrate inhibition models across different azo dye compounds

Microorganisms	**Substance and its concentration**	**System**	**Model**	**Kinetic parameters**	**References**
Stenotrophomonas maltophilia	Methyl Orange 100 mg L^{-1}	Batch	Haldane	μ_{max} =0.032 h^{-1}, K_i= 156 mg L^{-1} and K_s= 78 mg L^{-1}	(Anshuman Mishra, Singh, Mishra, Giri, & Singh, 2024)
Bacillus sp.	Acid Orange 7 25 mg L^{-1}	Integrated treatment system	Haldane	μ_{max} =0.1875 day^{-1}; K_s= 49.53 mg L^{-1}; K_i= 133.32 mg L^{-1}	(Sonwani et al., 2021)

Pseudomonas putida	Tectilon Yellow 2G 300 mg L^{-1}	Integrated treatment system	Haldane	μ_{max} = 0.3002 h^{-1} K_s= 117.6 mg L^{-1} K_i= 1039 mg L^{-1}	(R. Srinivasan, Kathiravan, & Gopinath, 2011)
Pseudomonas fluorescens	Acid Blue 113 50 mg L^{-1}	Integrated photocatalytic-fixed bed bioreactor	Haldane	μ_{max} =0.176 day^{-1} K_s=48.5 mg L^{-1} K_i=130 mg L^{-1}	(Tiwari, Sonwani, & Singh, 2022)
Lysinibacillus sp	Congo Red 50 mg L^{-1}	Packed bed bioreactor	Haldane	μ_{max} =0.061 day^{-1} K_s=37.47 mg L^{-1} K_i=631.97 mg L^{-1}	(Maurya, Swain, Sonwani, Verma, & Singh, 2022)
A. flavus	Reactive Black 5 100 mg L^{-1}	Batch	First order kinetic model	K= 0.01656 R^2 = 0.9997	(Gul et al., 2023)
Bacillus licheniformis	Brilliant Green 200 mg L^{-1}	Packed bed bioreactor	Han-Levenspiel kinetics	μ_{max}=0.185^{day-1} K_s=115 mg L^{-1}	(P. Tripathi, Tiwari, Sonwani, & Singh, 2023)
Lysinibacillus fusiformis KLM1 and *Lysinibacillus*	Congo Red	Moving bed biofilm	First-order kinetic model	K = 0.0381 h^{-1} R^2 =0.97	(Maurya et al., 2023)

macrolides KLM2	250 mg L^{-1}	reactor	and second-order (Grau) kinetic model	$K1$=0.0006 (L/mg.h) R^2 = 0.98	

4.3.2. The temperature-dependent variation in kinetic parameters

A thermodynamic experiment was carried out using *P. aeruginosa* JU_CHE_01 under batch cultivation using an optimized growth medium at temperatures between 30°C and 45°C to examine the role of temperature in modulating parameters of reaction kinetics such as specific growth rate as well as specific degradation rate. An Arrhenius plot was generated to assess the temperature-dependent association between specific degradation rate as well as specific growth rate within a range of temperatures encompassing both deactivation and activation circumstances (Adamberg, Kask, Laht, & Paalme, 2003). Temperature's influence on the rates of growth and degradation can be elucidated by referencing the Arrhenius equations (Eq. 13 & 14).

$$\ln \mu = \ln A^{/} - \frac{E^{/}_a}{RT} \quad \text{Eq. (13)}$$

$$\ln \nu = \ln A - \frac{E_a}{RT} \quad \text{Eq. (14)}$$

The variable v represents the specific degradation rate, while μ defines the specific growth rate. The activation frequency factors for growth and degradation are denoted as $A^{/}$ and A, respectively. R represents characteristic gas constant, while T indicates the absolute temperature. The $E^{/}_a$ denotes activation energy necessary for the process of growth, whereas E_a represents the activation energy required for the generation of products. The impact of temperature deactivation on specific degradation rate and specific growth rate can be mathematically represented by equations 15 and 16.

$$\ln \mu = \ln B^{/} + \frac{E^{/}_d}{RT} \quad \text{Eq. (15)}$$

$$\ln \nu = \ln B + \frac{E_d}{RT} \quad \text{Eq. (16)}$$

$E^{/}_d$ and E_d are independent variables that denote the deactivation energy for growth and degradation, respectively. The deactivation frequency factors for growth and degradation are

denoted as $B^{/}$ and B, respectively. Both activation and deactivation scenarios demonstrate that the system effectively conforms to the Arrhenius law. The empirical data demonstrates that the specific growth rate (μ) and specific degradation rate (v) exhibit an upward trend with temperature up to 37°C, but decline beyond this parameter. It has been established that the ideal temperature supporting bacterial growth and degradation of RR120 is 37^{o}C. Based on data from **Fig. 4.21a** and **Fig. 4.21b**, the activation energy required for cell proliferation and RR120 dye degradation was computed.

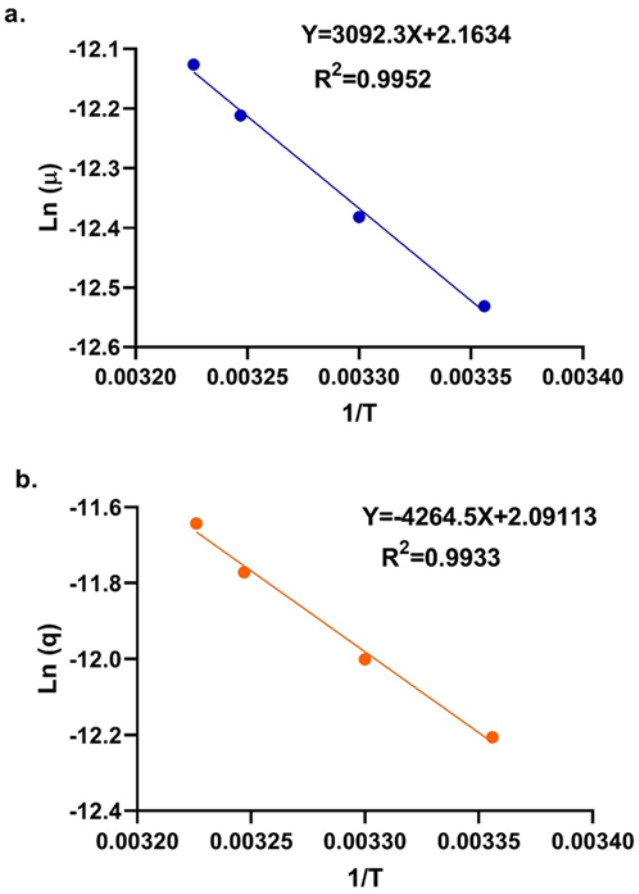

Figure 4.21: Illustrate the impact of temperature on Arrhenius plots (a) the specific growth rate (μ) (b) the degradation rate (q) observed under activation conditions

Figures 4.22a and **4.22b** illustrate the deactivation process at temperatures higher than 37°C. The observed activation and deactivation energy values for RR120 dye degradation and cell growth fall within the average range documented for biological systems. Cell growth activation energy for *Bacillus subtilis*, *Streptococcus thermophilus* St20, *L. plantarum* A6 and

Pyrococcus woesei is documented in the literature as 86, 8, 74, and 30.6 kJ/mol, respectively (Yuwono & Kokugan, 2008).

According to the obtained data, it may be concluded that the growth and RR120 dye degradation from *P. aeruginosa* JU_CHE_01 is very responsive to temperature, underscoring the need to select the most optimal temperature. A deviation from the optimal temperature might result in the inactivation of ribosomes and enzymes, consequently modifying the cell membrane fluidity and disrupts the movement of soluble substances (Phisalaphong, Srirattana, & Tanthapanichakoon, 2006).

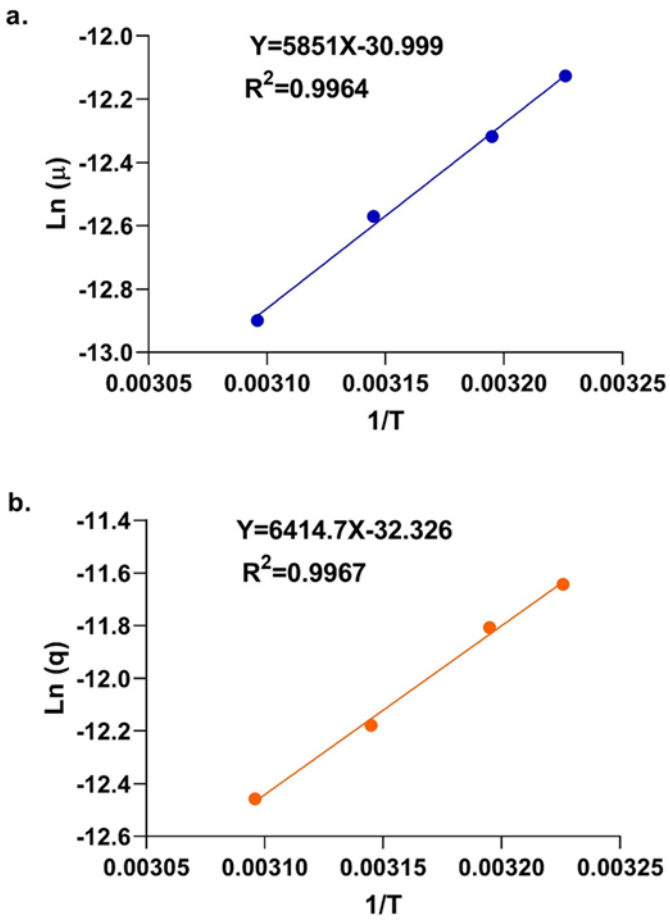

Figure 4.22: Arrhenius plots reveal the temperature dependence of (a) the specific growth rate (μ) (b) under deactivation situation, the specific degradation rate (q)

4.3.3. The impact of pH upon kinetic parameters

The effect of pH on several kinetic parameters was evaluated through an experiment, including specific growth rate and specific degradation rate. *P. aeruginosa* JU_CHE_01 was grown in batch culture using an optimal medium at pH values ranging from 6, 7, 8, 9, 10.

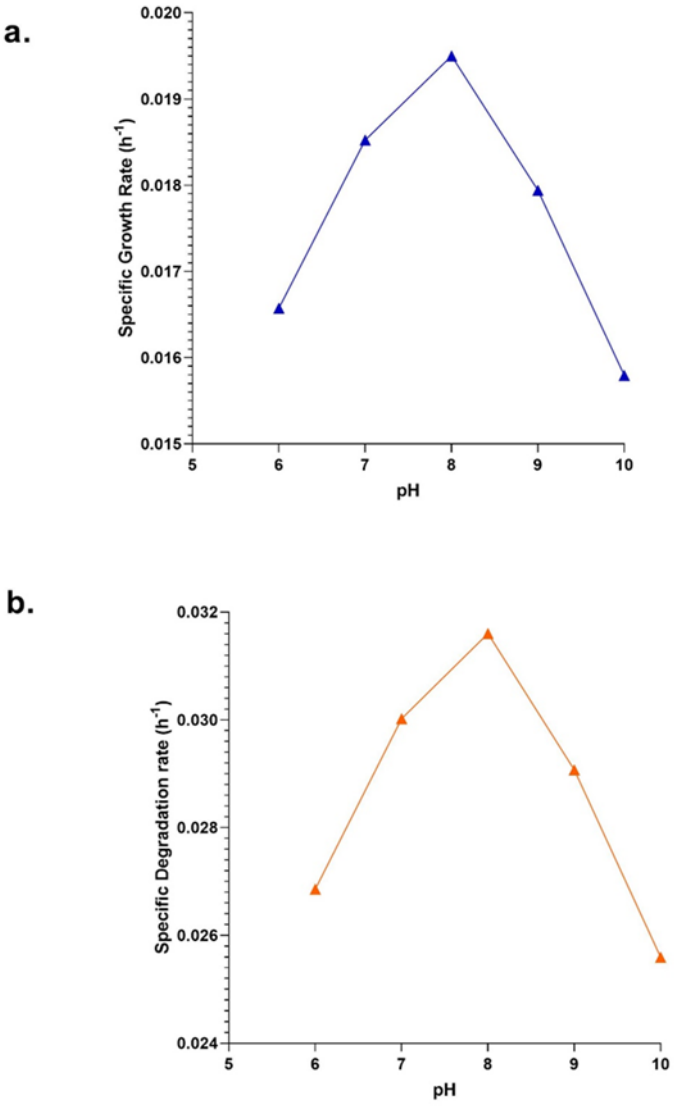

Figure 4.23: The role of pH in (a) specific growth rate and (b) specific degradation rate (q) at 37^{o}C

Figure 4.23 (a) and **(b)** illustrate the impact of pH on the specific growth rate as well as specific degradation rate, respectively. It is noted that the specific growth rate and specific degradation rate consistently rise as the pH level increases, up to a pH value of 8. Beyond this

threshold, both the specific growth rate and specific degradation rate decline. The impact of pH on the catalytic activity of enzymes released by microbial cells is anticipated since pH significantly influences the dynamic ionic interactions, leading to the obstruction of active sites (Yuwono & Kokugan, 2008). The data presented in **Figures 4.23 (a) and (b)** clearly demonstrate that pH significantly influences both the specific growth rate as well as specific degradation rate. After analysing the data, the pH-dependent enzymatic reaction rate for ionising enzymes can be described using the following scheme. This scheme influences either directly or indirectly bacterial growth and the degradation of RR120 dye (Adamberg et al., 2003).

$$EH \xrightleftharpoons{k_2} E^- + H^+$$
$$EH + S \xleftrightarrow{k_m} EHS \xrightarrow{k_{cat}} EH + P \qquad \text{Eq. (17)}$$
$$EH + H^+ \xrightleftharpoons{k_1} EH_2^+$$

An expression was given for the pH dependency of the specific growth rate (μ).

$$\mu = \frac{\mu_m[S]}{K_s^{'}[1+(\frac{K_{s2}}{[H^+]})+(\frac{[H^+]}{K_{s1}})]+[S]} \qquad \text{Eq. (18)}$$

Let μ_m represent the highest specific growth rate and K ⍰$_s$ denote the saturation constant. K_{S1} and K_{S2} pH-related inhibition constants that determine the specific growth rate.
That is:

$$\mu = \frac{\mu_m[S]}{K_{s.app}^{'}+[S]} \qquad \text{Eq. (19)}$$

Where

$$K_{s.app} = K_s^{'}[1+(\frac{K_{s2}}{[H^+]})+(\frac{[H^+]}{K_{s1}})] \qquad \text{Eq. (20)}$$

$$K_{s.app} = K_s^{'}.Y_s \qquad \text{Eq. (21)}$$

and

$$Y_s = [1 + (\frac{K_{s2}}{[H^+]}) + (\frac{[H^+]}{K_{s1}})] \quad \text{Eq. (22)}$$

Y_s represents the inhibition factor affecting pH-dependent specific growth rate.

An expression was given for the pH dependency of the specific degradation rate (v).

$$\nu = \frac{\nu_m[S]}{K_m^{'}[1 + (\frac{K_{m2}}{[H^+]}) + (\frac{[H^+]}{K_{m1}})] + [S]} \quad \text{Eq. (23)}$$

Where, maximum specific production rate and saturation constant are denoted by V_m and K ⍰$_m$, respectively. $K_{m1}$and $K_{m2}$are constants measured for pH inhibition. That is:

$$\nu = \frac{\nu_m[S]}{K_{m.app}^{'} + [S]} \quad \text{Eq. (24)}$$

Where,

$$K_{m.app} = K_m^{'}[1 + (\frac{K_{m2}}{[H^+]}) + (\frac{[H^+]}{K_{m1}})] \quad \text{Eq. (25)}$$

$$K_{m.app} = K_m^{'}.Y_p \quad \text{Eq. (26)}$$

and

$$Y_p = [1 + (\frac{K_{m2}}{[H^+]}) + (\frac{[H^+]}{K_{m1}})] \quad \text{Eq. (27)}$$

To get insight into the pH inhibition, a double reciprocal plot has been generated to analyse the correlation between concentration of substrate and both specific growth and degradation rates. The initial pH is used as the baseline parameter. These are illustrated in **Figures 4.24 (a) and (b)**. The linear graphs converge at a particular ordinate value, evidently

demonstrating the antagonistic relationship between pH and the current state of the system. The inhibitory parameters were calculated using the most suitable mathematical expressions for competitive inhibition, as presented by Adamberg et al. 2003 (Adamberg et al., 2003).

The minimal inhibitory constant is achieved at the optimal pH of 8, which is clearly located between pK1 and pK2. The rate of specific growth is determined by the range formed between pK1 and pK2, and production remains constant within this range (Shuler, 1992).

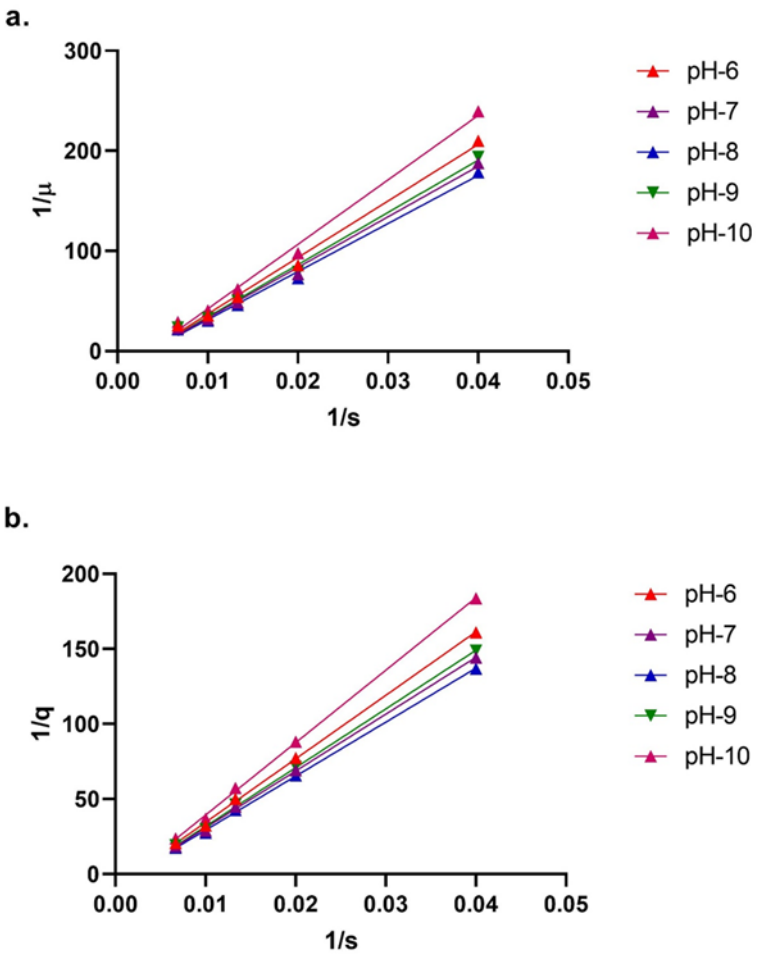

Figure 4.24: Lineweaver–Burk plot of (a) specific growth rate and (b) specific degradation rate at various pH

According to the previously described experiments, it may be inferred that pH significantly influences cellular activities and the associated kinetic parameters via activating and suppressing metabolic processes.

4.3.4. Phytotoxicity analysis

In plants, germination consists of imbibition of the seed, followed by radicle growth, and root lengthening (Nonogaki, Bassel, & Bewley, 2010) and it is disrupted by intricate metabolic processes connected to mutations carried on by external stress (Wei, Song, Tian, & Liu, 2014). An important physiological index for assessing the effects of different toxicants on plants is seed germination. The RSG (%), RRG (%), PI, and GI (%) values on RR120 dye and RR120 dye biodegraded solution in this investigation showed that this dye was consistently hazardous to all the seeds. According to the phytotoxicity analysis, the breakdown by-product was found to be less detrimental than the pure dye treatment on seeds. There was an increase in germination in the seeds subjected to degraded products. Since the dye solution in its crude form contains aromatic compounds that may function as micronutrients, all species of plants utilized in the investigation exhibited noticeable germination after being treated with it. However, these hazardous substances may build up in plants and potentially contaminate the food supply (Nouren et al., 2017). The PI and GI (%) indicate that root development in the control was maximal, followed by the RR120 dye degraded sample, with no growth observed in the RR120 dye solution (**Table 4.14**). Different seeds showed varying levels of sensitivity and tolerance potential, but overall the treated sample showed less toxicity to the seeds. The *Vigna mungo* and *Vigna radiata* seeds exhibited the least inhibition, followed by *Cicer arietinum* seeds (**Figure 4.25**). In contrast to the RR120 dye solution, which severely hindered root growth, the biodegraded sample was found to be significantly less toxic based on observations. Thus, RR120 dye was detoxified as a consequence of the isolated bacterial mediated biotransformation.

Table 4.14: Phytotoxicity testing on different seeds

Seed variant	Samples	Radicle Length (cm)	RRG%	RSG%	PI	GI
Vigna radiata	Distilled water	5.93 ± 0.5	100	100	0	100
	Crude dye	1.84 ± 0.1	31	80	0.69	24.8
	Degraded metabolite	4.49 ± 0.1	75	100	0.24	75
Vigna mungo	Distilled water	4.02 ± 0.3	100	100	0	100
	Crude dye	1.04 ± 0.1	26	80	0.74	20.8
	Degraded metabolite	3.29 ± 0.1	82	100	0.18	82
Cicer arietinum	Distilled water	2.32 ± 0.5	100	100	0	100
	Crude dye	1.41 ± 0.3	61	60	0.39	36.6
	Degraded metabolite	2.10 ± 0.2	90	100	0.09	90

Seed variant	Control	RR120	Biodegraded product
Vigna radiata			
Vigna mungo			
Cicer arietinum			

Figure 4.25: Examining the phytotoxicity of several seeds

CHAPTER 5

CONCLUSION AND FUTURE RECOMMENDATIONS

5.1. SUMMARY AND CONCLUSIONS

This current investigation involved the isolation of a robust and metabolically adaptable bacterial strain capable of decomposing RR120 dye from soil polluted with textile dyes, accompanied by biochemical and phylogenetic characterisation of the isolated strains. Thereafter, optimization of process parameters for RR120 dye was carried out with a pure bacterial strain. Finally, estimation of the kinetic parameters required in batch flasks for the biodegradation of the specific RR120 dye and the toxicological assessment of the significant dye degradation research of RR120 dye was done. In this circumstance, the subsequent outcomes were derived:

This work emphasizes the remarkable potential of *P. aeruginosa* JU_CHE_01, a gram-negative, facultative anaerobic bacterium, to achieve eco-friendly treatment of dye-laden wastewater. The strain exhibited remarkable catabolic plasticity, efficiently digesting elevated quantities (600 mg L^{-1}) of RR120 dye. Its remarkable metabolic capability allows it to function as an independent biocatalyst, rendering it an invaluable asset for the cleanup of high-strength dye effluent. The bacterium demonstrated resistance to ampicillin and cefradine while remaining sensitive to other evaluated antibiotics, a selective resistance profile that may affect its use in various environmental contexts.

The study utilized the Taguchi orthogonal array design to optimize essential physicochemical parameters for improved biodegradation efficiency. Importantly, under optimized conditions that is, pH 8.0, temperature 37 °C, 1.0 g L^{-1} of glucose and yeast extract, and 10% (v/v) inoculum-resulted in a 66.75% enhancement in RR120 dye degradation. Although glucose and yeast extract are frequently employed to facilitate microbial decomposition, their expense is a challenge for large-scale operations. Utilizing them at low concentrations (1.0 g L^{-1} each) in this study presents a cost-efficient strategy, reducing overall costs while maintaining performance integrity. The effective performance of *P. aeruginosa* JU_CHE_01 under static conditions, devoid of aeration, improves the energy effectiveness of the treatment process.

The kinetics study of facultative anaerobic biological growth and the degradation of RR120 by the isolated bacterium *P. aeruginosa* JU_CHE_01, which can decolorize 600 mg L^{-1} of RR120, marking the highest concentration recorded for biodegradation to date. The outcomes from the batch degradation studies indicated that *P. aeruginosa* JU_CHE_01 displayed substrate inhibition kinetics, with the Haldane model precisely representing the experimental outcomes. The biological kinetic parameters employed for biomass growth estimation included a maximum specific growth rate of μ_{max}= 0.18 h^{-1}, a half-saturation coefficient of

K_s= 345 mg L^{-1}, and an inhibition coefficient of K_i = 83.34. Post-treatment analysis was conducted to assess phytotoxicity of the biodegraded products by seed germination and root elongation assays on *Cicer arietinum, Vigna radiata*, and *Vigna mungo*. The results indicated a significant reduction in phytotoxicity during biodegradation, along with improved germination rates and root growth in treated samples relative to untreated controls. The findings demonstrate that the bacterial strain effectively degrades RR120 and mitigates its harmful environmental impacts. This work purposely employed a defined mineral medium to isolate and systematically assess the impact of different process factors on the biodegradation of RR120 by *P. aeruginosa* JU_CHE_01 under controlled laboratory circumstances.

The composition of actual textile wastewater is significantly more intricate and changeable, comprising mixed dyes, elevated salinity, changing pH, heavy metals, surfactants, and other organic loads, all of which may affect microbial activity and the effectiveness of dye breakdown. A significant obstacle in scaling the process is the existence of inhibitory chemicals and competition for electron donors, which may diminish biodegradation rates relative to those seen in mineral medium. The results of this investigation indicate that strain *P. aeruginosa* JU_CHE_01 can attain great decolourisation efficiency with minimum external nutrient supplementation (1 g L^{-1} glucose and yeast extract), implying significant metabolic adaptability. Although carbon and nitrogen supplies are necessary only at minimal concentrations, their extensive and prolonged application might lead to a significant rise in overall treatment expenses.

In practical applications, laboratory-grade supplements may be substituted by agro-wastes, cost-effective waste-derived carbon and nitrogen sources, or the inherent organic content of actual effluents, thus enhancing economic viability.

Future studies will aim to validate scalability and real-world applicability by treating actual textile effluents and assessing process performance in bench-scale and pilot-scale bioreactor systems, including sequencing batch reactors, anaerobic–aerobic hybrid reactors, and packed-bed reactors with immobilized cells. These investigations will evaluate operational stability under continuous flow, shock loads, and prolonged operation, in addition to the fate and toxicity of degradation intermediates. This study creates a solid platform for future reactor-based validation and process integration, linking laboratory findings with industrial wastewater treatment applications, while mineral medium-based research offers crucial mechanistic and process insights.

5.2. FUTURE RECOMMENDATIONS

In this thesis, the biodegradation of RR120 was evaluated using *P. aeruginosa* JU_CHE_01. A significant breakthrough was found and included in the thesis. However, the following works might be the future direction.

1) Although wild strain/ natural strain has lower efficiency as compared to recombinant strain. Therefore, a recombinant strain can be constructed with various dye degrading enzyme which can help to degrade versatile azo dye simultaneously which could be the future direction of the work.

2) Since bacteria are not directly involved to degrade RR120. However, enzymes which are responsible for biodegradation need to be characterized properly.

3) Various study suggested, a comprehensive biodegradation including aerobic and anaerobic has higher potentiality rather than using single process. Hence, biodegradation of RR120 may be further carried out to understand the degradation efficiency and toxicity of end product using comprehensive biodegradation process.

4) For commercial/large scale application a scale up study is very important and need to be developed using mathematical calculation. The development of the scale up equation might be the future direction of the research work.

Appendix-I

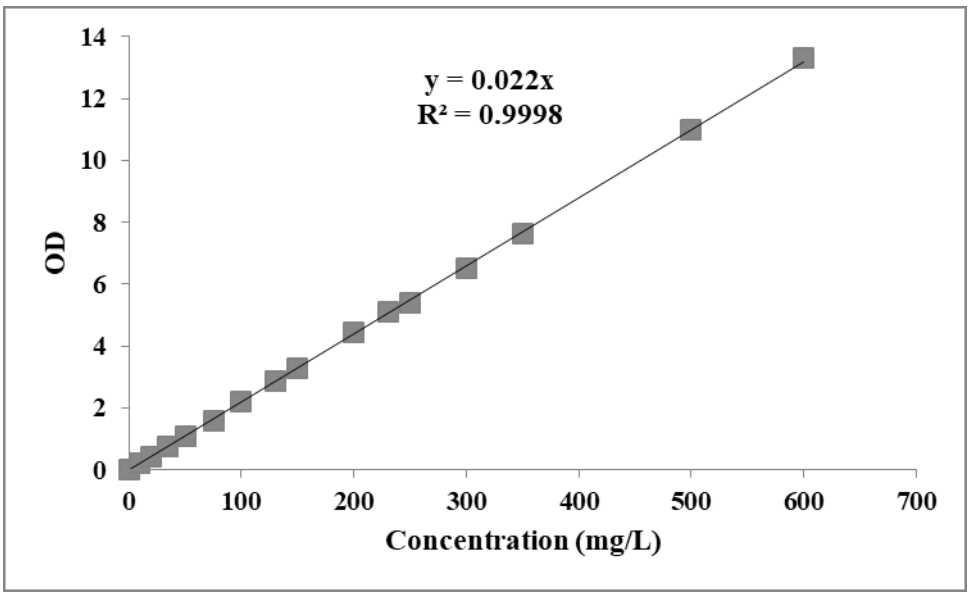

Figure A1: The Reactive Red 120 standard curve

Appendix-II

1. Mineral base medium (pH 7.0)

Glucose	0.5 g
Yeast Extract	0.5 g
K_2HPO_4	1.5 g
KH_2PO_4	0.5 g
$MgSO_4.7H_2O$	0.2 g
NaCl	0.5 g
$CaCl_2.2H_2O$	0.026 g
$FeSO_4.7H_2O$	0.0025 g
Distilled water	1,000.0 mL

2. **Nutrient Broth** (pH 7.0)

Peptone	5.0 g
Beef extract	3.0 g
NaCl	5.0 g
Distilled water	1,000.0 mL

3. **Nutrient Agar** (pH 7.0)

Peptone	5.0 g
Beef extract	3.0 g
Agar	15.0 g
NaCl	5.0 g
Distilled water	1,000.0 mL

4. MR-VP medium (pH 7.0**)**

Peptone	7.0 g
Dextrose	5.0 g
di-potassium phosphate	5.0 g
Distilled water	1,000.0 mL

5. Alpha (α)- napthol solution (Voges-Proskauer test reagent)

α- napthol	5.0 g
Ethyl alcohol	95.0 ml

5. Simmons Citrate agar

Magnesium sulfate	0.2 g
Ammonium dihydrogen phosphate	1.0 g
Dipotassium phosphate	1.0 g
Sodium citrate	2.0 g
Sodium chloride	5.0 g
Bromothymol blue	0.08 g
Agar	15.0 g
Distilled water	1,000.0 mL

6. Gram's iodine

Iodine	1.0 g
Potassium iodide	2.9 g
Distilled water	300.0 ml

7. Kovac's reagent

P-Dimethylaminobenzaldehyde	5.0 g
Amyl alcohol	75.0 ml
Hydrochloric acid (conc.)	25.0 ml

8. Motility study reagent

Carboxymethylcellulose	2.0 g
Sucrose (0.2 M)	98.0 ml
Distilled water	1,000.0 mL

9. Casein hydrolysis media (pH 7.2)

Skim milk powder	100.0 g
Peptone	5.0 g
Agar	15.0 g
Distilled water	1,000.0 mL

Appendix-III

Bacterial Characterization by Biochemical Tests

Catalase Test:

A nutrient agar medium was developed for cultivation

↓

Flasks and culture tubes were filled with the prepared medium

↓

Sterilization was carried out by autoclaving at 15 psi for 20 minutes

↓

The test organism was inoculated onto the prepared slants

↓

An un-inoculated agar slant functioned as the control

↓

Following incubation at 35°C, each slant with microbial growth received by hydrogen peroxide (3–4 drops)

↓

The presence or absence of gas bubbles in the culture was recorded

Oxidase Test:

The filter paper was folded into three similar sections and given the names of the corresponding organisms

↓

An aseptic inoculating loop was utilized to apply a loop of culture to the soaked filter paper

↓

The color of the smear was noted precisely 15-30 seconds after rubbing the cells on the moistened filter paper with the reagent

↓

A favorable response is indicated by a strong blue color

↓

After 10 seconds, a light violet or purple color was appeared an unfavorable result

Citrate Test:

Simmon's citrate agar medium was formulated and sterilized by autoclaving

↓

Five milliliters of the prepared medium were dispensed into culture tubes, and slants were created

↓

The inoculum was introduced onto the Simmon's citrate agar slants for culture

↓

Tubes without inoculation were kept as the control group

↓

The culture was kept at 37°C and incubated for 48 hours

↓

The slant culture was inspected for microbial growth and any changes in medium coloration

Methyl-Red and Voges-Proskauer Test:

The MRVP medium was made and sterilized under autoclave conditions

↓

Each tube was filled with a 5 mL aliquot of the broth

↓

The test microorganism was introduced into the tubes

↓

Tubes were placed in the incubator at 25°C for 48 hours

↓

To each tube, five drops of methyl red were administered

↓

The change in color of methyl red was observed for MR test

↓

To the other set of tubes, 12 drops of VP reagent-1 and two to three drops of VP reagent-II were added

↓

The medium was exposed to oxygen by gently shaking the tubes for 30 seconds with the caps removed

↓

The tubes were allowed to stand for 15–30 minutes and observed for color changes during the VP test

Indole Test:

The 1% tryptone broth was formulated and autoclaved at 15 psi for 20 minutes for sterilization

↓

The tryptone broth was inoculated with the test organism, and a control tube without inoculation was reserved

↓

Incubation occurred at 35°C for 48 hours, after which Kovac's reagent (1 mL) was introduced into the tubes

↓

The tubes were gently agitated every 10 to 15 minutes

↓

Tubes were left at rest for a short duration, enabling the reagent to reach the surface

↓

A cherry red layer forming at the top of the tubes was observed and recorded

Casein hydrolysis:

Skim milk agar was formulated and then sterilized via autoclaving

↓

Petri dishes were filled with the prepared media and set aside to become solid

↓

The organism was used to inoculate the plates

↓

48-hour incubation at 37°C was performed with all tubes kept in an inverted orientation

↓

The plates were observed clear zone around the line of growth

CHAPTER 7
REFERENCES

References

Aamr, A., & Cuiling, J. (2012). Bacterial influence on textile wastewater decolorization. *Journal of Environmental protection, 2012*.

Abbasiliasi, S., Tan, J. S., Ibrahim, T. A. T., Bashokouh, F., Ramakrishnan, N. R., Mustafa, S., & Ariff, A. B. (2017). Fermentation factors influencing the production of bacteriocins by lactic acid bacteria: a review. *Rsc Advances, 7*(47), 29395-29420.

Abe, F. R., Soares, A. M., de Oliveira, D. P., & Gravato, C. (2018). Toxicity of dyes to zebrafish at the biochemical level: Cellular energy allocation and neurotoxicity. *Environmental pollution, 235*, 255-262.

Adamberg, K., Kask, S., Laht, T.-M., & Paalme, T. (2003). The effect of temperature and pH on the growth of lactic acid bacteria: a pH-auxostat study. *International journal of food microbiology, 85*(1-2), 171-183.

Adomas, B., Sikorski, Ł., Bęś, A., & Warmiński, K. (2020). Exposure of Lemna minor L. to gentian violet or Congo red is associated with changes in the biosynthesis pathway of biogenic amines. *Chemosphere, 254*, 126752.

Aftab, U., Khan, M. R., Mahfooz, M., Ali, M., Aslam, S. H., & Rehman, A. (2011). Decolourization and degradation of textile azo dyes by Corynebacterium sp. isolated from industrial effluent. *Pakistan Journal of Zoology, 43*(1), 1-8.

Agrawal, S., Tipre, D., & Dave, S. (2019). Microbial Bioremediation of Azo Dyes in Textile Industry Effluent: A Review on Bioreactor-Based Studies. *Soil Microenvironment for Bioremediation Polymer Production* 131-171.

Agrawal, S., Tipre, D., & Dave, S. R. (2023). Biotreatment of azo dye containing textile industry effluent by a developed bacterial consortium immobilised on brick pieces in an indigenously designed packed bed biofilm reactor. *World Journal of Microbiology Biotechnology 39*(3), 1-16.

Agrawal, S., Tipre, D., Patel, B., & Dave, S. (2017). Bacterial decolourization, degradation and detoxification of Azo dyes: an eco-friendly approach. *Microbial Applications Vol. 1: Bioremediation Bioenergy* 91-124.

Ahmed, M., Mavukkandy, M. O., Giwa, A., Elektorowicz, M., Katsou, E., Khelifi, O., . . . Hasan, S. W. (2022). Recent developments in hazardous pollutants removal from wastewater and water reuse within a circular economy. *NPJ Clean Water, 5*(1), 1-25.

Ajaz, M., Rehman, A., Khan, Z., Nisar, M. A., & Hussain, S. (2019). Degradation of azo dyes by Alcaligenes aquatilis 3c and its potential use in the wastewater treatment. *Amb Express, 9*, 1-12.

Ajmal, A., Majeed, I., Malik, R., Iqbal, M., Nadeem, M. A., Hussain, I., . . . Nadeem, M. A. (2016). Photocatalytic degradation of textile dyes on Cu2O-CuO/TiO2 anatase powders. *Journal of Environmental Chemical Engineering, 4*(2), 2138-2146.

Aksu, Z., & Tezer, S. (2000). Equilibrium and kinetic modelling of biosorption of Remazol Black B by Rhizopus arrhizus in a batch system: effect of temperature. *Process Biochemistry, 36*(5), 431-439.

Al-Amrani, W. A., Lim, P.-E., Seng, C.-E., & Ngah, W. S. W. (2014). Factors affecting bio-decolorization of azo dyes and COD removal in anoxic–aerobic REACT operated sequencing batch reactor. *Journal of the Taiwan institute of Chemical Engineers, 45*(2), 609-616.

Al-Khaldi, F. A., Abusharkh, B., Khaled, M., Atieh, M. A., Nasser, M., Saleh, T. A., . . . Gupta, V. K. (2015). Adsorptive removal of cadmium (II) ions from liquid phase using acid modified carbon-based adsorbents. *Journal of Molecular Liquids, 204*, 255-263.

Al-Tohamy, R., Ali, S. S., Li, F., Okasha, K. M., Mahmoud, Y. A.-G., Elsamahy, T., . . . Sun, J. (2022). A critical review on the treatment of dye-containing wastewater: Ecotoxicological and health

concerns of textile dyes and possible remediation approaches for environmental safety. *Ecotoxicology Environmental Safety 231*, 113160.

AlAshkar, A., & Hassabo, A. G. (2021). Recent use of natural animal dyes in various field. *J Journal of Textiles, Coloration Polymer Science 18*(2), 191-210.

Ali, L., Alhassani, H., Karuvantevida, N., Rauf, M. A., & Ashraf, S. S. (2014). Efficient aerobic degradation of various Azo dyes by a Sphingomonas sp isolated from petroleum sludge. *Journal of Bioremediation Biodegredation 5*(3), 1.

Ali, N., Said, A., Ali, F., Raziq, F., Ali, Z., Bilal, M., . . . Iqbal, H. M. (2020). Photocatalytic degradation of congo red dye from aqueous environment using cobalt ferrite nanostructures: development, characterization, and photocatalytic performance. *Water, Air, Soil Pollution 231*, 1-16.

Ali, S. K., & Saleh, A. M. (2012). Spirulina-an overview. *International journal of Pharmacy Pharmaceutical sciences 4*(3), 9-15.

Allen, R. L. (2013). *Colour chemistry*: Springer Science & Business Media.

Almaguer, M., Carpio, R., Alves, T., & Bassin, J. (2018). Experimental study and kinetic modelling of the enzymatic degradation of the azo dye Crystal Ponceau 6R by turnip (Brassica rapa) peroxidase. *Journal of Environmental Chemical Engineering, 6*(1), 610-615.

Alzain, H., Kalimugogo, V., Hussein, K., & Karkadan, M. (2023). A Review of Environmental Impact of Azo Dyes. *Int. J. Res. Rev, 10*, 64-689.

Ameenudeen, S., Unnikrishnan, S., & Ramalingam, K. (2021). Statistical optimization for the efficacious degradation of reactive azo dyes using Acinetobacter baumannii JC359. *Journal of Environmental Management, 279*, 111512.

Amin, O. E., Aboul-Enein, A. M., Abd-Elsalam, I. S., Wahba, M. I., & El-Refai, H. A. (2022). Statistical, optimization, and thermodynamic studies on the production of alkaline protease using new local isolate of Bacillus Sp. *Egyptian Journal of Chemistry, 65*(4), 301-313.

Anastopoulos, I., Ahmed, M. J., Ojukwu, V. E., Danish, M., Stylianou, M., & Ighalo, J. O. (2024). A comprehensive review on adsorption of Reactive Red 120 dye using various adsorbents. *Journal of Molecular Liquids, 394*, 123719.

Anjaneya, O., Souche, S. Y., Santoshkumar, M., & Karegoudar, T. (2011). Decolorization of sulfonated azo dye Metanil Yellow by newly isolated bacterial strains: Bacillus sp. strain AK1 and Lysinibacillus sp. strain AK2. *Journal of hazardous materials, 190*(1-3), 351-358.

Anwar, F., Hussain, S., Ramzan, S., Hafeez, F., Arshad, M., Imran, M., . . . Abbas, N. (2014). Characterization of reactive red-120 decolorizing bacterial strain Acinetobacter junii FA10 capable of simultaneous removal of azo dyes and hexavalent chromium. *Water, Air, Soil Pollution 225*, 1-16.

Arshad, H., Imran, M., & Ashraf, M. (2020). Toxic effects of Red-S3B dye on soil microbial activities, wheat yield, and their alleviation by pressmud application. *Ecotoxicology Environmental Safety 204*, 111030.

Asmaly, H. A., Ihsanullah, Abussaud, B., Saleh, T. A., Laoui, T., Gupta, V. K., & Atieh, M. A. (2016). Adsorption of phenol on aluminum oxide impregnated fly ash. *Desalination Water Treatment 57*(15), 6801-6808.

Asmaly, H. A., Saleh, T. A., Laoui, T., Gupta, V. K., & Atieh, M. A. (2015). Enhanced adsorption of phenols from liquids by aluminum oxide/carbon nanotubes: comprehensive study from synthesis to surface properties. *Journal of Molecular Liquids, 206*, 176-182.

Atkar, A., Pabba, M., Sekhar, S. C., & Sridhar, S. (2021). Current limitations and challenges in the global textile sector. In *Fundamentals of Natural Fibres and Textiles* (pp. 741-764): Elsevier.

Ayed, L., Chaieb, K., Cheref, A., & Bakhrouf, A. (2009). Biodegradation of triphenylmethane dye Malachite Green by Sphingomonas paucimobilis. *World Journal of Microbiology and Biotechnology 25*, 705-711.

Ayed, L., Mahdhi, A., Cheref, A., & Bakhrouf, A. (2011). Decolorization and degradation of azo dye Methyl Red by an isolated Sphingomonas paucimobilis: biotoxicity and metabolites characterization. *Desalination, 274*(1-3), 272-277.

Ayed, L., Zmantar, T., Bayar, S., Cheref, A., Achour, S., Mansour, H. B., & Mzoughi, R. (2019). Potential use of probiotic consortium isolated from kefir for textile azo dye decolorization. *J Microbiol Biotechnol, 29*(10), 1629-1635.

Azanaw, A., Birlie, B., Teshome, B., & Jemberie, M. (2022). Textile effluent treatment methods and eco-friendly resolution of textile wastewater. *Case Studies in Chemical Environmental Engineering 6*, 100230.

Baeyer, A. (1883). Ueber die verbindungen der indigogruppe. *Berichte der deutschen chemischen Gesellschaft, 16*(2), 2188-2204.

Bai, Y.-N., Wang, X.-N., Zhang, F., Wu, J., Zhang, W., Lu, Y.-Z., . . . Zeng, R. J. (2020). High-rate anaerobic decolorization of methyl orange from synthetic azo dye wastewater in a methane-based hollow fiber membrane bioreactor. *Journal of hazardous materials, 388*, 121753.

Bailey, J. E., & Ollis, D. F. (2018). *Biochemical engineering fundamentals* (2nd ed.). New York: McGraw-Hill.

Balakrishnan, V. K., Shirin, S., Aman, A. M., de Solla, S. R., Mathieu-Denoncourt, J., & Langlois, V. S. (2016). Genotoxic and carcinogenic products arising from reductive transformations of the azo dye, Disperse Yellow 7. *Chemosphere, 146*, 206-215.

Balfour-Paul, J. (2012). *Indigo in the Arab world*: Routledge.

Banat, I. M., Nigam, P., Singh, D., & Marchant, R. (1996). Microbial decolorization of textile-dyecontaining effluents: a review. *Bioresource technology, 58*(3), 217-227.

Barathi, S., Aruljothi, K., Karthik, C., & Padikasan, I. A. (2020). Optimization for enhanced ecofriendly decolorization and detoxification of Reactive Blue160 textile dye by Bacillus subtilis. *Biotechnology Reports, 28*, e00522.

Barathi, S., Aruljothi, K., Karthik, C., Padikasan, I. A., & Ashokkumar, V. (2022). Biofilm mediated decolorization and degradation of reactive red 170 dye by the bacterial consortium isolated from the dyeing industry wastewater sediments. *Chemosphere, 286*, 131914.

Barathi, S., Karthik, C., Nadanasabapathi, S., & Padikasan, I. A. (2020). Biodegradation of textile dye Reactive Blue 160 by Bacillus firmus (Bacillaceae: Bacillales) and non-target toxicity screening of their degraded products. *Toxicology Reports, 7*, 16-22.

Basak, B., Bhunia, B., Dutta, S., Chakraborty, S., & Dey, A. (2014). Kinetics of phenol biodegradation at high concentration by a metabolically versatile isolated yeast Candida tropicalis PHB5. *Environmental Science Pollution Research 21*, 1444-1454.

Basutkar, M. R., Fatima, N., Chakra, P., Swami, R. S., Vishwaraj, S., & Shivannavar, C. (2019a). Decolorisation of reactive red 120 azo dye by micrococcus sp. *International journal of advanced research in biological sciences, 6*(5), 118-125.

Basutkar, M. R., Fatima, N., Chakra, P., Swami, R. S., Vishwaraj, S., & Shivannavar, C. (2019b). Decolorisation of reactive red 120 azo dye by micrococcus sp. *Int J Adv Res Biol Sci, 6*(5), 118-125.

Basutkar, M. R., & Shivannavar, C. T. (2019). Decolorization study of reactive Red-11 by using dye degrading bacterial strain Lysinibacillus boronitolerans CMGS-2. *Int. J. Curr. Microbiol. App. Sci., 8*(6), 1135-1143.

Behera, M., Nayak, J., Banerjee, S., Chakrabortty, S., & Tripathy, S. K. (2021). A review on the treatment of textile industry waste effluents towards the development of efficient

mitigation strategy: An integrated system design approach. *Journal of Environmental Chemical Engineering, 9*(4), 105277.

Benali, T., Habbadi, K., Khabbach, A., Marmouzi, I., Zengin, G., Bouyahya, A., . . . Achbani, E. H. (2020). GC–MS analysis, antioxidant and antimicrobial activities of Achillea odorata subsp. pectinata and Ruta montana essential oils and their potential use as food preservatives. *Foods, 9*(5), 1-17.

Benkhaya, S., M'rabet, S., & El Harfi, A. (2020a). Classifications, properties, recent synthesis and applications of azo dyes. *Heliyon, 6*(1).

Benkhaya, S., M'rabet, S., & El Harfi, A. (2020b). A review on classifications, recent synthesis and applications of textile dyes. *Inorganic Chemistry Communications, 115*, 107891.

Benkhaya, S., M'rabet, S., Lgaz, H., El Bachiri, A., & El Harfi, A. (2022). Dyes: classification, pollution, and environmental effects. *Dye biodegradation, mechanisms techniques: Recent advances* 1-50.

Bera, S. P., & Tank, S. (2021). Microbial degradation of Procion Red by Pseudomonas stutzeri. *Scientific Reports, 11*(1), 3075.

Berkessa, Y. W., Yan, B., Li, T., Jegatheesan, V., & Zhang, Y. (2020). Treatment of anthraquinone dye textile wastewater using anaerobic dynamic membrane bioreactor: Performance and microbial dynamics. *Chemosphere, 238*, 124539.

Berradi, M., Hsissou, R., Khudhair, M., Assouag, M., Cherkaoui, O., El Bachiri, A., & El Harfi, A. (2019). Textile finishing dyes and their impact on aquatic environs. *Heliyon, 5*(11).

Beydilli, M. I., Pavlostathis, S. G., & Tincher, W. C. (2000). Biological decolorization of the azo dye reactive red 2 under various oxidation–reduction conditions. *Water Environment Research, 72*(6), 698-705.

Bharathi, D., Nandagopal, J. G. T., Ranjithkumar, R., Gupta, P. K., & Djearamane, S. (2022). Microbial approaches for sustainable remediation of dye-contaminated wastewater: a review. *Archives of Microbiology, 204*(3), 169.

Bharathi, D., & Rajalakshmi, G. (2019). Microbial lipases: An overview of screening, production and purification. *Biocatalysis Agricultural Biotechnology 22*, 101368.

Bhatia, D., Sharma, N. R., Singh, J., & Kanwar, R. S. (2017). Biological methods for textile dye removal from wastewater: A review. *Critical Reviews in Environmental Science Technology 47*(19), 1836-1876.

Bhosale, S., Saratale, G., & Govindwar, S. (2006). Biotransformation enzymes in Cunninghamella blakesleeana (NCIM-687). *Journal of basic microbiology, 46*(6), 444-448.

Bhunia, B., Basak, B., Bhattacharya, P., & Dey, A. (2012). Kinetic studies of alkaline protease from Bacillus licheniformis NCIM-2042. *Journal of microbiology & biotechnology, 22*(12), 1758–1766.

Birmole, R. (2021). Evaluation of bacterial consortium and optimization of growth parameters for effective decolorization of azo dye reactive red 120. *Journal of Applied Biotechnology Reports, 8*(4), 428-439.

Birmole, R., & Aruna, K. (2019). Optimisation studies of reactive red 120 decolorisation by Shewanella haliotis RDB_1. *Journal of Global Biosciences, 8*, 6324-6367.

Brenner, D. J., Krieg, N. R., Staley, J. T., & Garrity, G. (2005). *Bergey's Manual of Systematic Bacteriology: Volume Two: The Proteobacteria (Part C)*: Springer.

Brüschweiler, B. J., & Merlot, C. (2017). Azo dyes in clothing textiles can be cleaved into a series of mutagenic aromatic amines which are not regulated yet. *Regulatory Toxicology Pharmacology 88*, 214-226.

Cannon, J., & Cannon, M. (1994). *Dye plants and dyeing*: Herbert Press Ltd.

Cardon, D., Prunac, S., & Andary, C. (1996). Yellow dyes of historical importance. Part II. Chemical analysis of weld ans saw-wort. In (Vol. 14, pp. 33-38): Dyes Hist Archaeol

Chakraborty, S., Basak, B., Dutta, S., Bhunia, B., & Dey, A. (2013). Decolorization and biodegradation of congo red dye by a novel white rot fungus Alternaria alternata CMERI F6. *Bioresource technology, 147*, 662-666.

Chang, J.-S., Chou, C., Lin, Y.-C., Lin, P.-J., Ho, J.-Y., & Hu, T. L. (2001). Kinetic characteristics of bacterial azo-dye decolorization by Pseudomonas luteola. *Water research, 35*(12), 2841-2850.

Chang, J.-S., Kuo, T.-S., Chao, Y.-P., Ho, J.-Y., & Lin, P.-J. (2000). Azo dye decolorization with a mutant Escherichia coli strain. *Biotechnology Letters, 22*, 807-812.

Chang, L., Meier, J., & Smith, M. (1997). Application of plant and earthworm bioassays to evaluate remediation of a lead-contaminated soil. *Archives of Environmental Contamination Toxicology 32*, 166-171.

Chen, A., Yang, B., Zhou, Y., Sun, Y., & Ding, C. (2018). Effects of azo dye on simultaneous biological removal of azo dye and nutrients in wastewater. *Royal Society Open Science, 5*(8), 180795.

Chen, B.-Y. (2002). Understanding decolorization characteristics of reactive azo dyes by Pseudomonas luteola: toxicity and kinetics. *Process Biochemistry, 38*(3), 437-446.

Chen, G., An, X., Li, H., Lai, F., Yuan, E., Xia, X., & Zhang, Q. (2021). Detoxification of azo dye Direct Black G by thermophilic Anoxybacillus sp. PDR2 and its application potential in bioremediation. *Ecotoxicology Environmental Safety 214*, 112084.

Chen, Y.-G., Huang, J.-H., Luo, R., Ge, H.-Z., Wołowicz, A., Wawrzkiewicz, M., . . . Kołodyńska, D. (2021). Impacts of heavy metals and medicinal crops on ecological systems, environmental pollution, cultivation, and production processes in China. *Ecotoxicology Environmental Safety 219*, 112336.

Cheng, H., Yuan, M., Zeng, Q., Zhou, H., Zhan, W., Chen, H., . . . Wang, Y. (2021). Efficient reduction of reactive black 5 and Cr (Ⅵ) by a newly isolated bacterium of Ochrobactrum anthropi. *Journal of hazardous materials, 406*, 124641.

Chequer, F. D., de Oliveira, G. A. R., Ferraz, E. A., Cardoso, J. C., Zanoni, M., & de Oliveira, D. P. (2013). Textile dyes: dyeing process and environmental impact. *Eco-friendly textile dyeing finishing 6*(6), 151-176.

Chequer, F. M. D., Angeli, J. P. F., Ferraz, E. R. A., Tsuboy, M. S., Marcarini, J. C., Mantovani, M. S., & de Oliveira, D. P. (2009). The azo dyes Disperse Red 1 and Disperse Orange 1 increase the micronuclei frequencies in human lymphocytes and in HepG2 cells. *Mutation Research/Genetic Toxicology Environmental Mutagenesis 676*(1-2), 83-86.

Chittal, V., Gracias, M., Anu, A., Saha, P., & Rao, K. B. (2019). Biodecolorization and biodegradation of azo dye reactive orange-16 by marine nocardiopsis sp. *Iranian Journal of Biotechnology, 17*(3), e1551.

Christen, P., Vega, A., Casalot, L., Simon, G., & Auria, R. (2012). Kinetics of aerobic phenol biodegradation by the acidophilic and hyperthermophilic archaeon Sulfolobus solfataricus 98/2. *Biochemical Engineering Journal, 62*, 56-61.

Christie, R. (2014). *Colour chemistry*: Royal society of chemistry, Cambridge, UK.

Chung, K.-T. (2016). Azo dyes and human health: A review. *Journal of Environmental Science Health, 34*(4), 233-261.

Chung, K.-T., & Cerniglia, C. E. (1992). Mutagenicity of azo dyes: structure-activity relationships. *Mutation Research/Reviews in Genetic Toxicology 277*(3), 201-220.

Clark, M. (2011). *Handbook of textile and industrial dyeing: principles, processes and types of dyes*: Elsevier.

Colin, N., Maceda-Veiga, A., Flor-Arnau, N., Mora, J., Fortuño, P., Vieira, C., . . . De Sostoa, A. (2016). Ecological impact and recovery of a Mediterranean river after receiving the effluent from a textile dyeing industry. *Ecotoxicology Environmental Safety 132*, 295-303.

Collivignarelli, M. C., Abbà, A., Miino, M. C., & Damiani, S. (2019). Treatments for color removal from wastewater: State of the art. *Journal of environmental management, 236*, 727-745.

Couto, N., Wood, J., & Barber, J. (2016). The role of glutathione reductase and related enzymes on cellular redox homoeostasis network. *Free radical biology medicine 95*, 27-42.

D'souza, D., Birmole, R., & Aruna, K. (2020). Optimization studies of the biodegradation of reactive red 120 by Shewanella putrefaciens RDB_2 isolated from textile effluent water. *International Journal of Recent Scientific Research, 11*(1), 37161-37178.

Dang, B.-T., Tran, D. P., Cao, H. T., Tomoaki, I., Pham, T.-T., Varjani, S., . . . Bui, X.-T. (2022). Comparison of degradation kinetics of tannery wastewater treatment using a nonlinear model by salt-tolerant Nitrosomonas sp. and Nitrobacter sp. *Bioresource Technology, 351*, 127000-127008.

Darwesh, O. M., Ali, S. S., Matter, I. A., & Elsamahy, T. (2021). Nanotextiles waste management: Controlling of release and remediation of wastes. In *Nanosensors and nanodevices for smart multifunctional textiles* (pp. 267-286): Elsevier.

Das, A., & Mishra, S. (2017). Removal of textile dye reactive green-19 using bacterial consortium: process optimization using response surface methodology and kinetics study. *Journal of Environmental Chemical Engineering, 5*(1), 612-627.

de Sousa, M. L., de Moraes, P. B., Lopes, P. R. M., Montagnolli, R. N., de Angelis, D. d. F., & Bidoia, E. D. (2012). Contamination by remazol red brilliant dye and its impact in aquatic photosynthetic microbiota. *Environmental Management Sustainable Development 1*(2), 129.

DeLuca, L. (2017). United Nations: Online data repositories and resources. *College Research Libraries News 78*(1), 41-45.

Dixit, S., & Garg, S. (2019). Development of an efficient recombinant bacterium and its application in the degradation of environmentally hazardous azo dyes. *International Journal of Environmental Science Technology 16*, 7137-7146.

Dong, H., Guo, T., Zhang, W., Ying, H., Wang, P., Wang, Y., & Chen, Y. (2019). Biochemical characterization of a novel azoreductase from Streptomyces sp.: application in eco-friendly decolorization of azo dye wastewater. *International journal of biological macromolecules, 140*, 1037-1046.

Donkadokula, N. Y., Kola, A. K., Naz, I., & Saroj, D. (2020). A review on advanced physico-chemical and biological textile dye wastewater treatment techniques. *Reviews in environmental science and bio/technology 19*(3), 543-560.

Dos Santos, A. B., Cervantes, F. J., & Van Lier, J. B. (2004). Azo dye reduction by thermophilic anaerobic granular sludge, and the impact of the redox mediator anthraquinone-2, 6-disulfonate (AQDS) on the reductive biochemical transformation. *Applied microbiology biotechnology 64*, 62-69.

Duran, N., & Esposito, E. (2000). Potential applications of oxidative enzymes and phenoloxidase-like compounds in wastewater and soil treatment: a review. *Applied catalysis B: environmental, 28*(2), 83-99.

Dutta, D., Arya, S., & Kumar, S. (2021). Industrial wastewater treatment: Current trends, bottlenecks, and best practices. *Chemosphere, 285*, 131245.

Dutta, S., Adhikary, S., Bhattacharya, S., Roy, D., Chatterjee, S., Chakraborty, A., . . . Rajak, P. (2024). Contamination of textile dyes in aquatic environment: Adverse impacts on aquatic

ecosystem and human health, and its management using bioremediation. *Journal of Environmental Management, 353*, 120103.
Dutta, S., Gupta, B., Srivastava, S. K., & Gupta, A. K. (2021). Recent advances on the removal of dyes from wastewater using various adsorbents: A critical review. *Materials Advances, 2*(14), 4497-4531.
Ebency, C. I. L., Rajan, S., Murugesan, A., Rajesh, R., & Elayarajah, B. (2013). Biodegradation of textile azo dyes and its bioremediation potential using seed germination efficiency. *International Journal of Current Microbiology Applied Sciences 2*(10), 496-505.

Edwards, V. H. (1970). The influence of high substrate concentrations on microbial kinetics. *Biotechnology bioengineering 12*(5), 679-712.

El Harfi, S., & El Harfi, A. (2017). Classifications, properties and applications of textile dyes: A review. *Applied Journal of Environmental Engineering Science, 3*(3), 311-320.
Elfarash, A., Mawad, A. M., Yousef, N. M., & Shoreit, A. A. (2017). Azoreductase kinetics and gene expression in the synthetic dyes-degrading Pseudomonas. *Egyptian journal of basic applied sciences 4*(4), 315-322.

Enaime, G., Baçaoui, A., Yaacoubi, A., Belaqziz, M., Wichern, M., & Lübken, M. (2020). Phytotoxicity assessment of olive mill wastewater treated by different technologies: effect on seed germination of maize and tomato. *Environmental Science Pollution Research 27*, 8034-8045.

Eteng, O. E., Moses, C. A., Ugwor, E. I., Enobong, J. E., Akamo, A. J., Adebekun, Y., . . . Ubana, E. (2022). Ingestion of Sudan IV-adulterated palm oil impairs hepato-renal functions and induces the overexpression of pro-inflammatory cytokines: A sub-acute murine model. *Egyptian journal of basic applied sciences, 9*(1), 11-22.
Falade, A. O., Nwodo, U. U., Iweriebor, B. C., Green, E., Mabinya, L. V., & Okoh, A. I. (2017). Lignin peroxidase functionalities and prospective applications. *MicrobiologyOpen, 6*(1), e00394.
Fazal, T., Razzaq, A., Javed, F., Hafeez, A., Rashid, N., Amjad, U. S., . . . Rehman, F. (2020). Integrating adsorption and photocatalysis: A cost effective strategy for textile wastewater treatment using hybrid biochar-TiO2 composite. *Journal of hazardous materials, 390*, 121623.
Feng, J., Yan, W., & Zhang, L. (2009). Synthesis of polypyrrole micro/nanofibers via a self-assembly process. *Microchimica Acta, 166*, 261-267.
Ferraz, E. R., Grando, M. D., & Oliveira, D. P. (2011). The azo dye Disperse Orange 1 induces DNA damage and cytotoxic effects but does not cause ecotoxic effects in Daphnia similis and Vibrio fischeri. *Journal of hazardous materials, 192*(2), 628-633.
Foguel, M. V., Ton, X.-A., Zanoni, M. V., Maria Del Pilar, T. S., Haupt, K., & Bui, B. T. S. (2015). A molecularly imprinted polymer-based evanescent wave fiber optic sensor for the detection of basic red 9 dye. *Sensors Actuators B: Chemical 218*, 222-228.

Franca, R. D. G., Vieira, A., Carvalho, G., Oehmen, A., Pinheiro, H. M., Crespo, M. T. B., & Lourenco, N. D. (2020). Oerskovia paurometabola can efficiently decolorize azo dye Acid Red 14 and remove its recalcitrant metabolite. *Ecotoxicology Environmental Safety 191*, 110007.

Galai, S., Korri-Youssoufi, H., & Marzouki, M. N. (2014). Characterization of yellow bacterial laccase SmLac/role of redox mediators in azo dye decolorization. *Journal of Chemical Technology Biotechnology 89*(11), 1741-1750.

Garg, N., Garg, A., & Mukherji, S. (2020). Eco-friendly decolorization and degradation of reactive yellow 145 textile dye by Pseudomonas aeruginosa and Thiosphaera pantotropha. *Journal of environmental management, 263*, 110383.
Garg, S. K., & Tripathi, M. (2013). Process parameters for decolorization and biodegradation of orange II (Acid Orange 7) in dye-simulated minimal salt medium and subsequent textile

effluent treatment by Bacillus cereus (MTCC 9777) RMLAU1. *Environmental monitoring assessment 185*, 8909-8923.

Gargava, P. (2021). Pollution control acts, rules & notifications issued thereunder. In: Pollution control law series PCLS/02/2021.

Gayathri, R., Kavi, A., Meena, P., Karthikeyan, S., & Ramesh, N. (2014). Biodegradation of azo dyes by using soil bacteria. *International Journal of Engineering Research & Technology, 3*, 738-741.

Ghaedi, M., Hajjati, S., Mahmudi, Z., Tyagi, I., Agarwal, S., Maity, A., & Gupta, V. (2015). Modeling of competitive ultrasonic assisted removal of the dyes–Methylene blue and Safranin-O using Fe3O4 nanoparticles. *Chemical Engineering Journal, 268*, 28-37.

Ghaly, A., Ananthashankar, R., Alhattab, M., & Ramakrishnan, V. V. (2014). Production, characterization and treatment of textile effluents: a critical review. *J Chem Eng Process Technol, 5*(1), 1-19.

Gholami, F., Zinatizadeh, A., Zinadini, S., McKay, T., & Sibali, L. (2020). An innovative jet loop-airlift bioreactor for simultaneous removal of carbon and nitrogen from soft drink industrial wastewater: Process performance and kinetic evaluation. *Environmental Technology Innovation 19*, 100772.

Gokilavani, S. A STUDY ON FACTORS INFLUENCING FOR LOGISTICS OPERATIONS–WITH SPECIAL REFERENCE TO TIRUPUR GARMENT EXPORT INDUSTRY, TAMILNADU.

Gomes, J. R. (2001). *Estrutura e propriedades dos corantes*: Barbosa e Xavier Lda., Braga, Portugal.

Goswami, D., Mukherjee, J., Mondal, C., & Bhunia, B. (2024). Bioremediation of azo dye: A review on strategies, toxicity assessment, mechanisms, bottlenecks and prospects. *Science of The Total Environment, 954*, 176426.

Goud, B. S., Cha, H. L., Koyyada, G., & Kim, J. H. (2020). Augmented biodegradation of textile azo dye effluents by plant endophytes: a sustainable, eco-friendly alternative. *Current Microbiology, 77*, 3240-3255.

Gregory, P. (1990). Classification of dyes by chemical structure. *The chemistry application of dyes,* 17-47.

Gul, R., Sharma, P., Kumar, R., Umar, A., Ibrahim, A. A., Alhamami, M. A., . . . Baskoutas, S. (2023). A sustainable approach to the degradation of dyes by fungal species isolated from industrial wastewaters: Performance, parametric optimization, kinetics and degradation mechanism. *Environmental Research, 216*, 114407-114418.

Guo, G., Tian, F., Zhao, Y., Tang, M., Liu, W., Liu, C., . . . Wang, S. (2019a). Aerobic decolorization and detoxification of Acid Scarlet GR by a newly isolated salt-tolerant yeast strain Galactomyces geotrichum GG. *International Biodeterioration Biodegradation, 145*, 104818.

Guo, G., Tian, F., Zhao, Y., Tang, M., Liu, W., Liu, C., . . . Wang, S. (2019b). Aerobic decolorization and detoxification of Acid Scarlet GR by a newly isolated salt-tolerant yeast strain Galactomyces geotrichum GG. *International Biodeterioration & Biodegradation, 145*, 104818.

Gupta, A. K., & Sinha, S. (2006). Chemical fractionation and heavy metal accumulation in the plant of Sesamum indicum (L.) var. T55 grown on soil amended with tannery sludge: Selection of single extractants. *Chemosphere, 64*(1), 161-173.

Gupta, V., Garg, S., Capalash, N., Gupta, N., & Sharma, P. (2015). Production of thermo-alkali-stable laccase and xylanase by co-culturing of Bacillus sp. and B. halodurans for biobleaching of kraft pulp and deinking of waste paper. *Bioprocess biosystems engineering, 38*, 947-956.

Gupte, S. A. (2012). Microbial remediation of azo dyes using bacterial consortium PES.

Hafeez, F., Farheen, H., Mahmood, F., Shahzad, T., Shahid, M., Iqbal, M., . . . Hussain, S. (2018). Isolation and characterization of a lead (Pb) tolerant Pseudomonas aeruginosa strain HF5 for decolorization of reactive red-120 and other azo dyes. *Annals of Microbiology, 68*, 943-952.

Han, J., Yang, D., Hall, D. R., Liu, J., Sun, J., Gu, W., . . . Krause, H. M. (2020). Toxicokinetics of brominated azo dyes in the early life stages of zebrafish (Danio rerio) is prone to aromatic substituent changes. *Environmental science technology, 54*(7), 4421-4431.

Han, K., & Levenspiel, O. (1988). Extended Monod kinetics for substrate, product, and cell inhibition. *Biotechnology and bioengineering, 32*(4), 430-447.

Hanne, L., Kirk, L., Appel, S., Narayan, A., & Bains, K. (1993). Degradation and induction specificity in actinomycetes that degrade p-nitrophenol. *Applied Environmental Microbiology, 59*(10), 3505-3508.

Haq, I., & Raj, A. (2018). Biodegradation of Azure-B dye by Serratia liquefaciens and its validation by phytotoxicity, genotoxicity and cytotoxicity studies. *Chemosphere, 196*, 58-68.

Haridevamuthu, B., Murugan, R., Seenivasan, B., Meenatchi, R., Pachaiappan, R., Almutairi, B. O., . . . Arockiaraj, J. (2024). Synthetic azo-dye, Tartrazine induces neurodevelopmental toxicity via mitochondria-mediated apoptosis in zebrafish embryos. *Journal of hazardous materials, 461*, 132524.

Hassan, M. M., & Carr, C. M. (2018). A critical review on recent advancements of the removal of reactive dyes from dyehouse effluent by ion-exchange adsorbents. *Chemosphere, 209*, 201-219.

Hatvani, N., & Mécs, I. (2001). Production of laccase and manganese peroxidase by Lentinus edodes on malt-containing by-product of the brewing process. *Process Biochemistry, 37*(5), 491-496.

Hocini, I., Benabbas, K., Khellaf, N., Djelal, H., & Amrane, A. (2019). Can duckweed be used for the biomonitoring of textile effluents? *Euro-Mediterranean Journal for Environmental Integration, 4*, 1-8.

Huang, X., Bo, X., Zhao, Y., Gao, B., Wang, Y., Sun, S., . . . Li, Q. (2014). Effects of compound bioflocculant on coagulation performance and floc properties for dye removal. *Bioresource technology, 165*, 116-121.

Hunger, K. (2007a). *Industrial dyes: chemistry, properties, applications*: John Wiley & Sons.

Hunger, K. (2007b). *Industrial dyes: chemistry, properties, applications* (Vol. 8): John Wiley & Sons.

Hussain, B., Sajad, M., Usman, H., Al-Ghanim, K. A., Riaz, M. N., Berenjian, A., . . . Show, P. L. (2022). Assessment of hepatotoxicity and nephrotoxicity in Cirrhinus mrigala induced by trypan blue-An azo dye. *Environmental Research, 215*, 114120.

Ihsanullah, I. (2020). MXenes (two-dimensional metal carbides) as emerging nanomaterials for water purification: Progress, challenges and prospects. *Chemical Engineering Journal, 388*, 124340.

Ihsanullah, I., Jamal, A., Ilyas, M., Zubair, M., Khan, G., & Atieh, M. A. (2020). Bioremediation of dyes: Current status and prospects. *Journal of Water Process Engineering, 38*, 101680.

Ikram, M., Naeem, M., Zahoor, M., Hanafiah, M. M., Oyekanmi, A. A., Ullah, R., . . . Gulfam, N. J. W. (2022). Biological degradation of the azo dye basic orange 2 by Escherichia coli: A sustainable and ecofriendly approach for the treatment of textile wastewater. *Water, 14*(13), 2063.

Ingamells, W. (1993). Colour for textiles. *Society of Dyers Colourists,* 2-5.

Islam, A., Teo, S. H., Taufiq-Yap, Y. H., Ng, C. H., Vo, D.-V. N., Ibrahim, M. L., . . . Awual, M. R. (2021). Step towards the sustainable toxic dyes removal and recycling from aqueous solution-A comprehensive review. *Resources, Conservation Recycling, 175*, 105849.

Islam, T., Repon, M. R., Islam, T., Sarwar, Z., & Rahman, M. M. (2023). Impact of textile dyes on health and ecosystem: A review of structure, causes, and potential solutions. *Environmental Science Pollution Research, 30*(4), 9207-9242.

Jadhav, A. C., & Jadhav, N. C. (2021). Treatment of textile wastewater using adsorption and adsorbents. In *Sustainable technologies for textile wastewater treatments* (pp. 235-273): Elsevier.

Jadhav, A. J., & Srivastava, V. C. (2013). Adsorbed solution theory based modeling of binary adsorption of nitrobenzene, aniline and phenol onto granulated activated carbon. *Chemical Engineering Journal, 229*, 450-459.

Jadhav, J., Parshetti, G., Kalme, S., & Govindwar, S. (2007). Decolourization of azo dye methyl red by Saccharomyces cerevisiae MTCC 463. *Chemosphere, 68*(2), 394-400.

Jadhav, U. U., Dawkar, V. V., Ghodake, G. S., & Govindwar, S. P. (2008). Biodegradation of Direct Red 5B, a textile dye by newly isolated Comamonas sp. UVS. *Journal of hazardous materials, 158*(2-3), 507-516.

Jafari, N., Soudi, M. R., & Kasra-Kermanshahi, R. (2014). Biodegradation perspectives of azo dyes by yeasts. *Microbiology, 83*, 484-497.

Jain, K., Shah, V., Chapla, D., & Madamwar, D. (2012). Decolorization and degradation of azo dye–Reactive Violet 5R by an acclimatized indigenous bacterial mixed cultures-SB4 isolated from anthropogenic dye contaminated soil. *Journal of hazardous materials, 213*, 378-386.

Jamee, R., & Siddique, R. (2019). Biodegradation of synthetic dyes of textile effluent by microorganisms: an environmentally and economically sustainable approach. *European journal of microbiology immunology, 9*(4), 114-118.

Jiang, L.-L., Li, K., Yan, D.-L., Yang, M.-F., Ma, L., & Xie, L.-Z. (2020). Toxicity assessment of 4 azo dyes in zebrafish embryos. *International journal of toxicology, 39*(2), 115-123.

Jin, X., Wu, C., Tian, X., Wang, P., Zhou, Y., & Zuo, J. (2021). A magnetic-void-porous MnFe2O4/carbon microspheres nano-catalyst for catalytic ozonation: Preparation, performance and mechanism. *Environmental Science Ecotechnology,7*, 100110.

Joshi, A. U., Hinsu, A. T., Kotadiya, R. J., Rank, J. K., Andharia, K. N., & Kothari, R. K. (2020). Decolorization and biodegradation of textile di-azo dye Acid Blue 113 by Pseudomonas stutzeri AK6. *3 Biotech, 10*(5), 214.

Kalme, S., Jadhav, S., Jadhav, M., & Govindwar, S. (2009). Textile dye degrading laccase from Pseudomonas desmolyticum NCIM 2112. *Enzyme Microbial Technology, 44*(2), 65-71.

Kalyani, D., Telke, A., Dhanve, R., & Jadhav, J. (2009). Ecofriendly biodegradation and detoxification of Reactive Red 2 textile dye by newly isolated Pseudomonas sp. SUK1. *Journal of hazardous materials, 163*(2-3), 735-742.

Kamal El-Dean, A. M., Ahmed, M. M., Mohamed, M. A., Hussain, S. M., & Hashem, E. Y. (2019). Mordant yellow 12 dye removal from wastewater using low cost modified sugarcane bagasse as an adsorbent. *Egyptian Sugar Journal, 12*, 130-149.

Kamali, M., Fazlpour, F., Karimi, F., Rezaee, A., Sadri, F., & Hosseini, S. F. (2023). A review of cytotoxic effects of azo dyes on brain-subregion. *Middle East Journal of Rehabilitation, Health Studies, 10*(2).

Kant, R. (2011). Textile dyeing industry an environmental hazard. *Natural Science, 4(1)*, 22-26.

Kapoor, R. T., Danish, M., Singh, R. S., Rafatullah, M., & HPS, A. K. (2021). Exploiting microbial biomass in treating azo dyes contaminated wastewater: Mechanism of degradation and factors affecting microbial efficiency. *Journal of Water Process Engineering, 43*, 102255.

Karcher, S., Kornmüller, A., & Jekel, M. (2002). Anion exchange resins for removal of reactive dyes from textile wastewaters. *Water research, 36*(19), 4717-4724.

Karim, M. E., Dhar, K., & Hossain, M. T. (2018). Decolorization of textile reactive dyes by bacterial monoculture and consortium screened from textile dyeing effluent. *Journal of Genetic Engineering Biotechnology, 16*(2), 375-380.

Kataria, J., Rawat, H., Tomar, H., Gaurav, N., & Kumar, A. (2022). Azo Dyes Degradation Approaches and Challenges: An Overview. *The Scientific Temper, 13*(02), 384-400.

Kaushik, P., & Malik, A. (2009). Fungal dye decolourization: recent advances and future potential. *Environment international, 35*(1), 127-141.

Khalaf, H. A., El-Sheekh, M. M., & Makhlof, M. E. (2023). Lychaete pellucida as a novel biosorbent for the biodegradation of hazardous azo dyes. *Environmental monitoring assessment, 195*(8), 929.

Khalaj, M., Kamali, M., Khodaparast, Z., & Jahanshahi, A. (2018). Copper-based nanomaterials for environmental decontamination–an overview on technical and toxicological aspects. *Ecotoxicology Environmental Safety, 148*, 813-824.

Khaled, J. M., Alyahya, S. A., Govindan, R., Chelliah, C. K., Maruthupandy, M., Alharbi, N. S., . . . Li, W.-J. (2022). Laccase producing bacteria influenced the high decolorization of textile azo dyes with advanced study. *Environmental Research, 207*, 112211.

Khalid, A., Arshad, M., & Crowley, D. E. (2008). Decolorization of azo dyes by Shewanella sp. under saline conditions. *Applied microbiology biotechnology, 79*, 1053-1059.

Khalid, A., Zubair, M., & Ihsanullah. (2018). A comparative study on the adsorption of Eriochrome Black T dye from aqueous solution on graphene and acid-modified graphene. *Arabian Journal for Science Engineering, 43*, 2167-2179.

Khan, M. D., Abdulateif, H., Ismail, I. M., Sabir, S., & Khan, M. Z. (2015). Bioelectricity generation and bioremediation of an azo-dye in a microbial fuel cell coupled activated sludge process. *PLoS One, 10*(10), e0138448.

Khan, M. D., Li, D., Tabraiz, S., Shamurad, B., Scott, K., Khan, M. Z., & Yu, E. H. (2021). Integrated air cathode microbial fuel cell-aerobic bioreactor set-up for enhanced bioelectrodegradation of azo dye Acid Blue 29. *Science of The Total Environment, 756*, 143752.

Khan, R., Bhawana, P., & Fulekar, M. (2013). Microbial decolorization and degradation of synthetic dyes: a review. *Reviews in Environmental Science Bio/Technology, 12*, 75-97.

Khataee, A., Dehghan, G., Ebadi, A., Zarei, M., & Pourhassan, M. (2010). Biological treatment of a dye solution by Macroalgae Chara sp.: Effect of operational parameters, intermediates identification and artificial neural network modeling. *Bioresource technology, 101*(7), 2252-2258.

Khataee, A., Vahid, B., Aghdasinia, H., & Bagheri, R. (2018). Semi-pilot scale fluidized bed reactor for removal of a textile dye through heterogeneous Fenton process using natural pyrite. *International journal of environmental science technology, 15*, 289-300.

Kimura, M. (1980). A simple method for estimating evolutionary rates of base substitutions through comparative studies of nucleotide sequences. *Journal of molecular evolution, 16*, 111-120.

Kishor, R., Purchase, D., Saratale, G. D., Ferreira, L. F. R., Hussain, C. M., Mulla, S. I., & Bharagava, R. N. (2021). Degradation mechanism and toxicity reduction of methyl orange dye by a newly isolated bacterium Pseudomonas aeruginosa MZ520730. *Journal of Water Process Engineering, 43*, 102300.

Knapp, J., & Newby, P. (1995). The microbiological decolorization of an industrial effluent containing a diazo-linked chromophore. *Water research, 29*(7), 1807-1809.

Kolekar, Y. M., Konde, P. D., Markad, V. L., Kulkarni, S. V., Chaudhari, A. U., & Kodam, K. M. (2013). Effective bioremoval and detoxification of textile dye mixture by Alishewanella sp. KMK6. *Applied microbiology and biotechnology, 97*(2), 881-889.

Koprivanac, N., Bosanac, G., Grabaric, Z., & Papic, S. (1993). Treatment of wastewaters from dye industry. *Environmental technology, 14*(4), 385-390.

Krithika, A., Gayathri, K. V., Kumar, D. T., & Doss, C. G. P. (2021). Mixed azo dyes degradation by an intracellular azoreductase enzyme from alkaliphilic Bacillus subtilis: a molecular docking study. *Archives of Microbiology, 203*, 3033-3044.

Kulkarni, A. N., Watharkar, A. D., Rane, N. R., Jeon, B.-H., & Govindwar, S. P. (2018). Decolorization and detoxification of dye mixture and textile effluent by lichen Dermatocarpon vellereceum in fixed bed upflow bioreactor with subsequent oxidative stress study. *Ecotoxicology Environmental Safety, 148*, 17-25.

Kulkarni, N., Shendye, A., & Rao, M. (1999). Molecular and biotechnological aspects of xylanases. *FEMS microbiology reviews, 23*(4), 411-456.

Kumar, A., Kumar, A., Singh, R., Singh, R., Pandey, S., Rai, A., . . . Rahul, B. (2020). Genetically engineered bacteria for the degradation of dye and other organic compounds. In *Abatement of environmental pollutants* (pp. 331-350): Elsevier.

Kumar, S., Stecher, G., & Tamura, K. (2016). MEGA7: molecular evolutionary genetics analysis version 7.0 for bigger datasets. *Molecular biology evolution, 33*(7), 1870-1874.

Kumar, V., Chandra, R., Thakur, I. S., Saxena, G., & Shah, M. P. (2020). Recent advances in physicochemical and biological treatment approaches for distillery wastewater. *Combined application of physico-chemical microbiological processes for industrial effluent treatment plant,* 79-118.

Kumari, L., Tiwary, D., & Mishra, P. K. (2016). Biodegradation of CI Acid Red 1 by indigenous bacteria Stenotrophomonas sp. BHUSSp X2 isolated from dye contaminated soil. *Environmental Science and Pollution Research, 23*(5), 4054-4062.

Kumari, S., Debnath, M., Hari Sonawane, S., Teja Malkapuram, S., & Mohan Seepana, M. (2022). Dye decolorization by Rhodococcus ruber strain TES III isolated from textile effluent wastewater contaminated soil. *ChemistrySelect, 7*(30), e202200421.

Kurade, M. B., Waghmode, T. R., Patil, S. M., Jeon, B.-H., & Govindwar, S. P. (2017). Monitoring the gradual biodegradation of dyes in a simulated textile effluent and development of a novel triple layered fixed bed reactor using a bacterium-yeast consortium. *Chemical Engineering Journal, 307*, 1026-1036.

Lade, H., Kadam, A., Paul, D., & Govindwar, S. (2015). Biodegradation and detoxification of textile azo dyes by bacterial consortium under sequential microaerophilic/aerobic processes. *EXCLI journal, 14*, 1-17.

Laing, I. (1991). The impact of effluent regulations on the dyeing industry. *Review of Progress in Coloration Related Topics, 21*(1), 56-71.

Lellis, B., Fávaro-Polonio, C. Z., Pamphile, J. A., & Polonio, J. C. (2019). Effects of textile dyes on health and the environment and bioremediation potential of living organisms. *Biotechnology Research Innovation, 3*(2), 275-290.

Leme, D. M., Primo, F. L., Gobo, G. G., da Costa, C. R. V., Tedesco, A. C., & de Oliveira, D. P. (2015). Genotoxicity assessment of reactive and disperse textile dyes using human dermal equivalent (3D cell culture system). *Journal of Toxicology Environmental Health, Part A, 78*(7), 466-480.

Li, H.-h., Wang, Y.-t., Wang, Y., Wang, H.-x., Sun, K.-k., & Lu, Z.-m. (2019). Bacterial degradation of anthraquinone dyes. *Journal of Zhejiang University. Science. B, 20*(6), 528.

Li, J. F., Rupa, E. J., Hurh, J., Huo, Y., Chen, L., Han, Y., . . . Mathiyalagan, R. (2019). Cordyceps militaris fungus mediated Zinc Oxide nanoparticles for the photocatalytic degradation of Methylene blue dye. *Optik, 183*, 691-697.

Li, K. (2003). The role of enzymes and mediators in white-rot fungal degradation of lignocellulose. In: ACS Publications.

Li, Y., Song, Z., Yuan, Y., Zhang, Q., & Zhu, H. (2020). Rheology improvement in an osmotic membrane bioreactor for waste sludge anaerobic digestion and the implication on agitation energy consumption. *Bioresource technology, 295*, 122313.

Liang, J., Ning, X.-a., Kong, M., Liu, D., Wang, G., Cai, H., . . . Yuan, Y. (2017). Elimination and ecotoxicity evaluation of phthalic acid esters from textile-dyeing wastewater. *Environmental pollution, 231*, 115-122.

Liang, J., Zhang, C.-M., & Zhu, C.-C. (2024). Toxic effects and mechanisms of cationic blue SD-GSL on Chlorella vulgaris before and after the biological decolorization process. *Chemosphere, 349*, 140947.

Lingappa, K., Ananda, S., Horti, S., Nabeela, B., & Mahesh, R. (2023). Bio-degradation of Azo dye by the Bacteria isolated from Textile Industry Effulent of Solapur district. *Research Journal of Chemistry and Environment, 27*(10), 1-5.

Lingappa, K., Ananda, S., Horti, S., Nabeela, B., & Mahesh, R. (2023). Bio-degradation of Azo dye by the Bacteria isolated from Textile Industry Effulent of Solapur district. *Research Journal of Chemistry Environment_, 27*, 10.

Liu, J., Fan, L., Yin, W., Zhang, S., Su, X., Lin, H., . . . Sun, F. (2023). Anaerobic biodegradation of azo dye reactive black 5 by a novel strain Shewanella sp. SR1: Pathway and mechanisms. *Journal of environmental management, 347*, 119073.

Liu, J., Xiong, J., Tian, C., Gao, B., Wang, L., & Jia, X. (2018). The degradation of methyl orange and membrane fouling behavior in anaerobic baffled membrane bioreactor. *Chemical Engineering Journal, 338*, 719-725.

Liu, W., You, Y., Sun, D., Wang, S., Zhu, J., & Liu, C. (2018). Decolorization and detoxification of water-insoluble Sudan dye by Shewanella putrefaciens CN32 co-cultured with Bacillus circulans BWL1061. *Ecotoxicology Environmental Safety, 166*, 11-17.

Liu, Y., Huang, L., Guo, W., Jia, L., Fu, Y., Gui, S., & Lu, F. (2017). Cloning, expression, and characterization of a thermostable and pH-stable laccase from Klebsiella pneumoniae and its application to dye decolorization. *Process Biochemistry, 53*, 125-134.

Livingston, A. G., & Chase, H. A. (1989). Modeling phenol degradation in a fluidized-bed bioreactor. *AIChE journal, 35*(12), 1980-1992.

Lobiuc, A., Olaru, S., Hancu, E. I., Costica, N., Fortuna, M. E., Zamfirache, M. M., & Constantinescu, G. (2018). Toxicity and removal of Direct Red 28 diazo dye in living polymeric systems. *Rev. Chim, 69*(7), 1628-1635.

Luong, J. (1987). Generalization of Monod kinetics for analysis of growth data with substrate inhibition. *Biotechnology Bioengineering, 29*(2), 242-248.

LYNCH, J. M., & MOFFAT, A. J. (2005). Bioremediation–prospects for the future application of innovative applied biological research. *Annals of Applied Biology, 146*(2), 217-221.

Mani, P., Fidal, V., Bowman, K., Breheny, M., Chandra, T., Keshavarz, T., & Kyazze, G. (2019). Degradation of azo dye (acid orange 7) in a microbial fuel cell: comparison between anodic microbial-mediated reduction and cathodic laccase-mediated oxidation. *Frontiers in Energy Research, 7*, 101.

Mani, S., & Bharagava, R. N. (2016). Exposure to crystal violet, its toxic, genotoxic and carcinogenic effects on environment and its degradation and detoxification for environmental safety. *Reviews of Environmental ContaminationToxicology, 237*, 71-104.

Manogaran, M., Manogaran, B., Othman, A. R., Gunasekaran, B., & Abd Shukor, M. Y. (2020). Decolourisation of Reactive Red 120 by a heavy metal-tolerant bacterium isolated from Juru River, Malaysia. *Bioremediation Science Technology Research, 8*(1), 23-26.

Manogaran, M., Yasid, N. A., Othman, A. R., Gunasekaran, B., Halmi, M. I. E., & Shukor, M. Y. A. (2021). Biodecolourisation of Reactive Red 120 as a sole carbon source by a bacterial

consortium—Toxicity assessment and statistical optimisation. *International journal of environmental research public health, 18*(5), 1-26.

Marcharchand, S., & Ting, A. S. Y. (2017). Trichoderma asperellum cultured in reduced concentrations of synthetic medium retained dye decolourization efficacy. *Journal of environmental management, 203*, 542-549.

Marzec, A. (2014). *The effect of dyes, pigments and ionic liquids on the properties of elastomer composites.* Université Claude Bernard-Lyon I; Uniwersytet łódzki,

Maurya, K. L., Swain, G., Kumar, M., Sonwani, R. K., Verma, A., & Singh, R. S. (2023). Biodegradation of Congo red dye using Lysinibacillus species in a moving bed biofilm reactor: continuous study and kinetic evaluation. *Applied Biochemistry Biotechnology, 195*(9), 5267-5279.

Maurya, K. L., Swain, G., Sonwani, R. K., Verma, A., & Singh, R. S. (2022). Biodegradation of Congo red dye using polyurethane foam-based biocarrier combined with activated carbon and sodium alginate: batch and continuous study. *Bioresource Technology, 351*, 126999-127005.

Mcyotto, F., Wei, Q., Macharia, D. K., Huang, M., Shen, C., & Chow, C. W. (2021). Effect of dye structure on color removal efficiency by coagulation. *Chemical Engineering Journal, 405*, 126674.

Meinert, C., Schürmann, M., Domeyer, J.-E., Poehlein, A., Daniel, R., & Steinbüchel, A. (2018). The unexpected function of a Flavin-dependent oxidoreductase from Variovorax paradoxus TBEA6. *FEMS microbiology letters, 365*(6), fny011.

Merdan, N., Eyupoglu, S., & Duman, M. N. (2017). Ecological and sustainable natural dyes. *Textiles clothing sustainability: sustainable textile chemical processes,* 1-41.

Milani, D., Bartlett, A. J., de Solla, S. R., Parrott, J. L., Intini, K. D., Legault, D., . . . Balakrishnan, V. K. (2018). Comparative toxicity of azo dyes to two infaunal organisms (Hexagenia spp. and Tubifex tubifex) in spiked-sediment exposures. *Environmental Science Pollution Research, 25*, 6937-6950.

Min, J., Xu, L., Fang, S., Chen, W., & Hu, X. (2020). Microbial degradation kinetics and molecular mechanism of 2, 6-dichloro-4-nitrophenol by a Cupriavidus strain. *Environmental Pollution, 258*, 113703-113712.

Miralles-Cuevas, S., Oller, I., Agüera, A., Llorca, M., Pérez, J. S., & Malato, S. (2017). Combination of nanofiltration and ozonation for the remediation of real municipal wastewater effluents: acute and chronic toxicity assessment. *Journal of hazardous materials, 323*, 442-451.

Mishra, A., Singh, R. S., Mishra, V., Giri, B. S., & Singh, D. (2024). Kinetics studies and effect of the process parameters on the biodegradation of methyl orange dye. *Journal of the Indian Chemical Society, 101*(10), 101334-101342.

Mishra, A., Takkar, S., Joshi, N. C., Shukla, S., Shukla, K., Singh, A., . . . Varma, A. (2022). An Integrative approach to study bacterial enzymatic degradation of toxic dyes. *Frontiers in Microbiology, 12*, 802544.

Mishra, B., Varjani, S., Iragavarapu, G. P., Ngo, H. H., Guo, W., & Vishal, B. (2019). Microbial fingerprinting of potential biodegrading organisms. *Current Pollution Reports, 5*, 181-197.

Mishra, B., Varjani, S., Kumar, G., Awasthi, M. K., Awasthi, S. K., Sindhu, R., . . . Zhang, Z. (2021). Microbial approaches for remediation of pollutants: Innovations, future outlook, and challenges. *Energy Environment, 32*(6), 1029-1058.

Mishra, G., & Tripathy, M. (1993). A critical review of the treatments for decolourization of textile effluent. *Colourage, 40*, 35-35.

Moghaddam, S. S., Moghaddam, M. A., & Arami, M. (2010). Coagulation/flocculation process for dye removal using sludge from water treatment plant: optimization through response surface methodology. *Journal of hazardous materials, 175*(1-3), 651-657.

Mohana, S., Shrivastava, S., Divecha, J., & Madamwar, D. (2008). Response surface methodology for optimization of medium for decolorization of textile dye Direct Black 22 by a novel bacterial consortium. *Bioresource technology, 99*(3), 562-569.

Mohanty, S. S., & Kumar, A. (2020). Optimization and kinetic studies on decolorization of Vat Green XBN by a newly isolated bacterial strain Proteus mirabilis PMS. *Journal of Water Process Engineering, 37*, 101529.

Mudhoo, A., Ramasamy, D. L., Bhatnagar, A., Usman, M., & Sillanpää, M. (2020). An analysis of the versatility and effectiveness of composts for sequestering heavy metal ions, dyes and xenobiotics from soils and aqueous milieus. *Ecotoxicology Environmental Safety, 197*, 110587.

Mukherjee, J., Lodh, B. K., Sharma, R., Mahata, N., Shah, M. P., Mandal, S., . . . Bhunia, B. (2023). Advanced oxidation process for the treatment of industrial wastewater: A review on strategies, mechanisms, bottlenecks and prospects. *Chemosphere*, 140473.

Mustafa, G., Zahid, M. T., Ali, S., Abbas, S. Z., & Rafatullah, M. (2021). Biodegradation and discoloration of disperse blue-284 textile dye by Klebsiella pneumoniae GM-04 bacterial isolate. *Journal of King Saud University-Science, 33*(4), 101442.

Narayanan, C., & Narayan, V. (2019). Biological wastewater treatment and bioreactor design: a review. *Sustainable Environment Research, 29*(1), 1-17.

Narayanan, M., Ali, S. S., & El-Sheekh, M. (2023). A comprehensive review on the potential of microbial enzymes in multipollutant bioremediation: Mechanisms, challenges, and future prospects. *Journal of Environmental Management, 334*, 117532.

Nejatbakhsh, S., Soodmand, A. M., Azimi, B., Farshchi, M. E., Aghdasinia, H., & Kazemian, H. (2023). Semi-pilot scale fluidized-bed reactor applied for the Azo dye removal from seawater by granular heterogeneous fenton catalysts. *Chemical Engineering Research Design, 195*, 1-13.

Ngo, A. C. R., & Tischler, D. (2022). Microbial degradation of azo dyes: approaches and prospects for a hazard-free conversion by microorganisms. *International Journal of Environmental Research Public Health, 19*(8), 4740.

Nikam, M., Patil, S., Patil, U., Khandare, R., Govindwar, S., & Chaudhari, A. (2017). Biodegradation and detoxification of azo solvent dye by ethylene glycol tolerant ligninolytic ascomycete strain of Pseudocochliobolus verruculosus NFCCI 3818. *Biocatalysis Agricultural Biotechnology, 9*, 209-217.

Nonogaki, H., Bassel, G. W., & Bewley, J. D. (2010). Germination—still a mystery. *Plant science, 179*(6), 574-581.

Nouren, S., Bhatti, H. N., Iqbal, M., Bibi, I., Kamal, S., Sadaf, S., . . . Safa, Y. (2017). By-product identification and phytotoxicity of biodegraded Direct Yellow 4 dye. *Chemosphere, 169*, 474-484.

Ogugbue, C. J., & Sawidis, T. (2011). Bioremediation and detoxification of synthetic wastewater containing triarylmethane dyes by Aeromonas hydrophila isolated from industrial effluent. *Biotechnology research international, 2011*(1), 967925.

Oguntade, O. A., Adetunji, M. T., Salako, F. K., Arowolo, T. A., & Azeez, J. O. (2018). Growth, dry matter and heavy metal uptake of potted Amaranthus cruentus L. as influenced by dye-laden wastewater. *Tropical Agriculture, 95*(2).

Oturkar, C. C., Nemade, H. N., Mulik, P. M., Patole, M. S., Hawaldar, R. R., & Gawai, K. R. (2011). Mechanistic investigation of decolorization and degradation of Reactive Red 120 by Bacillus lentus BI377. *Bioresource technology, 102*(2), 758-764.

Özkaya, B., Kaksonen, A. H., Sahinkaya, E., & Puhakka, J. A. (2019). Fluidized bed bioreactor for multiple environmental engineering solutions. *Water research, 150*, 452-465.

Panwar, P., Mahajan, P., & Kaushal, J. (2023). Microbial bioremediation of Azo dyes: An environmentally sustainable technology. *Remediation Journal, 33*(2), 151-165.

Parrott, J. L., Bartlett, A. J., & Balakrishnan, V. K. (2016). Chronic toxicity of azo and anthracenedione dyes to embryo-larval fathead minnow. *Environmental pollution, 210*, 40-47.

Patel, D. K., Tipre, D. R., & Dave, S. R. (2017). Enzyme mediated bacterial biotransformation and reduction in toxicity of 1: 2 chromium complex AB193 and AB194 dyes. *Journal of the Taiwan institute of Chemical Engineers, 77*, 1-9.

Patel, D. K., Tipre, D. R., & Dave, S. R. (2019). Application of a downflow microaerophilic fixed film (DFMFF) reactor for the treatment of dye house effluents using a developed bacterial consortium. *Environmental Sustainability, 2*, 145-155.

Patel Jay, N., Vaishnav Darshit, K., Joshi Pavan, R., & Tipre Devayani, R. (2023). Bacterial enzymes for azo dye degradation: an insight. *Research Journal of Chemistry and Environment, 27*(4), 135-148.

Paul, P. E. V., Sangeetha, V., & Deepika, R. G. (2019). Emerging trends in the industrial production of chemical products by microorganisms. *Recent developments in applied microbiology biochemistry,* 107-125.

Pearce, C., Lloyd, J., & Guthrie, J. (2003). The removal of colour from textile wastewater using whole bacterial cells: a review. *Dyes and Pigments, 58*(3), 179-196.

Periyasamy, A. P. (2024). Recent advances in the remediation of textile-dye-containing wastewater: prioritizing human health and sustainable wastewater treatment. *Sustainability, 16*(2), 495-535.

Phisalaphong, M., Srirattana, N., & Tanthapanichakoon, W. (2006). Mathematical modeling to investigate temperature effect on kinetic parameters of ethanol fermentation. *Biochemical Engineering Journal, 28*(1), 36-43.

Piątkowska, M., Jedziniak, P., Olejnik, M., Żmudzki, J., & Posyniak, A. (2018). Absence of evidence or evidence of absence? A transfer and depletion study of Sudan I in eggs. *Food chemistry, 239*, 598-602.

Pinheiro, L. R. S., Gradíssimo, D. G., Xavier, L. P., & Santos, A. V. (2022). Degradation of azo dyes: bacterial potential for bioremediation. *Sustainability, 14*(3), 1510.

Pokharia, A., & Ahluwalia, S. S. (2013). Isolation and screening of dye decolorizing bacterial isolates from contaminated sites. *Textiles Light Industrial Science and Technology, 2*(2), 54-61.

Popli, S., & Patel, U. D. (2015). Destruction of azo dyes by anaerobic–aerobic sequential biological treatment: a review. *International Journal of Environmental Science Technology, 12*, 405-420.

Prasad, A. A., & Rao, K. B. (2010). Physico chemical characterization of textile effluent and screening for dye decolorizing bacteria. *Global journal of biotechnology and biochemistry, 5*(2), 80-86.

Prasad, K. K., Mohan, S. V., Rao, R. S., Pati, B. R., & Sarma, P. (2005). Laccase production by Pleurotus ostreatus 1804: Optimization of submerged culture conditions by Taguchi DOE methodology. *Biochemical Engineering Journal, 24*(1), 17-26.

Qi, J., Anke, M. K., Szymańska, K., & Tischler, D. (2017). Immobilization of Rhodococcus opacus 1CP azoreductase to obtain azo dye degrading biocatalysts operative at acidic pH. *International Biodeterioration Biodegradation, 118*, 89-94.

Qiu, H., Shen, F., Yin, A., Liu, J., Wu, B., Li, Y., . . . Xu, B. (2022). Biodegradation and detoxification of azo dyes by halophilic/halotolerant microflora isolated from the salt fields of Tibet autonomous region China. *Frontiers in Microbiology, 13*, 877151.

Rai, H. S., Bhattacharyya, M. S., Singh, J., Bansal, T., Vats, P., & Banerjee, U. (2005). Removal of dyes from the effluent of textile and dyestuff manufacturing industry: a review of emerging techniques with reference to biological treatment. *Critical reviews in environmental science technology, 35*(3), 219-238.

Rai, R., & Vijayakumar, B. (2023). Myco-Remediation of Textile Dyes Via Biosorption by Aspergillus tamarii Isolated from Domestic Wastewater. *Water, Air, Soil Pollution, 234*(8), 542.

Rajamohan, N., & Rajasimman, M. (2013). Kinetic modeling of dye effluent biodegradation by Pseudomonas stutzeri. *Engineering,Technology Applied Science Research, 3*(2), 387-390.

Rajendran, R., Kiruthika, S., Saranya, P., Mohan, A., & Vaishali, C. (2021). Biodecolorization of azo dye mixture (Remazol Brilliant Violet 5r and Reactive Red 120) by indigenous bacterial consortium obtained from dye contaminated soil. *Research square*, 1-12.

Rápó, E., Posta, K., Csavdári, A., Vincze, B. É., Mara, G., Kovács, G., . . . Tonk, S. (2020). Performance comparison of Eichhornia crassipes and Salvinia natans on azo-dye (Eriochrome Black T) phytoremediation. *Crystals, 10*(7), 565.

Rathod, J., & Archana, G. (2013). Molecular fingerprinting of bacterial communities in enriched azo dye (Reactive Violet 5R) decolorising native acclimatised bacterial consortia. *Bioresource technology, 142*, 436-444.

Rawat, D., Mishra, V., & Sharma, R. S. (2016). Detoxification of azo dyes in the context of environmental processes. *Chemosphere, 155*, 591-605.

Rezouga, F., Hamdi, M., & Sperandio, M. (2009). Variability of kinetic parameters due to biomass acclimation: case of para-nitrophenol biodegradation. *Bioresource technology, 100*(21), 5021-5029.

Rippon, J. A., & Evans, D. J. (2020). Improving the properties of natural fibres by chemical treatments. In *Handbook of natural fibres* (pp. 245-321): Elsevier.

Robinson, T., McMullan, G., Marchant, R., & Nigam, P. (2001). Remediation of dyes in textile effluent: a critical review on current treatment technologies with a proposed alternative. *Bioresource technology, 77*(3), 247-255.

Rondon, H., El-Cheikh, W., Boluarte, I. A. R., Chang, C.-Y., Bagshaw, S., Farago, L., . . . Shu, L. (2015). Application of enhanced membrane bioreactor (eMBR) to treat dye wastewater. *Bioresource technology, 183*, 78-85.

Rusan, M. J., Albalasmeh, A. A., Zuraiqi, S., & Bashabsheh, M. (2015). Evaluation of phytotoxicity effect of olive mill wastewater treated by different technologies on seed germination of barley (Hordeum vulgare L.). *Environmental Science Pollution Research, 22*, 9127-9135.

Saha, I., Datta, S., & Biswas, D. (2023). Mechanistic approach on comparative biosorption of dyes by extracellular polymer of Ochrobactrum pseudintermedium C1 utilizing waste mineral lubricating oil. *Bioremediation Journal*, 1-20.

Saha, P., Madliya, S., Khare, A., Subudhi, I., & Bhaskara Rao, K. V. (2023). Enzymatic biodegradation, kinetic study, and detoxification of reactive Red-195 by Halomonas meridiana isolated from marine sediments of Andaman Sea, India. *Environmental Technology, 44*(17), 2648-2667.

Sahu, A., & Poler, J. C. (2024). Removal and degradation of dyes from textile industry wastewater: Benchmarking recent advancements, toxicity assessment and cost analysis of treatment processes. *Journal of Environmental Chemical Engineering*, 113754.

Saitou, N., & Nei, M. (1987). The neighbor-joining method: a new method for reconstructing phylogenetic trees. *Molecular biology evolution, 4*(4), 406-425.

Salokhe, M., & Govindwar, S. (1999). Effect of carbon source on the biotransformation enzymes in Serratia marcescens. *World journal of microbiology biotechnology, 15*(2), 229-232.

Sandhibigraha, S., Chakraborty, S., Bandyopadhyay, T., & Bhunia, B. (2020). A kinetic study of 4-chlorophenol biodegradation by the novel isolated Bacillus subtilis in batch shake flask. *Environmental Engineering Research, 25*(1), 62-70.

Saratale, G., Humnabadkar, R., & Govindwar, S. (2007). Study of mixed function oxidase system in Aspergillus ochraceus (NCIM 1146). *Indian Journal of Microbiology, 47*, 304-309.

Saratale, G. D., Chien, L.-J., & Chang, J. S. (2010). Enzymatic treatment of lignocellulosic wastes for anaerobic digestion and bioenergy production. In *Environmental Anaerobic Technology: Applications and New Developments* (pp. 279-308): World Scientific.

Saratale, R., Saratale, G., Chang, J.-S., & Govindwar, S. (2009a). Ecofriendly degradation of sulfonated diazo dye CI Reactive Green 19A using Micrococcus glutamicus NCIM-2168. *Bioresource technology, 100*(17), 3897-3905.

Saratale, R., Saratale, G., Chang, J., & Govindwar, S. (2009b). Ecofriendly degradation of sulfonated diazo dye CI Reactive Green 19A using Micrococcus glutamicus NCIM-2168. *Bioresource technology, 100*(17), 3897-3905.

Saratale, R., Saratale, G., Kalyani, D., Chang, J.-S., & Govindwar, S. (2009). Enhanced decolorization and biodegradation of textile azo dye Scarlet R by using developed microbial consortium-GR. *Bioresource technology, 100*(9), 2493-2500.

Saratale, R. G., Saratale, G. D., Chang, J.-S., & Govindwar, S. P. (2011). Bacterial decolorization and degradation of azo dyes: a review. *Journal of the Taiwan Institute of Chemical Engineers, 42*(1), 138-157.

Sarim, K. M., Kukreja, K., Shah, I., & Choudhary, C. K. (2019). Biosorption of direct textile dye Congo red by Bacillus subtilis HAU-KK01. *Bioremediation Journal, 23*(3), 185-195.

Sarkar, P., Show, S., Tiwari, H., & Dey, A. (2024). Strategic utilization of groundnut shell (Arachis hypogaea) immobilized bacterial consortium for enhanced 4-nitrophenol remediation: statistical optimization, kinetic modeling, and reusability. *Biomass Conversion Biorefinery, 14*(2), 2733-2744.

Sarvajith, M., Reddy, G. K. K., & Nancharaiah, Y. (2018). Textile dye biodecolourization and ammonium removal over nitrite in aerobic granular sludge sequencing batch reactors. *Journal of hazardous materials, 342*, 536-543.

Savin, I.-I., & Butnaru, R. (2008). Wastewater characteristics in textile finishing mills. *Environmental Engineering Management Journal, 7*(6).

Saxena, A., & Gupta, S. (2020). Bioefficacies of microbes for mitigation of Azo dyes in textile industry effluent: A review. *BioResources, 15*(4), 9858-9881.

Saxena, G., Kishor, R., Saratale, G. D., & Bharagava, R. N. (2020). Genetically modified organisms (GMOs) and their potential in environmental management: constraints, prospects, and challenges. *Bioremediation of Industrial Waste for Environmental Safety,* 1-19.

Schirmer, C., Nussbaumer, T., Schöb, R., Pörtner, R., Eibl, R., & Eibl, D. (2018). Development, engineering and biological characterization of stirred tank bioreactors. *Biopharmaceuticals. InTech*, 87-108.

Schmidt, C., Berghahn, E., Ilha, V., & Granada, C. (2019). Biodegradation potential of Citrobacter cultures for the removal of amaranth and congo red azo dyes. *International Journal of Environmental Science Technology, 16*(11), 6863-6872.

Selvaraj, D., Leena, R., & Kamal, D. (2015). Toxicological and histopathological impacts of textile dyeing industry effluent on a selected teleost fish Poecilia reticulata. *Asian Journal of Pharmacology Toxicology, 3*(10), 26-30.

Selvaraj, V., Karthika, T. S., Mansiya, C., & Alagar, M. (2021). An over review on recently developed techniques, mechanisms and intermediate involved in the advanced azo dye degradation for industrial applications. *Journal of molecular structure, 1224*, 129195.

Sen, S. K., Raut, S., Bandyopadhyay, P., & Raut, S. (2016). Fungal decolouration and degradation of azo dyes: a review. *Fungal Biology Reviews, 30*(3), 112-133.

Senthilvelan, T., Rathore, H. S., Gomathi, E., Panda, R. C., Issac, P. K., Guru, A., & Arockiaraj, J. (2023). The enzymatic decolorization of leather azo dyes (AB 113 and AB 52) using crude fungal laccase: an eco-friendly approach towards pollution reduction. *Biomass Conversion Biorefinery,* 1-13.

Sghaier, I., Guembri, M., Chouchane, H., Mosbah, A., Ouzari, H. I., Jaouani, A., . . . Neifar, M. (2019). Recent advances in textile wastewater treatment using microbial consortia. *Text. Eng. Fash. Technol, 5*(3), 134-146.

Shabir, M., Yasin, M., Hussain, M., Shafiq, I., Akhter, P., Nizami, A.-S., . . . Park, Y.-K. (2022). A review on recent advances in the treatment of dye-polluted wastewater. *Journal of Industrial Engineering Chemistry, 112*, 1-19.

Shah, M. P. (2019). Bioremediation of azo dye. In *Microbial wastewater treatment* (pp. 103-126): Elsevier.

Shalini, & Setty, Y. P. (2019). Multistage fluidized bed bioreactor for dye decolorization using immobilized polyurethane foam: a novel approach. *Biochemical Engineering Journal, 152*, 107368.

Sharma, A., Kumar, V., Shahzad, B., Ramakrishnan, M., Singh Sidhu, G. P., Bali, A. S., . . . Khanna, K. (2020). Photosynthetic response of plants under different abiotic stresses: a review. *Journal of Plant Growth Regulation, 39*, 509-531.

Sharma, J., Sharma, S., & Soni, V. (2021). Classification and impact of synthetic textile dyes on Aquatic Flora: A review. *Regional Studies in Marine Science, 45*, 101802.

Sharma, K., Sharma, P., Dhiman, S. K., Chadha, P., & Saini, H. S. (2022). Biochemical, genotoxic, histological and ultrastructural effects on liver and gills of fresh water fish Channa punctatus exposed to textile industry intermediate 2 ABS. *Chemosphere, 287*, 132103.

Shekhawat, N. S., Patra, S. K., Patra, A. K., & Bag, B. (2024). A novel environmental friendly and sustainable process for textile dyeing with sulphur dyes for cleaner production. *Chemical Engineering Journal, 479*, 147329.

Shi, B., Li, G., Wang, D., Feng, C., & Tang, H. (2007). Removal of direct dyes by coagulation: the performance of preformed polymeric aluminum species. *Journal of hazardous materials, 143*(1-2), 567-574.

Shi, Y., Yang, Z., Xing, L., Zhang, X., Li, X., & Zhang, D. (2021). Recent advances in the biodegradation of azo dyes. *World Journal of Microbiology Biotechnology, 37*, 1-18.

Shindhal, T., Rakholiya, P., Varjani, S., Pandey, A., Ngo, H. H., Guo, W., . . . Taherzadeh, M. J. (2021). A critical review on advances in the practices and perspectives for the treatment of dye industry wastewater. *Bioengineered, 12*(1), 70-87.

Shu, D., Fang, K., Liu, X., Cai, Y., An, F., Qu, G., & Liang, Y. (2019). Cleaner pad-steam dyeing technology for cotton fabrics with excellent utilization of reactive dye. *Journal of Cleaner Production, 241*, 118370.

Shuler, M. L. (1992). Bioprocess enzineering. *Prentice-Hall*, 412-420.

Siddiqui, S. I., Allehyani, E. S., Al-Harbi, S. A., Hasan, Z., Abomuti, M. A., Rajor, H. K., & Oh, S. (2023). Investigation of Congo red toxicity towards different living organisms: a review. *Processes, 11*(3), 807.

Siemiatycki, J., Richardson, L., Straif, K., Latreille, B., Lakhani, R., Campbell, S., . . . Boffetta, P. (2004). Listing occupational carcinogens. *Environmental health perspectives, 112*(15), 1447-1459.

SILVA, W. J. D., SILVA, M. R., & Takashima, K. (2015). Preparation and characterization of Zno/CuO semiconductor and photocatalytic activity on the decolorization of direct red 80 azodye. *Journal of the chilean chemical society, 60*(4), 2749-2751.

Singh, A., Pal, D. B., Mohammad, A., Alhazmi, A., Haque, S., Yoon, T., . . . Gupta, V. K. (2022). Biological remediation technologies for dyes and heavy metals in wastewater treatment: New insight. *Bioresource technology, 343*, 126154.

Singh, B. J., Chakraborty, A., & Sehgal, R. (2023). A systematic review of industrial wastewater management: Evaluating challenges and enablers. *Journal of Environmental Management, 348*, 119230.

Singh, G. B., Vinayak, A., Mudgal, G., & Kesari, K. K. (2024). Azo dye bioremediation: An interdisciplinary path to sustainable fashion. *Environmental Technology & Innovation, 36*, 103832.

Singh, H., Raj, S., Kumar, D., Sharma, S., Bhatt, U., & Soni, V. (2021). Bioremediation Potential of Duckweed (Lemna Gibba) in The Decolorization of CI Basic Green 4 and Chlorophyll a Fluorescence Analysis: Understanding Plant Performance.

Skanda, S., Bharadwaj, P., Kar, S., Sai Muthukumar, V., & Vijayakumar, B. (2023). Bioremoval capacity of recalcitrant azo dye Congo red by soil fungus Aspergillus arcoverdensis SSSIHL-01. *Bioremediation Journal, 27*(1), 32-43.

Slokar, Y. M., & Le Marechal, A. M. (1998). Methods of decoloration of textile wastewaters. *Dyes pigments, 37*(4), 335-356.

Sodaneath, H., Lee, J.-I., Yang, S.-O., Jung, H., Ryu, H. W., & Cho, K.-S. (2017). Decolorization of textile dyes in an air-lift bioreactor inoculated with Bjerkandera adusta OBR105. *Journal of Environmental Science Health, Part A, 52*(11), 1099-1111.

Solayman, H., Hossen, M. A., Abd Aziz, A., Yahya, N. Y., Leong, K. H., Sim, L. C., . . . Zoh, K.-D. (2023). Performance evaluation of dye wastewater treatment technologies: A review. *Journal of Environmental Chemical Engineering, 11*(3), 109610.

Solis-Oba, M. M., Solís, A., Pérez, H. I., Manjarrez, N., & Flores, M. (2012). Microbial decolouration of azo dyes. *Process Biochemistry, 47*(12), 1723-1748.

Solís, M., Solís, A., Pérez, H. I., Manjarrez, N., & Flores, M. (2012). Microbial decolouration of azo dyes: a review. *Process Biochemistry, 47*(12), 1723-1748.

Soni, V., Keswani, K., Bhatt, U., Kumar, D., & Singh, H. (2021). In vitro propagation and analysis of mixotrophic potential to improve survival rate of Dolichandra unguis-cati under ex vitro conditions. *Heliyon, 7*(2).

Sonwani, R. K., Pandey, S., Yadav, S. K., Giri, B. S., Katiyar, V., Singh, R. S., & Rai, B. N. (2021). Construction of integrated system for the treatment of Acid orange 7 dye from wastewater: Optimization and growth kinetic study. *Bioresource Technology, 337*, 125478-125484.

Sonwani, R. K., Patel, D., Singh, A., Singh, R. S., & Rai, B. N. (2023). Intensified biodegradation of Congo red dye by mixed culture in a sequential bioreactor: Kinetics and phytotoxicity studies. *Indian Journal of Experimental Biology, 61*(10), 739-745.

Srinivasan, R., Kathiravan, M. N., & Gopinath, K. P. (2011). Degradation of Tectilon Yellow 2G by hybrid technique: Combination of sonolysis and biodegradation using mutant Pseudomonas putida. *Bioresource Technology, 102*(3), 2242-2247.

Srinivasan, S., Bankole, P. O., & Sadasivam, S. K. (2022). Biodecolorization and degradation of textile azo dyes using Lysinibacillus sphaericus MTCC 9523. *Frontiers in Environmental Science, 10*, 1-13.

Srivastava, A., Rani, R. M., Patle, D. S., & Kumar, S. (2022). Emerging bioremediation technologies for the treatment of textile wastewater containing synthetic dyes: a comprehensive review. *Journal of Chemical Technology Biotechnology, 97*(1), 26-41.

Srivatsav, D., Devi, S., Reddy, V., & Venkant, S. (2019). Microbial Degradation of Azo Dyes From Textile Industry-Review. *International Journal of Engineering Research Technology, 8*(11), 429-435.

Suzuki, H., Abe, T., Doi, K., & Ohshima, T. (2018). Azoreductase from alkaliphilic Bacillus sp. AO1 catalyzes indigo reduction. *Applied microbiology biotechnology, 102*, 9171-9181.

Szyguła, A., Guibal, E., Ruiz, M., & Sastre, A. M. (2008). The removal of sulphonated azo-dyes by coagulation with chitosan. *Colloids Surfaces A: Physicochemical Engineering Aspects, 330*(2-3), 219-226.

Taguchi, G., & Phadke, M. S. (1984). Quality engineering through design optimization. *Quality control, robust design, the Taguchi method,* 77-96.

Taieb, I., Ben Younes, S., Messai, B., Mnif, S., Mzoughi, R., Bakhrouf, A., . . . Ellafi, A. (2021). Isolation, characterization and identification of a new lysinibacillus fusiformis strain zc from metlaoui phosphate laundries wastewater: Bio-treatment assays. *Sustainability, 13*(18), 10072.

Takkar, S., Tyagi, B., Kumar, N., Kumari, T., Iqbal, K., Varma, A., . . . Mishra, A. (2022). Biodegradation of methyl red dye by a novel actinobacterium Zhihengliuella sp. ISTPL4: Kinetic studies, isotherm and biodegradation pathway. *Environmental Technology Innovation, 26*, 102348.

Tang, A. Y., & Kan, C. w. (2020). Non-aqueous dyeing of cotton fibre with reactive dyes: A review. *Coloration Technology, 136*(3), 214-223.

Teerapatsakul, C., Parra, R., Keshavarz, T., & Chitradon, L. (2017). Repeated batch for dye degradation in an airlift bioreactor by laccase entrapped in copper alginate. *International Biodeterioration Biodegradation, 120*, 52-57.

Tekere, M., Jacob-Lopes, E., & Zepka, L. Q. (2019). Microbial bioremediation and different bioreactors designs applied. *Biotechnology and bioengineering,* 1-19.

Telke, A. A., Kalyani, D. C., Dawkar, V. V., & Govindwar, S. P. (2009). Influence of organic and inorganic compounds on oxidoreductive decolorization of sulfonated azo dye CI Reactive Orange 16. *Journal of hazardous materials, 172*(1), 298-309.

Tian, F., Guo, G., Zhang, C., Yang, F., Hu, Z., Liu, C., & Wang, S.-w. (2019). Isolation, cloning and characterization of an azoreductase and the effect of salinity on its expression in a halophilic bacterium. *International journal of biological macromolecules, 123*, 1062-1069.

Tian, F., Wang, Y., Guo, G., Ding, K., Yang, F., Wang, H., . . . Liu, C. (2021). Enhanced azo dye biodegradation at high salinity by a halophilic bacterial consortium. *Bioresource technology, 326*, 124749.

Tippabathani, J., Nellore, J., Kathirkannan, P., & Nachiyar, C. V. (2022). Developmental effects of three textile chemicals on locomotor activity, antioxidant markers and acetylcholine esterase activity in zebrafish. *Indian Journal of Experimental Biology, 58*(03), 212-218.

Titchou, F. E., Zazou, H., Afanga, H., El Gaayda, J., Akbour, R. A., Nidheesh, P. V., & Hamdani, M. (2021). Removal of organic pollutants from wastewater by advanced oxidation processes and its combination with membrane processes. *Chemical Engineering Processing-Process Intensification, 169*, 108631.

Tiwari, H., Sonwani, R. K., & Singh, R. S. (2022). A comprehensive evaluation of the integrated photocatalytic-fixed bed bioreactor system for the treatment of Acid Blue 113 dye. *Bioresource Technology, 364*, 128037-128045.

Tounsadi, H., Metarfi, Y., Taleb, M., El Rhazi, K., & Rais, Z. (2020). Impact of chemical substances used in textile industry on the employee's health: Epidemiological study. *Ecotoxicology environmental safety, 197*, 110594.

Trautmann, N. M., & Krasny, M. E. (1998). *Composting in the classroom: Scientific inquiry for high school students*: Kendall/Hunt Publishing Company.

Tripathi, A., & Srivastava, S. (2011). Ecofriendly treatment of azo dyes: biodecolorization using bacterial strains. *International Journal of Bioscience, Biochemistry Bioinformatics, 1*(1), 37.

Tripathi, P., Tiwari, S., Sonwani, R. K., & Singh, R. S. (2023). Assessment of biodegradation kinetics and mass transfer aspects in attached growth bioreactor for effective treatment of brilliant green dye from wastewater. *Bioresource Technology, 381*, 129111-129121.

Unuofin, J. O., Okoh, A. I., & Nwodo, U. U. (2019). Aptitude of oxidative enzymes for treatment of wastewater pollutants: a laccase perspective. *Molecules, 24*(11), 2064.

Usha, M., Sasirekha, B., Bela, R., Devi, S., Kamalini, C., Manasa, G., & Neha, P. (2012). Batch, repeated batch and continuous degradation of Reactive Black 5 and Reactive Red 120 dye by immobilized bacteria. *Journal of Scientific & Industrial Research, 71*, 504-510.

Vandevivere, P. C., Bianchi, R., & Verstraete, W. (1998). Treatment and reuse of wastewater from the textile wet-processing industry: Review of emerging technologies. *Journal of Chemical Technology Biotechnology: International Research in Process, Environmental Clean Technology, 72*(4), 289-302.

Varjani, S., & Upasani, V. N. (2019). Influence of abiotic factors, natural attenuation, bioaugmentation and nutrient supplementation on bioremediation of petroleum crude contaminated agricultural soil. *Journal of environmental management, 245*, 358-366.

Varjani, S., Upasani, V. N., & Pandey, A. (2020). Bioremediation of oily sludge polluted soil employing a novel strain of Pseudomonas aeruginosa and phytotoxicity of petroleum hydrocarbons for seed germination. *Science of The Total Environment, 737*, 139766.

Varjani, S. J., & Upasani, V. N. (2017). A new look on factors affecting microbial degradation of petroleum hydrocarbon pollutants. *International Biodeterioration Biodegradation, 120*, 71-83.

Ventura-Camargo, B. d. C., Maltempi, P. P., & Marin-Morales, M. A. (2011). The use of the cytogenetic to identify mechanisms of action of an azo dye in Allium cepa meristematic cells. *J Environ Anal Toxicol, 1*(3), 1-12.

Vikrant, K., Giri, B. S., Raza, N., Roy, K., Kim, K.-H., Rai, B. N., & Singh, R. S. (2018). Recent advancements in bioremediation of dye: current status and challenges. *Bioresource technology, 253*, 355-367.

Wahla, A. Q., Iqbal, S., Anwar, S., Firdous, S., & Mueller, J. A. (2019). Optimizing the metribuzin degrading potential of a novel bacterial consortium based on Taguchi design of experiment. *Journal of hazardous materials, 366*, 1-9.

Walters, A., Santillo, D., & Johnston, P. (2005). An overview of textiles processing and related environmental concerns. *Greenpeace Research Laboratories, Department of Biological Sciences, University of Exeter, UK*.

Wang, B., Wang, Z., Chen, T., & Zhao, X. (2020). Development of novel bioreactor control systems based on smart sensors and actuators. *Frontiers in Bioengineering Biotechnology, 8*, 1-15.

Wang, H., Zheng, X.-W., Su, J.-Q., Tian, Y., Xiong, X.-J., & Zheng, T.-L. (2009). Biological decolorization of the reactive dyes Reactive Black 5 by a novel isolated bacterial strain Enterobacter sp. EC3. *Journal of hazardous materials, 171*(1-3), 654-659.

Wang, J., & Chen, H. (2020). Catalytic ozonation for water and wastewater treatment: Recent advances and perspective. *Science of The Total Environment, 704*, 135249.

Wang, S.-J., & Loh, K.-C. (1999). Modeling the role of metabolic intermediates in kinetics of phenol biodegradation. *Enzyme and Microbial Technology, 25*(3-5), 177-184.

Wang, W., & Keturi, P. H. (1990). Comparative seed germination tests using ten plant species for toxicity assessment of a metal engraving effluent sample. *Water, Air, Soil Pollution, 52*, 369-376.

Wang, Z., Liang, J., & Liang, Y. (2013). Decolorization of Reactive Black 5 by a newly isolated bacterium Bacillus sp. YZU1. *International Biodeterioration & Biodegradation, 76*, 41-48.

Wanyonyi, W. C., Onyari, J. M., Shiundu, P. M., & Mulaa, F. J. (2019). Effective biotransformation of reactive black 5 dye using crude protease from Bacillus cereus strain KM201428. *Energy Procedia, 157*, 815-824.

Waring, D. R., & Hallas, G. (2013). *The chemistry and application of dyes*: Springer Science & Business Media.

Wasi, S., Tabrez, S., & Ahmad, M. (2013). Use of Pseudomonas spp. for the bioremediation of environmental pollutants: a review. *Environmental monitoring and assessment, 185*, 8147-8155.

Wei, H., Song, S., Tian, H., & Liu, T. (2014). Effects of phenanthrene on seed germination and some physiological activities of wheat seedling. *Comptes Rendus. Biologies, 337*(2), 95-100.

Weigle, P. (1974). *Ancient dyes for modern weavers*: Watson-Guptill Publications.

Welham, N. J., Willis, P. E., & Kerr, T. (2000). Mechanochemical formation of metal–ceramic composites. *Journal of the American Ceramic Society, 83*(1), 33-40.

Wielewski, L. P., Zuccolotto, T., Soares, M., Prola, L. D. T., & Liz, M. V. d. (2020). Degradation of the textile dye reactive black 5 by basidiomycetes. *Revista Ambiente Água, 15*, e2464.

Will, Y., McDuffie, J. E., Olaharski, A. J., & Jeffy, B. D. (2016). *Drug discovery toxicology: From target assessment to translational biomarkers*: John Wiley & Sons.

Wu, J., Doan, H., & Upreti, S. (2008). Decolorization of aqueous textile reactive dye by ozone. *Chemical Engineering Journal, 142*(2), 156-160.

Xu, K.-Z., Ma, H., Wang, Y.-J., Cai, Y.-J., Liao, X.-R., & Guan, Z.-B. (2020). Extracellular expression of mutant CotA-laccase SF in Escherichia coli and its degradation of malachite green. *Ecotoxicology environmental safety, 193*, 110335.

Xu, X.-R., & Li, X.-Z. (2010). Degradation of azo dye Orange G in aqueous solutions by persulfate with ferrous ion. *Separation purification technology, 72*(1), 105-111.

Xuejiao, A., Yi, C., Ningjian, L., Shulin, Z., Liuwei, W., & Qinghua, Z. (2023). Green and sustainable approach for decoloration and detoxification of azo dye by bacterial-mediated thermo-halotolerant dye-decolorizing peroxidase (DyP). *Process Biochemistry, 130*, 334-346.

Yang, Y., Jiang, C., Wang, X., Fan, L., Xie, Y., Wang, D., . . . Zhuang, X. (2024). Unraveling the potential of microbial flocculants: preparation, performance, and applications in wastewater treatment. *Water, 16*(14), 1-18.

Yano, T., & Koga, S. (1969). Dynamic behavior of the chemostat subject to substrate inhibition. *Biotechnology bioengineering, 11*(2), 139-153.

Yaseen, D., & Scholz, M. (2019). Textile dye wastewater characteristics and constituents of synthetic effluents: a critical review. *International journal of environmental science technology, 16*, 1193-1226.

Yeap, K. L., Teng, T. T., Poh, B. T., Morad, N., & Lee, K. E. (2014). Preparation and characterization of coagulation/flocculation behavior of a novel inorganic–organic hybrid polymer for reactive and disperse dyes removal. *Chemical Engineering Journal, 243*, 305-314.

You, S.-J., & Teng, J.-Y. (2009). Anaerobic decolorization bacteria for the treatment of azo dye in a sequential anaerobic and aerobic membrane bioreactor. *Journal of the Taiwan Institute of Chemical Engineers, 40*(5), 500-504.

Yuwono, S. D., & Kokugan, T. (2008). Study of the effects of temperature and pH on lactic acid production from fresh cassava roots in tofu liquid waste by Streptococcus bovis. *Biochemical Engineering Journal, 40*(1), 175-183.

Zafar, S., Bukhari, D. A., & Rehman, A. (2022). Azo dyes degradation by microorganisms–An efficient and sustainable approach. *Saudi Journal of Biological Sciences, 29*(12), 103437.

Zahran, S. A., Ali-Tammam, M., Hashem, A. M., Aziz, R. K., & Ali, A. E. (2019). Azoreductase activity of dye-decolorizing bacteria isolated from the human gut microbiota. *Scientific Reports, 9*(1), 5508.

Zambrano, J., García-Encina, P. A., Hernández, F., Botero-Coy, A. M., Jiménez, J. J., & Irusta-Mata, R. (2023). Kinetics of the removal mechanisms of veterinary antibiotics in synthetic wastewater using microalgae–bacteria consortia. *Environmental Technology Innovation, 29*, 103031-103044.

Zarei, A., Biglari, H., Amiri, R., Ebrahimzadeh, G., Narooie, M. R., Mehrizi, E. A., & Mobini, M. (2017). The removal of blue 71 from aqueous solution using cotton pod ash. *Pollution Research, 36*(3), 489-497.

Zhang, H., Zhang, J., Zhang, X., & Geng, A. (2018). Purification and characterization of a novel manganese peroxidase from white-rot fungus Cerrena unicolor BBP6 and its application in dye decolorization and denim bleaching. *Process Biochemistry, 66*, 222-229.

ZHANG, X., & FLURKEY, W. H. (1997). Phenoloxidases in Portabella mushrooms. *Journal of food science, 62*(1), 97-100.

Zheng, X., Fu, D., Cheng, J., Tang, R., Chu, M., Chu, P., . . . Yin, S. (2021). Effects of hypoxic stress and recovery on oxidative stress, apoptosis, and intestinal microorganisms in Pelteobagrus vachelli. *Aquaculture, 543*, 736945.

Zhu, X., Chen, J., Qiu, K., & Kuai, B. (2017). Phytohormone and light regulation of chlorophyll degradation. *Frontiers in Plant Science, 8*, 1911.

Zhu, Y., Wang, W., Ni, J., & Hu, B. (2020). Cultivation of granules containing anaerobic decolorization and aerobic degradation cultures for the complete mineralization of azo dyes in wastewater. *Chemosphere, 246*, 125753.

Zhuang, M., Sanganyado, E., Zhang, X., Xu, L., Zhu, J., Liu, W., & Song, H. (2020). Azo dye degrading bacteria tolerant to extreme conditions inhabit nearshore ecosystems: optimization and degradation pathways. *Journal of environmental management, 261*, 110222.

Zollinger, H. (2003). *Color chemistry: syntheses, properties, and applications of organic dyes and pigments*: John Wiley & Sons.

Zou, H., Ning, X.-a., Wang, Y., & Zhou, F. (2019). The agricultural use potential of the detoxified textile dyeing sludge by integrated Ultrasound/Fenton-like process: A comparative study. *Ecotoxicology Environmental Safety, 172*, 26-32.

Deepa Goswami
12.02.26